MITOTIC SLIPPAGE IN NONCANCER CELLS INDUCED BY A MICROTUBULE DISRUPTOR, DISORAZOLE C_1, AND THE NOVEL ROLE FOR GPIBA IN CYTOKINESIS AND TETRAPLOIDIZATION IN CANCER CELLS

by

Fengfeng Xu

BS, University of Science and Technology of China, 2004

Submitted to the Graduate Faculty of

Arts and Sciences in partial fulfillment

of the requirements for the degree of

Doctor of Philosophy

University of Pittsburgh

2010

UNIVERSITY OF PITTSBURGH

ARTS AND SCIENCES

This dissertation was presented

by

Fengfeng Xu

It was defended on

March 25, 2010

and approved by

Lewis A. Jacobson, PhD, Professor

Kirill Kiselyov, PhD, Assistant Professor

James M. Pipas, PhD, Professor

Billy W. Day, PhD, Professor

Dissertation Advisor: William S. Saunders, PhD, Associated Professor

MITOTIC SLIPPAGE IN NONCANCER CELLS INDUCED BY A MICROTUBULE DISRUPTOR, DISORAZOLE C_1, AND THE NOVEL ROLE FOR GPIBA IN CYTOKINESIS AND TETRAPLOIDIZATION IN CANCER CELLS

Fengfeng Xu, PhD

University of Pittsburgh, 2010

Disorazole C_1 (DZ) is a synthesized polyene macrodiolide, originally identified as a minor metabolite from the myxobacterium fermentation broth. I examined the cellular responses to DZ in noncancer and cancer cells, and compared the results to vinblastine and taxol. In noncancer cells, DZ induced a prolonged mitotic arrest, followed by mitotic slippage, which was associated with cyclin B degradation, but did not require p53. Four apoptosis detection assays, including examination of poly(ADP-ribose) polymerase cleavage, cytochrome C release, mitochondrial depolarization, and annexin V staining, were conducted and demonstrated little induction of apoptosis in noncancer cells treated with DZ. However, I observed an activated apoptotic pathway in cancer cells, suggesting that normal and malignant cells respond differently to DZ, and indicating a potential therapeutic application for this compound.

GpIbα is a transmembrane subunit of the von Willebrand factor receptor on platelet surfaces, functioning in platelet adhesion and activation. Recent research has revealed that GpIbα also plays roles in transformation and genomic instability as an oncoprotein. In my studies, GpIbα colocalized with F-actin and filamin A, an actin-binding protein, at the cleavage furrow in anaphase cells, suggesting a novel role for GpIbα in cytokinesis. However, when GpIbα was

overexpressed in noncancer cells with p53 knockdown, GpIbα, F-actin, and filamin A became mislocalized. RhoA, a cytokinesis regulator, was localized asymmetrically, although Aurora B, an important cytokinesis kinase, retained its correct localization. Additionally, anaphase bridges were observed in these GpIbα-overexpressing cells, along with elevated percentages of cytokinesis failure and binucleation, indicating that GpIbα overexpression led to cytokinesis defects/failure and tetraploidization. Conversely, in cancer cells that endogenously overexpress GpIbα, I observed decreases in the percentages of binucleation and mitotic defects upon GpIbα knockdown. Furthermore, down-regulation of Aurora B was demonstrated to mediate the mechanism through which GpIbα overexpression led to cytokinesis failure, and the filamin A-binding domain and the signal peptide of GpIbα were shown to be indispensible for this mechanism. These results add a new component of the existing cancer cell genetic instability pathways, by suggesting that overexpression of GpIbα in cancer cells disrupts normal cytokinesis and causes tetraploidization through down-regulation of Aurora B.

TABLE OF CONTENTS

LIST OF FIGURES

ACKNOWLEDGEMENTS

First and foremost, I would like to thank my PhD advisor, Dr. William S. Saunders, for giving me wonderful projects to work on, and for guiding me along the way with his insightful suggestions and discussions on science to allow me becoming a mature scientist. He has always been my teaching mentor, and I have learned a lot from him by observing and assisting in his teaching, as well as discussing and practising my own teaching with him. He is a kind and extremely supportive advisor, who I cannot thank enough.

I would also like to thank my current and past committee members Dr. Lewis Jacobson, Dr. Kirill Kiselyov, Dr. James Pipas, Dr. Billy Day, Dr. John Lazo, and Dr. Susan Gilbert. Their continuous support and valuable comments and suggestions for all of my projects and especially my thesis are greatly appreciated.

I would like to express my sincerest gratitude and appreciation to my collaborators, Dr. Edward Prochownik, Dr. Kirill Kiselyov, Dr. John Lazo, Dr. Peter Wipf, Dr. Youjun Li (a post-doc in Dr. Prochownik's lab) and Youssef Rbaibi (a previous member of in Dr. Kiselyov's lab). I have always enjoyed our scientific discussions and would like to thank all of my collaborators for sharing scientific ideas, reagents, equipment and cell lines. In addition, I would also like to thank Dr. Jeffery Brodsky, Dr. Jeffery Hildebrand, Dr. Lewis Jacobson, Dr. Valerie Oke, and Dr. Fumihiko Nakamura (Harvard) for sharing their equipments and reagents. I have special thanks

to Dr. Eric Polinko and Hernan Brizuela for numerous help with solving computer and software problems.

About the Saunders lab, I would like to say that I feel very lucky to be a part of this lab, as we are just like one big family. We have discussed scientific ideas, helped each other through experiments, written and edited our manuscripts and enjoyed our time in and out of the lab. Ruta Sahasrabudhe and previous lab member Dr. Qian Wu, I thank you for being my great friends and for all of the happy times we have spent together. Jennifer Glasser, you are always helpful, I thank you for maintaining the lab. Most importantly, I would like to thank ***Kristen Bartoli***, you will be my forever sister. I cannot find enough words to thank you for everything, yes, I mean everything. I would also take this chance to thank the Bartoli family, who are extremely nice and are just like my extended family in the US. ☺

I would also like to thank the entire Biological Sciences department, for being a great and supportive work environment. I particularly would like to thank Brodsky's lab, Kiselyov's lab, and Hendrix's lab for the great times we shared. I want to thank Cathy Barr, Crystal Petrone, Pat Dean, and Hillary for all of the heart-warming conversations, encouragement and help throughout my graduate school years. I also would like to thank Tom Harper for his help in confocal microscope and for taking care of the auto-processor for Western blotting.

I would like to take this chance to thank Dr. Valerie Oke, Dr. Susan Godfrey, Dr. Lydia Daniels, Dr. Richard Sherwin, and Carol LaFave for all your help during my teaching, I learned a lot from all of you and appreciate all your suggestions.

I dedicate this work to my beloved family. My mom, you have waited for such a long time to see this, I owe you everything. My husband, my daughter May, my parents-in-law, my sister-in-law and my brother-in-law, I thank you all for all of your support. Especially, I would

like to thank my parents-in-law for taking care of my daughter in the past four years so that I could completely focus on my research. I cannot express all into words my gratitude to my family, as I would not have been able to accomplish what I have achieved without any of you. I love you all.

1.0 CHAPTER I. INTRODUCTION

1.1 MICROTUBULES

Microtubules (MTs), actin filaments, and intermediate filaments are the three major types of the cytoskeletal filaments in mammalian cells. MTs originate from the microtubule organizing center (MTOC) in the cytoplasm of cells (Vorobjev and Nadezhdina, 1987), and participate in a variety of essential cellular activities, such as providing roadways for the intracellular transportation and the localization of mRNAs (Hirokawa, 2006) and membrane-bound organelles (Apodaca, 2001), and function in mitosis (Inoue and Ritter, 1975).

Actin filaments, on the other hand, are the bases for structures associated with cellular morphology and motility, such as stress fibers, filopodia, microvilli, and lamellipodia, just to name a few (DeRosier and Tilney, 2000; Hotulainen and Lappalainen, 2006; Medalia et al., 2007; Small, 1994). Moreover, actin filaments also play important roles in completion of cytokinesis, which will be discussed in the "CYTOKINESIS" section of this chapter. Intermediate filaments are beyond the scope of my research, and therefore will not be discussed.

1.1.1 Structural components and general assembly of MTs

MTs are composed of α and β-tubulins, which are both globular proteins with molecular weights of approximately 55 kilodaltons. The α and β-tubulins form heterodimers through noncovalent bonds, and assemble together in an alternating order to form linear protofilaments; 13 parallel protofilaments then associate with one another to form a MT, which is a long and hollow cylinder with an outer diameter of 25 nm (Evans et al., 1985). Generally speaking, MTs are more rigid than actin filaments, but not as strong as intermediate filaments.

Both α and β-tubulins contain nucleotide binding sites; however, only β-tubulin can hydrolyze guanosine 5'-triphosphate (GTP) into guanosine diphosphate (GDP), which is known to influence polymer stability (Spiegelman et al., 1977; Weisenberg et al., 1976). When a MT is polymerizing, the GTP-bound α/β tubulin heterodimers are added to one end of this MT, while the tubulin dimers internal to this MT polymer hydrolyze GTP to GDP (David-Pfeuty et al., 1977; MacNeal and Purich, 1978). Hence, there are usually GTP molecules bound to the polymerizing end of a MT, referred to as the "GTP cap" (Carlier, 1982; Mitchison and Kirschner, 1984). MTs can also depolymerize, characterized by the disassociation of tubulin subunits from the end of a shrinking MT (Figure 1). It is thought that the loss of the GTP cap results in rapid depolymerization, while the regaining of the GTP cap results in rescue by favoring polymerization (Carlier and Pantaloni, 1978; Carlier and Pantaloni, 1981).

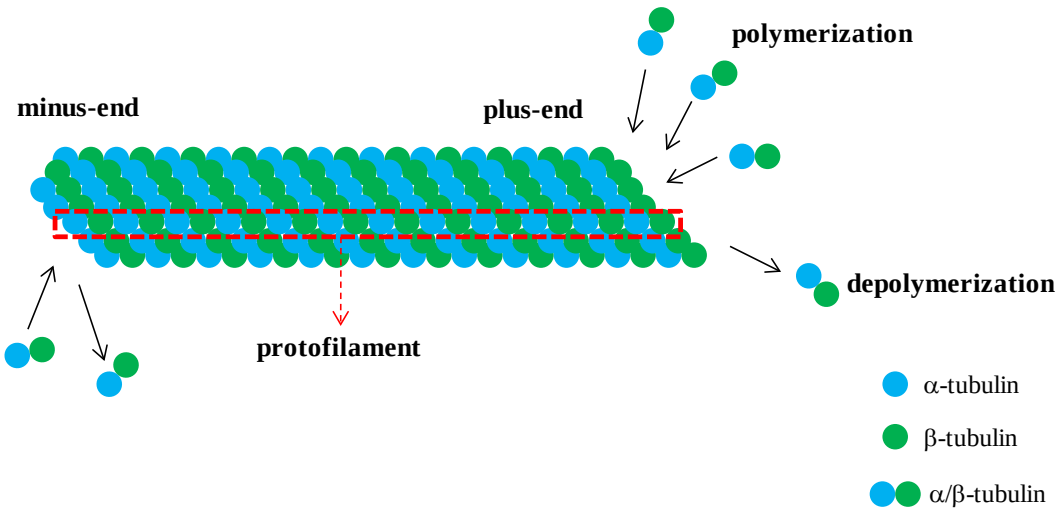

Figure 1 MT structure and dynamic features.

MTs are built with protofilaments, which are composed of α/β tubulin dimers. Polymerization and depolymerization at the ends of MTs are the basis of their dynamic features, allowing them to grow and shrink for rapidly reorganization.

1.1.2 Structures of the MTs in mammalian cells

MTs are polymer structures with polarities, and the plus-end is defined as the end of MTs where β-tubulins are exposed (Allen and Borisy, 1974). In mammalian cells, the plus-ends of MTs are oriented towards the cell boundary, where the growth and shrinkage primarily occur, while their minus-ends are anchored at the MTOC, also known as the centrosome, where MTs nucleate (Dammermann et al., 2003). These MTs form an astral network in interphase cells, but this organization is changed during mitosis.

The centrosome is localized next to the nucleus in mammalian cells, and is composed of a pair of orthogonally positioned centrioles, which are surrounded by the pericentriolar material (PCM). Centrioles, the cylindrical structures with a diameter of 100-200 nm and a length of 100-400 nm, consist of nine short MT triplets (Lange and Gull, 1996; Marshall, 2001), while PCMs

contain γ-tubulin ring complexes, which are thought to serve as the templates to nucleate MTs (Moritz et al., 2000).

During mitosis, MTs are completely re-organized. In an early phase of mitosis, the original and newly-duplicated centrosomes move towards the opposing sides of cells to form two poles; the MTs nucleate from these two poles and spread out in an astral array accordingly. Over time, these MTs orient into highly organized mitotic spindles, and facilitate mitotic and cytokinesis progression.

1.1.3 The dynamic features of MTs

MT polymers are usually very dynamic, due to the fact that polymerization and depolymerization can occur at the same time, but at the different ends of a MT polymer, which is termed "treadmilling". Alternatively, polymerization and depolymerization can occur at the same end of a MT polymer, but at different times, which is referred to as "dynamic instability" (Hotani and Miyamoto, 1990).

1.1.3.1 Dynamic instability

The most important feature for MTs is their dynamic instability, which describes the phenotype when the end of a filament grows for a certain period of time, then undergoes a sudden shrinkage; some time later after a "pause", this end can begin to grow again (Shelden and Wadsworth, 1993; Walker et al., 1988). In mammalian cells, this switch between the growing and shrinking states of MTs can occur several times per minute.

Dynamic instability is essential for cells because it allows for the rapid re-organization of MTs, ensuring that their functions are achieved efficiently and effectively. Some examples that

require MT dynamic instability are mitotic cells, which will be discussed in the section of "CELL CYCLE" of this chapter, as well as neurons that grow towards their targets in response to their environmental clues (Sabry et al., 1991).

The dynamics of MTs can be influenced by MT-associating proteins (MAPs), most of which bind to tubulin subunits and stabilize MTs against disassembly (Maccioni and Cambiazo, 1995; Wu et al., 2008). In addition, MT motors, proteins that 'walk' along MTs by hydrolyzing ATP, can also affect the dynamics of MTs. One such example is during cell division, wherein a family of MT motors depolymerizes MTs to control the length of mitotic spindles, therefore contributing to the regulation of mitotic progression (Varga et al., 2009). Besides the MAPs and motors, certain small molecule inhibitors can also interfere with MT dynamics by depolymerizing MTs or hyper-stabilizing MTs, as discussed below.

1.1.4 Small molecule inhibitors of MTs

1.1.4.1 MT disruptors

There are many types of MT disruptors, including vinca alkaloids, nocodazole, and colchicine. An example of the vinca alkaloids is vinblastine, which was originally identified from the *Vinca rosea* plants, and it has now been synthetically produced and widely used in clinics. Vinblastine binds to β-tubulin at the vinca-binding site near the exchangeable GTP binding site (Chaudhuri et al., 1998; Himes et al., 1976). The major effect of vinblastine and other vinca alkaloids is to cause MT depolymerization and suppress MT dynamics.

A second example of MT disruptors is colchicine, originally identified from the *Colchicum* plants. It has been shown that colchicine binds to β-tubulin at the intradimer interface with α-tubulin, which is different from the vinca-binding site. Colchicine weakens the

lateral interactions between tubulins, and therefore inhibits the polymerization at low concentrations and promotes the depolymerization at high concentrations (Ravelli et al., 2004).

Nocodazole is another classical MT disruptor that is widely used in research. It has been reported that the binding site for nocodazole overlaps with the colchicine-binding site on β-tubulins (Lin and Hamel, 1981). The cellular responses to nocodazole have also been extensively studied, some of which will be mentioned in Chapter II.

1.1.4.2 MT stabilizers

Taxol or paclitaxel, a natural product identified from the *Taxus brevifolia* plant, is a classical example of a MT stabilizer. Taxol has been reported to bind to β-tubulin with a 1:1 stoichiometry in a deep hydrophobic cleft near the surface, which is distinct from the colchicine- and vinca-binding sites. Taxol can modify the structures of MTs to hyper-stabilize them, therefore inhibiting MT dynamics. At high concentrations, taxol can increase the polymer mass by favoring the addition of the tubulin subunits and inhibiting their disassociation from MTs (Arnal and Wade, 1995; Lowe et al., 2001; Parness and Horwitz, 1981; Snyder et al., 2001).

Another type of MT stabilizer is epothilone B, originally found in metabolites from *Sorangium cellulosum* myxobacterium. Epothilone B also binds to the tubulin dimer with a 1:1 ratio and hyper-stabilizes MTs. Although there is no obvious homology between the structures of epothilone B and taxol, epothilone B competes for the taxol binding site, with kinetics similar to taxol itself, indicating that epothilone B possibly has a similar binding site and/or utilizes a similar mechanism of action as taxol to hyper-stabilize MTs (Bollag et al., 1995).

1.2 CELL CYCLE.

A typical growth-division cycle of eukaryotic cells contains four phases: 1) the first gap phase (G1 phase), 2) the DNA synthesis phase (S phase), 3) the second gap phase (G2 phase) and 4) mitosis (M phase), among which the first three phases are part of interphase (Figure 2). There is another optional phase, called G0, of which terminally-differentiated or quiescent cells are found that are considered to have dropped out from the regular cell cycle and need specific stimuli to re-enter it. In mammals, the active cycles of growth and division are most common during development and tissue regeneration, while the majority of cells in the developed adult mammals are differentiated and no longer dividing.

1.2.1 General regulation of cell cycle

Cell cycle progression is controlled by cyclin-dependent kinases (cdks) that are in turn regulated by cyclin association, phosphorylation/dephosphorylation, and association of inhibitor proteins (CKIs). Levels of cyclins vary at different phases in the cell cycle (Figure 2), and cdks are serine/threonine kinases that can be activated by their specific cyclins, and phosphorylate various protein substrates either to activate or inactive them for cell cycle progression. One such example is cyclin D. Cyclin D can activate cdk4 and cdk6 by forming complexes with them, which hyperphosphorylate Rb proteins to inhibit Rb's interaction with the E2F transcription factor, thereby allowing E2F to transcribe proteins needed for cell proliferation during G1 phase (Johnson, 1995; Khleif et al., 1996).

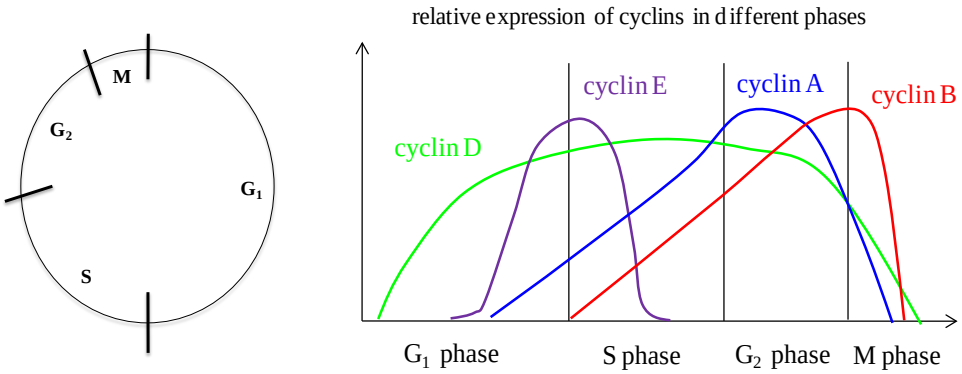

Figure 2 Cell cycle and cyclins.

The cell cycle is typically divided into G1, S, G2 and M phases, and cyclin levels fluctuate during the cell cycle.

Besides cyclins, phosphatases can also activate cdks by dephosphorylating inhibitory sites, therefore promoting the cell cycle. For example, in the G1 phase, cdc25A facilitates the activation of cdk2 through dephosphorylating Tyr15 and Thr14 residues on cdk2, which contributes to the hyperphosphorylation of Rb proteins and results in cell cycle progression into S phase (Gu et al., 1992).

The cdks' activities can be negatively regulated by cyclin kinase inhibitors (CKIs). One such example is p21, a critical downstream target of the well-known tumor suppressor protein p53 (Dulic et al., 1994; el-Deiry et al., 1994). p21 can be up-regulated in response to cell-cell contact, serum starvation or senescence (Dotto, 2000). It causes cell cycle arrest through several mechanisms, one of which is to bind to cdk2 and inhibit its function in promoting cellular proliferation (Morisaki et al., 1999). Other examples of CKIs also include p15, p16, p18, p19, p27, p57, just to name a few (Donjerkovic and Scott, 2000).

My research has been focused on the regulation and execution of mitosis and cytokinesis in cancer and noncancer cells. Therefore, the details of mitosis progression will be discussed

below. Cytokinesis will be introduced in a separate section following this "CELL CYCLE" section.

1.2.2 G2/M transition

The G2/M transition requires the activation of a maturation promoting factor (MPF), consisting of cyclin B and cdk1 (Nurse, 1990). Thr14 and Tyr15 residues on cdk1 are phosphorylated, which keeps the MPF inactive, at approximately the same time when cyclin B expression begins during G2 phase (Atherton-Fessler et al., 1993; Mueller et al., 1995; Norbury et al., 1991). As the cell cycle progresses, cyclin B continues to accumulate, and cdc25 phosphatases dephosphorylate cdk1 at these Thr14 and Tyr15 residues to activate cdk1, which will promote the G2/M transition (Berry and Gould, 1996; Nilsson and Hoffmann, 2000).

1.2.3 Mitosis

Once cells enter mitosis, a series of events occur, including mitotic spindle assembly, chromosome alignment, chromosome segregation, and final partitioning of the cytoplasm including all cytoplasmic organelles by cytokinesis. All of these events are tightly regulated and monitored by checkpoints to ensure the high fidelity of cell division. There are multiple major steps in mitosis: prophase, prometaphase, metaphase, anaphase, and telophase (cytokinesis), which will be introduced separately below.

1.2.3.1 Prophase/prometaphase

During prophase or prometaphase, chromatin is condensed by the condensin complexes to prepare for the stable attachment to mitotic spindles in a later stage of mitosis (Losada, 2007). The two sister chromatids join together at special regions called centromeres and are held by the ring-like structures known as cohesins (Nasmyth, 2005; Uhlmann, 2004). Each of the sister chromatids assemble a kinetochore, a disc-shaped protein structure, at the centromere region of the chromosomes (Brinkley and Stubblefield, 1966; Rieder, 1982; Ris and Witt, 1981).

Centrosomes, which begin to duplicate at the G1/S transition and complete a single round of duplication prior to the onset of mitosis (Tsou and Stearns, 2006), begin to separate towards opposing sides of the cell during prophase, utilizing forces generated and modulated by MT motor proteins (Roof et al., 1992; Sawin et al., 1992; Tanenbaum et al., 2008). This organization of centrosomes in dividing cells allows chromosomes to be retained between the two centrosomes after nuclear envelope breakdown (NEB).

1.2.3.2 Prometaphase/metaphase

In prophase, the nuclear envelope begins to be broken into fragments, and by prometaphase the fragments become totally disassembled, allowing the kinetochores on each sister chromatid to be accessible (Georgatos et al., 1997; Salina et al., 2002). Meanwhile, the highly dynamic MTs that emanate from the two separated centrosomes begin “search and capture”, which describes when the plus-ends of the MTs dynamically grow and shrink, until they are in contact with the kinetochores on chromosomes and become more stable (Kirschner and Mitchison, 1986).

The purpose of MT “search and capture” during prometaphase/metaphase is to establish the bi-oriented attachment for each chromosome, which is the most stable form of the MT-

kinetochore attachments. During this process, inaccurate attachments may also occur, including 1) monotelic attachment, where one sister chromatid is attached to MTs from one pole while the other sister chromatid is not attached (Figure 3A), 2) syntelic attachment, where both sister chromatids are attached to MTs from the same pole (Figure 3B), or 3) merotelic attachments, where one sister chromatid is attached to MTs from both poles (Figure 3C). These mismatches are not stable, and most of them are corrected before the onset of anaphase. The monotelic and syntelic attachments can be monitored by spindle assembly checkpoint (SAC), which will be discussed later in this section, while the merotelic attachment is detected in an Aurora B-dependent manner.

It has been demonstrated that Aurora B and its partners play critical roles in monitoring and correcting merotelic attachments by phosphorylating their substrates at the kinetochores and promoting turnover of incorrectly-attached kinetochore MTs. The chromosomes with the merotelic attachment appear to be tilted to the metaphase plate at a certain angle, suggesting that MTs from the erroneous spindle pole may be pulled closer to the inner centromere where Aurora B is highly accumulated (Cimini et al., 2003; Cimini et al., 2006). With the help of sensor proteins at the inner centromere, Aurora B phosphorylates the kinetochore protein Hec1, thus promoting the detachment of the incorrectly-attached MTs from the kinetochore (DeLuca et al., 2006). Furthermore, the MT motor protein MCAK, another substrate of Aurora B, is also found at the centromere of the merotelic chromosomes. MCAK increases the depolymerization rate of the detached MTs from the incorrect spindle pole, therefore opening more binding sites on the kinetochore for MTs from the correct pole (Knowlton et al., 2006; Ohi et al., 2003).

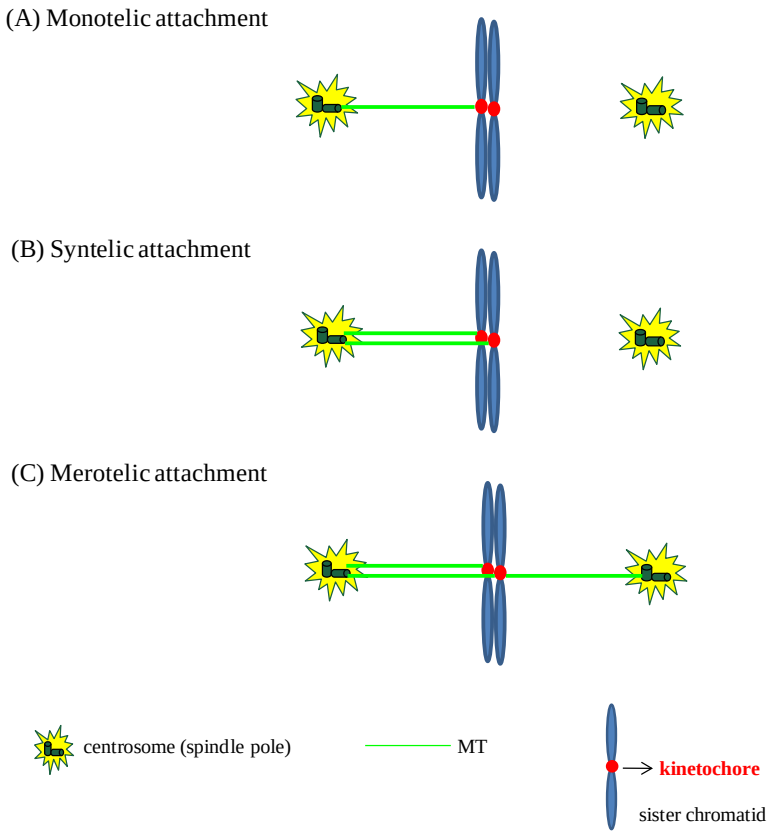

Figure 3 Abnormal MT-kinetochore attachments.

(A) Monotelic attachment. Only one of the two kinetochores in a pair of sister chromatids is attached to MTs from one spindle pole. (B) Syntelic attachment. Both kinetorchores in a pair of sister chromatids are attached to MTs from the same spindle pole. (C) Merotelic attachement. One kinetochore is attached to MTs from two spindle poles.

At the end of prometaphase or during metaphase, the bi-oriented chromosomes congress and align on the metaphase plate, a center plate with equivalent distances from both spindle poles in the cell. This is mediated by MTs and their motor proteins (Foley and Kapoor, 2009).

1.2.3.3 Metaphase/anaphase

Prior to segregation in anaphase, all chromosomes need to be correctly attached to MTs from both spindle poles; even when there is only one chromosome that is not properly attached

to MTs, the cell will not execute anaphase. This is regulated by the SAC, which was first observed as a checkpoint in response to impaired spindle assembly during mitosis, but later found to monitor interactions between kinetochores and MT spindles rather than the spindle assembly itself (Hardwick et al., 1999; Hoyt et al., 1991; Musacchio and Hardwick, 2002; Taylor et al., 2004).

The most critical regulator for the onset of anaphase is the anaphase-promoting complex/cyclosome (APC/C), a large multiprotein E3 ubiquitin ligase that requires association with cdc20 to exert its mitotic function (Hwang et al., 1998; Morgan, 1999). When there are unattached kinetochores in metaphase, however, three SAC proteins, MAD2, BUBR1/MAD3, and BUB3, form a mitotic checkpoint complex (MCC) that concentrates at the free kinetochores in a MT motor-dependent manner and bind to cdc20. This binding prevents the cdc20-dependent APC/C activation, therefore inhibiting the onset of anaphase (Fang et al., 1998; Hardwick et al., 2000; Shannon et al., 2002; Sudakin et al., 2001; Wu et al., 2000).

As mitosis progresses, SAC proteins including MAD1 and MAD2 begin to disassociate from the kinetochores after MT attachment, freeing cdc20 and allowing APC/C activation (Hoffman et al., 2001; Howell et al., 2001; King et al., 2000; Maiato et al., 2004). These activated APC/C complexes can in turn ubiquitinate several protein substrates, leading to their degradation (Glotzer et al., 1991; Pfleger and Kirschner, 2000; Sudakin et al., 1995). Among all such substrates, securin and cyclin B are the most important ones for mitotic progression, due to the reason below.

The key event in anaphase is sister chromatid segregation; however, prior to anaphase onset, sister chromatid pairs are held tightly together by cohesions (Darwiche et al., 1999; Uhlmann et al., 1999). An enzyme called separase is responsible for cohesin cleavage. When it

is bound to cyclin B or securin (before satisfying the SAC), however, separase cannot exert its catalytic activities (Holland and Taylor, 2006; Holloway et al., 1993; Wirth et al., 2006; Zou et al., 1999). Therefore, not until the APC/C-dependent degradation of cyclin B and securin occurs is separase able to cleave cohesin and free the chromatids for their poleward movements needed for mitotic progression.

In summary, the SAC is constantly active in metaphase when there are unattached kinetochores present. When all kinetochores are attached to MTs from the proper spindle poles, the SAC is satisfied and anaphase is initiated by the activation of APC/C complexes. Chromosomes then segregate towards opposite poles, followed by spindle elongation and the movement of centrosomes away from each other.

MTs during metaphase are very dynamic in order to meet the need of the "search and capture" model; however, in anaphase, the MTs need to be stable, in order to provide the structural bases for chromosome segregation (Mallavarapu et al., 1999). Phosphatase cdc14, which is activated by separase, has been demonstrated to reduce MT dynamics by promoting the localization of MT-stabilizing proteins, therefore facilitating the poleward movements of sister chromatids (Higuchi and Uhlmann, 2005; Khmelinskii et al., 2007; Stegmeier et al., 2002).

1.2.3.4 Telophase

Telophase is the last step in mitosis, which is when chromosomes begin to decondense at the two poles and the nuclear envelopes begin to form around them utilizing the nuclear envelope fragments from the mother cell (Hernandez-Verdun and Gautier, 1994). Simultaneously, cytokinesis occurs to partition the mother cell cytoplasm into two daughter cells, which will be discussed in the next section of this chapter. The entire cell cycle is now

completed, and these daughter cells may start another round of the cell cycle in response to proper intrinsic or extrinsic cues.

1.3 CYTOKINESIS.

Cytokinesis is the final step of cell division, when one mother cell is split into two daughter cells by equal partition of cytoplasmic materials. This process is mediated by multiple cellular events, including formation of the cleavage furrow (CF) at the center of the dividing cell, formation of the contractile ring that produces forces needed for the CF ingression, and membrane trafficking events that deposit the new membrane materials at the interface between the two daughter cells.

The central spindles, comprising bundles of anti-parallel and overlapping MTs, have been reported to play vital roles in regulation of CF formation and ingression. As cytokinesis progresses, the central spindles become thinner and thinner, later developing into a compact structure termed the “midbody” near which the final abscission occurs, physically separating the mother cell into two daughter cells (Glotzer, 2004; Mastronarde et al., 1993).

1.3.1 CF formation

There are three models that have been proposed to explain how the CF forms during cytokinesis (Figure 4). The first model is the astral stimulation model (Figure 4A). In this model, astral MTs, which are non-central-spindle MTs that radiate from spindle poles, are thought to contain stimuli that trigger the CF formation during cytokinesis (Rappaport, 1961). The equatorial cortex that is in the center of a dividing cell is influenced by the astral MTs from both of the

spindle poles; therefore, the equatorial cortex contains the most signals to stimulate the formation of the CF. This model is supported by the classical torus experiment, where two spindles in one cytoplasm are sufficient to induce the formation of an additional CF in the absence of chromosomes (Rappaport, 1961; Rappaport, 1985).

The second model is the astral relaxation model (Figure 4B), in which the astral MTs are hypothesized to cause a reduction in cortical contractility (White, 2005). In this model, the cell cortex around the pole regions is thought to have a higher astral MT density than the equatorial cortex, thus containing more relaxation signals, and is less contractile than the equatorial area (Wolpert, 1960). This leads to the CF formation at the equatorial area. This astral relaxation model is opposite to the astral stimuli model, because the underlying assumptions for the distributions and densities of astral MTs in the dividing cells are different.

More recently, the third model: the central spindle model, seems to be more likely (Figure 4C). It is possible that the central spindles, which position at the center of the dividing cell, send certain signals to trigger the formation of the CF (Giansanti et al., 2001). This model is consistent with the report where the CF fails to form in cells that lack central spindles but maintain normal appearances of astral MTs (Adams et al., 1998; Somma et al., 2002). This central spindle model is challenged by other experiments, however, where cells depleted of key components of the central spindle regulators can still form CFs in *C. elegans* embryos, although these cells cannot complete cytokinesis (Jantsch-Plunger et al., 2000; Powers et al., 1998; Raich et al., 1998). Therefore, it is plausible that dividing cells utilize both the astral MT-dependent and the central spindle-dependent mechanisms to form the CF.

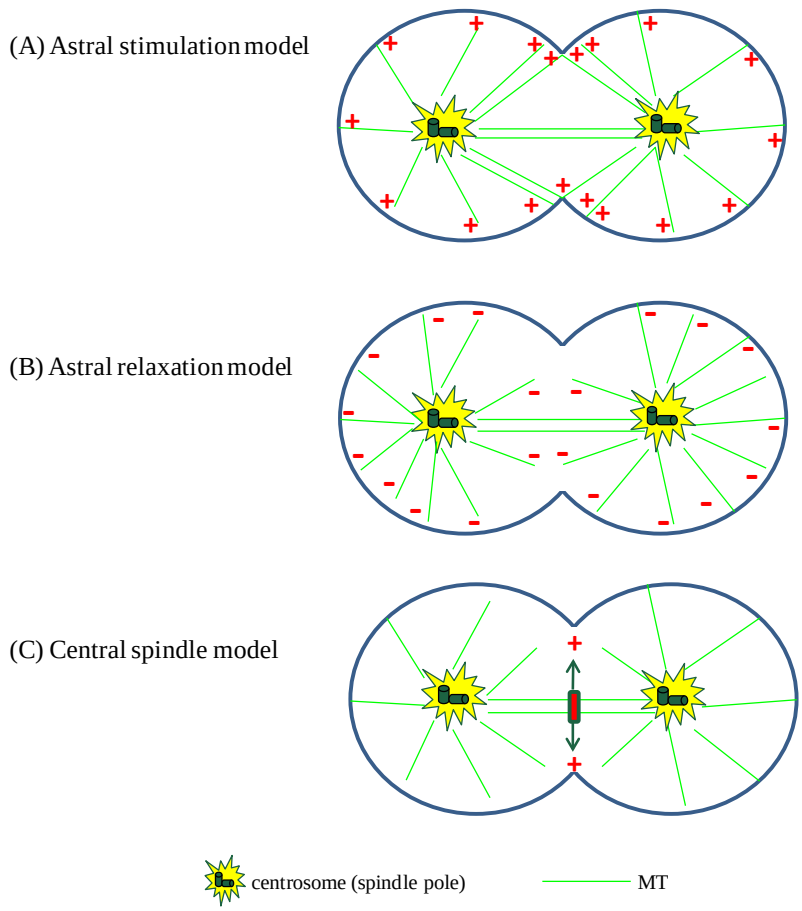

Figure 4 Models for CF formation.

(A) Astral stimulation model. MTs are hypothesized to positive signals ("+") that can trigger CF formation. The center part of the cell membrane is hypothesized to contain the highest density of MTs, as MTs from both spindle poles meet there, and CF formation can be initiated at the center part of cell membrane. (B) Astral relaxation model. MTs are hypothesized to contain negative signals ("-") that can reduce cortical contractility. The cell cortex around the pole regions is hypothesized to contain higher MT densities than the center part of the cell membrane, thus holding more relaxation signals allowing CF formation to initiate at the center part of the cell membrane. (C) Central spindle model. The central spindles in the center of the cell are hypothesized to signals to trigger CF formation ("+"), therefore the center part of the membrane receives the most signals to initiate the formation of CF.

Interestingly, Aurora B and its regulators, such as INCENP and survivin, have been reported to influence or induce the CF formation, although their exact roles remain unclear. Aurora B and its partners may function through regulating central spindle MTs to control the CF formation (Adams et al., 2000; Bolton et al., 2002; Cheeseman et al., 2002; Honda et al., 2003; Kaitna et al., 2000; Romano et al., 2003). Additionally, Aurora B has been recently reported to generate a "spatial phosphorylation gradient" at the center of the central spindles, through targeting to a subset of the MTs that activate Aurora B (Fuller et al., 2008). This creates a positive feedback loop to organize the MTs and to provide the spatial information needed for positioning the cleavage site in mammalian cells.

1.3.2 Contractile ring formation and contraction

The contractile ring is composed of F-actin and its motor protein myosin II, which generates the contractile forces for CF ingression. It has been suggested that central spindle formation may be required for contractile ring assembly, as the contractile ring does not form in *Drosophila* cells containing defective central spindles, consistent with its role in CF formation (Giansanti et al., 1998; Williams et al., 1995). Below I will introduce some general information on F-actin and myosin II first, followed by the possible mechanisms of contractile ring contraction during cytokinesis.

1.3.2.1 F-actin

As introduced in the first section, actin filaments (F-actin) are one type of the cytoskeletal structures that play critical roles in various cellular activities. These activities include cell

motility, cell migration, muscle contraction and cytokinesis (Pollard and Berro, 2009; Pollard and Cooper, 2009).

The structures of F-actin

G-actin (global actin) and F-actin (filamentous actin) are the two major forms of actins in the cell. F-actin is the polymer structure consisting of the G-actin subunits, which can polymerize or depolymerize at different ends to rapidly change its configuration and location (Wanger et al., 1985; Wanger and Wegner, 1985).

Small molecule inhibitors of F-actin

There are several groups of small molecules that can alter F-actin polymer structures. One such example is the phalloidins, which bind along the sides of the F-actin and stabilize the F-actin structure. Cytochalisins, on the other hand, bind to the plus-ends of the F-actin, and prevent the new subunits from adding to the existing F-actin (Cooper, 1987). These two molecules are frequently used in research. For example, the fluoro-labeled phalloidins can be used to visualize F-actin in fixed cells (Wulf et al., 1979), and the cytochalasins are used to depolymerize F-actin networks in cells.

The actin nucleation proteins

The key molecule to nucleate unbranched actin filaments is formin, which is associated with the fast-growing ends of the F-actin, the plus-ends (Goode and Eck, 2007). Formins are suggested to remain bound to the plus-end when new actin monomers are added to the same end, thereby preventing the binding of the other plus end-associated proteins which can potentially destabilize F-actin (Kovar and Pollard, 2004; Watanabe and Higashida, 2004). It has been demonstrated that formin can be activated by the GTPase RhoA, which turns off the auto-

inhibition mechanism of formin, therefore allowing polymerization of F-actin (Li and Higgs, 2005; Otomo et al., 2005; Wallar et al., 2006).

The actin cross-linking proteins

Besides nucleating proteins like formin, there are other molecules that affect the organizations and structures of F-actin. These include the proteins that organize actin filaments into the parallel bundles, such as α-actinin and villin (George et al., 2007; Pelletier et al., 2003), and the proteins that crosslink actin filaments into a gel-like network, such as filamin (Weihing, 1985).

There are three types of filamins identified in human cells, including the most abundant and widely distributed filamin A, the less broadly expressed filamin B, and the filamin C that is predominantly expressed in the muscle tissues (Stossel et al., 2001). Filamin A has been shown to cross-link actin filaments most potently; for example, even one filamin A dimer per actin is sufficient to induce actin gelation by facilitating the pointed ends of the actin filaments to intersect with the sides of other actin filaments (Brotschi et al., 1978). It has been demonstrated that *in vivo* filamin A is a dimer with two large polypeptides joined together at their C-terminus, and interacts with the F-actin through its actin-binding-domain located on its N-terminus (Weihing, 1985). In addition, at least 20 other binding partners of filamin A have been identified, most of which bind to the C-terminus of filamin A.

It is therefore not surprising that filamin A may be involved in various cellular events because of the diversity of its binding partners. For example, filamin A directly associates with β-integrin, which mediates the interactions between an adhesion cell and its extracellular matrix (ECM), and functions in related signaling and adhesion pathways (Calderwood et al., 2000; MacPherson and Fagerholm; Pfaff et al., 1998). In addition, filamin A can also bind to some

Rho family GTPases and their regulators and effectors, including RhoA, Rac, cdc42, a Rho kinase ROCK, and a guanine nucleotide exchange factor (GEF) Trio, suggesting possible roles for filamin A in the GTPase-related signaling pathways (Bellanger et al., 2000; Ohta et al., 1999; Pi et al., 2002; Ueda et al., 2003).

1.3.2.2 Myosin II, a major actin motor protein

Myosins are a superfamily of the F-actin motors that utilize ATP to generate power for movements of cargoes. More than 15 classes of myosins have been identified (Sellers, 2000), but I will only focus on the most relevant one to my research, myosin II, which was initially investigated to elucidate the muscle contraction mechanism, and was later found to also function in non-muscle cells.

The structure of myosin II

Before assembly of the contractile structure, myosin II is a dimer, consisting of two heavy chains and four associated light chains. The heavy chain is further divided into three domains: the globular head domain that associates with the F-actin and contains an ATPase as the motor domain, the neck domain that allows the interaction with the myosin light chain and provides a level arm to transduce the force generated by the motor domain, and lastly the tail domain that homodimerizes to form an α-helix coiled tail and interacts with cargoes (Hodge et al., 1992; Kelley et al., 1992; Maeda et al., 1991). There are two types of myosin light chains per heavy chain, one is the myosin essential light chain (MELC) and the other is the myosin regulatory light chain (MRLC), which wrap around the neck domain of the myosin heavy chain (Harrington and Rodgers, 1984).

The activities of myosin II rely largely on the phosphorylation status of the MRLC. For example, the monophosphorylation of the MRLC at Ser19 is reported to increase the stability of myosin II and to allow the interaction with F-actin, while the diphosphorylation of MRLC at both Ser19 and Thr18 can further stabilize myosin II, promoting its activities more efficiently than monophosphorylation (Ikebe and Hartshorne, 1985a; Ikebe and Hartshorne, 1985b; Ikebe et al., 1986).

The regulation of myosin II

As the activities of myosin II predominantly depend on the phosphorylation of the MRLC, the kinases and phosphatases for MRLC are therefore the most important regulators for myosin II. Many proteins are known to phosphorylate the MRLC *in vitro* and some *in vivo*, including the myosin light chain kinase (MLCK), the Rho kinase (ROCK), citron kinase, Aurora B, p21-activated kinase (PAK) and integrin-linked kinase (ILK) (Amano et al., 1996; Goeckeler et al., 2000; Matsumura et al., 2001; Muranyi et al., 2002; Yamashiro et al., 2003; Yokoyama et al., 2005), although only the first four kinases have been reported to be the relevant candidates for myosin II regulation during cytokinesis in cells, as described below (Chew et al., 2002; Eda et al., 2001; Kosako et al., 1999; Madaule et al., 1998; Poperechnaya et al., 2000; Yokoyama et al., 2005).

MLCK is found to localize at the CF and becomes activated before the ingression of the CF during cytokinesis (Poperechnaya et al., 2000). It is thought that Aurora B may phosphorylate MLCK in cells to inhibit the activity of MLCK, as it does *in vitro* (Dulyaninova and Bresnick, 2004). It is also suggested that Aurora B can directly influence the activities of myosin II by phosphorylating the Ser19 residue (Murata-Hori et al. 2002), therefore suggesting a possible crosstalk between central spindles and the contractile ring. ROCK, another MRLC

kinase, is also believed to play important roles in CF formation and ingression by the contractile ring, as inhibition of ROCK delays furrow ingression (Kosako et al., 2000). Citron kinase, another Rho effector, is localized at the CF in the mammalian cells (Eda et al., 2001). Overexpression of a constitutively active citron mutant is reported to result in abnormal contraction of the cortex, leading to cytokinesis failure (Madaule et al., 1998).

1.3.3 Models of contractile ring contraction

As introduced earlier, the contractile ring assembles at the CF during cytokinesis, which is primarily composed of actin filaments, myosin II and their regulators. The contractile ring is responsible for generating the forces needed for the CF ingression.

It is reported that the actin proteins found in the contractile ring during cytokinesis are predominately from the reorganization of the existing actin network, rather than the newly synthesized actin molecules (Cao and Wang, 1990), although the detailed mechanism of how the contractile ring contracts remains unknown. There are three models that try to explain the mechanism, which are summarized below (Figure 5).

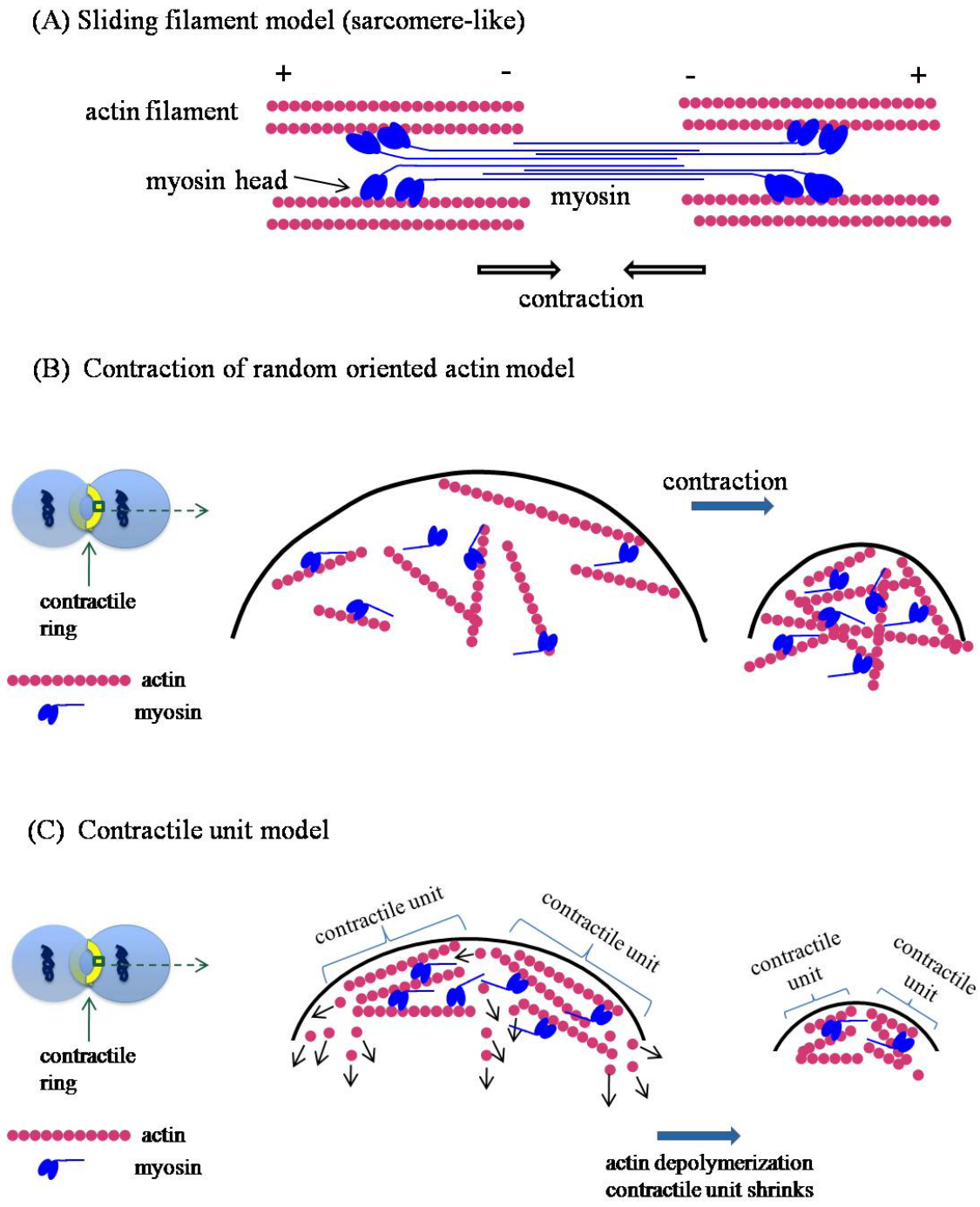

Figure 5 Models for actin arrangement in the contractile ring and contractile force generation during CF ingression.

(A) Sliding filament model (sarcomere-like). Actin and myosin in contractile rings are hypothesized to organize and generate forces in a manner similar to sarcomeres of muscle cells. Actin filaments arrange into bundles while myosin are attached to the actin bundles. When myosin move towards the plus-ends of

actin filaments, the two sets of actin bundles are brought closer together, resulting in contraction. (B) Contraction of random oriented actin model. Actin filaments in contractile rings are hypothesized to display an irregular orientation. Myosin exerts forces using these randomly-oriented actin filaments, resulting in contraction. (C) Contractile unit model. Similar to the sliding filament model in that actin filament and myosin motors arrange into individual "contractile units" along the contractile ring, however within each unit, the organization of actin does not have to be anti-parallel. Depolymerization of actin is hypothesized to be the major cause of the 'shrinkage' of each contractile unit, therefore leading to the contraction of the whole ring.

The first model, which is the most classical model, is based on the specific organization of actin-myosin in the muscles, termed the sarcomeres (Figure 5A). It is thought that in the contractile ring during cytokinesis the F-actin and myosin II organize into sarcomere-like arrays and generate forces similar to the "sliding filament" theory, which describes how the myosin II molecules slide along the actin filaments in the sarcomeres during the muscle contraction (Schroeder, 1975). This model is reasonable, as the electron microscopy (EM) examinations of dividing cells have directly shown thin layers of the actin filaments and myosin in the contractile rings (Arnold, 1969; Kamasaki et al., 2007; Maupin and Pollard, 1986; Sanger and Sanger, 1980; Schroeder, 1968; Schroeder, 1970; Schroeder, 1972; Takiguchi, 1991; Tucker, 1971).

Besides the first model, there are two alternative models that propose the non-sarcomere-like organizations of the actin filaments in contractile rings during cytokinesis. In the second model, the actin proteins are thought to form irregularly-oriented homogenous bundles, and myosin II generates the forces utilizing these actin filaments (Figure 5B) (Kruse et al., 2001; Kruse and Julicher, 2000; Kruse and Julicher, 2003; Tanaka-Takiguchi et al., 2004). In the third model, the contractile forces are hypothesized to come from the depolymerization dynamics of the actin filaments in the contractile ring (Zumdieck et al., 2007). This model is furthered by the

concept of “contractile units”, which was proposed to explain the proportionality observed between the initial ring size and the constant constriction rate. These contractile units are shortened at a steady rate by actin depolymerization during the CF ingression (Figure 5C) (Carvalho et al., 2009).

1.3.4 Abscission

During the progression of cytokinesis, the CF continues to ingress while the contractile ring keeps contracting, until only a thin canal is left connecting the two daughter cells. This canal structure contains the midbody, providing a platform for binding of many abscission-related proteins, as more than 100 proteins have been identified at the midbody by proteomic studies, including the regulators for the MTs, the actin filaments and membrane trafficking proteins (Eggert et al., 2006; Skop et al., 2004), which all may contribute to the final abscission of the cell.

In order to execute abscission, F-actin in the contractile ring needs to disassemble. This is thought to be controlled by the inactivation of its upstream regulator RhoA, as the RhoA activating nucleotide exchange factor ECT2 was observed to gradually decrease, at the same time as cellular progression through cytokinesis (Chalamalasetty et al., 2006; Saito et al., 2004; Simon et al., 2008).

1.3.4.1 Three models of abscission

Although the exact mechanism of abscission is not fully understood, there are three models for the possible mechanisms of abscission (Figure 6). The first model is the mechanic rupture model, which describes an abrupt rupturing of the canal when the two daughter cells

migrate away from each other, exerting enough traction forces on the canal that it breaks (Figure 6A). This rupture event results in membrane holes that are hypothesized to be closed using mechanism similar to the cellular wound healing process, as is supported by the observation that the similar molecules are required for both abscission and healing of single-cell/multicellular wounds (Bement et al., 1999; Benink and Bement, 2005; Darenfed and Mandato, 2005).

The second model is based on plasma membrane constriction (Figure 6B). In this model, a spiral filament plays a key role in mediating the membrane curvature, and eventually leading to abscission (Hanson et al., 2008; Wollert et al., 2009).

The third model is a membrane deposit/fusion model where membrane-containing vesicles derived from the endocytosis and/or secretory pathways involving Golgi/ER systems, are deposited near the midbody and vesicles are fused together to separate the two daughter cells (Figure 6C), which is discussed below.

1.3.4.2 The membrane trafficking and deposit/fusion in cytokinesis

Membranes and vesicle trafficking have recently been demonstrated to be essential for completion of cytokinesis, especially in the third model proposed above, as secretory vesicles and the endocytosis vesicles are observed at abscission regions. For example, a yeast protein complex, the exocyst, that is responsible for the delivery of secretory vesicles to the plasma membrane, is observed to localize at the divisional site. Furthermore, knockdown of the exocyst is reported to cause abscission defects (Fielding et al., 2005; Gromley et al., 2005), indicating a possible role for the secretory pathways in cytokinesis.

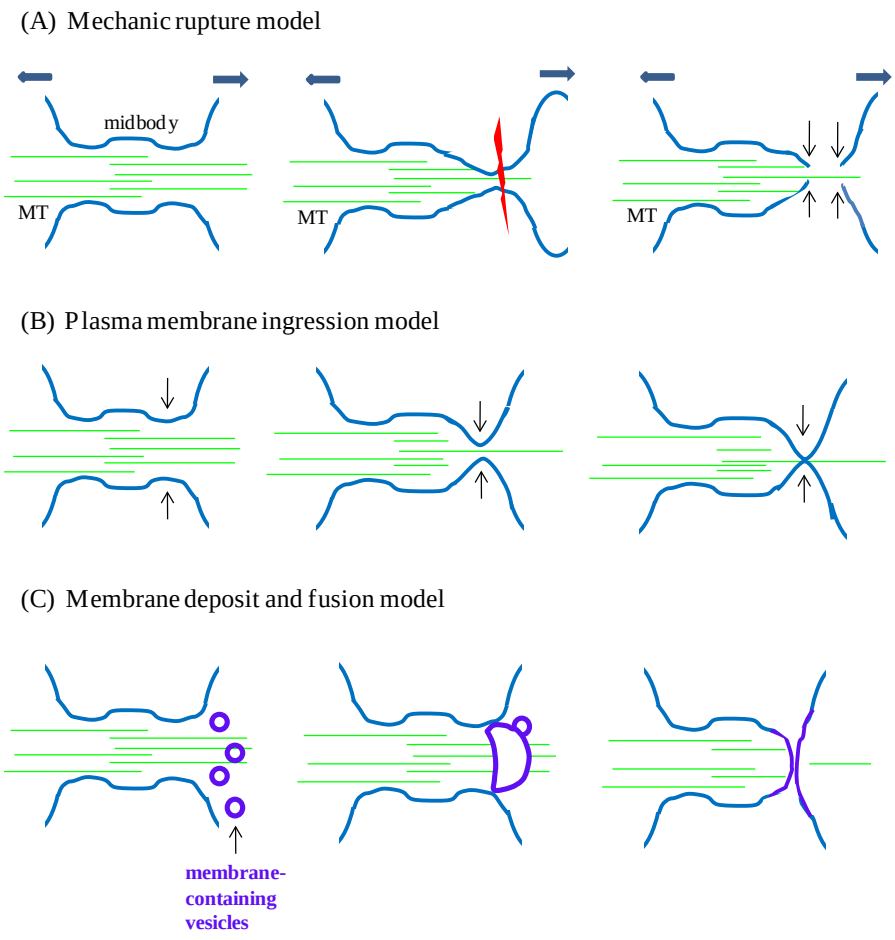

Figure 6 Models for abscission.

(A) Mechanic rupture model. At the end of cytokinesis, two daughter cells migrate away from each other, exerting forces on the "canal" between them, therefore resulting in an abrupt rupture of the canal to physically separate daughter cells. This leaves 'holes' on the membrane at the broken parts, which will be closed using mechanisms similar to the wound-healing process. (B) Plasma membrane ingression model. Both sides of the cortical membrane near the midbody bend until they meet each other, followed by membrane fusion to generate two separated daughter cells. (C) Membrane deposit and fusion model. Membrane-containing vesicles, derived from the endocytosis and/or secretory pathways involving Golgi/ER systems, are deposited near the midbody. These vesicles fuse together and separate daughter cells.

In addition to the secretory pathways, endosome recycling appears to also be involved in cytokinesis. For example, inhibition of dynamin, a protein that functions in the clathrin-coat-

dependent endocytosis, results in defects in the CF ingression during cytokinesis (Konopka et al., 2006; Thompson et al., 2002). Additionally, in *Drosophila* embryos, the F-actin and the membranes are reported to form a unit, which is recruited to the ingressing CF during cytokinesis, via the endosome-derived vesicles along the central spindles (Albertson et al., 2008), confirming a possible relationship between the membrane trafficking and the completion of cytokinesis.

1.3.5 The checkpoint during cytokinesis

Similar to the mitotic checkpoint SAC, there is a cytokinesis checkpoint used to ensure the accurate segregation of chromosomes at the last step of cell division, known as the abscission checkpoint. This checkpoint was first identified in yeast in 2006, and was named as "NoCut" pathway (Norden et al., 2006). Recently in 2009, further research has indicated an Aurora B-dependent pathway as the abscission checkpoint in mammalian cells, similar to the yeast NoCut pathway, with some minor differences (Steigemann et al., 2009).

Both of the yeast NoCut and the mammalian abscission checkpoint pathways seem to respond to the presence of the DNA that are present in the middle of the divisional site during cytokinesis, most of time in the form of anaphase DNA bridges. There are several defective events in the earlier stages of mitosis that can contribute to the anaphase DNA bridge formation, including the incomplete chromosome decatenation (Chan et al., 2007), dysfunctional telomeres (Maser and DePinho, 2002; Stewenius et al., 2005) and the dicentric chromosomes (Acilan et al., 2007), indicating the necessity and importance of this abscission checkpoint.

In the NoCut pathway, the yeast homolog of Aurora kinase Ipl1 is activated by the unsegregated chromosomes, which delays the abscission by targeting the two anillin-like

proteins to the bud neck (Norden et al., 2006). Final completion of cytokinesis is postponed, therefore allowing more time for this yeast to resolve the lagging DNA bridges at the divisional site. The physiological significance of this checkpoint is thought to be to prevent the premature cutting through the chromosomes, which may lead to the DNA damage and harm the cell (Norden et al., 2006). Further investigation revealed the key trigger for the NoCut pathway is the interaction between chromatins and Ipl1, involving Ahc1, a histone acetyltransferase component, therefore suggesting that the lagging chromatin may need to be acetylated to trigger the NoCut response by interacting with Ipl1 (Kelly et al., 2007; Mendoza et al., 2009).

The abscission checkpoint, which is conserved with the yeast NoCut pathway, has been recently identified in the mammalian cells, with Aurora B kinase being the key regulator. It is demonstrated that the lagging chromosomes during cytokinesis sustain the activities of Aurora B, therefore delaying the abscission and also preventing the CF regression by phosphorylating a MT kinesin, MKLP1, to stabilize the contractile ring structure (Steigemann et al., 2009). It is interesting to note that in yeasts, the NoCut pathway prevents the premature abscission, whereas in mammalian cells, the NoCut-like abscission checkpoint prevents the CF regression and tetraploidization. More details of these pathways need to be elucidated, which will contribute to our current knowledge of the cytokinesis checkpoints.

1.4 CYTOKINESIS FAILURE, TETRAPLOIDIZATION AND TUMORIGENESIS.

As mentioned previously, each step of the cell cycle is strictly regulated; in addition, there are checkpoints present to monitor and/or cope with potential damages or mistakes. However, sometimes cells may still exhibit defects (DNA damage, missegregation of chromosomes, etc.)

that they fail to overcome, therefore generating abnormal or problematic outcomes. One such example is when a cell fails in cytokinesis, resulting in a binucleated cell, meaning one cell that contains two nuclei. This cell contain double amount of the genetic materials, therefore it is also a tetraploid cell.

1.4.1 Tetraploidization formation

Cytokinesis failure is the most common pathway that can generate tetraploid cells, but it is not the only one, as tetraploidization may also arise from other defects, including the defective DNA replication or damage repair pathways, and other physiological-relevant mechanisms, as discussed below.

1.4.1.1 Tetraploidization from divisional defects and cytokinesis failure

Cytokinesis failure can occur due to defective cytokinesis machinery, such as disassembly of the contractile ring components, or in response to errors during chromosome segregation. One such example of the latter is the chromosome nondisjunction, when chromatid pairs fail to separate properly, triggering CF regression and cytokinesis failure, and resulting in tetraploid progeny (Shi and King, 2005).

Other examples of chromosome segregation defects that can potentially lead to cytokinesis failure include lagging chromosomes, which may be a result of chromosomes with merotelic kinetochore attachments in an earlier stage of mitosis, and anaphase bridges, which arise from chromosomes containing two centromeres (Acilan et al., 2007; Shi and King, 2005).

1.4.1.2 Tetraploidization from DNA replication defects

It has been suggested that defects in DNA replication or damage repair pathways may also hinder cytokinesis, thus generating tetraploid cells. One piece of supporting evidence comes from the fact that a DNA replication initiation complex component Orc6 and a DNA damage repair factor BRCA2 are both localized to the CF in mammalian cells, and the elimination of these proteins results in abnormal cytokinesis and tetraploid daughter cells (Daniels et al., 2004; Prasanth et al., 2002).

1.4.1.3 Tetraploidization from other mechanisms

Some other pathways to generate tetraploid cells are found in physiological conditions, such as endoreplication and cell-cell fusion. Endoreplication, or endomitosis, describes a cell undergoing more than one round of DNA replication without cell division (Zimmet and Ravid, 2000). This process is an essential step for megakaryocyte maturation, which will be discussed in Chapter III. Cell-cell fusion is observed during the development of liver tissues, in order to generate terminally differentiated polyploid cells (Duelli et al., 2005; Ogle et al., 2005).

1.4.2 Tetraploidy and tumorigenesis

Having extra nuclei might not interfere with the interphase functions of cells, however, it becomes intrinsically hard for these cells to accurately separate their chromosomes during mitosis, as they contain not only doubled amounts of chromosomes, but sometimes also doubled number of centrosomes, which may cause multipolar spindle (MPS) formation and erroneous cell division.

Tetraploidy is conventionally believed to associate with tumorigenesis for many reasons. The first evidence is that tetraploid cells have been observed in a variety of human solid tumors by flow cytometry and cytogenetic studies, (Dutrillaux et al., 1991; Ewers et al., 1984; Kallioniemi et al., 1988; Wijkstrom et al., 1984). In addition, tetraploidy is considered to be one of the early events during tumor formation, and may lead to chromosomal instability and aneuploidy (Galipeau et al., 1996; Olaharski et al., 2006). Furthermore, *in vitro* experiments and computer modeling have confirmed that tetraploidy can serve as an intermediate towards aneuploidy through the loss and gains of chromosomes (Andreassen et al., 1996; Shackney et al., 1989). Therefore, this information allows researchers to hypothesize that tetraploidy can lead to tumorigenesis, possibly through generating aneuploid progenies.

This hypothesis is supported by an *in vitro* experiment, where tetraploid cells generated by cell-cell fusion can undergo transformation (Duelli and Lazebnik, 2007; Duelli et al., 2007). More convincingly, recent effort has been devoted to directly testing this hypothesis by using xenograft models. A strong support comes from a direct observation that malignant mammary epithelial tumors develop when tetraploid cells generated by blocking cytokinesis in p53-/- mammary epithelial cells are subcutaneously transplanted into nude mice (Fujiwara et al., 2005). Furthermore, another group of researchers have also demonstrated that the tetraploid Rat1a cells generated by overexpressing a c-Myc downstream target, after inoculation into immune-compromised mice result in rapid and large tumor formation (Li et al., 2008). Similarly, a recent study also demonstrates aggressive mammary tumor growth in nude mice, after they were injected with sorted tetraploid cells that were obtained from Aurora B-overexpressing murine epithelial cells (Nguyen et al., 2009). These data all agree with the hypothesis that tetraploidy leads to tumorigenesis.

1.4.3 How does tetraploidy lead to tumorigenesis

As tetraploidy has been demonstrated to cause tumorigenesis, one must be wondering how exactly tetraploid cells induce and/or facilitate tumor formation, which will be discussed in the remaining part of this section.

1.4.3.1 Tetraploidy and DNA damage

Tetraploid cells have been reported to exhibit DNA damage such as DNA breakages on the chromosomes. For example, when compared with the diploid controls, a higher frequency of γ-H2AX foci, a DNA double strand break (DSB) marker, has been observed in human tetraploid fibroblasts, indicating more DNA damage in these tetraploid cells (Fujiwara et al., 2005; Hau et al., 2006).

Why tetraploidy leads to DNA damage is not known, but some hypotheses have been proposed to explain these observation. The first is the possibility that having a doubled number of the nuclei (2 versus 1) can cause twice the amount of the spontaneous DNA damage in cells, which may then overwhelm the DNA damage repair system (Storchova et al., 2006), thus resulting in more DNA breaks if left unrepaired; although this hypothesis is challenged by the possibility that the DNA damage repair proteins may also be expressed twice as much. Therefore, there is another potential explanation for the DNA damage in tetraploid cells. Due to chromosomal instability, proteins that are essential for the DNA damage repair pathways can be suppressed or even missing, by the heterozygosity of the chromosomes containing their respective gene locus, leaving unfixed DNA damage accumulate overtime. As DNA damage, especially DSB, is relevant to my studies, I will briefly discuss the cellular responses to DNA damage.

DNA damage response

DNA damage in cells can arise from intracellular or extracellular cues. The intracellular cues include inaccurately replicated DNA, and reactive oxygen/nitrogen species, which are byproducts from the natural metabolic pathways (Wiseman and Halliwell, 1996). The extracellular cues include ionizing radiation (IR), ultraviolet (UV) light and reactive chemicals (Iliakis et al., 2003; Orren et al., 1995; Sorenson and Eastman, 1988a; Sorenson and Eastman, 1988b). If unfixed, these DNA changes may alter the genetic materials and interfere with normal cell division, therefore there are multiple DNA damage monitoring and repair systems in cells, which can sense and fix the problems, and hinder or resume cell cycle progression accordingly.

There are three major components of the DNA damage monitoring system, including sensors, transducer, and effectors. The sensors detect DNA damage, sending signals through the transducers, and finally triggering the effectors to take action, arresting the cell cycle, and allowing more time to repair the damaged DNA.

Two important *effector* proteins in DSB monitoring pathways include p53 and the cdc25 family of phosphatases. p53 is the most classical tumor suppressor protein, which also plays a central role in the DNA damage monitoring system, and decides the fate of the cell: either arrest in the cell cycle, or cell death (Giaccia and Kastan, 1998; Prives and Hall, 1999; Vousden, 2000). The protein expression levels and activities of p53 are regulated by post-transcriptional modifications, such as phosphorylation and acetylation (Appella, 2001; Appella and Anderson, 2001). In normal conditions, the level of p53 is kept low due to an Mdm2-dependent ubiquitylation and degradation pathway (Liang and Clarke, 2001; Marine and Lozano). Upon DNA damage, p53 is phosphorylated at Ser15, which results in inhibition of p53's interaction with Mdm2, therefore stabilizing p53 (Banin et al., 1998; Canman et al., 1998; Shieh et al.,

1997). One key transcriptional target of p53 is p21, which can inhibit cyclin D/cdk4, cyclin A/cdk2 and cyclin E/cdk2 complexes, and arrest cells prior to entering S phase (el-Deiry et al., 1994), as introduced previously in the "CELL CYCLE" section of this chapter. This cell cycle arrest is critical to allow enough time for the DNA damage repair system to function, hence preventing cells from replicating the damaged DNA, and ensuring the high fidelity of the inheritance of the genetic materials in cells.

Cdc25 phosphatases are the other family of the effector proteins. Upon DNA damage, cdc25 proteins are phosphorylated at inhibitory sites by chk1 and chk2, which are activated in a ATM-dependent manner (Chaturvedi et al., 1999; Matsuoka et al., 1998; Peng et al., 1997; Sanchez et al., 1997). This leads to an inhibition of cdc25 phosphatase activities, therefore suppressing the activities of the cyclin B complexes, by maintaining the inhibitory phosphorylation at the Tyr15 residue on cyclin B, therefore arresting cells at G2/M transition (Furnari et al., 1997).

While cell cycle is arrested by the above-mentioned effectors, DNA damage repair pathways are activated, however those pathways are beyond the scope of my research, thus will not be discussed.

1.4.4 Tetraploidy, aneuploidy and chromosomal instability

Although the exact mechanism through which tetraploid cells cause tumor formation remains unknown, it is suggested that aneuploidy and/or chromosomal instability that arises from tetraploid cell division might mediate this mechanism (Lengauer et al., 1997; Thompson and Compton, 2008). Chromosomal instability is defined as the accelerated rate of chromosome gains or losses, leading to aneuploidy, a state that describes cells having an abnormal

chromosome number. Aneuploidy is often found in cancer cells and is believed to facilitate tumor formation (Weaver and Cleveland, 2006). Intuitively, gaining more copies of oncogenes, whose protein products favor cell proliferation, or losing gene copies of tumor suppressor genes, whose protein products block cell division, can contribute to the hyper-proliferation of cells, by altering the expression of the relevant proteins. Examples of these two categories of proteins are discussed below.

1.4.4.1 Oncoproteins

There are different types of oncoproteins that have been identified to promote cell proliferation and transformation, including various mitogens, kinases, GTPases and transcription factors. It has been conventionally accepted that cancer results from a series of gene mutations, some of which convert proto-oncogenes to actively expressed oncogenes, which can be transcribed and translated into oncoproteins. c-Myc is one of the most classical and relevant oncoprotein for my studies, which functions as a transcription factor.

The c-Myc gene has been reported to be amplified in various human cancers, including breast carcinomas, lung carcinomas, and colon carcinomas, in addition, c-Myc protein has been found to be overexpressed in almost 1/3 of colon and breast carcinomas, as well as other cancers including cervical carcinomas, osteosarcomas, glioblastomas, and myeloid leukemias (Augenlicht et al., 1997; Erisman et al., 1985; Escot et al., 1986; Little et al., 1983; Mariani-Costantini et al., 1988; Melhem et al., 1992; Munzel et al., 1991). A well-known example is the Burkitt's lymphoma (BL), in which the activated c-Myc functions as a key factor. It has been found that chromosome 8, which contains the c-Myc locus, can undergo translocation with chromosome 14, 2, and 22, which contain the immunoglobin (Ig) heavy chain locus, resulting in

the juxtaposition of c-Myc to the Ig locus, which is responsible for BL (Casares et al., 1993; Crews et al., 1982; Dalla-Favera et al., 1982; Shen-Ong et al., 1982; Taub et al., 1982).

As it is largely associated with various tumors, c-Myc has gained a lot of attention from cancer researchers in the past 28 years. Although how exactly c-Myc causes and/or facilitates tumor formation still remains a mystery, there are some hypotheses trying to elucidate the role(s) for c-Myc in tumorigenesis.

One hypothesis is that, c-Myc may increase the general protein expression rates, by up-regulating the expression of proteins that are involved in the transcription or translation machineries, such as RNA polymerases, ribonucleases, and rRNA-modifying enzymes, just to name a few (Gomez-Roman et al., 2006; Schlosser et al., 2003). In addition, as more and more downstream targets of c-Myc have been identified, some of the c-Myc targets have shown the capability to recapitulate multiple genomic instability phenotypes similar to c-Myc, indicating other possible mechanisms mediating the tumorigenesis process caused by c-Myc (Li et al., 2008). One such mechanism is through up-regulating a c-Myc downstream target protein GpIbα and causing cytokinesis failure and tetraploidization, which I will discuss in the Chapter III.

1.4.4.2 Tumor suppressor proteins

In contrast to oncoproteins, tumor suppressor proteins function as negative regulators of cell proliferation, among them the most classical one is p53, which is a multi-functional protein that is known as “guardian of the genome”. Diverse roles of p53 in cells include directly functioning in DNA damage monitor pathways, as discussed earlier in this section, and more generally, acting as a transcription factor. Numerous targets regulated by p53 have been identified, ranging from proteins involved in cell cycle control, immune response, motility, migration, cell death, senescence, to factors functioning in DNA metabolism and energy

metabolism (Olovnikov et al., 2009; Polager and Ginsberg, 2009; Roger et al., 2006). For example, p53 can either transcriptionally suppress the synthesis of proteins that can promote cell proliferation, such as c-Myc and survivin (Hoffman et al., 2002; Sachdeva et al., 2009), or transcriptionally up-regulate the synthesis of proteins that can inhibit cell cycle progression, such as p21, a classical cyclin kinase inhibitor (CKI) discussed in the "CELL CYCLE" section of this chapter, therefore p53 tend to inhibit cell proliferation (Dulic et al., 1994; el-Deiry et al., 1994).

2.0 CHAPTER II. MITOTIC SLIPPAGE IN NONCANCER CELLS INDUCED BY A MICROTUBULE DISRUPTOR, DISORAZOLE C1.

Figures 7, 8B, 11A, 12, 13A, C, D, 14, 15, 16, 17A, B, C, 18 have been published in (Xu et al.)

2.1 INTRODUCTION

As discussed in Chapter I, various compounds can inhibit the dynamics of MTs by depolymerizing or hyper-stabilizing MTs, therefore interfering with the normal processes of cell division. Hence these compounds can be used to hinder the uncontrolled proliferation of tumor cells in cancer patients; in fact, many of these compounds are either in clinical trials or on the market already as anticancer drugs. For example, taxol is commercially available to treat breast, lung, bladder and head and neck cancers (Rowinsky et al., 1990), while vinblastine and other vinca alkaloids are used in the treatment of leukemia, lymphoma, small cell lung, breast cancer, and other malignancies (Rowinsky and Donehower, 1991). Although these drugs are effective in certain cancer patients, more anticancer drug candidates are still in great demand, due to intrinsic and acquired resistance to existing drugs, and cytotoxic effects of current therapies.

Disorazoles are a family of 29 macrodiolides identified from the fermentation broth of myxobacteria *Sorangium cellulosum* (Jansen, et al. 1994), a strain of the gram-negative “slime bacteria” that glide or walk on their hosts in the soil, rotting plants and animal dung

(Reichenbach, 2001). Besides the disorazoles, *Sorangium cellulosum* also produce other metabolites, such as epothilones (Altaha et al., 2002; Trivedi et al., 2008), tubulysins (Sasse et al., 2000), chondramides (Rachid et al., 2006), just to name a few. It is interesting to note that among these metabolites, disorazoles and tubulysins are newly-identified MT inhibitors (Hopkins and Wipf, 2009; Sasse et al., 2000), while epothilones are one type of MT stabilizers that are currently in the clinical trials (Kuppens, 2006). It remains unknown why the myxobacteria *Sorangium cellulosum* generate these different compounds during fermentation, which can interfere with the structure and dynamics of MTs; and while beyond the scope of the current study, it may be intriguing to study the reason behind this biological phenotype and its impact on the evolutionary adaption of *Sorangium cellulosum.*

Among the 29 disorazoles, disorazole A_1 is the major component which contributes to approximately 70% of the relative mass of all disorazoles isolated from *Sorangium cellulosum* (Jansen, et al. 1994). Disorazole A_1 has been demonstrated to inhibit MT polymerization, therefore arresting cells at M phase and inducing apoptosis in various cancer cell lines at the picomolar concentrations(Elnakady et al., 2004).

Disorazole C_1, which will be referred to as DZ for the rest of my thesis, is a very rare component of the fermentation products of *Sorangium cellulosum*; however, it receives more attention from researchers, probably due to its higher therapeutic potential, as DZ does not contain the chemically reactive divinyl oxirane and (*E*,*Z*)-dienyl oxazole moieties, which disorazole A_1 has (Wipf and Graham, 2004; Wipf et al., 2006) (Figure 7). Several research groups have reported different strategies to chemically synthesize DZ (Wipf and Graham, 2004), thus making further biological studies of DZ feasible, despite DZ's extremely low yield in the natural fermentation products of *Sorangium cellulosum.*

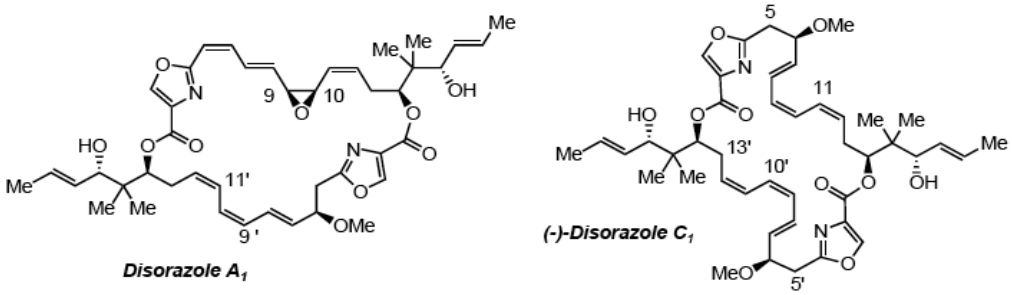

Figure 7 Chemical structures of disorazole A_1 and disorazole C_1 (DZ).

In a preliminary small-molecule screen, DZ has been shown to depolymerize MTs and to induce mitotic arrest (Wipf et al., 2006). In a follow-up study, Tierno *et al.* have demonstrated that DZ might bind to tubulin subunits at a unique site, which is distinct from the known vinca-binding site, and blocking the polymerization of the MTs (Tierno et al., 2009). DZ has also been observed to cause apoptosis and premature senescence in certain cancer cell lines (Tierno et al., 2009; Wipf et al., 2006). All of this research has been focused on the responses of cancer cells to DZ, but no results were obtained yet to compare the responses to this compound in noncancer cells with those in cancer cells. Therefore in my studies I investigated noncancer cells' responses to DZ, and contrasted the different fates of cancer and noncancer cells after the treatment of DZ.

2.2 RESULTS

2.2.1 DZ depolymerizes MTs, causing mitotic arrest and inhibiting cell proliferation

Generally speaking, MT depolymerizers, when applied to cells, can exhibit two classical features: mitotic arrest and proliferation inhibition, which are both associated with their ability to interfere with the structures and dynamics of MTs. Therefore, as a newly synthesized MT disruptor, DZ was examined for these classical effects, by using cultured human cancer and noncancer cells.

2.2.1.1 DZ depolymerizes MTs from their plus-ends in both cancer and noncancer cells

In order to visualize the MTs in cells, immunofluorescence was employed with antibodies against α-tubulin. An oral squamous cell carcinoma cell line UPCI:SCC103 (a gift from Dr. Susanne Gollin, University of Pittsburgh) was used as a representative for cancer cells, and a retinal pigmented epithelial cell line immortalized by human telomerase reverse transcriptase (RPE-hTERT) was used as a representative for noncancer cells. Both of these two cell lines were treated with DZ, at concentrations close to DZ's IC_{50}s, as determined by different cell lines (Tierno et al., 2009). As demonstrated in Figure 8A, DZ depolymerized the MTs in both cancer and noncancer cells, with a similar effectiveness and severity, suggesting that DZ can interfere with the MTs in both cancer and noncancer cells.

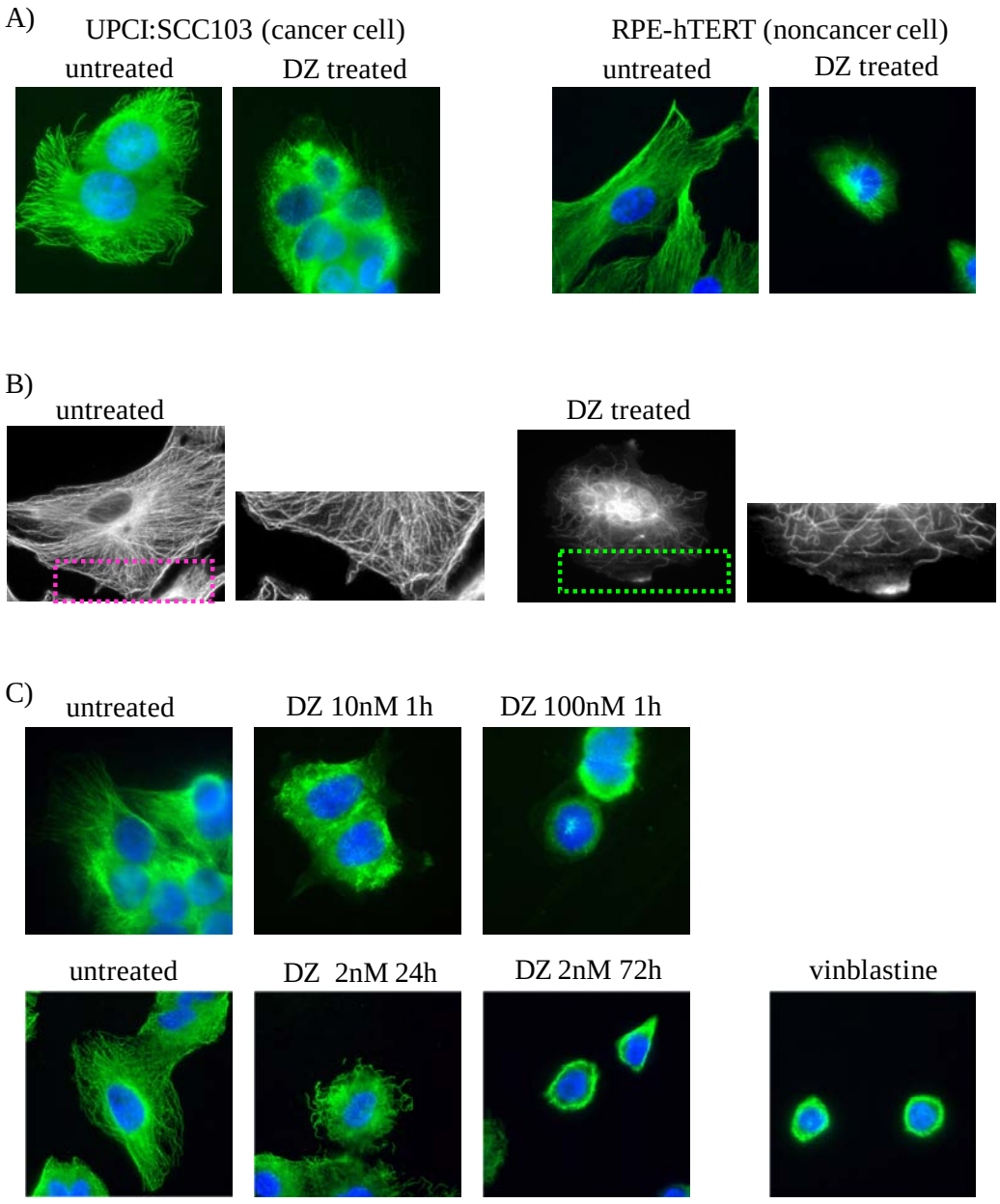

Figure 8 DZ depolymerizes the MTs in both cancer and noncancer cells, in a time- and dose-dependent manner, and this depolymerization is from the plus-ends of the MTs.

(A) The UPCI:SCC103 cells (cancer cells) and the RPE-hTERT cells (noncancer cells) were treated with 10 nM of DZ for 1 hour before fixation. Cells were stained with the antibodies against a-tubulin to visualize the MTs (green). The nuclei were labeled by DAPI (blue). (B) Left: before the DZ treatment, the MTs were intact in the RPE-hTERT cells, where the plus-ends of the MTs reached the vicinity of the boundary of a cell. Right: after the DZ treatment, the plus-ends of the MTs depolymerized, and could no

longer reach the boundary of the cell. (C) Top: The UPCI:SCC103 cells were treated with different doses of DZ for 1 hour before fixation. Bottom: The A549 cells were treated with 2nM of DZ for different times before fixation. Bottom right: The A549 cells were treated with vinblastine for 72 hours. The cells were stained with the antibodies against a-tubulin to visualize the MTs (green). The nuclei were labeled by DAPI (blue).

Next, I examined which ends of the MTs were disrupted by DZ. Immunofluorescence data revealed that in all cell lines tested, including RPE-hTERT, UPCI:SCC103, a human lung adenocarcinoma cell line A549, and a monkey kidney cell line COS-7, the MTs seemed to depolymerize from the plus-ends (Figure 8B). This result is not surprising, because the minus-ends of MTs in cells are normally embedded in the centrosomes, therefore are less dynamic than the plus-ends of MTs, which can be easily influenced by small inhibitory compounds such as DZ.

Lastly, DZ's ability to depolymerize MTs was demonstrated to be both concentration-dependent and time-dependent. As indicated in Figure 8C, higher concentrations of DZ resulted in fuller depolymerization of MTs; similarly, longer exposures of DZ also led to more complete depolymerization. It is worth noting that after a complete disruption of MTs, some α-tubulin stained structures seemed to accumulate around the nuclei, forming bundles. This phenotype was not DZ-specific, as the vinblastine-treated cells also demonstrated the similar bundle-like MT structures around the nuclei (Figure 8C). Furthermore, this observation was also consistent with data reported in an earlier literature for other tubulin inhibitors (Kruczynski et al., 1998), suggesting that after disruption by small inhibitory molecules, MTs might organize into these perinuclear structures in cells.

2.2.1.2 DZ-caused depolymerization is mostly irreversible

Some MT inhibitors exhibit reversible effects, while some others are irreversible after application. Therefore I tested whether the depolymerizing effects of DZ on MTs could be reversed after wash-out, in both RPE-hTERT and UPCI:SCC103 cells. A known reversible MT inhibitor nocodazole was used as a control.

After drug treatments, cells were washed for three times with the drug-free medium, and released for up to 6 days, immunofluorescence analyses was then performed to determine the integrity of MT structures after the release. As shown in Figure 9A, B, the nocodazole-treated cells restored their MT networks at day 3, which looked almost exactly the same as the astral organization of MTs in the untreated cells, while the DZ-treated cells did not show recover at day 3. Even at day 6, the RPE-hTERT cells released from DZ treatment contained only several short MT filaments that are bundled together near the nuclei, but these MTs were not organized into any meaningful structures that can be close to a normal MT network. Therefore, these data suggest that the depolymerizing effect of DZ on MTs was mostly irreversible in both cancer and noncancer cells, which may be a result of irreversible binding of DZ to MTs in these cells.

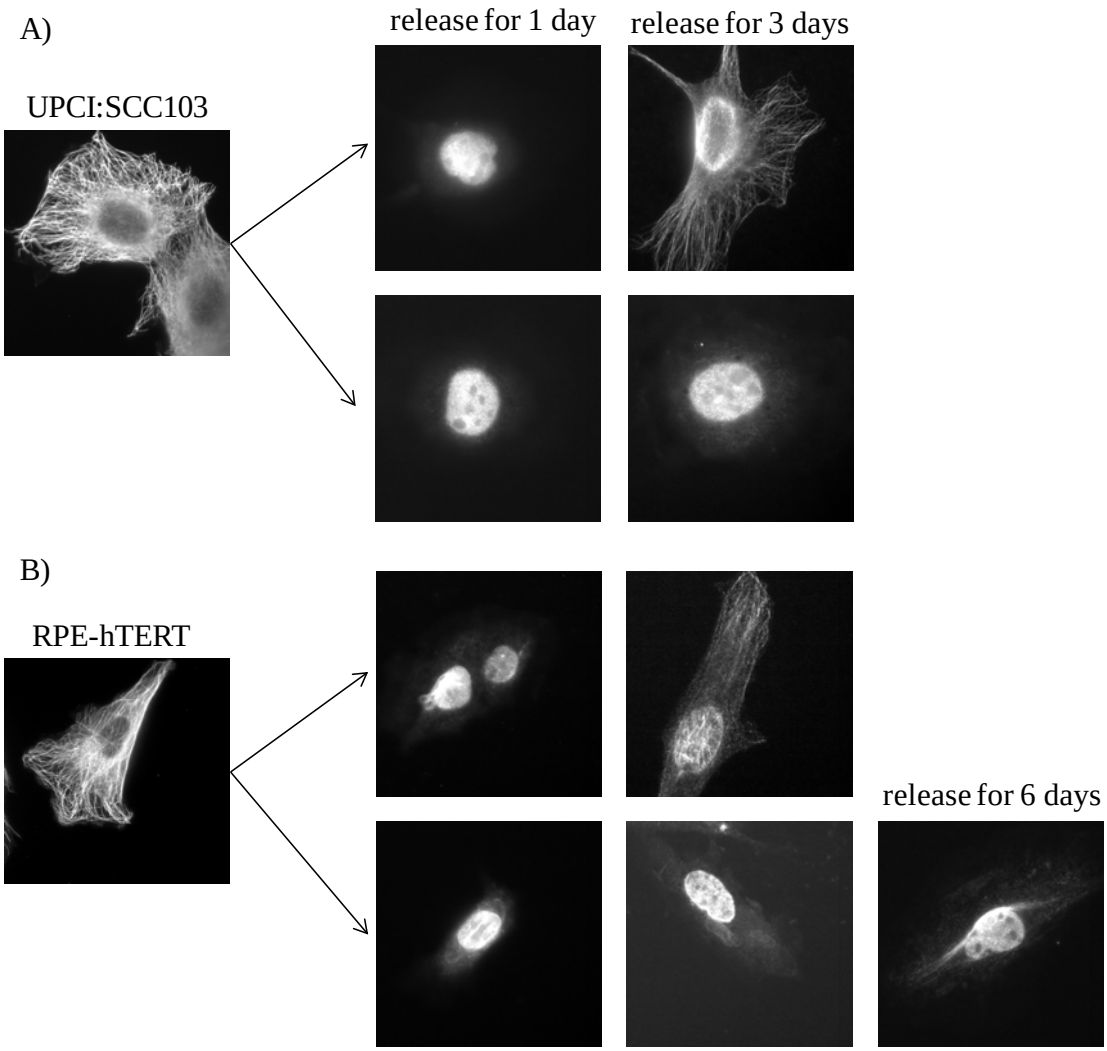

Figure 9 The depolymerization effect of DZ on the MTs is mostly irreversible, in both the cancer and noncancer cells.

(A) The UPCI:SCC103 cells were treated with 25 nM of nocodazole or 25 nM of DZ for 1 hour, followed by three washes with the drug-free medium, and released for 1 day or 3 days. The cells were then fixed and stained with the antibodies against a-tubulin to visualize the MTs. (B) The RPE-hTERT cells were subjected to the same treatment as in (A). Bottom right: 6 days after the release from the DZ treatment, longer strings of the MTs appeared around the nuclei of the RPE-hTERT cells, but they were not organized into the normal MT network.

2.2.1.3 DZ's effect on the *in vitro* polymerized MTs that are stabilized with taxol

DZ has been demonstrated to depolymerize MTs from their plus-ends in mammalian cells, therefore its effects on MTs polymerized *in vitro* were also analyzed. As shown in Figure 10A, the *in vitro* polymerized MTs were typically straight linear elements with no curving, and they were not as long as the MTs in mammalian cells. When DZ was added, these strings appeared almost unaffected, although some of them might be slightly shorter than the controls. To conclude these results, DZ's effects on the MTs polymerized *in vitro* were much less than its dramatic effects on the MTs in mammalian cells, in fact the *in vitro* polymerized MTs were almost unaffected by the addition of DZ.

A possible explanation for this large difference in DZ's effects on MTs is that *in vivo* (cell) experiments and *in vitro* experiments were performed at different temperatures and contained different buffers. Therefore, I conducted another *in vitro* experiment, which was similar to the previous one, but changed the temperature and buffers to mimic the *in vivo* (cell) experiments. It seems that this new protocol interfered with the normal *in vitro* polymerization of MTs, as the number of MT short strings was significantly reduced when compared with the experiment done with the standard protocol. However, my preliminary data still appeared to be similar to the previous findings, which were that the DZ-treated MTs were almost identical but maybe a little shorter than the DMSO-treated controls (Figure 10B), suggesting that the temperatures and buffers may not be the explanation for the different effects of DZ observed *in vitro* and *in vivo* (cell).

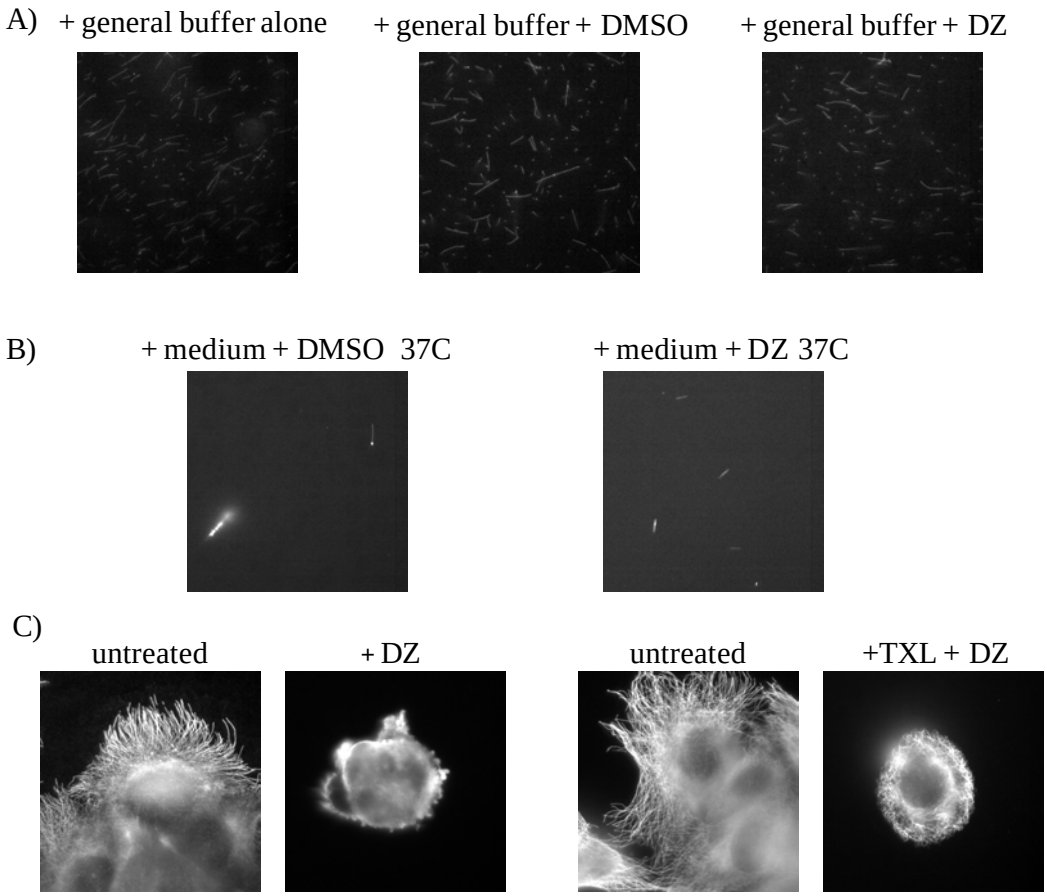

Figure 10 DZ exerts little effect on the MTs polymerized in vitro when stabilized by taxol.

(A) *in vitro*-polymerized MTs. Left: the MTs were polymerized *in vitro*. Middle: the MTs were polymerized *in vitro*, and then treated with DMSO for 30 minutes. Right: the MTs were polymerized *in vitro*, and then treated with 100 nM of DZ for 30 minutes. (B) Similar experiments as in (A), except for using the UPCI:SCC103 culture medium instead of the general buffer in the standard protocol, and using 37°C instead of the room temperature. (C) Left: The UPCI:SCC103 cells treated with 100 nM of DZ demonstrated almost completely depolymerized MTs. Right: The UPCI:SCC103 cells that were pre-treated with taxol, and then treated with 100 nM of DZ, demonstrated the disrupted, but not completely depolymerized, MTs. Cells were fixed and stained with the antibodies against a-tubulin to visualize the MTs.

These distinct effects on MTs observed in cells and *in vitro* after DZ treatment might actually originate from different stabilization properties of DZ in these two systems. For

example, cells may metabolize DZ, whereas *in vitro*, DZ may become unstable in the environment needed for the *in vitro* MT polymerization reaction.

In addition, it is worth noting that taxol, a MT stabilizer, was required in the *in vitro* MT polymerization protocol, but was not added in the *in vivo* (cell) experiment. Therefore the different effects of DZ between the *in vitro* and *in vivo* (cell) experiments may be explained by a hypothesis that taxol hyper-stabilized the MTs polymerized *in vitro* and canceled the depolymerizing effect of DZ. To test this, UPCI:SCC103 were pre-treated with taxol before the addition of DZ. Interestingly, the taxol-stabilized MTs in UPCI:SCC103 cells seemed to be less affected by DZ, as demonstrated by the residual short MT filaments in these cells, which looked like a shrank structure of the normal star-like MT network, compared with the complete disruption of MTs found in UPCI:SCC103 cells that were only treated with DZ (Figure 10C). These data support the hypothesis that taxol may interfere with the effects of DZ on MTs, hence generating the different results in the *in vitro* and *in vivo* (cell) experiments.

Another possibility to explain the different effects of DZ between the *in vitro* and *in vivo* (cell) experiments is that, although the same concentrations of DZ were added to the cells and to the *in vitro* polymerization reactions, the effective concentrations of DZ on MTs might not be the same. For example, the cells might absorb and keep accumulating this compound in the cytoplasm, therefore ending up with a higher effective concentration of DZ than what was added initially, however the effective concentration in the *in vitro* reactions would be the same as what was added initially, hence the MTs in cells were affected more severely, than the MTs in the *in vitro* experiments.

2.2.1.4 DZ causes mitotic arrest in cancer cells and noncancer cells

DZ has been shown to potently disrupt the MTs in both RPE-hTERT and UPCI:SCC103 cells, therefore DZ would presumably arrest these cells at M phase, because cell division can not proceed without intact MTs. Hence, the mitotic indices were examined by 4,6-diamidino-2-phenylindole (DAPI)-stained nuclei, before and after DZ treatment, using both RPE-hTERT and UPCI:SCC103 cells. The condensed bright nuclei indicate cells in mitosis, while the decondensed oval-shaped nuclei indicate cells in interphase (Figure 11A).

A classical method to determine the mitotic index is to count cells at random areas on a coverslip, and divide the number of the mitotic cells by the total number of the cells counted. As expected, increases in the mitotic indices were observed in both RPE-hTERT and UPCI:SCC103 cells after 16 hours treatment of DZ, indicating that cells are arrested in mitosis after DZ exposure (Figure 11A). It is interesting to note that the fold changes of the mitotic indices in both cell lines are almost identical. This may be related to the previous observation that DZ seemed to disrupt MTs at a similar level in both RPE-hTERT and UPCI:SCC103 cells, therefore might causing a comparable level of damages to the mitotic spindles in both cell lines when they divide.

2.2.1.5 DZ inhibits the cell proliferation

A general consequence of the treatment of MT disruptors is that cell proliferation would be inhibited, therefore I analyzed DZ's effect on the viabilities of cancer cells and non-cancer cells. the assay chosen utilizes the compound 3-(4,5-dimethylthiazol-2-yl)-5-(3-carboxymethoxyphenyl)-2-(4-sulfophenyl)-2H-tetrazolium (MTS), which can be bioreduced into a color product, mediated by NADPH or NADH generated by the dehydrogenase in the metabolically active cells (Berridge and Tan, 1993; Cory et al., 1991). This MTS assay directly

measures the quantity of electrons transferred during metabolism in living cells by recording the absorbance at 490 nm, which reflects the relative numbers of living cells. MTS assays are hence commonly used to determine the relative viability of cells before and after treatments.

MTS data suggest that DZ treatment caused decreases in the energy flow of all tested cell lines, including cancer cells and noncancer cells, which reflected the decreased viabilities in these cells after their exposure to DZ (Figure 11B). It interesting to note that the viabilities of RPE-hTERT and UPCI:SCC103 were affected to comparable levels after DZ treatment, while a cancer cell A549 and a monkey cell line COS-7 seemed to be more resistant to DZ, as their viabilities were not markedly reduced after exposure to DZ, when compared with RPE-hTERT and UPCI:SCC103. Interestingly, when A549 cells were treated with another MT disruptor, vinblastine, little reduction in viability was observed, similar to the results obtained after DZ treatment (Figure 11B).

These data revealed that DZ is a very potent compound, which can inhibit the proliferation of both cancer and noncancer cells. However, unfortunately some cancer cell lines such as A549 may have demonstrated resistance towards DZ, suggesting that not all cancer cells could respond to DZ effectively. The reason for A549 cells failed to effectively respond to MT disruptors will be discussed in the section of “Speculations and discussions”.

2.2.2 DZ causes centrosome disorganization

My previous data suggeste that MTs in cells were severely disrupted by DZ from their plus-ends, therefore I was curious whether the minus-ends of the MTs would also be affected. As centrosomes are where the minus-ends of MTs are embedded, the organization and distribution

of centrosomes were analyzed before and after DZ treatment, by examine a centrosome protein p150 (Askham et al., 2002).

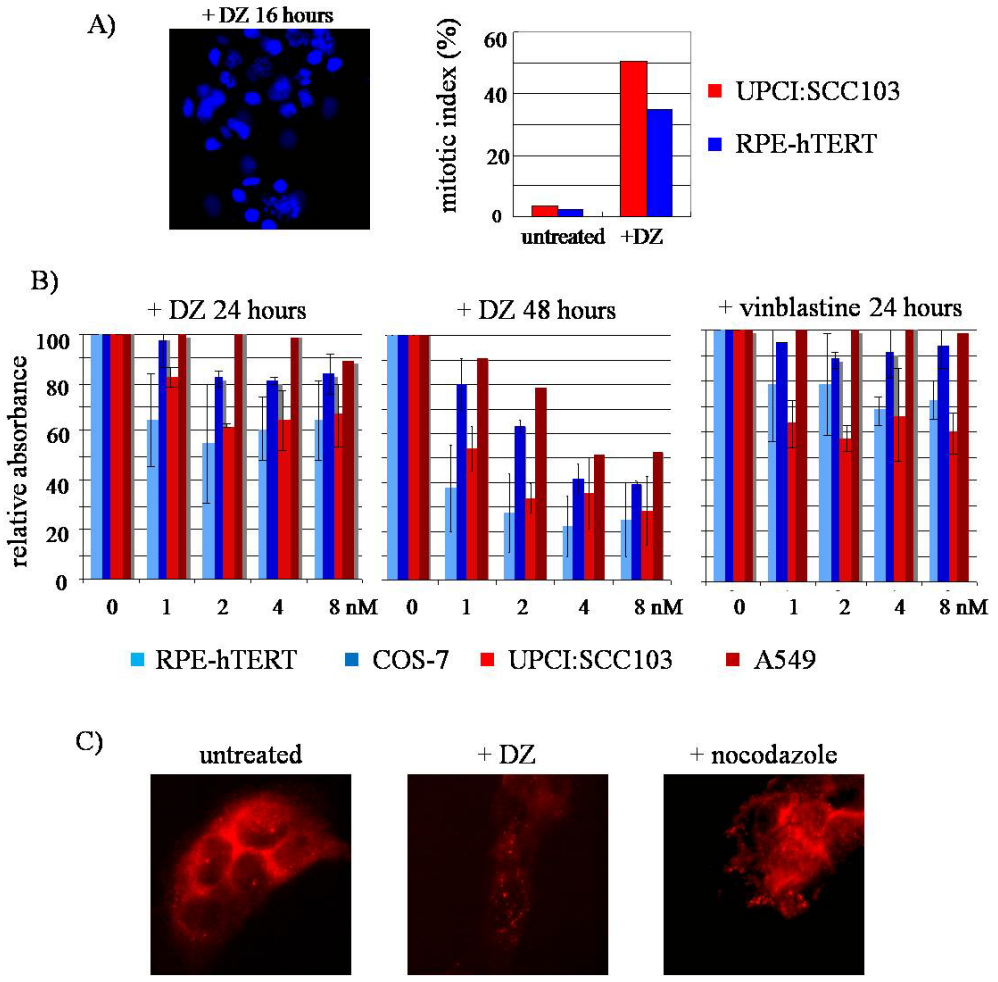

Figure 11 DZ causes the mitotic arrest and the inhibition of the cell proliferation, meanwhile also triggers the split distribution pattern of a centrosome protein p150.

(A) The cells treated with 50 nM of DZ for 16 hours demonstrated increases in their mitotic indexes. Left: the cells were fixed with methanol after the 16 hour treatment of DZ, and nuclei were labeled using DAPI (blue). Right: quantification of the mitotic indices before and after the DZ treatment, in both the UPCI:SCC103 cells and RPE-hTERT cells. (B) Four cell lines (RPE-hTERT, COS-7, UPCI:SCC103 and A549) were treated with different doses of DZ (1 nM, 2 nM, 4 nM and 8 nM) for different time courses (24 hours and 48 hours). Their cell viabilities were evaluated by the MTS assay. Vinblastine treatment was used to be compared with DZ. (C) The localization and distribution of p150 in cells was changed after the DZ

treatment. The UPCI:SCC103 cells treated with DZ or nocodazole were fixed and stained with antibodies against p150 (red).

In most of the untreated cells, the staining of p150 represents the centrosome, by one bright dot per cell, localized next to the nucleus (Figure 11C). However, in cells treated with DZ, p150 exhibited an altered distribution pattern, where there were several p150 positive foci scattered in the cytoplasm of one cell, indicating a change in the localization or the organization of centrosomes, or their relevant structural components (Figure 11C).

This change in the centrosome localization or distribution by DZ treatment may be explained by the possibility that, the depolymerizing effects on the minus-ends of MTs by MT disruptors alters the centrosome structures and/or organizations. If this hypothesis is correct, other MT disruptors should exert similar effects on the centrosomes. Indeed, when MTs were depolymerized by nocodazole, p150 also demonstrated the same split pattern, same as that was observed in the DZ-treated cells (Figure 11C), supporting the hypothesis that the disorganized centrosome is a result of the MT depolymerization caused by the MT disruptors.

2.2.3 DZ causes nuclear fragmentation in the noncancer cells, which is mitotic slippage

My data so far has demonstrated that DZ depolymerizes MTs from their plus-ends and disturb centrosome structure, causing mitotic arrest and inhibiting cell proliferation. Furthermore, these effects seemed to be comparable in both UPCI:SCC103 and RPE-hTERT cells. In the following studies, I will mainly discuss the cellular responses to a 38-hour treatment using 10nM of DZ of RPE-hTERT cells, which were different from cancer cells' responses to the same treatment.

2.2.3.1 RPE-hTERT cells demonstrate nuclear fragmentation after DZ treatment, which is not associated with apoptosis

As shown previously, RPE-hTERT cells' viability decreased markedly upon DZ treatment; therefore I asked whether these cells underwent apoptosis, a classical cellular response to many MT inhibitors of various cell lines. Using DAPI staining, abnormally shaped nuclei were observed in the DZ-treated RPE-hTERT cells, which was characterized by several small fragments of nuclei clustering together, instead of one oval-shaped nucleus in untreated cells (Figure 12A).

RPE-hTERT cells treated with DZ do not demonstrate high percentages of annexin-V staining

To test whether this nuclear fragmentation was a result from apoptosis, I performed annexin-V staining, which is widely used as an apoptosis detection assay. Annexin-V can bind to the phosphatidylserine, which is normally localized on the inner side of the cell membrane, but can be flipped to the outer side of the membrane when cells are undergoing apoptosis, thus annexin-V signals indicate apoptosis (van Engeland et al., 1998; Vermes et al., 1995). Surprisingly, the RPE-hTERT cells treated with DZ for 38 hours only demonstrated a small percentage of cells with positive annexin-V staining, while majority of these DZ-treated cells demonstrated nuclear fragmentation (Figure 12C), suggesting that the observed nuclear fragmentation is probably not a phenotype associated with apoptosis. Interestingly, RPE-hTERT cells treated with vinblastine or taxol, also demonstrated low percentages of annexin-V positive signals, regardless of the high percentages of nuclear fragmentation (Figure 12C), suggesting that DZ affects RPE-hTERT cells similarly to the other MT inhibitors.

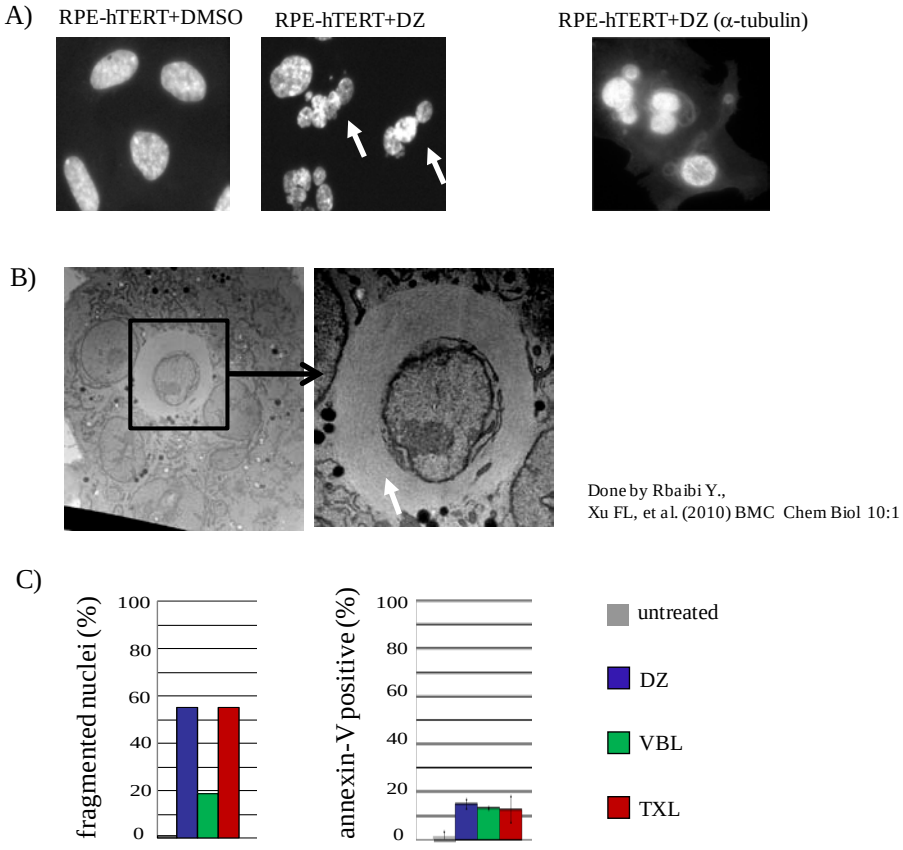

Figure 12 The RPE-hTERT cells treated with DZ demonstrate nuclear fragmentation.

(A) The RPE-hTERT cells were treated with 10 nM of DZ or DMSO for 38 hours. Left two images: the nuclei before and after the DZ treatment, visualized by DAPI. The arrows point to the fragmented nuclei in the DZ-treated RPE-hTERT cells. Right: the residual MTs visualized by antibodies to a-tubulin in the DZ-treated RPE-hTERT cells. (B) EM images of DZ-treated RPE-hTERT cells. Right: a zoom-in picture of the fragmented nuclei, which contained filament-like structures (white arrow). (C) Left: the percentages of the nuclear fragmentation phenotype in the RPE-hTERT cells treated with 10 nM of DZ, or 100 nM of vinblastine or 1 mM of taxol for 38 hours. Right: the percentages of apoptosis in the RPE-hTERT cells treated with 10 nM of DZ, or 100 nM of vinblastine or 1 mM of taxol for 38 hours, examined by annexin-V staining.

Cytochrome C is not released in RPE-hTERT cells treated with DZ

In order to further confirm that the nuclear fragmentation observed in the DZ-treated RPE-hTERT cells was not accompanied by apoptosis, three other apoptosis detection assays were employed. Apoptosis is a well-studied multi-step cellular process, during which cytochrome C release from the mitochondria is considered to be one of the most critical events (Cai et al., 1998). Therefore immunofluorescence was utilized to visualize whether cytochrome C was released in the cells treated with DZ.

As shown in Figure 13A, cytochrome C in the untreated RPE-hTERT cells formed long or short filament-like structures, with bright staining signals. H_2O_2-treated cells were used as a positive control to demonstrate apoptosis, where cytochrome C staining became very faint and diffuse, and only some thin filament-like structures were left. However, RPE-hTERT cells treated with 10 nM of DZ for 38 hours, which was the same treatment that induced the nuclear fragmentation, did not demonstrate the dim and diffuse cytochrome C distribution patterns, as observed in the H_2O_2-treated apoptotic cells; instead the cytochrome C staining in these DZ-treated cells was bright, and appeared to be more similar to that of the untreated cells. These data, together with the low percentages of annexin-V positive cells, suggest that DZ does not induce apoptosis in RPE-hTERT cells after the 38 hour-treatment of DZ.

When vinblastine and taxol were used to compare with DZ, I also observed similar phenotypes of the cytochrome C distributions (Figure 13A), suggesting that DZ behaves similarly to vinblastine and taxol. Intriguingly, in the untreated cells, cytochrome C seemed to align along the MTs, indicating a possible relationship between the structures of the MTs and the distribution of cytochrome C in mammalian cells (Figure 13B).

Mitochondria are not depolarized in the DZ-treated RPE-hTERT cells

We also tested mitochondria depolarization, which is another commonly-used marker for apoptosis. As a membrane-enclosed structure, the mitochondria possess membrane potentials under normal conditions, however when cells are undergoing apoptosis, mitochondrial membrane permeability increases, leading to depolarization of the inner membrane of mitochondria and rupture of the outer membrane, consequently resulting in cytochrome C release from these mitochondria (Dussmann et al., 2003; Heiskanen et al., 1999; Scarlett et al., 2000). Therefore, I analyzed the mitochondria potential in the DZ-treated RPE-hTERT cells, and used H_2O_2 treated cells as a positive control for apoptosis.

MitoTracker is a fluor-conjugated probe to detect the membrane potential of the mitochondria in cells, therefore was used to visualize the mitochondria in untreated and DZ-treated RPE-hTERT cells. In the untreated cells, the morphologies of mitochondria were similar to the cytochrome C staining patterns, both demonstrating filament-like structures (Figure 13A). Most, if not all, of the cytochrome C could be found overlapping with the mitochondria, consistent with the fact that under normal conditions cytochrome C is restricted on the inner membranes of mitochondria. However, when apoptosis occurred in the cells treated with H_2O_2, an extremely faint staining of the mitochondria was observed, where most of the filament-like mitochondrial structures had vanished (Figure 13A), indicating a dramatic loss of the membrane potential in these mitochondria, a signature for the activated apoptosis pathway. However, in the DZ-treated cells, this signature faint staining was not observed, instead, the mitochondria in the cells treated with DZ looked more like those in the untreated cells (Figure 13A), suggesting little or no apoptosis occurred in the RPE-hTERT cells treated with DZ, consistent with the previous negative annexin-V and cytochrome C results.

Again, when vinblasine and taxol were used, similar results were obtained, indicating that DZ's effects on RPE-hTERT cells are similar to those caused by other MT inhibitors.

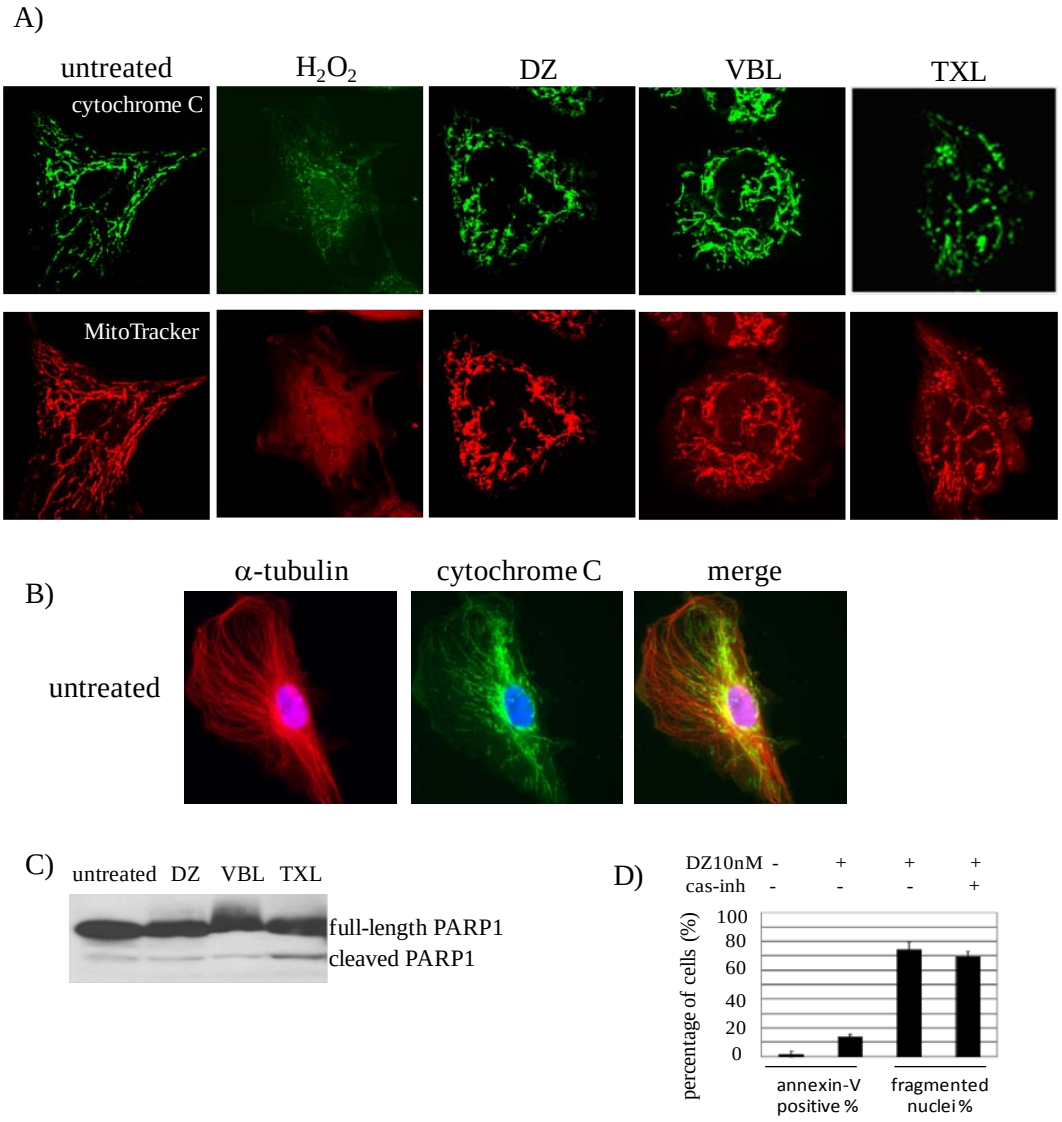

Figure 13 The RPE-hTERT cells treated with DZ do not undergo apoptosis.

(A) The RPE-hTERT cells that were treated with 10 nM of DZ, or 100 nM of vinblastine or 1 mM of taxol for 38 hours were examined by the confocal microscopy analyses. The H_2O_2-treated cells were used as a positive control for apoptosis. The first row: the cells were fixed and stained with the antibodies against the cytochrome C. The second row: the cells were incubated with MitoTracker before fixation to visualize the polarized mitochondria. (B) The RPE-hTERT cells were fixed and co-stained with the antibodies against a-

tubulin (red) and cytochrome C (green). The nuclei were visualized by DAPI (blue). (C) The RPE-hTERT cells were treated with 10 nM of DZ, or 100 nM of vinblastine or 1 mM of taxol for 38 hours, and subjected to Western blot analyses for PARP1 cleavage. (D) The nuclear fragmentation in the DZ-treated RPE-hTERT cells with or without caspase inhibitors. cas-inh: caspase inhibitors, including caspase-3/7, -8, and -9 inhibitors, which were used in a combination to inhibit all the major caspases responsible for apoptosis. The annexin-V assays were used for the detection of apoptosis in the RPE-hTERT cells treated with 10 nM of DZ for 38 hours.

poly(ADP-ribose) polymerase 1 are not cleaved after DZ treatment in RPE-hTERT cells

A central event during apoptosis is the caspase-mediated protease cascade: when a series of caspases, including caspase-3, caspase-8 and caspase-9, are activated by the apoptotic signaling pathways, many protein targets are cleaved, one such target is poly(ADP-ribose) polymerase 1 (PARP1), and the cleavage of PARP1 confirms an irreversible commitment to cell death (Bharti et al., 2005; Duriez and Shah, 1997; Soldani and Scovassi, 2002). Full-length PARP1 is a protein with a molecular weight of 116 kilodaltons; and during apoptosis, PARP1 is cleaved into a product of 89 kilodaltons and a smaller product of 24 kilodaltons. Therefore, Western blotting analysis was utilized to examine whether PARP1 was cleaved in the DZ-treated RPE-hTERT cells, to see whether apoptosis occurred in these cells.

As demonstrated in Figure 13C, there were hardly any cleavage products after DZ or vinblastine treatment in RPE-hTERT cells when compared with untreated cells, while only a insignificant cleavage band was observed in the RPE-hTERT cells treated with taxol, indicating that the 38-hour treatment of MT inhibitors, which could induce the nuclear fragmentation, could not activate the classical apoptosis pathways in RPE-hTERT cells, consistent with previous observations.

Nuclear fragmentation in cells treated with DZ is caspase-independent

So far, four different apoptosis detection assays have been employed, and all suggested that, although DZ treatment induced a high frequency of nuclear fragmentation in RPE-hTERT cells, it did not induce a comparable level of apoptosis. These results led to a conclusion that the nuclear fragmentation observed in DZ-treated RPE-hTERT cells is not apoptosis. To further confirm this, caspase inhibitors that can prevent the activities of caspase-3, -8 and -9 were used, and no effect of these caspase inhibitors was observed on the percentages of nuclear fragmentation in the DZ-treated RPE-hTERT cells (Figure 13D). Hence, this nuclear fragmentation phenotype was confirmed not to be caused by apoptosis, or other caspase-dependent activities.

Nuclear fragmentation induced by DZ is mitotic slippage

As discussed above, the DZ-caused nuclear fragmentation was not a result of apoptosis, what exactly this phenotype was from therefore remained unknown. Researching through the literature, I found that the nuclear fragmentation observed in DZ-treated cells was similar to the products formed after mitotic slippage, which describes when cells that are originally arrested in M phase escape from this arrest, and generating progenies with abnormally shaped nuclei (Elhajouji et al., 1998).

In order to directly examine whether mitotic slippage was the reason for the nuclear fragmentation observed after DZ treatment, I attempted to transfect RPE-hTERT cells with the GFP-tagged histone protein H2B (H2B-GFP) plasmid to label the nuclei, hence I could utilize live-cell imaging to visualize the changes of the nuclei after DZ treatment in real-time. However, the transfection efficiency using RPE-hTERT cells was very low, despite of the use of

various transfection reagents and protocols. Therefore, UPCI:SCC40-H2B-GFP cells were employed, which is an oral squamous cell carcinoma cell line stably transfected with H2B-GFP.

UPCI:SCC40-H2B-GFP cells were treated with 10nM of DZ for 16 hours, to allow them to arrest at M phase prior to imaging, at which time their chromosomes were highly condensed. During the following 9.5 hours of recording, most of the mitotically-arrested cells exited mitosis, decondensed their chromosomes, and finally formed fragmented nuclei that persisted until the end of recording (Figure 14A). This is consistent with the description of classical mitotic slippage. After quantification, 70% of the recorded samples (16/23) demonstrated this mitotic slippage, resulting in fragmentation of the nuclei, which was very similar to what was observed in DZ-treated RPE-hTERT cells. Meanwhile, an additional 13% of recorded samples underwent a transient mitotic slippage, which was immediately followed by cell death. These cells originally demonstrated condensed chromosomes due to mitotic arrest, which then become decondensed, recondensed again, and quickly fragmented into many small pieces, indicating an abrupt cell death. Another 13% of cells were found to undergo mitotic catastrophe, which is a type of cell death during mitosis, characterized by the observation that the originally condensed chromosomes directly formed many small and highly condensed fragments without an intermediate process of decondensing. Lastly, I also observed one cell that remained arrested in mitosis and never exited, possibly indicating that the cell has entered senescence, as a response to the DZ treatment, which is consistent with the previous report (Tierno et al., 2009).

Therefore, I concluded that the nuclear fragmentation observed in the DZ-treated cells is a phenotype generated after mitotic slippage. It is interesting to note that in the live-cell imaging experiment, the cancer cell line UPCI:SCC40-H2B-GFP also demonstrated some cell death or senescence besides mitotic slippage, within the 25.5 (16+9.5=25.5) hours after addition of DZ.

These data suggest that cancer cells might have more complicated responses to DZ than RPE-hTERT cells did, consistent with the previously-reported senescence phenotype seen in cancer cells after DZ treatment (Tierno et al., 2009), which will be discussed in the section of the "Speculations and discussions".

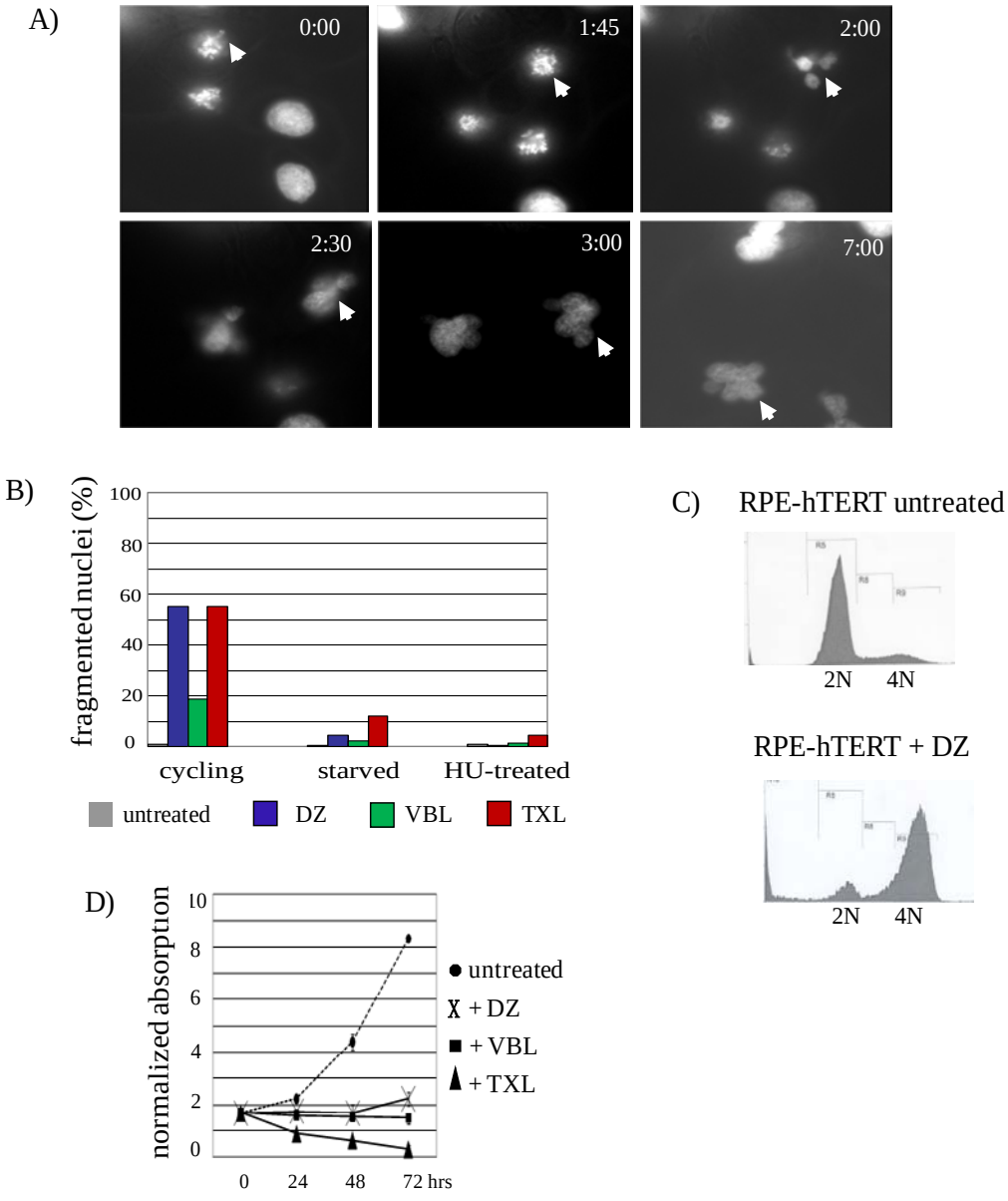

Figure 14 The nuclear fragmentation phenotype observed in the DZ-treated RPE-hTERT cells is actually mitotic slippage, which generates tetraploid cells.

(A) The end products of the mitotic slippage were the fragmented nuclei, visualized by live-cell imaging. The UPCI:SCC40 cells stably-transfected with GFP-H2B were treated with 10 nM of DZ for 16 hours prior to the 7-hour live-cell microscopy videoing. The arrows point to a cell that was first arrested in mitosis due to the DZ treatment, and then underwent mitotic slippage, resulting in the fragmented nuclei. Timestamps: hours:minutes. (B) Mitotic slippage required active cell cycling. Serum-starvation or 4 mM of hydroxyurea (HU) were used to stop the cell cycle prior to the treatment of 10 nM of DZ, or 100 nM of vinblastine, or 1 mM of taxol for 38 hours. (C) Flow cytometry analysis of the RPE-hTERT cells treated with 10 nM of DZ for 38 hours. (D) The cell proliferation was halted after the treatment of 10 nM of DZ, or 100 nM of vinblastine or 1 mM of taxol, demonstrated by the MTS assay.

Nuclear fragmentation induced by DZ is dependent on active cell cycle progression

The data so far suggested that the nuclear fragmentation observed in the DZ-treated cells was mitotic slippage, in order to confirm it, a further question was analyzed: was active cell cycling required for the nuclear fragmentation? The hypothesis is that if nuclear fragmentation is truly a phenotype associated with the cell cycle (as mitotic slippage is), stopping cell cycle progression would prevent nuclear fragmentation from occurring.

Two different methods were employed to arrest the cell cycle. One was serum starvation, which stopped cell cycle at G0/G1 phase, due to a lack of the growth stimuli to promote proliferation, while the other method was the treatment of hydroxyurea (HU), a ribonucleotide reductase inhibitor that can block DNA synthesis, therefore arresting cells in S phase (Cooper, 2003; Koc et al., 2004).

These two treatment arrested cells at different phases in the cell cycle, but both yielded the same effect: the nuclear fragmentation that were observed in the cycling cells after DZ treatment was now inhibited (Figure 14B), consistent with the above hypothesis. In fact, the

cells arrested at either G0/G1 phase or S phase seemed to demonstrate the same oval-shaped nuclei after DZ treatment, as those of interphase cells, with little or no condensed nuclei in the population, demonstrating little or no mitosis. Therefore, although DZ depolymerized their MTs, these pre-arrested cells probably did not become arrested at mitosis, as they were not cycling before the DZ treatment, hence mitotic slippage could not occur. These data again confirmed that the nuclear fragmentation observed after DZ treatment is indeed mitotic slippage, not a cell cycle-independent event.

The cells that slip from mitotic arrest after DZ treatment contain a 4N DNA content

Cells that slipped from the mitotic arrest caused by DZ theoretically contain doubled amounts of chromosomes, which were duplicated before mitosis. To test it, flow cytometry was employed to analyze the DNA contents in cells before and after the DZ treatment. As demonstrated in Figure 14C, untreated cells were mostly 2N in terms of their DNA contents, while a very small amount of cells demonstrated 4N DNA contents, which were of the mitotic population. However, after 38 hours of treatment with 10 nM of DZ, most cells demonstrated 4N DNA contents, while only a small portion still had 2N DNA content (Figure 14C), indicating that most RPE-hTERT cells after 38 hours of DZ treatment are tetraploid cells. These cells may not be able to proliferate again, due to a post-mitotic checkpoint, which will be discussed later in the model in the "Speculations and discussions" section of this chapter.

Consistently, the proliferation assays also revealed that, instead of the exponential growth of untreated cells, DZ-treated cells stopped proliferation, similar to the vinblastine or taxol-treated cells (Figure 14D). Therefore, my data suggest that the DZ-treated noncancer cells are

first arrested at mitosis, then abnormally escaped from this mitotic arrest, forming fragmented nuclei with 4N DNA contents, and these cells would probably not divide any further.

2.2.3.2 Mitotic slippage in cells treated with DZ is dependent on cyclin B degradation

It has been indicated that the nocodazole-treated cells undergo mitotic slippage because their spindle assembly checkpoint (SAC) cannot completely prevent a slow but continuous degradation of cyclin B (Brito and Rieder, 2006). Hence I tested the hypothesis that the mitotic slippage observed in the DZ-treated cells was also dependent on the destruction of cyclin B.

A series of time points were taken every four hours from 0 to 48 hours after the DZ treatment. At each time point, Western blotting was employed to monitor the protein level of cyclin B, and the percentage of nuclear fragmentation was recorded. In order to ensure the cyclin B level and the percentage of nuclear fragmentation were representing the same population, one coverslip was placed in each 60mm petri dish, and cells for this experiment were seeded evenly on this petri dish. After 24 hours of cell culture, DZ was added into the culture medium for the indicated time, and finally the coverslips were fixed and mitotically-arrested and slipped cells were counted, while the rest of the cells on the petri dish were subjected to Western blotting analysis.

As shown in Figure 15A, before DZ was added, the unsynchronized cell population demonstrated low levels of cyclin B, because most of the cells were not in mitosis. After DZ was added, cyclin B quickly accumulated within 4 hours of treatment; meanwhile mitotic index increased gradually, as a result from the fact that more and more cells entered M phase but none of them could finish mitosis due to the disrupted MTs by DZ. At 16 hours after treatment, about half of the cells were arrested in mitosis and cyclin B remained at a high level. Afterward, the fragmented nuclei started to appear, while the mitotic population was slowly replaced by this

percentage of nuclear fragmentation. At 36 hours, the percentage of nuclear fragmentation peaked and persisted through the end of this experiment. Interestingly the level of cyclin B was sharply reduced after 36 hours, indicating that the SAC failed to prevent cyclin B degradation in the DZ-treated cells, therefore giving these cells a chance to escape from the mitotic arrest.

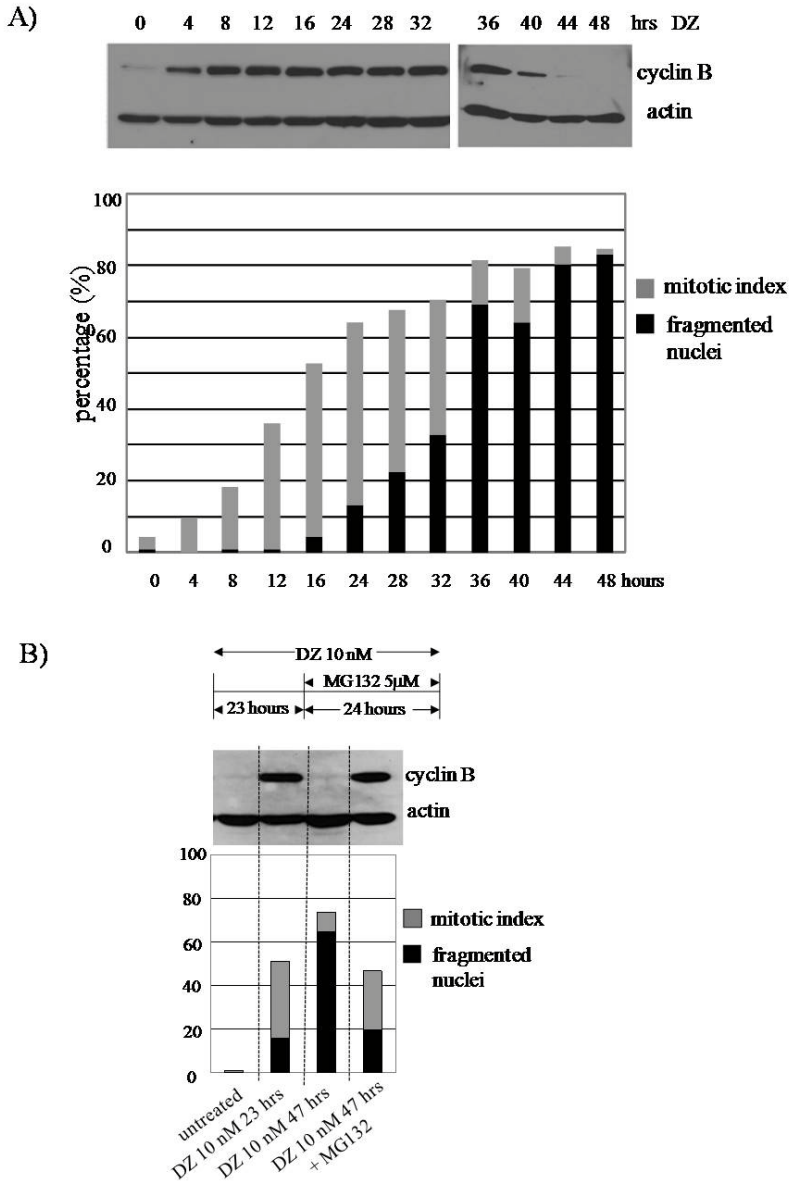

Figure 15 Cyclin B degradation is required for mitotic slippage. The RPE-hTERT cells were treated with 10 nM of DZ in the following experiments.

(A) Top: immunoblot analyses of cyclin B during a time course from 4 to 48 hours after the DZ treatment. Actin was used as a loading control. Bottom: the percentages of the mitotic slippage and the mitotic indexes analyzed at the same time points as in the top panel. (B) Top: a schematic experimental design. The cells were treated with DZ for 47 hours in total. 5 mM MG132 was added 23 hours after DZ was added, to avoid a toxicity effect on the cells. Bottom: the cyclin B protein levels and the percentages of mitotic slippage were analyzed as indicated in the above experimental design.

These results suggested that the mitotic slippage in the DZ-treated cells was accompanied by cyclin B destruction, consistent with my hypothesis. However, a more direct test would be to see whether mitotic slippage could still occur, when the degradation of cyclin B was blocked. Therefore MG132, a cell-permeable potent proteasome inhibitor, was used. As MG132 has been reported to cause G1 arrest and apoptosis in some cell lines (Zhang et al., 2008), and as the RPE-hTERT cells treated with MG132 for 48 hours in my experiment were mostly detached from the petri dish, I decided to add MG132 in the middle of the DZ treatment. At the 24-hour time point post addition of DZ, the cells were already arrested in mitosis and about to begin mitotic slippage, therefore adding MG132 at this time could prevent the cyclin B degradation for the purpose of my studies, without causing as much toxicity as the prolonged treatment (48 hours).

As we expected, 24 hours after DZ was added, RPE-hTERT cells demonstrated low levels of mitotic slippage while a great portion of cells were still arrested in mitosis, along with a high level of cyclin B. After MG132 was added, even at 47-hour time point post DZ treatment (23 hours after MG132 addition), cells still demonstrated similar phenotypes as the 24-hour time point post DZ treatment, which was characterized by high percentages of mitotic indices, low percentages of mitotic slippage, and high levels of cyclin B (Figure 15B). In a control experiment where MG132 was not added, mitotic slippage occurred in the majority of the

population at the 47-hour time point post DZ treatment as expected, at the same time the mitotic index was very low and cyclin B was almost completely eliminated (Figure 15B). These data clearly indicated that the protease activity, plausibly for cyclin B destruction, was required for mitotic slippage to occur in the DZ-treated cells.

Collectively, my data demonstrated that mitotic slippage in the DZ-treated RPE-hTERT cells is dependent on cyclin B degradation, which could be a result from a weak or a gradual leaking SAC. As discussed in the "CELL CYCLE" section of Chapter I, the APC/C complex is responsible for the ubiquitination of cyclin B and securin, for their sequential proteolysis; but the activities of APC/C is normally repressed, by the binding of cdc20 to MCC proteins, when unattached or weakly attached kinetochores are present. Therefore, a question remains whether APC is slowly attenuated to mediate this mitotic slippage observed in the DZ-treated cells and if so, how, which will be discussed in the model in the section of "Speculations and discussions".

2.2.3.3 The role for p53 in mitotic slippage in the cells treated with DZ

p53 has been conventionally believed to play essential roles in the cell cycle regulation, for example, p53 is shown to control the G1 and G2/M cell cycle checkpoints (Agarwal et al., 1995). Therefore, I analyzed whether p53 played a role in the mitotic slippage observed in the DZ-treated cells.

Western blotting analysis was used to test whether p53 was stabilized upon DZ treatment in the RPE-hTERT cells, by taking a series of time points. The results demonstrated that, within 4 hours after DZ's addition, p53 level was dramatically increased, indicating the stabilization of p53, which persisted through the 48-hour time point, the end of this experiment (Figure 16A). Comparable results were observed in the cells treated with vinblastine or taxol, suggesting that p53 is up-regulated in the noncancer cells in response to the MT inhibition.

Next, in order to test whether the mitotic slippage could still occur in the absence of p53, small interfering RNA (siRNA)-mediated knockdown of p53 was performed. Western blotting was employed to verify the efficiency of knockdown; ionizing radiation (IR), which is known to cause DNA damage and stabilize p53, was used to confirm the knockdown of p53 (Figure 16B). These RPE-hTERT cells with p53 knockdown were treated with DZ, and the percentages of nuclear fragmentation were quantified to demonstrate the levels of mitotic slippage. Surprisingly, after DZ treatment, RPE-hTERT cells with p53 knockdown continued to undergo mitotic slippage, similar to the control cells containing the intact p53. What's more interesting is that, these p53-knockdown cells showed even a higher percentage of mitotic slippage after the DZ treatment, than their respective control cells (Figure 16B). These results indicate that p53 is not required for the mitotic slippage observed in the DZ-treated cells, rather it might interfere with the process of mitotic slippage.

To further confirm this result, HFF-hTERT-shp53, an immortalized noncancer cell line that was stably depleted of p53 via shRNA, and its respective control cell line HFF-hTERT, were employed (a gift from Dr. Edward Prochownik, Children's Hospital, University of Pittsburgh). Western blotting analyses revealed an almost complete depletion of p53 in HFF-hTERT-shp53 cells, even after the IR treatment. Consistently, the DZ-treated HFF-hTERT-shp53 cells also demonstrated mitotic slippage, although these stable cell lines did not show an increase in mitotic slippage after the DZ treatment, when compared with their control cells (Figure 16C), which was slightly different form the results obtained in the RPE-hTERT cells with transient knockdown. Furthermore, vinblastine and taxol treatments also demonstrated similar results, supporting the conclusion that p53 was dispensable for mitotic slippage.

Collectively, the mitotic slippage does not require p53, interestingly p53 might play an inhibitory role during the process of mitotic slippage. The reason why the stable-knockdown cell lines showed slightly different results than the transient-knockdown cells may be due to the possibility that, in the stable-knockdown cells, certain proteins that are involved in the p53-dependent pathways to regulate mitotic slippage might have been compromised during the selection procedure to generate stable cell lines, therefore an increase in mitotic slippage after DZ treatment would not be observed in these stable cell lines. The exact role for p53 to block mitotic slippage is not yet understood, but will be discussed in the model in the section of "Speculations and discussions".

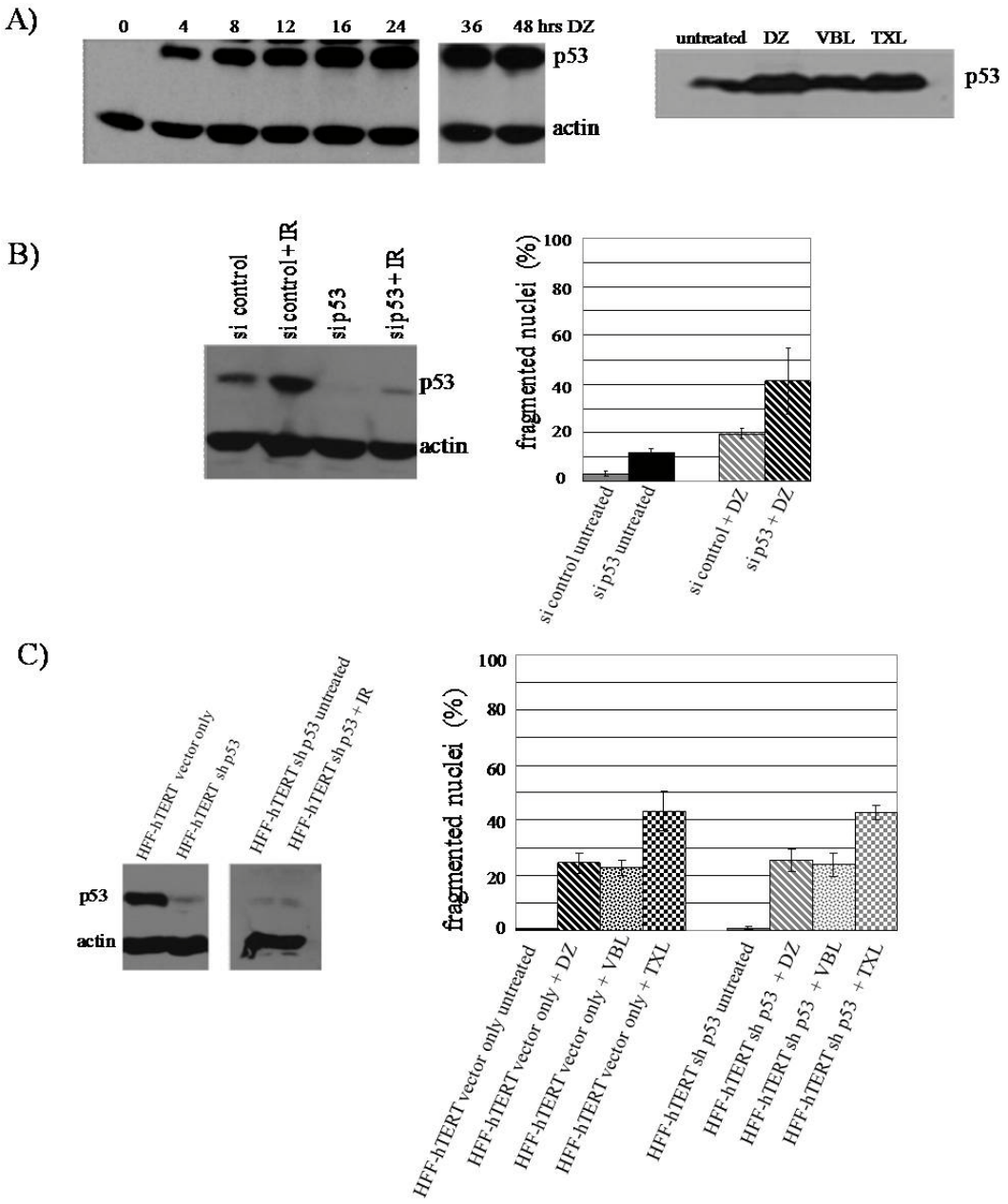

Figure 16 p53 is stabilized in the RPE-hTERT cells after DZ treatment, but is not required for mitotic slippage.

(A) Left: immunoblot analyses of p53 in the RPE-hTERT cells treated with 10 nM of DZ, for different time courses ranging from 4 to 48 hours. Right: immunoblot analyses of p53 in the RPE-hTERT cells treated with 10 nM of DZ, or 100 nM of vinblastine or 1 mM of taxol for 38 hours. (B) Left: immunoblot analyses of p53 in RPE-hTERT cells containing wild type p53 or p53 knockdown. Right: the percentages of mitotic slippage in the RPE-hTERT p53-wild type and p53-knockdown cells treated with 10 nM of DZ, or 100

nM of vinblastine or 1 mM of taxol for 38 hours. (C) Left: immunoblot analyses of p53 in the HFF-hTERT vector only and the HFF-hTERT shp53 (stable-knockdown) cells to confirm the successful knockdown of p53. Right: the percentages of the mitotic slippage in the HFF-hTERT vector only and the HFF-hTERT shp53 cells treated with 10 nM of DZ, or 100 nM of vinblastine or 1 mM of taxol for 38 hours.

2.2.4 DZ-treated cancer cells activate the apoptosis pathways, unlike the noncancer cells

As demonstrated above, RPE-hTERT cells were arrested in M phase after DZ treatment, then underwent mitotic slippage in a cyclin B degradation-dependent and p53-independent manner. The end products of this mitotic slippage were cells with 4N DNA contents, which probably would not proliferate any further due to their intact p53. Meanwhile, apoptosis pathways were not activated in these RPE-hTERT cells treated with DZ.

Similarly, when I examined another noncancer cell line HFF-hTERT after the treatment of DZ, no cleavage of PARP1 protein was observed, indicating that no apoptosis was executed in these HFF-hTERT cells treated with DZ. I also used primary cells UP3 (gift from Dr. Susan Gollin) to confirm that apoptosis pathways were not activated in the DZ-treated noncancer cells (Figure 17A).

However, cancer cells apparently responded to DZ differently from the noncancer cells. As shown in Figure 17B and C, all tested cancer cells, including four oral squamous cell carcinoma cells UPCI:SCC40, UPCI:SCC70, UPCI:SCC78, UPCI:SCC103, as well as U-2 OS and HeLa cells, demonstrated PARP1 cleavage after a 38-hour treatment with 10 nM of DZ, indicating that apoptosis was executed in these DZ-treated cancer cell lines. Similar PARP1 cleavage was observed when these cancer cells were treated with vinblastine and taxol, confirming that cancer cells tend to undergo apoptosis in response to MT inhibitors.

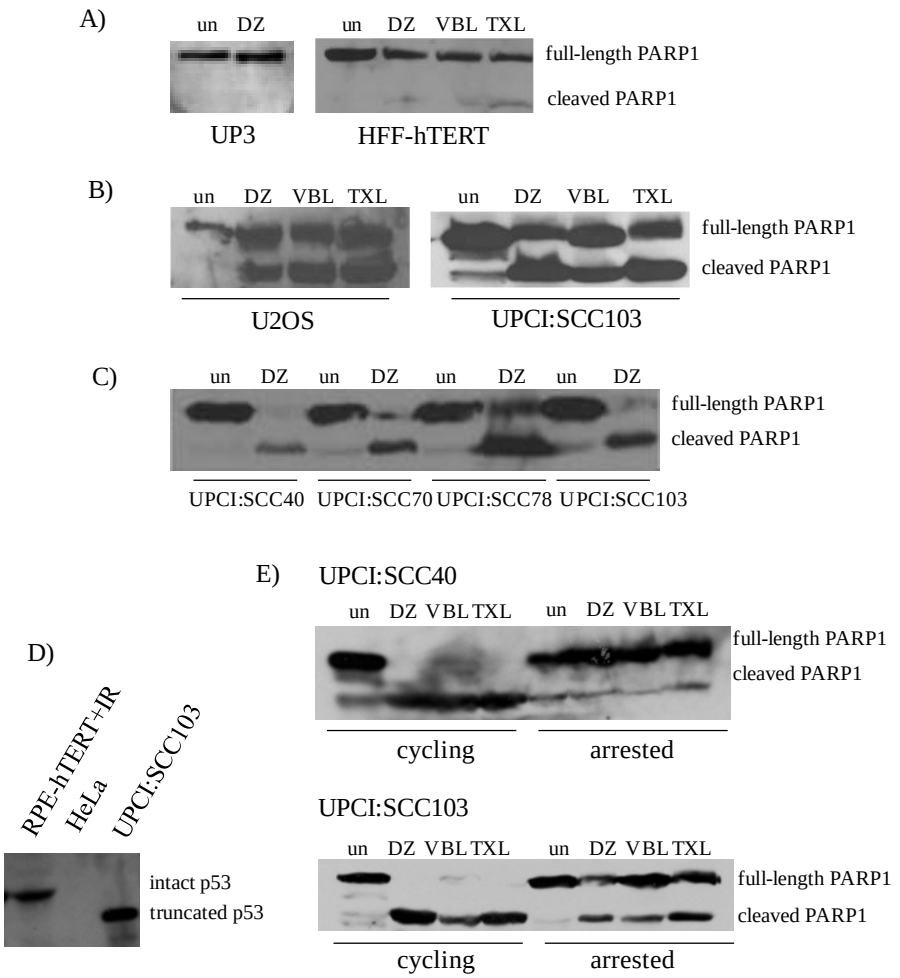

Figure 17 Unlike the DZ-treated noncancer cells that do not undergo apoptosis, cancer cells activate the apoptosis pathways in response to DZ.

PARP1 cleavage was used to indicate apoptosis, examined by the immunoblot analyses in the following experiments. un: untreated. (A) immunoblot analyses of PARP1 cleavage after 10 nM of DZ treatment for 38 hours in noncancer cells (UP3, HFF-hTERT). (B) and (C) immunoblot analyses of PARP1 cleavage in different cancer cell lines after 10 nM of DZ treatment for 38 hours. (D) p53 in RPE-hTERT (after IR treatment), HeLa, UPCI:SCC103 cells. (E) immunoblot analyses of PARP1 cleavage after the treatment of 10 nM of DZ, or 100 nM of vinblastine or 1 mM of taxol for 38 hours, in the cycling or non-cycling (serum-starved) cancer cells.

2.2.4.1 The apoptosis pathways activated in DZ-treated cancer cells does not require p53

It is known that p53 is either mutated or missing in many cancer cells. My Western blotting data also revealed that UPCI:SCC103 cells contain a truncated p53, whose molecular weight is less than the full-length p53 (Figure 17D). In addition, HeLa cells do not possess a stable p53, as Western blotting could not detect p53 in HeLa cells (Figure 17D), also consistent with previous reports (Liang et al., 1995). Therefore, the apoptosis pathways activated by DZ do not require p53, at least in some cancer cell lines.

2.2.4.2 The apoptosis pathways activated in some DZ-treated cancer cells seem to require active cell cycling

Lastly, I was curious to find out whether the apoptosis pathways induced by DZ in cancer cells were also dependent on active cell cycling, as was the mitotic slippage. Therefore, UPCI:SCC40 cells were serum-starved to stop the normal progression of their cell cycle, prior to the DZ treatment. Interestingly, little or no PARP1 cleavage was observed in these non-cycling UPCI:SCC40 cells treated with DZ, or vinblastine and taxol (Figure 17E), indicating that the apoptosis induced by the MT inhibitors in UPCI:SCC40 cells depended on active cell cycling.

Similarly, the non-cycling UPCI:SCC103 cells exposed to the MT inhibitors demonstrated less PARP1 cleavage, when compared with the cycling UPCI:SCC103 cells receiving the same treatment (Figure 17E). These results suggest that the activated apoptosis pathways in some DZ-treated cancer cells require active cell cycle progression, although their detailed mechanism needs further examination.

2.3 SUMMARY

In this chapter, I explored and contrasted the cellular responses of cancer and noncancer cells to a newly-synthesized MT disruptor, DZ. Common effects caused by typical MT disruptors including MT depolymerization, mitotic arrest and proliferation inhibition, were all observed in both cancer and noncancer cells after the DZ treatment. In addition, DZ could induce apoptosis in cancer cells, but not in noncancer cells. Instead, mitotic slippage was observed in the DZ-treated noncancer cells, which was highly dependent on the destruction of cyclin B, but did not require p53. DZ was also demonstrated to have similar effects as other MT inhibitors, such as vinblastine and taxol, suggesting a therapeutic potential for this compound.

2.4 SPECULATIONS AND DISCUSSIONS

Besides my results as summarized above, there are also a few interesting observations that will be further analyzed below and may be worth further investigation in the future.

2.4.1 p53's potential role in mitotic slippage

As demonstrated previously, the mitotic slippage observed in the DZ-treated RPE-hTERT cells seemed not to depend on p53; moreover, when p53 was transiently knockdown in the RPE-hTERT cells, a slight increase in the percentage of cells undergoing mitotic slippage was observed after DZ treatment, suggesting that p53 might negatively regulate the process of mitotic slippage.

Therefore, I speculate that p53 could play an inhibitory role in the mitotic slippage, through down-regulation of cdc20, a key molecule to activate the APC/C complex for cyclin B degradation. It has been demonstrated that the ectopically expressed p53 can repress the expression of cdc20 by directly binding to the promoter of the cdc20 DNA sequence, thus causing chromatin remodeling to inhibit its transcription (Banerjee et al., 2009); therefore, it is plausible that the p53 proteins that were stabilized by DZ treatment could also interfere with cdc20 expression, thus holding back the activities of APC/C and hindering the proteolysis of cyclin B, the key event for mitotic slippage.

If p53 indeed plays an inhibitory role in mitotic slippage; I could therefore propose a model where p53 is involved in the two sequential "checkpoints" in response to DZ or other MT inhibitors (Figure 18). The first checkpoint is the classical SAC, which arrests cells at mitosis when MTs are disrupted. p53 may facilitate this SAC by down-regulating cdc20 and inhibiting the activation of APC/C, as described above. However, SAC sometimes may be "leaky" or attenuated by unknown mechanism (even with the assistance of stabilized p53); hence cells may abnormally exit from the mitotic arrest, becoming arrested at the post-mitotic G1 phase, due to a post-mitotic checkpoint, which is very likely to involve p53 as a central regulator based on previous publications (Blagosklonny et al., 2004; Lanni and Jacks, 1998), and which will be discussed further in a later part of this section.

On the other hand, it is also possible that the increased percentages of mitotic slippage observed in the DZ-treated cells after p53 knockdown, may be simply due to the fact that cells proliferate faster in the absence of p53, which is demonstrated in the previous reports (Jones et al., 1997), as well as observed during my culturing of the HFF-hTERT-shp53 and control HFF-hTERT cells. Intuitively, when the overall cell cycle is accelerated by the p53 knockdown, the

time needed for cells to exit from mitotic arrest may be shortened accordingly, hence generating a higher percentage of mitotic slippage in these cells with p53 knockdown.

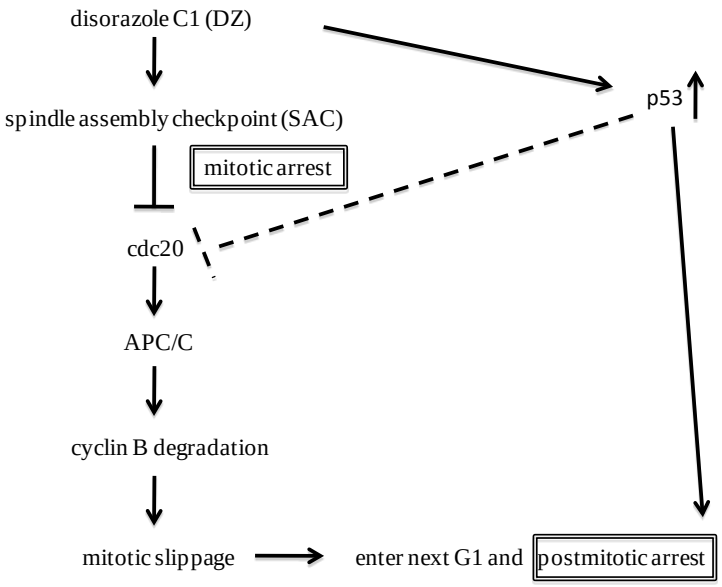

Figure 18 Model: the response of noncancer cells to the microtubule inhibitors.

DZ is proposed to activate two sequential cell cycle checkpoints. The first is the APC-dependent arrest at mitosis; when that fails, a second arrest at G1 is observed. p53 stabilization may mediate both events, but is not required for the mitotic slippage that acts independent of the conventional p53-dependent apoptosis pathways. APC/C: anaphase-promoting complex/cyclosome.

2.4.2 How does nuclear fragmentation take place? Are MTs involved?

One of the key phenotypes observed in the noncancer cells treated with DZ was that they underwent mitotic slippage and formed fragmented nuclei. It remains unknown why these cells failed to generate the interphase nuclei, as normal cell would do when they exit mitosis. The biggest difference between these mitotic-slipped cells and the normal cells is that these mitosis-slipped cells lost the integrity of MTs after the treatment of DZ. Therefore it could be likely that the nuclear fragmentation is a result from the disturbed MT or centrosomal structures.

Indeed, the immunofluorescence images of these RPE-hTERT cells that were treated with DZ and underwent mitotic slippage demonstrated some bundle-like structures that were stained positively by α-tubulin antibodies and seemed to wrap around the fragmented nuclei (Figure 12A). Furthermore, with the help with our collaborator Rbaibi Youssef, electron microscopy (EM) was employed and revealed filaments around these fragmented nuclei in DZ-treated cells (Figure 12B). It would be informative if immuno EM could be employed to identify whether these filaments were MTs, and knowing the exact organization of the residual MTs around the fragmented nuclei would be useful to confirm the possible functions of MTs in the process of nuclear fragmentation.

It could be possible that the residual MT filaments actively accumulate around the different groups of decondensed chromosomes in a mitotic-slipped cell, therefore *actively* causing the fragmented nuclei. Alternatively, it could also be possible that when the chromosomes become decondensed as the cell abnormally exits from the mitotic arrest, the nuclear envelop tries to reassemble around the chromosomes, but in an irregular manner (maybe utilizing some MT-independent mechanism), causing the fragmented nuclei, which is then followed by the residual MTs *passively* accumulating around these newly-formed fragmented nuclei. A third possibility could be that the MTs might play a role in guiding the nuclear envelop reassembly, therefore disrupting MTs could interfere with the nuclear envelop re-formation around the decondensed chromosomes, therefore leading to several fragmented small nuclei.

2.4.3 Final fate of the noncancer cells exited from the mitotic arrest

The RPE-hTERT cells that were arrested at mitosis by DZ presumably have already duplicated their chromosomes; therefore, they become tetraploid cells with fragmented nuclei after mitotic

slippage. As introduced previously, tetraploid cells might generate problematic products that are associated with polyploidy, aneuploidy or genomic instability, if they undergo more rounds of cell division. Interestingly, there is a specific checkpoint called the "post-mitotic checkpoint", which has been reported to cause G1 arrest in the cells that have abnormally exited from the mitotic arrest (Blagosklonny et al., 2004), therefore preventing further proliferation of these cells. It is plausible that the DZ-treated RPE-hTERT cells that demonstrated 4N DNA contents and fragmented nuclei were also arrested at G1 phase by this post-mitotic checkpoint.

This post-mitotic checkpoint is thought to depend on the p53 activation, which in turn up-regulates p21 (Blagosklonny et al., 2004), thus arresting cells at G1 phase as introduced in the "CELL CYCLE" section of Chapter I. As the stabilization of p53 in the DZ-treated RPE-hTERT cells was observed (Figure 16), my data is therefore consistent with the prediction that these cells may be arrested by the post-mitotic checkpoint.

The final fate of these RPE-hTERT cells after the DZ treatment might be an interesting question. Presumably they are arrested at G1 phase after the 38 hours of DZ treatment, but the long-term effect of DZ on cells has not been tested. At the day 3 after the addition of DZ, RPE-hTERT cells still did not demonstrate apoptosis (data not shown), hence these cells may eventually end up in senescence, similar to what was reported in some DZ-treated cancer cells (Tierno et al., 2009). Alternatively, these RPE-hTERT cells may ultimately execute some cell death pathways long after the DZ treatment, which is beyond the scope of this analysis but might still be appealing to investigate in the future.

2.4.4 Cancer cells versus noncancer cells *or* apoptosis-prone cells verse apoptosis-reluctant cells?

It is interesting to note the different responses to DZ between certain cancer and noncancer cells: the cancer cells executed apoptosis while the noncancer cells did not. These data suggest a therapeutic potential of DZ, however, what cellular event determines these completely different cellular fates is not clear. In addition, it is possible that not all cancer cells would execute apoptosis in response to DZ (or vinblastine and taxol), for example the human lung adenocarcinoma A549 cells, whose viability was only marginally affected by the DZ treatment, could be one of these exceptions in cancer cells. It is worth noting that A549 have been previously categorized into the apoptosis-reluctant cells (Blagosklonny et al., 2006; Demidenko and Blagosklonny, 2004), therefore these cells might be intrinsically hard to activate the apoptosis pathways due to a possible defect in their apoptosis pathways.

One plausible explanation for the little effect of DZ on A549 cells may be that, A549 cells express ABCB1 transporters on their plasma membranes, which are ATP-driven pumps mediating the export of many drugs from the cytoplasm (Becker et al., 1992; Mercier et al., 2004; Oguri et al., 2008). Hence, the real concentration of drugs in A549 cells can be much lower than what was added, resulting in little effect of the drugs on A549 cells. Indeed, other researchers have reported the docetaxel-resistance and vincristine-resistance A549 cells with the ABCB1-dependent or ABCB1-independent mechanisms (Chiu et al.), supporting the hypothesis that the low effect of DZ on A549 cells could be due to the overexpressed ABCB1 transporters on the membrane of A549 cells.

Therefore, it is possible that noncancer cells and some cancer cells belong to the group of apoptosis-reluctant cells, which do not execute the apoptosis pathways upon MT inhibitor

treatments. Meanwhile, other cancer cell lines, especially the oral squamous cell carcinoma cells, HeLa, and U2-OS, may belong to the group of the apoptosis-prone cells (Blagosklonny, 2007). The cellular-level reasons behind the differences between the apoptosis-reluctant and apoptosis-prone cells are still not understood. It might be explained by the different expression levels of ABCB1 transporter, or similar transporter, as described above.

2.4.5 Apoptosis in the DZ-treated cancer cells

Apoptosis induced in the cancer cells after the DZ treatment may be more complicated than it appears. There are many different apoptosis pathways (Janz et al., 2007; Peled et al., 1996), some cancer cells may utilize p53-dependent pathways while others can use p53-independent pathways. Therefore, although all of the tested cancer cell lines demonstrated PARP1 cleavage after DZ treatment, the mechanisms may be different. For example, U-2 OS cells have been reported to contain wild-type p53 (Kastan et al., 1992), which may be involved in the apoptosis pathways activated after the DZ treatment; however, HeLa and UPCI:SCC103 cells do not have full-length p53 (Figure 17), hence the apoptosis pathways activated in these two cell lines after the treatment of DZ must be p53-independent.

In addition, although the phenotype of nuclear fragmentation was mainly observed in the DZ-treated RPE-hTERT cells, this cannot exclude the possibility that the cancer cells might also undergo mitotic slippage. It is possible that some of the cancer cells first exit from the mitotic arrest, and then activate their cell death responses. Hence it might be likely that in the same time frame, the noncancer cells treated with DZ only start to abnormally exit from the mitotic arrest, while the cancer cells treated with DZ have already finished mitotic slippage and have decided to commit to apoptosis. For example, the UPCI:SCC40-H2B-GFP cells used for live-cell imaging

indeed demonstrated mitotic slippage, as early as the 16-25 hours post DZ treatment; and by the 38 hour after the DZ treatment, these cells have already exhibited a almost complete cleavage of PARP1, indicating that apoptosis dominantly took place at the 38 hour after addition of DZ. Therefore, the conclusion is that after 38 hours treatment of 10 nM of DZ, the cancer cells activated apoptosis, whereas the noncancer cells only exited the mitosis arrest (mitotic slippage) and probably were arrested again by the post-mitotic checkpoint.

3.0 CHAPTER III. THE NOVEL ROLE FOR GPIBA IN CYTOKINESIS AND TETRAPLOIDIZATION IN CANCER CELLS.

Figures 39 are 40 have been published in (Li et al.).

3.1 INTRODUCTION

GpIbα is the key subunit of the von Willebrand factor (vWF) receptor, which is a complex composed of multiple glycoproteins identified on the surfaces of platelets and megakaryocytes. Each vWF receptor complex consists of 2 molecules of GpIbα and 4 molecules of GpIbβ that are disulfide-linked, in addition to 2 molecules of GPIX and 1 molecule of GPV that are non-convalently associated with GpIbα/β, therefore the vWF receptor is also referred to as the GpIb/IX/V complex (Luo et al., 2007; Rivera et al., 2000).

The interaction between vWFs and GpIb/IX/V complexes has been reported to be essential for the initiation of platelet adhesion to the ECM, or to the already adherent platelets (Beumer et al., 1995; Kulkarni et al., 2000), therefore it is critical for blood clotting. Patients lacking GpIb/IX/V complexes or possessing dysfunctional GpIb/IX/V complexes, suffer from the Bernard Soulier syndrome (BSS), a strong bleeding diathesis (Clemetson and Clemetson, 1995). More specifically, GpIbα is shown to play a central role in mediating the interaction

between vWFs and GpIb/IX/V complexes during hemostasis, and mice with deficient GpIbα also demonstrate the bleeding diathesis phenotypes, similar to the BSS patients (Denis et al., 1998; Ware et al., 2000).

In platelets and differentiated megakaryocytes, GpIbα is found to be expressed and localized at the cell cortex (Debili et al., 1992; Moran et al., 2000; Ulsemer et al., 2001). It is a large protein composed of 610 amino acids, with a molecular weight of 140 kilodaltons, due to the extensive glycosylation after protein translation. There are four domains in GpIbα, including an amino-terminal domain, a heavily glycosylated mucin-like stalk, a single transmembrane domain and a cytoplasmic tail domain.

The N-terminus of GpIbα contains several leucine-rich repeats, and is the major ligand binding domain, where the vWF and the thrombin bind (Takamatsu et al., 1986; Yamamoto et al., 1991). In addition, other molecules such as TSP-1, high-molecular-weight kininogen, coagulation factors XI and XII have also been shown to bind to the N-terminus of GpIbα (Baglia et al., 2002; Bradford et al., 1997; Bradford et al., 2000; Jurk et al., 2003).

The mucin-like stalk of GpIbα contains many glycosylation sites, for example, it is estimated that there are five O-linked sites for every 13 amino acids (Andrews et al., 2003; Lopez et al., 1998). It is suggested that these posttranslational modifications may potentially be important for the GpIbα–mediated functions, as glycosylation is generally related to protein folding, stability and receptor binding (Delos et al., 2002; Garcia-Campayo et al., 2002; Konrad and Kudlow, 2002).

The cytoplasmic domain of GpIbα is vital for its localization and functions. For instance, filamin A has been demonstrated to interact with the C-terminal tail of GpIbα, which anchors the entire GpIb/IX/V complex to the cell cortex of platelets (Feng et al., 2003; Xu et al., 1998).

Furthermore, although the mechanism through which GpIbα initiates platelet aggregation is not completely clarified, it is suggested that the proteins associated with the cytoplasmic domain of GpIbα mediate this mechanism. Just to name a few examples, calmodulin and 14-3-3ζ are found to interact with GpIbα through its C-terminal tail, therefore suggesting that certain signaling pathways involving phosphatidylinositol 3-kinase (PI-3K), focal adhesion kinase (FAK), GTPase-activating proteins, Src-related tyrosine kinases, and/or tyrosine phosphatases, might be responsible for the aggregation and activation of platelets (Du, 2007; Ozaki et al., 2005).

In addition to its well-known importance in platelet activation and adhesion, GpIbα has recently been suggested by the laboratory of Dr. Edward V. Prochownik at Children's Hospital of Pittsburgh, to be involved in the tumorigenesis pathways downstream of the classic oncoprotein c-Myc. Firstly, GpIbα was identified as one of the most up-regulated proteins by c-Myc (Rogulski et al., 2005a; Rogulski et al., 2005b), and secondly, the overexpression of GpIbα has been related to the induction of tetraploid cells (Li et al., 2007). A later paper from the Prochownik lab further demonstrated that when the Rat1a cells overexpressing GpIbα are subcutaneously inoculated into nude mice large tumors develop, suggesting a tumorigenic consequence to GpIbα overexpression (Li et al., 2008).

In addition, GpIbα is widely overexpressed in various human cancer cells, but not in noncancer cells (Li et al., 2008), implying a link between GpIbα overexpression and tumor formation in human cells. Interestingly, deletion mutants of GpIbα that block the induction of tetraploidization demonstrate less transformation properties (Li et al., 2009), emphasizing the importance of tetraploidization in the tumorigenesis process. I therefore investigated the mechanism through which GpIba overexpression leads to tetraploidization.

3.2 RESULTS

3.2.1 GpIbα in interphase

As demonstrated by the Prochownik lab, GpIbα is expressed in non-platelet cells without expression of the other subunits of the vWF receptor (Li et al., 2009), suggesting that GpIbα might play certain roles unrelated to the platelet/megakaryocyte system, which leads to the following investigation.

Immunofluorescence was first employed to analyze the localization of GpIbα in interphase non-platelet cells, such as RPE-hTERT, HFF-hTERT, HeLa and UPCI:SCC103 cells. However, the antibodies against GpIbα did not recognize specific structures containing GpIbα in these cells during interphase, except for a slight accumulation of signals near the nuclei, where endoplasmic reticulum (ER) presumably localizes (Figure 19A). This may be due to the fact that GpIbα is a highly glycosylated membrane protein that needs to go through ER for the posttranslational modifications. Meanwhile, a different approach was adopted, by ectopically expressing the GFP-tagged GpIbα in HeLa cells, which demonstrated a specific localization of GpIbα' on the cortex of interphase non-platelet cells that will be analyzed below (Figure 19B).

3.2.1.1 GpIbα is colocalized with F-actin and filamin A on the cell cortex

As demonstrated in Figure 19B, some of the GpIbα protein has been found to localize on the cell cortex and form filament-like structures. Interestingly, when rhodamine-labeled phalloidin was used to stain the F-actin in these cells, a partial overlap between GpIbα and F-actin was observed, suggesting that at least a portion of GpIbα proteins were co-localized with

F-actin in non-platelet cells. Similar co-localization was also observed in another cell line, UPCI:SCC103, that was transfected with the GFP-tagged GpIbα (data not shown), therefore ruling out the possibility that the cortical localization of GpIbα was cell type-specific.

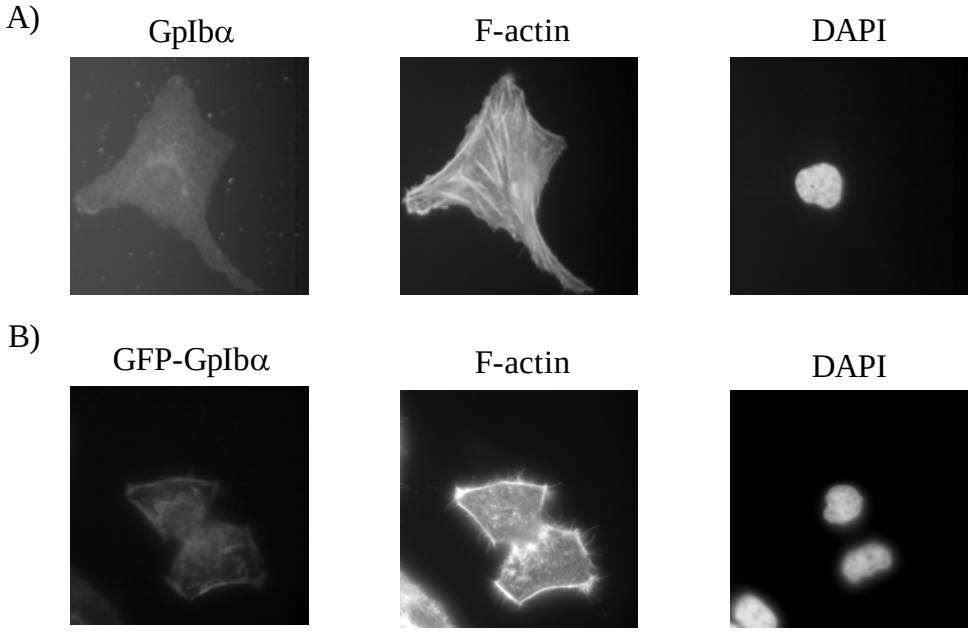

Figure 19 GpIbα in interphase non-platelet cells.

(A) RPE-hTERT cells, or (B) HeLa cells with GFP-GpIba, were fixed and stained with antibodies against GpIba. The actin filaments were visualized by rhodamine-phalloidin, and the nuclei were labeled by DAPI.

These results are not surprising, as GpIbα in platelets has been reported to anchor the entire GpIb/IX/V complex to the F-actin network underneath the plasma membrane, by interacting with filamin A, the major cross-linker for F-actin (Feng et al., 2003). Therefore, it seems that in non-platelet cells, GpIbα could also link to the F-actin network through filamin A.

To better visualize the colocalization between GpIbα and F-actin, confocal microscopy analysis was employed. A series of sections (about 10-12) were conducted for each single HeLa cell transfected with GFP-GpIbα, and stained with rhodamine-phalloidin. Indeed, the confocal

microscopy results also revealed that GpIbα formed filaments, and some of these GpIbα filaments were partially co-localized with the F-actin bundles (Figure 20A).

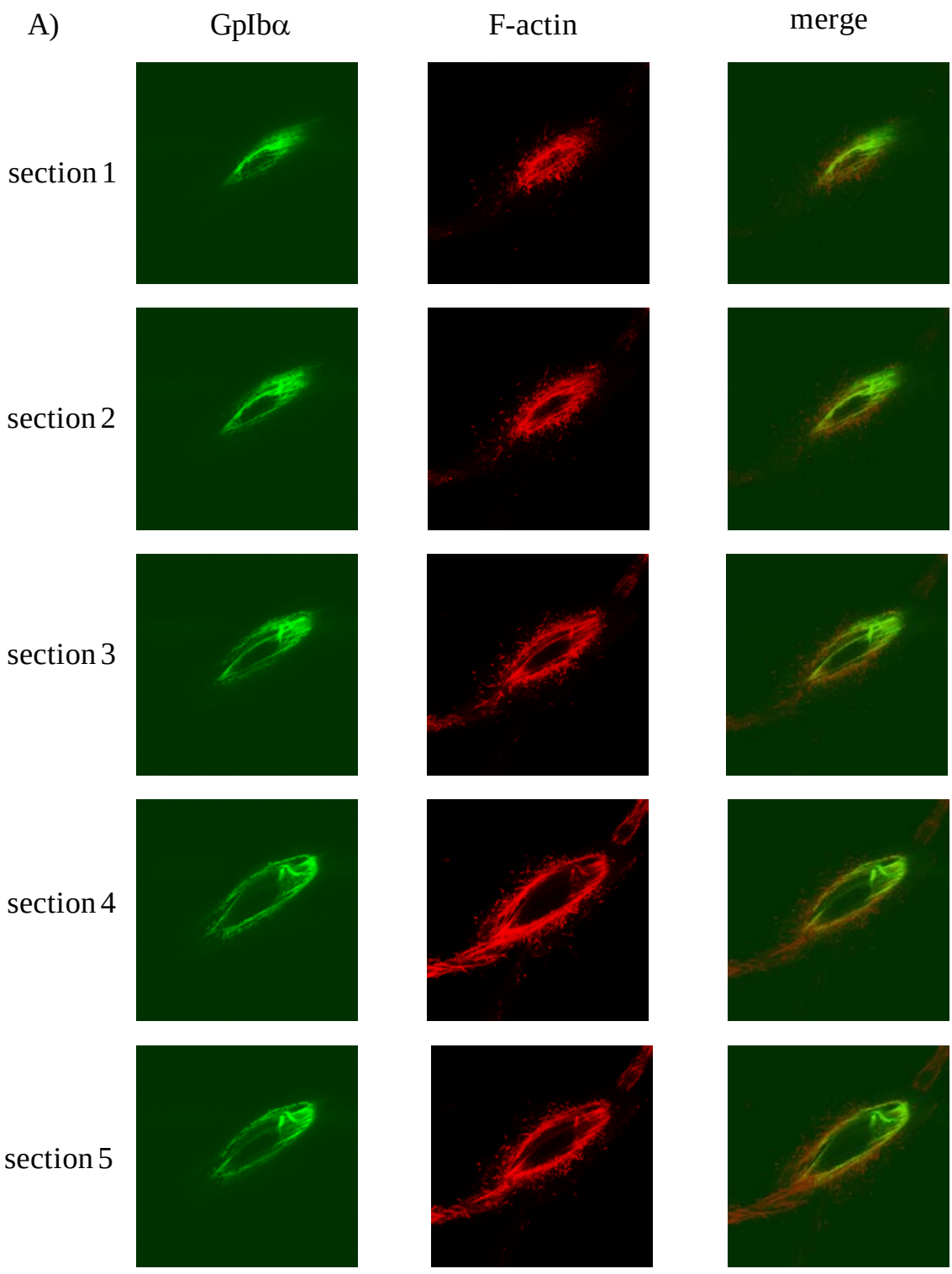

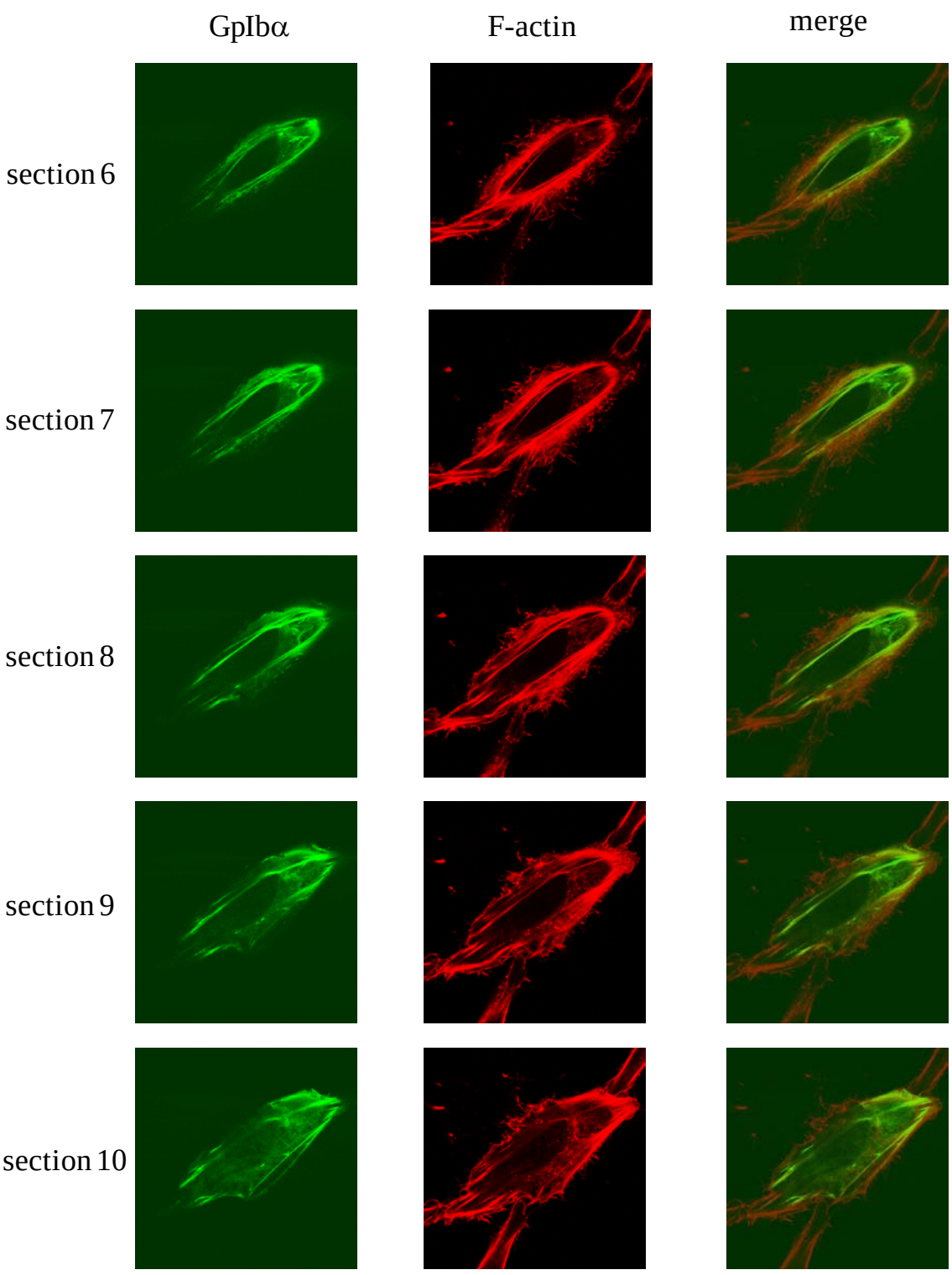
GpIbα
F-actin
merge
section 6
section 7
section 8
section 9
section 10

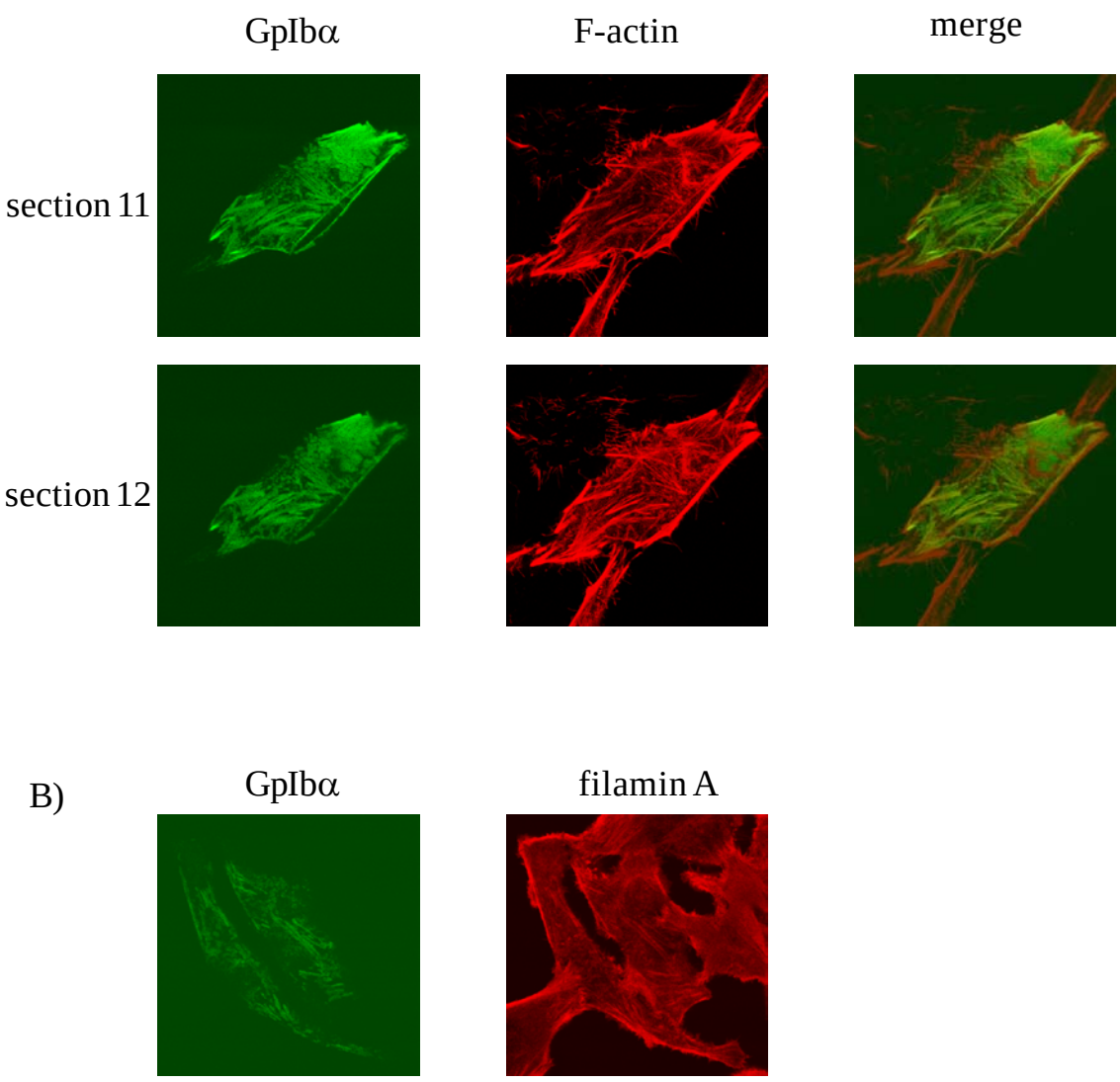

Figure 20 GpIbα, filamin A, and F-actin colocalization on the cell cortex, examined by confocal microscopy.

(A) HeLa cells transfected with GFP-GpIbα were fixed and stained with rhodamine-phalloidin. The samples were subjected to 12 optical sections with confocal microscope. Green: GFP-GpIbα. Red: F-actin. (B) The HeLa cells transfected with GFP-GpIbα were fixed and stained with antibodies against filamin A before the confocal microscopy analyses. Green: GFP-GpIbα. Red: filamin A. Pictures are representatives of at least 20 samples that were examined in each experiment.

Next, I examined filamin A in these HeLa cells transfected with GFP-GpIbα by immunofluorescence. Similarly, a partial co-localization between filamin A and GpIbα was also observed (Figure 20B), suggesting that in non-platelet cells, GpIbα, filamin A and F-actin may form a complex, which can localize to the cell cortex.

It is interesting to note that there are other GpIbα filaments that were not co-localized with F-actin, suggesting that GpIbα may have multiple localizations and functions. It is also interesting to note that GpIbα seemed to form thick bundles at the bottom of a cell, and there appeared to be diffuse GpIbα proteins in the last serial section, which was the plane where the cell made contact with the ECM, suggesting that GpIbα might have additional functions in cell-cell or cell-ECM adhesion or signaling pathways. This is possibly due to the fact that GpIbα binds to filamin A, and filamin A is known to interact with integrins (Sharma et al., 1995), which are key proteins involved in the cell-cell/ECM adhesion and cell signaling pathways, controlling the morphology and motility of the cell (Brown and Hogg, 1996; Faull and Ginsberg, 1996), however this is beyond the scope of my research, and therefore will not be discussed in this chapter.

3.2.1.2 GpIbα's distributions in cells examined by cellular fractionation

As some of the GpIbα proteins appeared to be diffuse in the cytoplasm of cells, as demonstrated by the confocal microscopy analysis, I took another approach to examine whether these GpIbα proteins were freely soluble molecules in the cytoplasm. HeLa cells transiently transfected with GFP-GpIbα were subjected to cellular fractionation, where whole cells were lysed and separated into three fractions. The first fraction contained cytosolic proteins that were extracted from the cells, after digitonin permeabilized the plasma membrane; the second fraction

contained membrane proteins and their associated proteins, which were extracted by a different detergent, NP-40, from the pellet formed after the first digitonin extraction; while the last fraction was a pellet containing everything left over that was not solubilized by the NP-40 extraction, and was instead solubilized by sodium dodecyl sulfate (SDS).

Theoretically, freely soluble molecules in the cytoplasm should be enriched in the first fraction, while the membrane proteins and their associated structures should be enriched in the second fraction. Indeed, the cytosolic protein marker GAPDH accumulated mostly in the first fraction, whereas the membrane protein maker CD44 was mostly found in the second faction, indicating the cellular fractionation was successful (Figure 21).

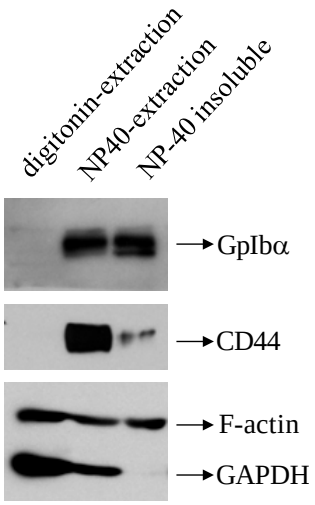

Figure 21 Cellular fractionation of HeLa cells transfected with GFP-GpIbα.

Cellular fractionation was carried out as described in the section of "Materials and Methods". The first fraction: digitonin-extracted faction that contained cytosolic proteins. The second fraction: the NP40-extracted fraction that contained membrane proteins and associated proteins. The third fraction: the NP40 insoluble fraction that contained everything that failed to be extracted by NP40, including nuclear proteins and insoluble cytoskeletal components, as well as unlysed cells. GAPDH was used as a control for the soluble proteins in the cytoplasm, and CD44 was used as a control for the membrane proteins.

However, I did not observe any GpIbα in the first fraction, indicating that none of GpIbα proteins were soluble in the cytoplasm. At least half of GpIbα was enriched in the second fraction and some in the third fraction, suggesting that GpIbα were associated with certain membrane structures, for example, the plasma membrane and/or the F-actin networks connected to the plasma membrane. Alternatively, as ER and its associated proteins were also enriched in the second fraction (data not shown), it would not be surprising to find that the membrane protein GpIbα, which needs to go through ER for posttranslational modifications, were also found in this faction.

It is interesting to note that actin was found in all of these three fractions, possibly due to the fact that cells contain both soluble actin proteins as well as polymerized actin filaments. The soluble actin was enriched in the first fraction, while some actin filaments, that are associated with the plasma membrane, could be co-fractionated with the membrane in the second fraction. In addition, some actin proteins have been reported to localize within the nuclei, therefore it was not surprising to observe them in the third faction.

In conclusion, the cellular fractionation data demonstrated that GpIbα was not freely soluble in the cytoplasm, suggesting that the seemingly 'diffuse' staining of GpIbα observed during confocal analysis was most likely associated with membrane structures within cells.

So far, these data suggest that GpIbα was partially co-localized with filamin A and the F-actin network on the cell cortex, and may be involved in certain actin-related functions in non-platelet cells. Meanwhile, it was also possible that GpIbα played additional roles, such as functioning in focal adhesion or signal transduction that are related to the adhesive interaction, as some portion of GpIbα seemed to localize at the focal planes of cells close to the ECM, and as the GpIbα binding partner filamin A is known to interact with integrins.

3.2.1.3 The cortical localization of GpIbα depends on the F-actin network, but not on the MTs

In order to investigate whether the GpIbα's interphase localization was dependent on F-actin, HeLa cells expressing GFP-GpIbα were treated with cytochalasin D to disrupt their F-actin networks, and were then subjected to confocal microscopy analysis. As expected, when F-actin lost its normal organization in cells, GpIbα was also disrupted and mislocalized (Figure 22A), indicating the dependency on F-action for GpIbα's cortical localization in interphase cells. Interestingly, some of the disrupted GpIbα appeared to still colocalize with the residual F-actin, suggesting that the localization of GpIbα was determined by the localization of F-actin.

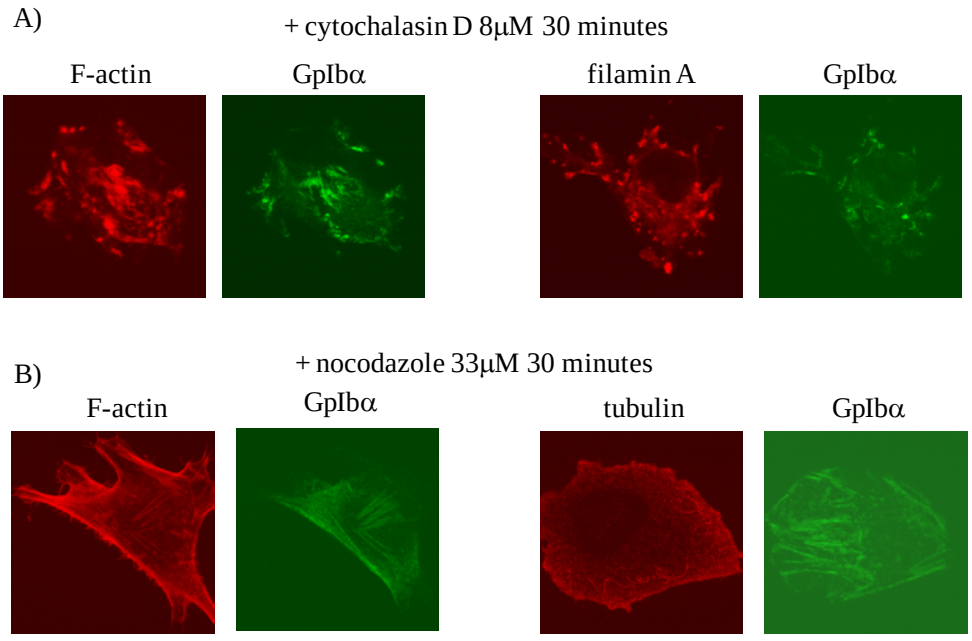

Figure 22 The cortical localization of GpIbα in cells is dependent on the actin network, not the MT network.

(A) The HeLa cells transfected with GFP-GpIbα were treated with 8 mM of cytochalasin D for 30 minutes before fixation, which were then stained with antibodies against filamin A or rhodamine-phalloidin. Samples were subjected to confocal microscopy analyses. Red: F-actin or filamin A. Green: GFP-GpIbα.

(B) The HeLa cells transfected with GFP-GpIbα were treated with 33 mM of nocodazole for 30 minutes, then stained with antibodies against α-tubulin or rhodamine-phalloidin. Red: F-actin or α-tubulin. Green: GFP-GpIbα. Pictures are representatives of at least 15 samples that were examined in each experiment.

However, when cells were treated with MT inhibitor nocodazole to disrupt their MTs, the organization of GpIbα was not affected, evidenced by the filament-like structures of GpIbα on the cell cortex after nocodazole treatment (Figure 22B). Therefore, the organization and localization of GpIbα in non-platelet cells seemed to depend on the F-actin network, but not the MT network.

3.2.1.4 GpIbα and the ER

Li *et al.* have demonstrated by Western blot analysis that GpIbα is predominantly found in the ER fractions of the Rat1a cells ectopically expressing GpIbα (Li et al., 2009). However, to my surprise, there was very little sign of ER localization of GpIbα in the HeLa cells that I examined. A typical ER localization would be enrichment around the nucleus, where the ER is localized. However, in the previous confocal analysis using HeLa cells transfected with GFP-GpIbα cells, most of GpIbα demonstrated filament-like structures on the cell boundary, and some enrichment towards the bottom of the cell, which seemed to be different from the predominant ER localization observed by Li *et al* by using fractionation. I have also expressed GFP only in HeLa cells as a control and did not observe any particular localization of GFP, which were diffuse throughout the cells (data not shown). This experiment rules out the possibility that the GFP localized on the cell cortex and forced GpIbα to localize to the cell cortex, although it still does not rule out the possibility that the localization of GpIbα is

influenced by the GFP tag. As I will demonstrate later in this chapter, the mitotic localization of GFP-GpIbα was verified by immunofluorescence microscopy analysis, therefore validating this experimental approach.

To further investigate this issue, I compared the localization of GpIbα with an ER marker protein, calnexin (Wada et al., 1991), by performing immunofluorescence staining with antibodies against calnexin using HeLa cells expressing GFP-GpIbα, and subjected these cells to confocal microscopy analysis. As indicated in Figure 23, calnexin formed many concentrated foci in an area around the nuclei in multiple focal planes, representing the localization of the ER in cells. Meanwhile, GpIbα still demonstrated the localization on the cell cortex, and showed very little colocalization with calnexin, suggesting that the GFP-GpIbα that was ectopically expressed in HeLa cells was not predominantly associated with ER.

These different results on ER localization of GpIbα may originate from the different cells that were used: the research of Li *et al.* utilized Rat1a cells transfected with GpIbα, and my studies relied on HeLa cells transfected with GFP-GpIbα. Rat1a cells are immortalized rat embryo fibroblasts that do not overexpress GpIbα endogenously, whereas HeLa cells have been demonstrated to contain endogenously overexpressed GpIbα (Li et al., 2008). As GpIbα is a large membrane protein that needs to undergo complicated posttranslational modifications, overexpression of it in Rat1a cells may result in an overload of the ER, therefore causing an accumulation of the overexpressed GpIbα in the ER of the Rat1a cells. On the other hand, HeLa cells may be able to tolerate the ectopic expression of GpIbα, due to its endogenous high level of GpIbα proteins, therefore demonstrating little accumulation of GpIbα in the ER of HeLa cells.

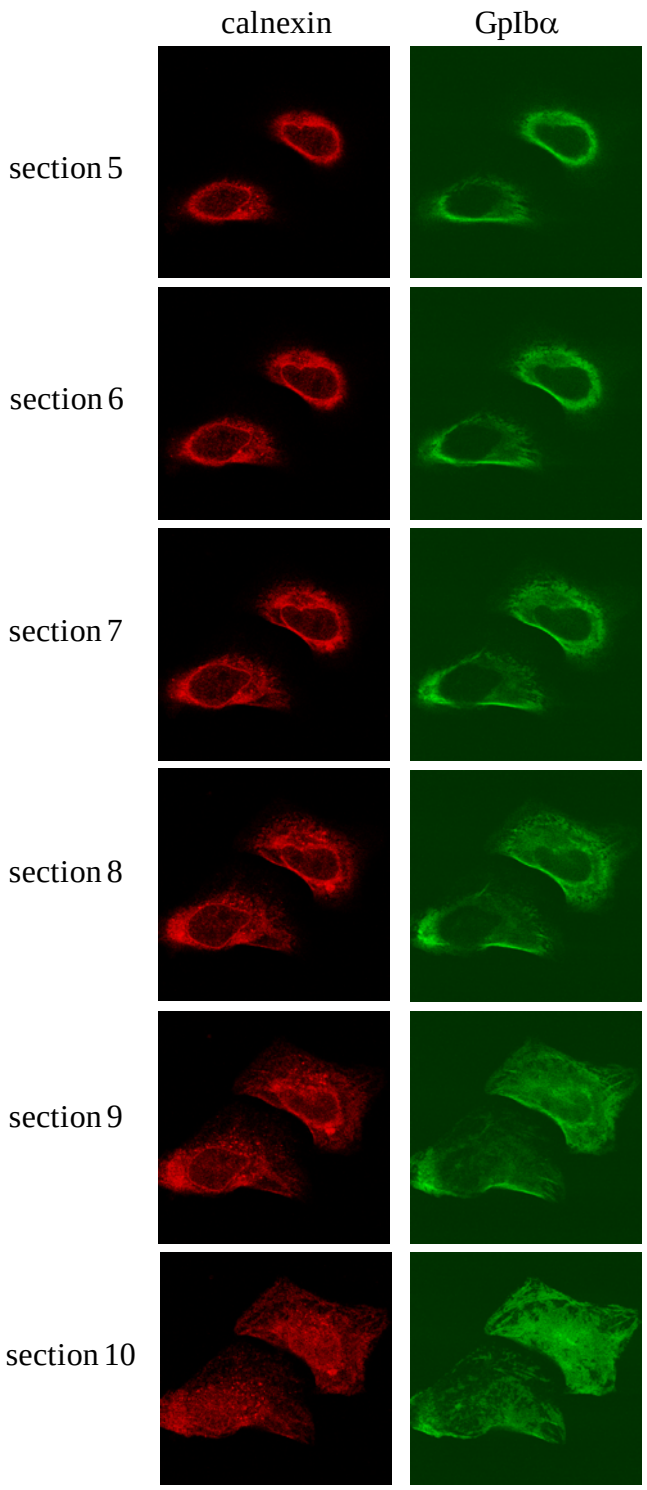

Figure 23 GpIbα and ER in the interphase cells, as examined by confocal microscopy.

The HeLa cells transfected with GFP-GpIbα were fixed and stained with antibodies against calnexin, an ER maker protein, and subjected to the confocal microscopy analyses. Green: GpIbα. Red: calnexin. Pictures are representatives of at least 15 samples that were examined in each experiment.

Alternatively, these different results may arise from the possibility that, there might be two subpopulations of GpIbα proteins that could be detected by the different experimental approaches in these two studies. Rat1a cells transfected with GpIbα were subjected to Western blot in Li *et al.*'s study, using an antibody against GpIbα, while HeLa cells in my study was transfected with GFP-labeled GpIbα and subjected to microscopic analysis. It was interesting to note that the antibody against GpIbα were generated using the highly glycosylated extracellular domain of GpIbα from platelets as the antigen (Berndt et al., 1988). Therefore, the GpIbα proteins localized in ER, which were probably undergoing extensive glycosylation, may be more likely to be detected by this antibody. On the contrary, the GpIbα proteins located on the cell cortex, which might not be as glycosylated, or might have been cleaved and lost certain portions of the extracellular domain as in activated platelets (Bonnefoy et al., 2006), may not be recognized by this antibody.

3.2.2 GpIbα in mitotic cells

The above studies have focused on interphase GpIbα, which revealed that in non-platelet cells, GpIbα proteins were localized on the cell cortex in an F-actin dependent manner, and were partially co-localized with F-actin and filamin A, besides its other localizations and/or functions in interphase cells. What is more interesting is that during these analyses, GpIbα was found to

demonstrate a specific localization in mitosis and cytokinesis. Besides, GpIbα has also been suggested to be related to cytokinesis as that the overexpressed GpIbα promotes binucleation, a product of cytokinesis failure (Li et al., 2007), therefore the potential functions of GpIbα in cell division is investigated below.

3.2.2.1 GpIbα is enriched at the dividing site and the CF

HeLa cells transfected with GFP-GpIbα were subjected to live-cell imaging, to follow the localization of GpIbα during mitosis in real-time, which is shown in Figure 24A. Firstly, when the cell started to round up for mitosis, GpIbα was enriched at the cell cortex, as a bright ring localized at the boundary of the cell, which was consistent with its interphase localization at the cell cortex. As the cell continued mitotic progression, GpIbα began to symmetrically concentrate at the dividing site, which was in the middle of the cell. This site later became the CF during cytokinesis, where GpIbα still persisted to be concentrated, until the end of cytokinesis. Afterwards, the two daughter cells were ready to separate and enter G1 phase, that's when GpIbα began to re-organize into the filament-like structures on the cell cortex, as observed previously in interphase cells. This localization pattern seemed to suggest that GpIbα could play a role in cytokinesis.

Furthermore, when HeLa cells transfected with GFP-GpIbα were fixed, some of the cells did demonstrate the same CF localization of GpIbα as describes above, while others did not. This observation will be discussed later in this section, as a specific phenotype in cancer cells but not in noncancer cells. Immunofluorescence results using fixed noncancer cells, such as RPE-hTERT and HFF-hTERT cells, all demonstrated that GpIbα was concentrated at the CF during normal cytokinesis, as shown in Figure 24B and analyzed below.

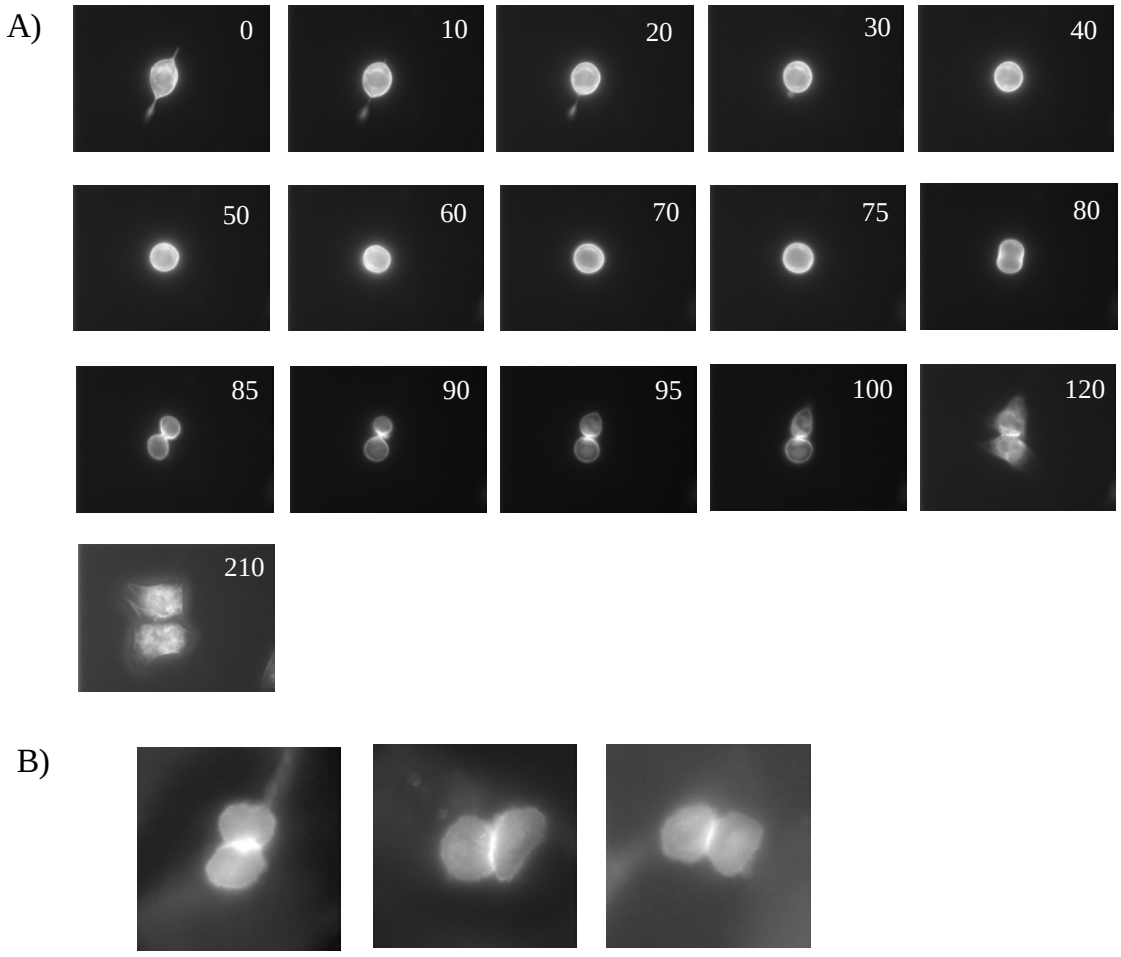

Figure 24 GpIbα is enriched at the CF during cytokinesis.

(A) The HeLa cells transfected with GFP-GpIbα were subjected to live-cell imaging analyses, demonstrating that GpIbα was first localized at the boundary of the dividing cell, then enriched at the divisional site, and later the CF until the completion of cell division. Timestamp: minutes. (B) Immunofluorescence analysis confirmed the CF localization of GpIbα during cytokinesis. The HFF-hTERT and the RPE-hTERT cells were fixed and stained with antibodies against GpIbα.

3.2.2.2 GpIbα is co-localized with F-actin, filamin A and myosin II at the CF during cytokinesis

In order to further investigate the CF localization of GpIbα, double-immunofluorescence was employed to stain cells with antibodies against GpIbα and another known cytokinesis

protein, for example actin, the major component of the contractile ring. As expected, GpIbα was found to co-localize with F-actin at the CF during cytokinesis. Similarly, antibodies against myosin II heavy chain (MHC) were used to represent the localization of myosin II, and GpIbα was also found to co-localize with MHC. Lastly, filamin A localization was examined, and not surprisingly, GpIbα co-localized with filamin A at the CF (Figure 25A, B, C). Therefore, during cytokinesis, GpIbα was localized at the CF, where it co-localized with F-actin, myosin II and filamin A, again indicating a possible role for GpIbα during cytokinesis.

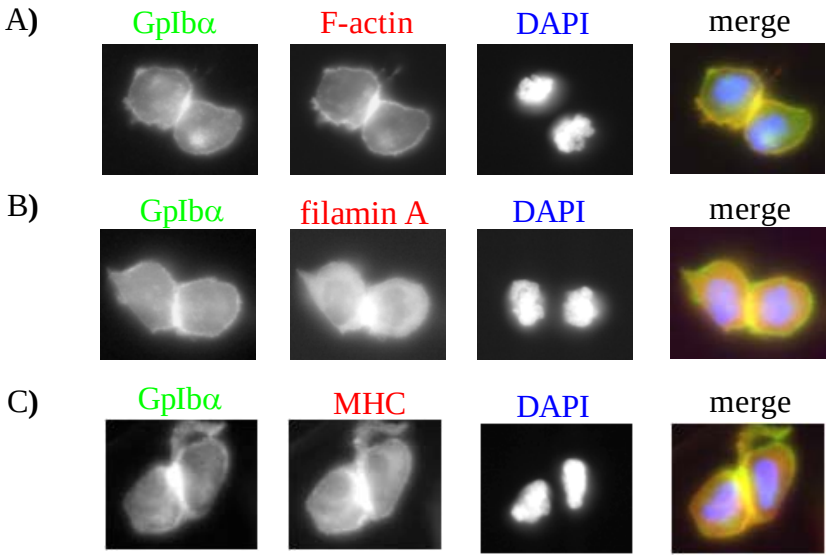

Figure 25 GpIbα co-localized with F-actin, filamin A and myosin II during cytokinesis in noncancer cells.

HFF-hTERT cells were fixed and co-stained with antibodies against GpIbα and F-actin (A), or filamin A (B), or myosin heavy chain (MHC), representing myosin II (C). The nuclei were visualized by DAPI.

Interestingly, although these four proteins, GpIbα, F-actin, myosin II and filamin A, were all found at the CF during cytokinesis, their localizations did not completely overlap, suggesting that all of the four proteins may not form one single complex; rather, there may be hierarchies in

their organizations, where some of them may be integrated into one complex while other(s) may only interact with the complex at some time, which will be further discussed later in this section. It is also important to note again that these above immunofluorescence analyses were performed using the noncancer cell lines HFF-hTERT and/or RPE-hTERT, as the cancer cells demonstrated completely different localization patterns of these proteins, which will also be examined in a later section.

3.2.3 GpIbα overexpression inhibits cytokinesis

A major theme of my studies was to elucidate the possible mechanism(s) through which GpIbα overexpression can cause tumorigenesis, which was provoked by the fact that GpIbα overexpression is commonly observed in cancer cells, and that cells overexpressing GpIbα can cause tumor formation in nude mice (Li et al., 2008). Hence, after the brief investigation of GpIbα in normal conditions, as described above, I began to explore the phenotype caused by GpIbα overexpression.

3.2.3.1 GpIbα overexpression interferes with the localization of the cytokinesis apparatus

It has been demonstrated that cells containing overexpressed GpIbα exhibit high percentages of binucleation (Li et al., 2007), hence it was hypothesized that GpIbα overexpression may cause cytokinesis defects, such as erroneous assembly of cytokinesis machineries, which then led to cytokinesis failure, generating binucleated progenies. Therefore, immunofluorescence analyses were performed to examine the localization of key cytokinesis

proteins in the GpIbα-overexpressing cell line HFF-hTERT-shp53+GpIbα cells, and their control HFF-hTERT-shp53 cells.

Theoretically, using HFF-hTERT-GpIbα cells and comparing them with HFF-hTERT control cells would be the best approach for my study, however these HFF-hTERT-GpIbα cells stopped dividing during culture and demonstrated senescence-like morphologies. This may be a result from the GpIbα overexpression-caused DNA damage (Li et al., 2008), which activated p53 and hindering the normal cell cycle progression. Therefore in order to examine cytokinesis, p53 has to be removed to allow these cells to continue going through mitosis.

GpIbα, F-actin, myosin II and filamin A are mislocalized in HFF-hTERT-shp53+GpIbα cells

Contrary to its CF localization in normal conditions, F-actin was found to be missing from the CF in at least half of the dividing HFF-hTERT-shp53+GpIbα cells. Similarly, filamin A and myosin II also demonstrated mislocalization during cytokinesis, even GpIbα itself was observed to disappear from the CF in more than half of the dividing population, suggesting that GpIbα overexpression impaired the localizations of key cytokinesis proteins (Figure 26A, B, C, D).

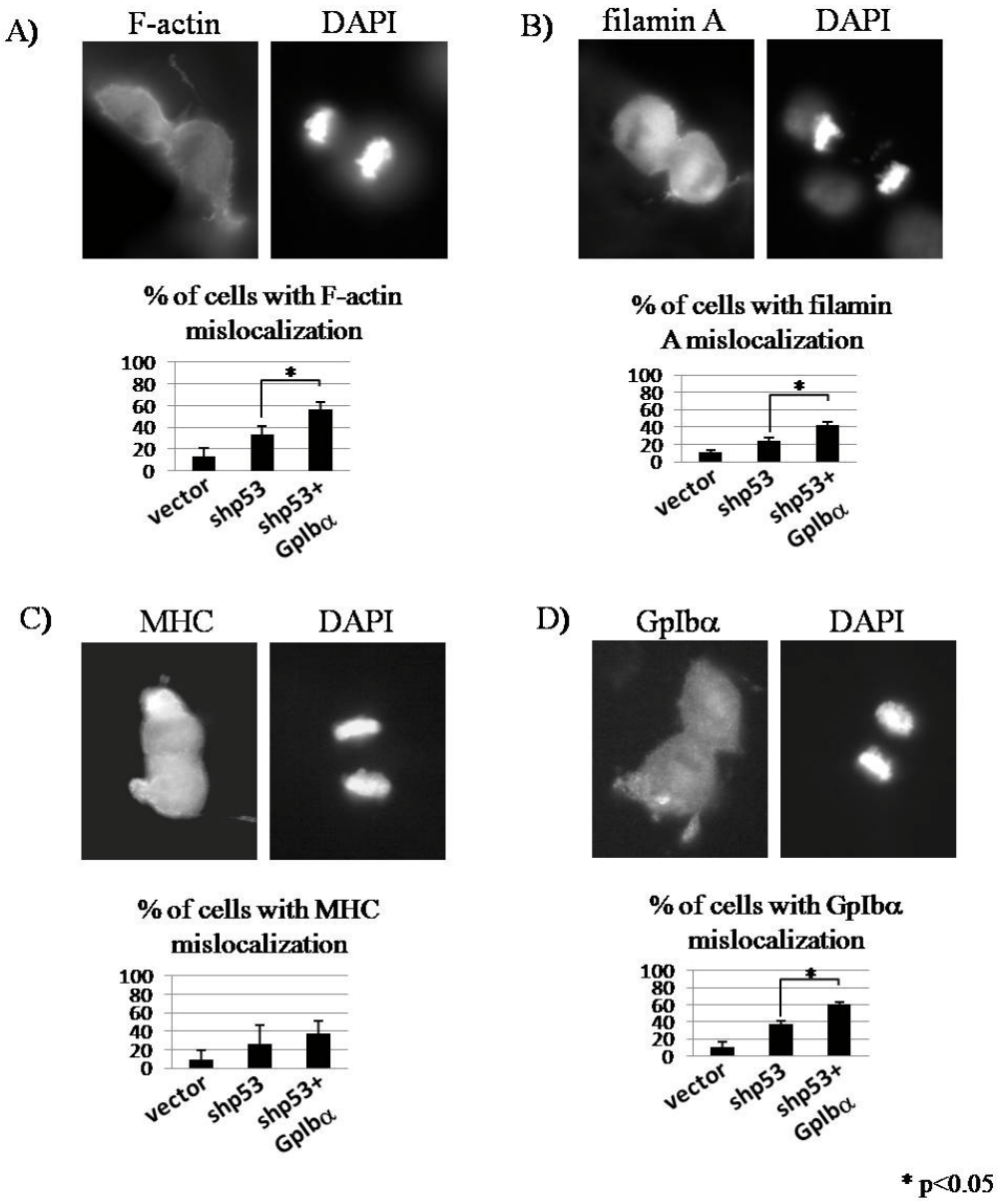

Figure 26 GpIbα overexpression in noncancer cells causes the mislocalization of cytokinesis-related proteins: F-actin, myosin II, filamin A and GpIbα itself.

The localizations of F-actin (A), filamin A (B), myosin II (C), and GpIbα (D) during cytokinesis were examined in HFF-hTERT-shp53+GpIbα cells, and compared to their control HFF-hTERT-shp53 cells by immunofluorescence. Top: a representative image of protein mislocalization during cytokinesis. Nuclei were stained with DAPI. Bottom: quantification of protein mislocalization during cytokinesis in HFF-hTERT-vector, HFF-hTERT-shp53, and HFF-hTERT-shp53+GpIbα cells.

GpIbα, F-actin and filamin A are mislocalized in the same cell, but myosin II is not

It has been suggested earlier in this section that, GpIbα, F-actin, filamin A and myosin II did not demonstrate a complete overlap of their staining patterns at the CF during normal cytokinesis, possibly due to the different hierarchies in their organizations. Indeed, when I closely examined the mislocalization phenotypes of these proteins in the HFF-hTERT-shp53+GpIbα cells using double-immunofluorescence, I noticed that when GpIbα was mislocalized in a cell, F-actin or filamin A was mislocalized in greater than 95% of the cases (Figure 27A, B). However, MHC staining did not follow the same pattern, for example, when GpIbα was mislocalized in a cell, MHC could still be enriched at the CF in about 50% of the cases, indicating that myosin II could have a different localization pattern than GpIbα, F-actin and filamin A (Figure 27C).

These data suggest that GpIbα, F-actin and filamin A may form a hypothetical complex and localize to or mislocalize from the CF, as one entity, which will need further investigation to test this hypothesis. Meanwhile, myosin II may only interact with this complex at some time, but not necessarily be an integrated part of this complex.

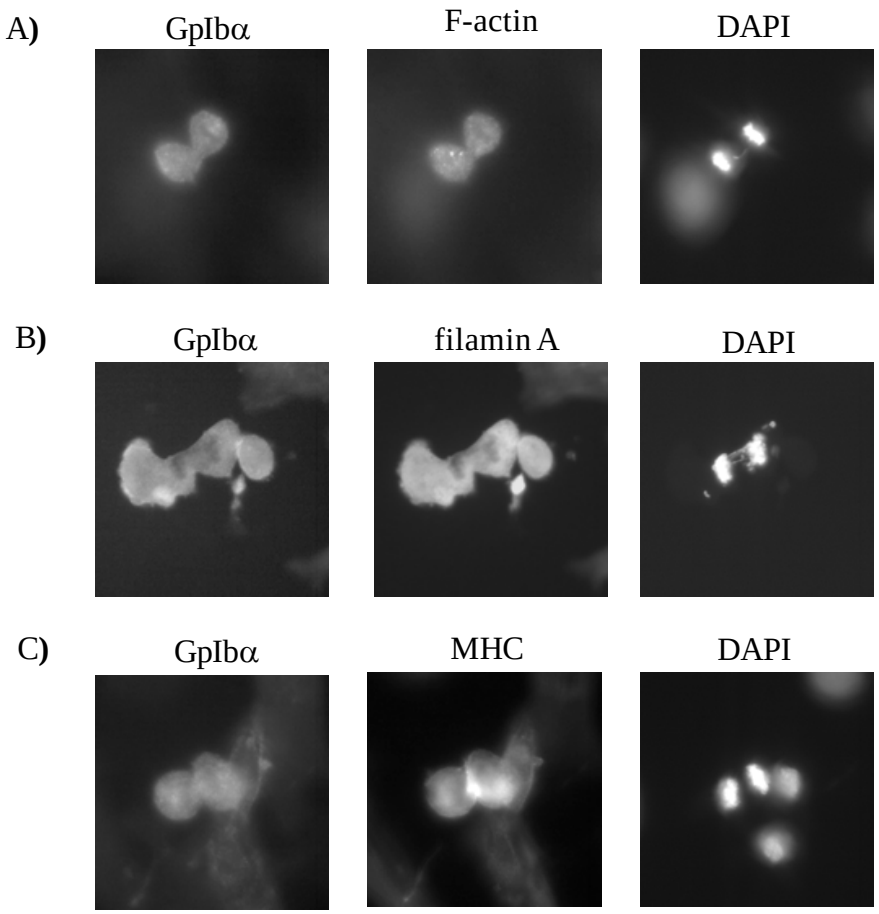

Figure 27 In greater than 95% of cells that demonstrated GpIbα mislocalization, filamin A or F-actin was also mislocalized within the same cell, however, mislocalization of myosin II did not correlate with the mislocalization of GpIbα in the same cell.

Double immunofluorescence analyses were performed using antibodies against GpIbα and actin (A), or GpIbα and filamin A (B), or GpIbα and MHC (C), in HFF-hTERT-shp53+GpIbα cells. Note that in (C), the cell demonstrated GpIbα mislocalization, but myosin II seemed to localize correctly at the CF.

F-actin and filamin A are not affected in interphase GpIbα-overexpressing cells

As F-actin and filamin A have been found to be mislocalized during cytokinesis when GpIbα was overexpressed, I was curious about whether they may also mislocalize during interphase in GpIbα-overexpressing cells. Interestingly, F-actin and filamin A seemed to form

normal filaments on the cell cortex in the GpIbα-overexpressing cells, which was indistinguishable from that observed in the control cells (Figure 28A). Moreover, Western blot analysis has shown that the actin protein levels stayed the same in cells overexpressing GpIbα (Figure 28B), indicating that the protein level and localization of F-actin during interphase was not controlled by the expression levels of GpIbα.

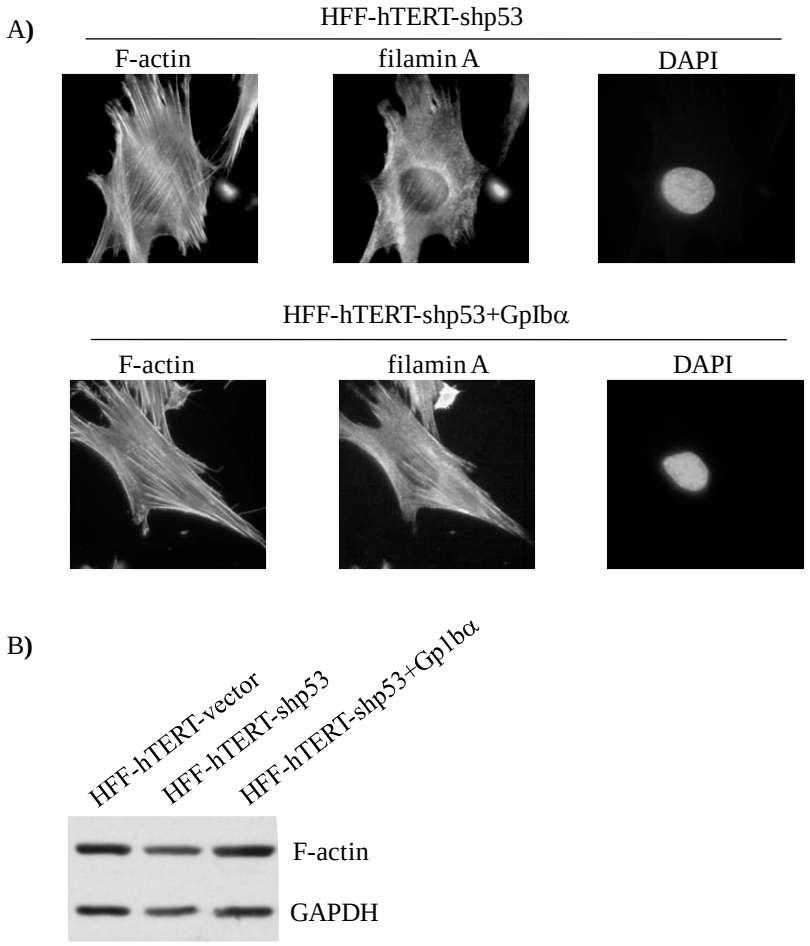

Figure 28 During interphase, GpIbα overexpression affects neither the localization of F-actin and filamin A, nor the expression of actin in cells.

(A) The HFF-hTERT-shp53+GpIbα cells and their control HFF-hTERT-shp53 cells were fixed and stained with antibodies against filamin A. The actin filaments were visualized by rhodamine-phalloidin. The nuclei were labeled by DAPI. (B) The HFF-hTERT-vector, HFF-hTERT-shp53, HFF-hTERT-shp53+GpIbα

cells were lysed and subjected to immunoblot analyses using antibodies against actin. GAPDH was used as a loading control.

These results suggest that the abnormal organization of F-actin and filamin A upon GpIbα overexpression was only specific to cytokinesis, which may be a result of a deregulated cytokinesis-related pathway that had no impact on the cytoskeleton organization in interphase.

RhoA demonstrates asymmetrical localization in the HFF-hTERT-shp53+GpIbα cells

Besides the two contractile ring components actin and myosin II, RhoA was also analyzed in the GpIbα-overexpressing cells, for two reasons. The first is that RhoA is a central cytokinesis regulator, which controls the activities of myosin II through an effector kinase ROCK, and also controls the polymerization of F-actin in the contractile ring by regulating formin (Piekny et al., 2005). The second reason is that filamin A, the GpIbα-interacting partner, has been demonstrated to bind to RhoA and ROCK directly (Pi et al., 2002; Ueda et al., 2003). As GpIbα itself, filamin A and F-actin were absent from the CF during cytokinesis in the HFF-hTERT-shp53+GpIbα cells, one can predict that the localization of RhoA would also be altered in these cells.

As expected, RhoA demonstrated a different localization pattern in the GpIbα-overexpressing cells when compared with controls. In normal conditions, RhoA was found to be symmetrically enriched at both sides of the dividing site, which later became the CF (Figure 29A); however, when GpIbα was overexpressed, RhoA was asymmetrically localized (Figure 29B, C), suggesting a defect in RhoA's localization during cytokinesis.

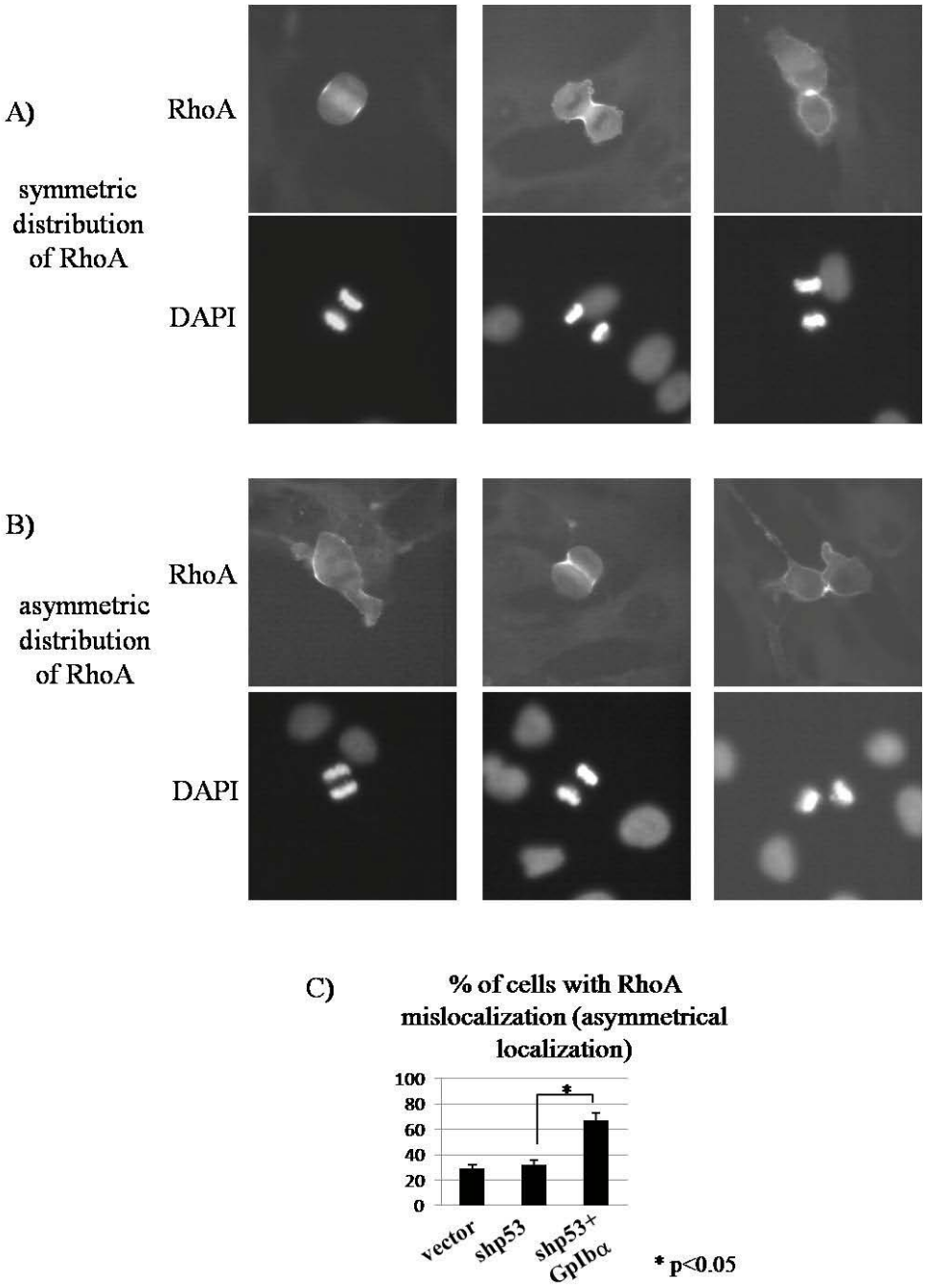

Figure 29 GpIbα overexpression in noncancer cells causes asymmetrical localization of RhoA during cytokinesis.

(A) The normal symmetrical localization of RhoA at the divisional site. The HFF-hTERT-shp53 cells at different stages of cytokinesis were fixed with trichloroacetic acid and stained with RhoA. DAPI was used to visualize the nuclei. (B) The asymmetrical localization of RhoA during cytokinesis. HFF-hTERT-

shp53+GpIbα cells were fixed and analyzed as in (A). (C) The quantification of the asymmetrical localization of RhoA during cytokinesis in the HFF-hTERT-vector, HFF-hTERT-shp53 and HFF-hTERT-shp53+GpIbα cells.

This asymmetric localization of RhoA was slightly different from the mislocalization of GpIbα, F-actin and filamin A, which demonstrated complete absence from the CF or even the entire cell, suggesting that the distributions and activities of RhoA may be obstructed by a different pathway and/or different protein regulator than what affected the GpIbα, F-actin and filamin A localizations during cytokinesis.

Aurora B is not mislocalized in the HFF-hTERT-shp53+GpIbα cells

Up till now GpIbα, F-actin, filamin A, myosin II and RhoA all demonstrated defective localization in the HFF-hTERT-shp53+GpIbα cells, I next examined another cytokinesis-related protein Aurora B kinase.

As shown in Figure 30A, Aurora B was located at the CF region in HFF-hTERT control cells. Upon a closer look, in normal controls, Aurora B seemed to form many short strings, which were mostly parallel and occupied the majority part of the space constrained by the CF (Figure 30B).

At a later stage of cytokinesis, Aurora B became very concentrated, as the "canal" that connected the two daughter cells became thinner. Interestingly, this localization pattern was not changed in the GpIbα-overexpressing cells (Figure 30C, D), suggesting that Aurora B localization was not affected by GpIbα-overexpression, therefore not all proteins in the cytokinesis machinery were prevented from localizing normally.

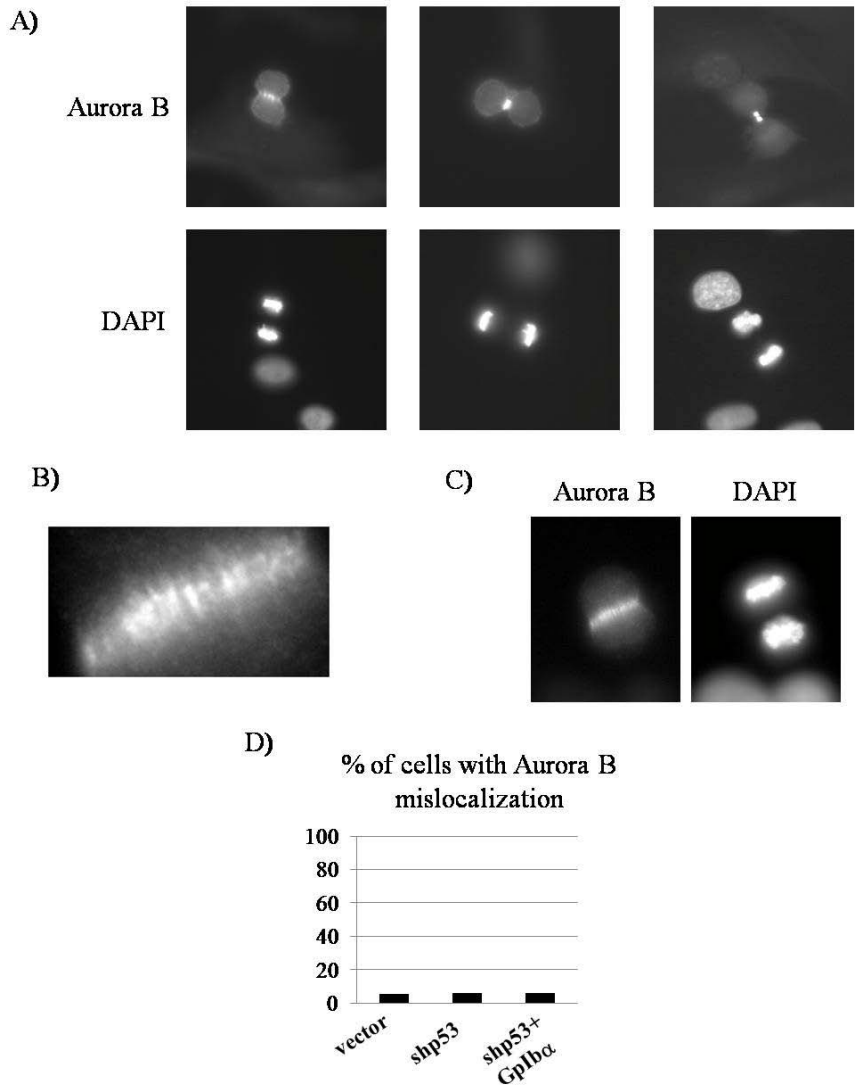

Figure 30 GpIbα overexpression does not affect the localization of Aurora B during cytokinesis.

(A) The localization of Aurora B at the divisional site. The HFF-hTERT-shp53 cells at different stages of cytokinesis were fixed and stained with antibodies against Aurora B. (B) A zoomed-in picture of Aurora B at the divisional site demonstrated the filament-like patterns of Aurora B. (C) The localization of Aurora B in the GpIbα-overexpressing cells. (D) The quantification of Aurora B mislocalization in the HFF-hTERT-vector, HFF-hTERT-shp53, HFF-hTERT-shp53+GpIbα cells.

It is interesting to note that the proteins which have demonstrated defective localizations during cytokinesis in the GpIbα-overexpressing cells are mostly proteins that localize at the cell

cortex, cytoskeletons, and their interactants, in other words, proteins closer to the outside surface of the CF. On the contrary, the proteins that did not demonstrate mislocalization (Aurora B) is known to associate with MTs during cytokinesis (Delaval et al., 2004; Maerki et al., 2009), meaning that, it is localized on the central spindles inside of the "canal", not on the cell surface. Therefore, these differences may suggest that the mechanism by which GpIbα overexpression interferes with cytokinesis, is probably functioning through affecting the cortical cytoskeleton and/or its associated proteins during cytokinesis.

3.2.3.2 GpIbα overexpression directly interferes with completion of cytokinesis

As GpIbα overexpression resulted in the mislocalization of multiple cytokinesis proteins, one may predict that cytokinesis would be also affected. Therefore live-cell imaging was employed to follow the completion of cell division in various cell lines.

As expected, a 4-fold increase in the percentage of cytokinesis failure was observed in HFF-hTERT-shp53+GpIbα cells, when compared with their respective control cells (Figure 31A), confirming that overexpression of GpIbα indeed inhibits the completion of cytokinesis, therefore generating tetraploid progenies. Consistently, binucleation frequency also increased in the GpIbα-overexpressing cells when compared with controls, as shown in Figure 31B.

My data so far have demonstrated that overexpression of GpIbα in noncancer HFF cells caused defective localizations of cytokinesis-related proteins, and failure of cytokinesis. Interestingly, as revealed by Li *et al.*, all the cancer cell lines they tested contained endogenous overexpression of GpIbα (Li et al., 2008), therefore one can predict that cancer cells may demonstrate similar cytokinesis defects as HFF-hTERT-shp53+GpIbα cells, and the endogenous

overexpression of GpIbα in cancer cells may be the cause for their divisional defects, which is discussed below.

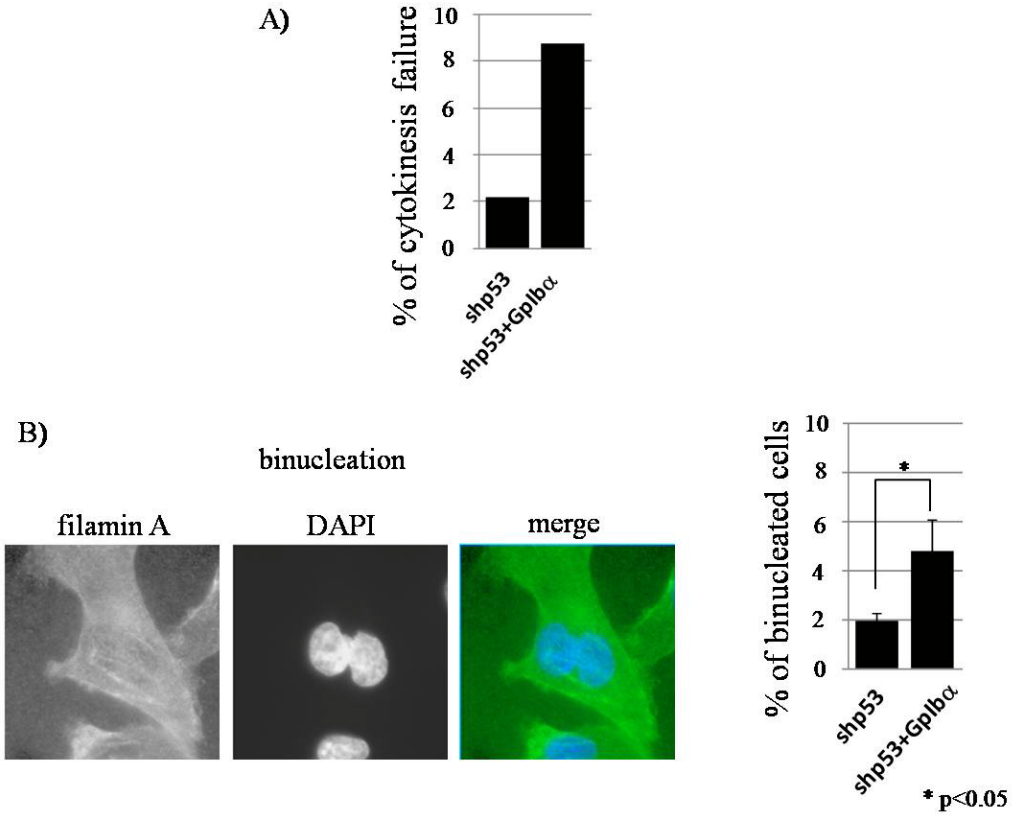

Figure 31 GpIbα overexpression causes cytokinesis failure and binucleation.

(A) Live-cell imaging was used to quantify the frequency of cytokinesis failure in the HFF-hTERT-shp53+GpIbα cells and control HFF-hTERT-shp53 cells. (B) Immunofluorescence analyses were used to determine the binucleation ratio in the HFF-hTERT-shp53+GpIbα cells and control HFF-hTERT-shp53 cells. Left: an example of binucleated cells. filamin A staining was used to visualize the boundary of the cell. DAPI was used to label the nuclei. Right: quantification of binucleated cells.

3.2.4 GpIbα overexpression is associated with cytokinesis defects in cancer cells

As predicted, cancer cells may demonstrate cytokinesis defects, for example, mislocalization of cytokinesis-related proteins and binucleation. Hence, four cancer cell lines were employed,

including the cervical adenocarcinoma epithelial cell line HeLa, two oral squamous cell carcinoma cell lines UPCI:SCC103, UPCI:SCC40 and the liver adenocarcinoma cell line SK-HEP, which were subjected to a series of immunofluorescence analyses to investigate their divisional defects.

3.2.4.1 Cancer cells demonstrated similar mislocalization of cytokinesis proteins and high percentages of binucleation

As expected, all of the four cancer cell lines demonstrated high percentages of GpIbα mislocalization in the dividing population, similar mislocalization was also observed for F-actin, filamin A and RhoA (Figure 32A, C), indicating that the cytokinesis apparatus in cancer cells were indeed defective. These phenotypes were very close to what was previously observed in HFF-hTERT-shp53+GpIbα cells, suggesting that the HFF-hTERT-shp53+GpIbα cells could serve as a model cell line to study GpIbα effects in cancer cells.

In addition, the percentages of binucleation were also analyzed in these four cancer cell lines, interestingly I found a correlation between the mislocalization of cytokinesis-related proteins and the percentage of binucleation as shown in Figure 32B. Cell lines that demonstrated high percentages of cells with mislocalized cytokinesis proteins also demonstrated relatively high frequencies of binucleation, suggesting that the defective localization of cytokinesis-related proteins might contribute to cytokinesis failure, therefore generating binucleated cells. The HFF-hTERT-shp53+GpIbα cells also appeared to behave similarly to the four cancer cell lines, as these HFF-hTERT-shp53+GpIbα cells have also demonstrated high percentages of both protein mislocalization and binucleation, confirming that HFF-hTERT-shp53+GpIbα cells could be used to study cytokinesis defects-related features of cancer cells.

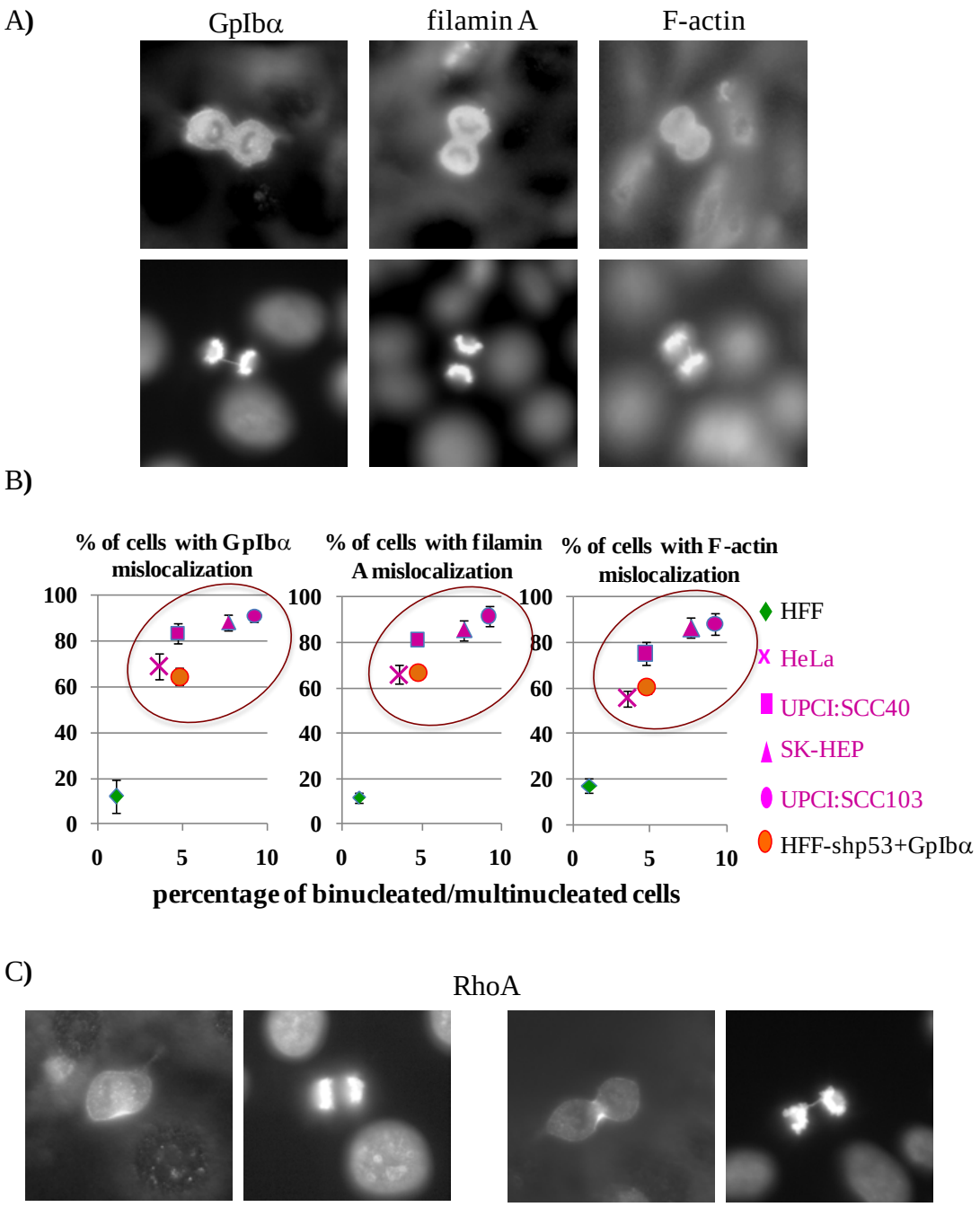

Figure 32 Cancer cells demonstrate mislocalization of the cytokinesis-related proteins similar to what was observed in the HFF-hTERT-shp53+GpIbα cells, and these mislocalizations seem to be correlated with the binucleation/multinucleation frequencies.

Four cancer cell lines, HeLa, UPCI:SCC40, SK-HEP, and UPCI:SCC103 were fixed and stained with various antibodies to examine the localization of GpIbα, filamin A, F-actin, and RhoA during cytokinesis.

(A) Images demonstrating the mislocalization of GpIbα, filamin A and F-actin. (B) The relationship between the percentages of the cytokinesis-related protein mislocalization and the frequencies of binucleation/multinucleation. (C) The asymmetrical localization of RhoA during cytokinesis.

3.2.4.2 GpIbα overexpression is a cause of mitotic/cytokinesis defects in HeLa cells

Now that GpIbα overexpression seemed to be related to binucleation and mislocalization of cytokinesis proteins in cancer cells, the next question to be addressed was: did GpIbα overexpression cause cytokinesis failure in cancer cells?

Besides mislocalization of cytokinesis proteins and binucleation, there are other types of mitotic/cytokinesis defects commonly observed in cancer cell lines, for example multipolar spindles (MPSs), anaphase bridges, lagging chromosomes, and micronuclei (Figure 33A), which may all contribute to cytokinesis failure and/or genomic instability as discussed in the "CYTOKINESIS FAILURE, TETRAPLOIDIZATION AND TUMORIGENESIS" section of Chapter I. In order to answer the above-proposed question, HeLa cells were employed as a representative of cancer cells. The percentages of all these defects were quantified and compared between HeLa-shGpIbα cells, in which GpIbα proteins were knocked-down by shRNA, and their respective control HeLa-shvector cells.

3.2.4.3 GpIbα knockdown decreases some mitotic/cytokinesis defects from HeLa cells

As demonstrated in Figure 33B, the frequencies of MPSs, anaphase bridges, lagging chromosomes, micronuclei, and binucleation were all significantly reduced in HeLa cells after GpIbα knockdown, suggesting that the endogenous overexpression of GpIbα was responsible for these mitotic/cytokinesis defects. In order to verify that these results were truly due to GpIbα knockdown, a shRNA resistant GpIbα (murine GpIbα, mGpIbα) was expressed in HeLa-

shGpIbα cells. As expected, the frequencies of these mitotic/cytokinesis defects were all mostly restored in HeLa-shGpIbα-mGpIbα cells (Figure 33B), confirming that GpIbα overexpression was the cause for the MPSs, anaphase bridges, lagging chromosomes, micronuclei and binucleation observed in HeLa cells.

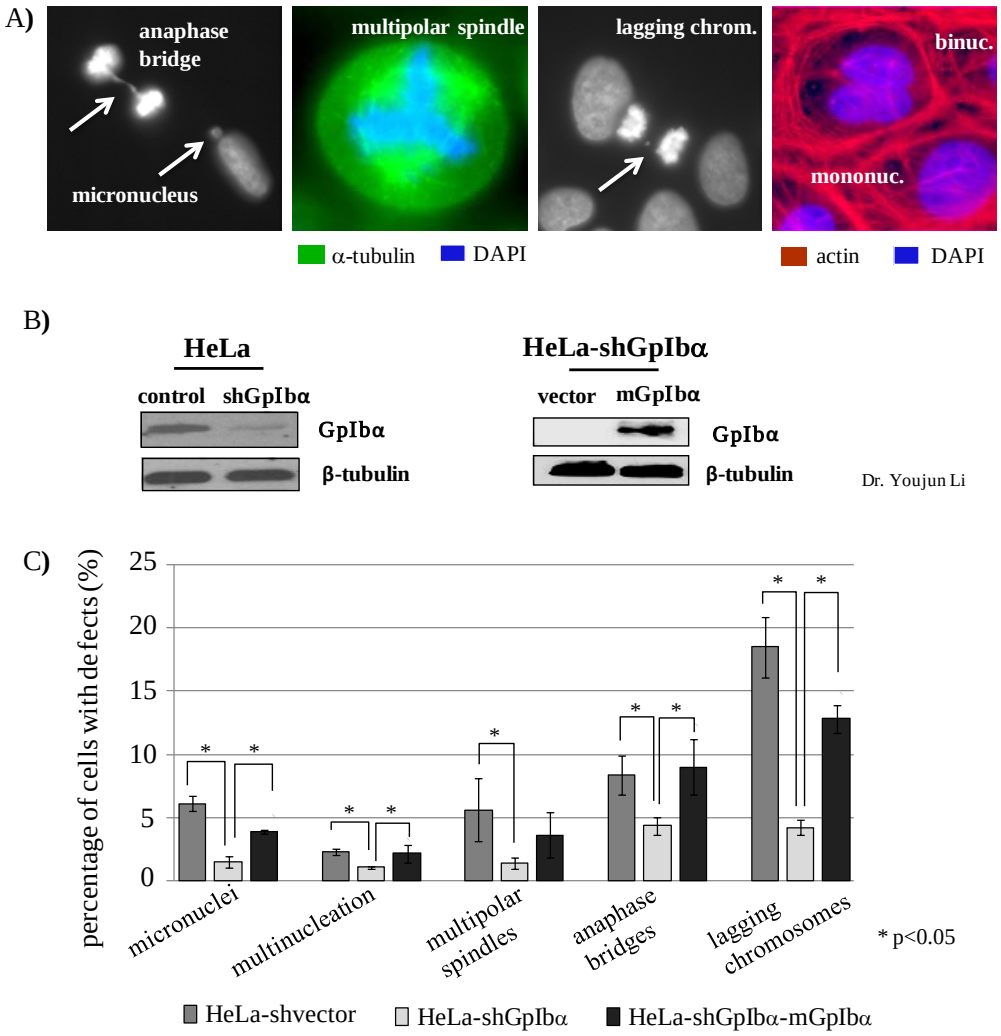

Figure 33 Overexpression of GpIbα was partially responsible for many of the mitosis/cytokinesis defects observed in HeLa cells.

(A) Examples of mitotic/cytokinesis defects in HeLa cells: anaphase bridges, micronuclei (indicated by arrows), multipolar spindles, lagging chromosomes (indicated by arrows), and binucleation. HeLa cells were fixed and staining with antibodies against a-tubulin or rhodamine-phalloidin. DNA was visualized by

DAPI. (B) Western blotting analysis to verify successful knockdown of GpIbα via shRNA in HeLa cells and overexpression of a shRNA-resistant mGpIbα in these cells. (C) Quantification of the percentages of each mitotic/cytokinesis defect as shown in (A), using HeLa-shvector cells, HeLa-shGpIbα cells (HeLa cells with stably knockdown of GpIbα), and HeLa-shGpIbα-mGpIbα cells (HeLa cells with stable knockdown of GpIbα, and overexpression of a shRNA-resistant mouse GpIbα).

All of the divisional defects that were significantly reduced after GpIbα knockdown in HeLa cells were not observed in the same cell. This is because most of the cells that exhibited mitotic/cytokinesis defects observed were not in the same stage of cell division, such as MPSs were observed in metaphase, anaphase bridges were observed in anaphase, while binucleation was observed in interphase. However, these mitotic/cytokinesis defects might actually be mechanistically related. For example, the lagging chromosomes during mitosis might become the micronuclei in interphase, if they were not resolved. In addition, binucleation might be a result of anaphase bridges, which could inhibit the normal completion of cell division, leading to failure of cytokinesis and binucleation. Therefore, it is possible that GpIbα overexpression may affect one or several central regulators in cell division, but generating many various phenotypes of mitotic/cytokinesis defects.

3.2.4.4 GpIbα knockdown does not decrease the percentages of cytokinesis-related protein mislocalization in HeLa cells

The percentages of cells with mislocalization of GpIbα, F-actin and filamin A during cytokinesis were analyzed using HeLa-shGpIbα cells, and results were compared with those in their respective controls, HeLa-shvector cells. Surprisingly, there were only marginal decreases in the percentages of cells with mislocalization of these proteins after GpIbα knockdown, even

when blinded analysis was completely employed, to ensure the objectiveness and accuracy of the data (Figure 34A, B, C).

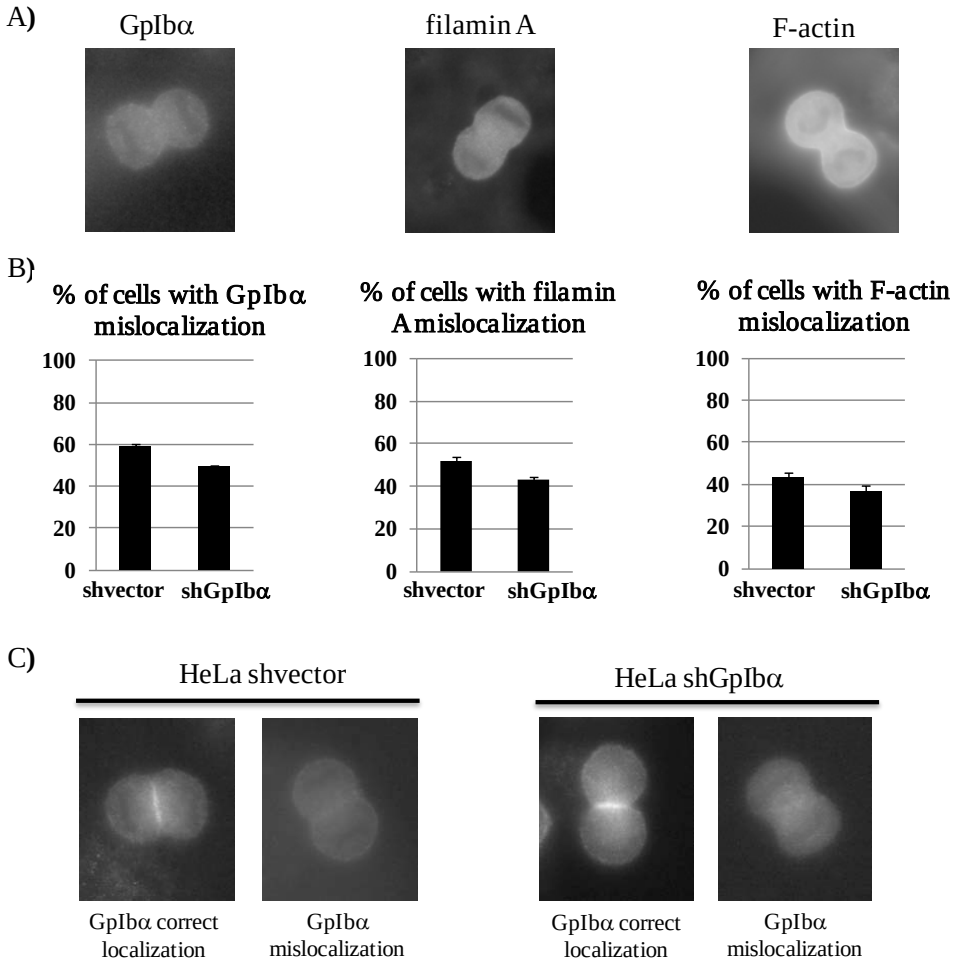

Figure 34 Knockdown of GpIbα does not rescue the mislocalization of cytokinesis-related proteins in HeLa cells.

(A) HeLa cells were fixed and stained with antibodies against GpIbα, filamin A, and F-actin, which demonstrated mislocalization during cytokinesis. (B) The percentages of GpIbα, filamin A, and F-actin mislocalization during cytokinesis in HeLa cells with and without the knockdown of GpIbα. (C) Example images of GpIbα at the CF in HeLa cells with and without the knockdown of GpIbα.

These results suggest that knockdown of GpIbα rescued many mitotic/cytokinesis defects in HeLa cells, but failed to correct the mislocalization of the cytokinesis-related proteins. Therefore it is possible that there are different pathways contributing to these different divisional defects, among which GpIbα overexpression only affected some, but not others, for example, mislocalization of cytokinesis-related proteins may be caused by a GpIbα-independent pathway. Alternatively, the mislocalization phenotypes of cytokinesis-related proteins could be influenced by multiple causes, GpIbα overexpression was only one of them. There may also be other possible explanations, which will be addressed in the section of "Speculations and discussions" later in this chapter.

3.2.4.5 Abnormally localized GpIbα in U-2 OS cells during cytokinesis

As demonstrated earlier, GpIbα was found to be mislocalized from the CF during cytokinesis in the majority of the HeLa, UPCI:SCC103, UPCI:SCC40, and SK-HEP cancer cells, as well as HFF-hTERT-shp53+GpIbα cells that were generated to reproduce the GpIbα overexpression seen in cancer cells. However, when I examined the localization of GpIbα in another cancer cell line U-2 OS, which was derived from human osteosarcoma, an unusual phenotype was observed.

As shown in Figure 35A, instead of being almost completely absent from the mitotic cells, GpIbα in U-2 OS formed dots with various sizes and various numbers per cell during cytokinesis. Although it was consistent with the previous observation that GpIbα was not found to accumulate at the CF, it was not clear why there were aggregates of GpIbα in the mitotic U-2 OS cells.

It may be possible that the aggregates of GpIbα in U-2 OS cells were due to an overloaded ER, therefore antibodies against calnexin, the ER marker protein, were used, and the dividing U-2 OS cells were co-stained with GpIbα and calnexin. Surprisingly, calnexin did not demonstrate a dot-like distribution as GpIbα did during cytokinesis (Figure 35B), which suggest that the aggregated GpIbα was probably not associated with the ER in U-2 OS cells during cytokinesis. Furthermore, interphase cells co-stained with antibodies against GpIbα and calnexin confirmed that calnexin-labeled ER seem to be normal in the interphase U-2 OS cells (Figure 35C), therefore, overexpressed GpIbα may have a different fate in U-2 OS cells during cell division.

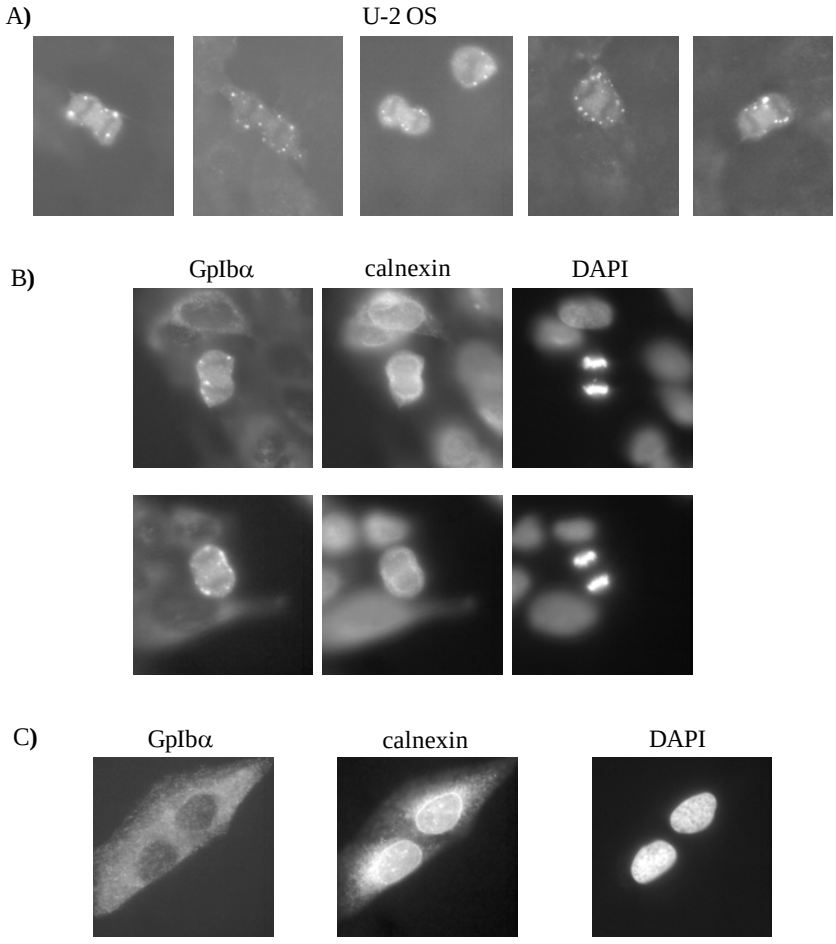

Figure 35 Abnormal localization of GpIbα in U-2 OS cells.

(A) U-2 OS cells were fixed and stained with antibodies against GpIbα, which demonstrated aggregation-like foci during cytokinesis. (B, C) U-2 OS cells were fixed and co-stained with antibodies against GpIbα and calnexin. DAPI was used to visualize the nuclei. (B) mitotic U-2 OS cells. (C) interphase U-2 OS cells.

Collectively, my data demonstrated that GpIbα overexpression causes many mitotic/cytokinesis flaws in certain cancer cells, which lead to cytokinesis failure and tetraploidization, although there may be additional factors or mechanisms interfering with this completion of cell division. Hence, I sought to investigate how exactly the overexpression of GpIbα could induce cytokinesis defects, by using the HFF cell system that mimicked cancer cells.

3.2.5 Potential mechanism of GpIbα overexpression interferes with cytokinesis

Based on my studies and related work from the Prochownik lab, the mechanism through which GpIbα overexpression impaired cytokinesis, is beginning to be understood. Hence, I will first discuss the important domains of GpIbα that mediated this possible mechanism, then address a key factor, the anaphase bridges, and a key protein mediator of this mechanism, the down-regulated Aurora B, before concluding a model at the end of this section.

3.2.5.1 The capability to bind to filamin A is required for overexpressed GpIbα to inhibit cytokinesis

As mentioned in the “Introduction” section of this chapter, GpIbα contains several important domains, one of which is the signal peptide at the N-terminus of GpIbα that directs the newly-synthesized GpIbα proteins to enter ER, mostly for posttranslational modifications,

glycosylation. The second important domain is the filamin A binding domain, located at the C-terminus of GpIbα, which is responsible for mediating the interaction between GpIbα and filamin A. Both of these domains have been reported to be critically associated with the transforming features of the GpIbα-overexpressing cells, and their genomic instability (Li et al., 2009). Therefore, I examined whether the signal peptide and filamin A binding domains are essential for the overexpressed GpIbα to interfere with cytokinesis.

Mutated GpIbα lacking the signal peptide was overexpressed in HFF-hTERT-shp53 cells, interestingly these cells did not demonstrate an elevated level of binucleation, when compared with their controls (Figure 36A). These data suggest that the signal peptide was indispensible for the overexpressed GpIbα to cause binucleation. Furthermore, the percentages of cytokinesis failure were compared between cells overexpressing full-length GpIbα, GpIbα mutant lacking the signal peptide, and the vehicle control, using live-cell imaging. Consistently, GpIbα mutant lacking the signal peptide did not induce a higher percentage of cytokinesis failure when overexpressed in the HFF-hTERT-shp53 cells (Figure 36A), confirming the importance of the signal peptide. These results suggest that overexpressed GpIbα needs to go through the ER in order to impair cytokinesis, which may be due to the requirement of glycosylation to become a fully functional protein.

I next investigated whether the filamin A binding domain of GpIbα was also needed for the overexpressed GpIbα to interfere with cytokinesis, and analyzed this question using the same approach as mentioned above. The mutated GpIbα lacking the filamin A binding domain was overexpressed in the HFF-hTERT-shp53 cells. Similarly, this GpIbα mutant lost its ability to induce higher percentages of binucleation and cytokinesis failure when overexpressed in noncancer cells, as demonstrated by immunofluorescence and live-cell imaging (Figure 36A).

Therefore, binding to filamin A also seemed to be required for the overexpressed GpIbα to cause cytokinesis failure and binucleation, thus suggesting a mechanism directly involving filamin A, or alternatively, filamin A may regulate the stability of the overexpressed GpIbα, hence indirectly contribute to the mechanism. This will be discussed in the section of "Speculations and discussions".

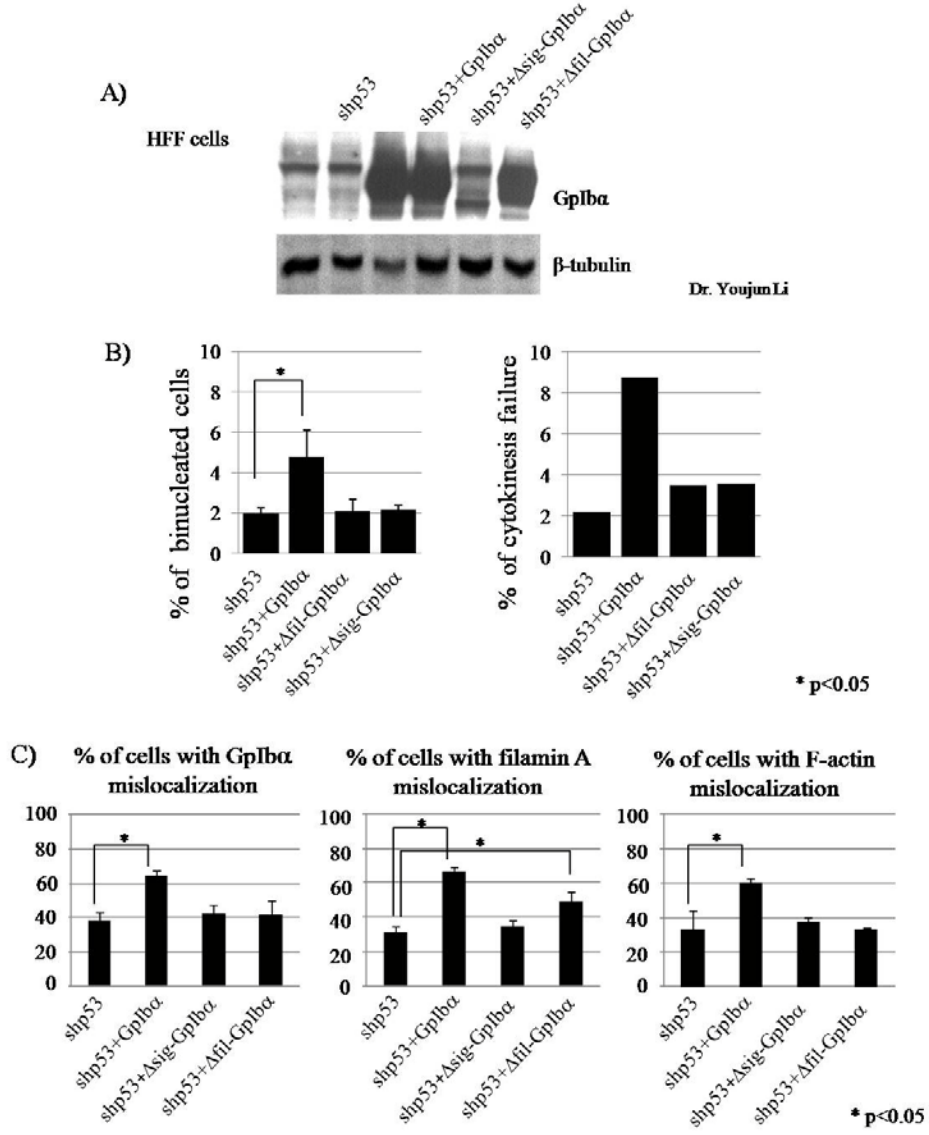

Figure 36 The signal peptide and the filamin A-binding domain are indispensible for the overexpressed GpIbα to impair cytokinesis.

(A) Western blotting analysis to verify the overexpression of either full-length GpIbα, or the filamin A-binding domain deleted GpIbα (Δfil-GpIbα), or the peptide domain deleted GpIbα (Δsig-GpIbα) in HFF cells. (B) The percentages of binucleation and cytokinesis failure were analyzed by immunofluorescence and live-cell imaging, respectively. HFF-hTERT-shp53 cells were transfected with either full-length GpIbα, or the filamin A-binding domain deleted GpIbα (Δfil-GpIbα), or the peptide domain deleted GpIbα (Δsig-GpIbα). (C) The percentages of GpIbα, filamin A, and F-actin mislocalization during cytokinesis in the cell lines used in (B). Overexpression of full length GpIbα significantly increased the percentages of binculeation and mislocalization of cytokinesis-related proteins (indicated by *), while overexpression of GpIbα mutant failed to induce a significant increase in binucleation or the percentages of cells with mislocalization of cytokinesis-related proteins, except that the percentage of cells with mislocalization of filamin A during cytokinesis was increased after overexpression of the filamin A-binding domain deleted GpIbα (Δfil-GpIbα).

Furthermore, the localization of cytokinesis-related proteins were also analyzed in HFF-hTERT-shp53 cells overexpressing either the signal peptide-deleted GpIbα or the filamin A binding domain-deleted GpIbα. As demonstrated in Figure 36B, the percentages of cells with GpIbα, F-actin and filamin A mislocalization during cytokinesis were almost unchanged before and after overexpression of either GpIbα mutants, except that the percentage of cells with filamin A mislocalization during cytokinesis was increased after the filamin A binding domain-deleted GpIbα was overexpressed. These data indicate that both the signal peptide and the filamin A binding domain were indispensible for the overexpressed GpIbα to inhibit the localizations of cytokinesis-related proteins.

Taken together, these data demonstrated that the overexpressed GpIbα proteins need to go through the ER, possibly for glycosylation, as well as interaction with filamin A, in order to

inhibit cytokinesis and generating tetraploid cells, and this inhibition of cytokinesis seems to be linked with the mislocalization of cytokinesis-related proteins.

3.2.5.2 DNA damage and anaphase bridges may contribute to the cytokinesis failure induced by GpIbα overexpression

Li *et al.* have observed higher levels of DSB DNA damage in the GpIbα-overexpressing cells (Li et al., 2008); it was also interesting to note that in my studies, more anaphase bridges seemed to be present in the GpIbα-overexpressing cells than their respective controls. As discussed in the "CYTOKINESIS" section of Chapter I, anaphase bridges can inhibit normal cytokinesis machineries that are required for the CF ingression, therefore, the mechanism of GpIbα overexpression causing cytokinesis failure may be explained by the hypothesis that GpIbα overexpression induces DNA damage, leading to anaphase bridge formation and eventually interfering with cytokinesis.

In order to test this hypothesis, IR treatment was employed to induce more DSB DNA damage and anaphase bridges in the HFF-hTERT-shp53+GpIbα cells. Indeed, the percentages of anaphase bridges were significantly increased after IR; however, surprisingly, the percentages of mislocalization of GpIbα did not show a dramatic increase (Figure 37A), suggesting that the increased anaphase bridges failed to trigger more mislocalization of cytokinesis-related proteins in the IR-treated HFF-hTERT-shp53+GpIbα cells.

Upon a closer look of these HFF-hTERT-shp53+GpIbα cells after IR treatment, I observed that there was a subpopulation of cells with anaphase bridges and mislocalization of cytokinesis-related proteins, as well as a subpopulation of cells demonstrating anaphase bridges and correct localization of cytokinesis-related proteins (Figure 37B), although the latter was rare.

Similarly, among the cells that did not contain anaphase bridges, there was a subpopulation which demonstrated mislocalization and another subpopulation which exhibited correct localization. These data suggest a complicated relationship between anaphase bridges and mislocalization of cytokinesis-related proteins, which will be discussed in the section of "Speculations and discussions".

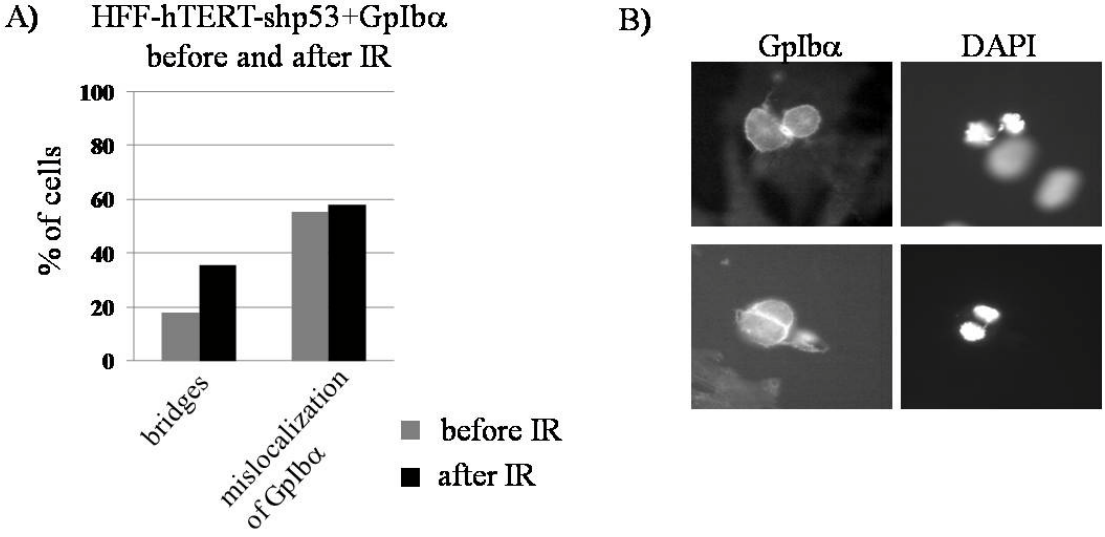

Figure 37 The IR treatment induces more anaphase bridges in the HFF-hTERT-shp53+GpIbα cells, however it fails to increase the percentage of cytokinesis-related protein mislocalization.

(A) The percentages of anaphase bridges and mislocalization of GpIbα during cytokinesis before and after the IR treatment. HFF-hTERT-shp53+GpIbα cells were treated with 2 Gy of g-radiation and then released for 24 hours before fixation. (B) Examples of HFF-hTERT-shp53+GpIbα cells containing normal-like localization of GpIbα in the presence of the anaphase bridge. Cells were fixed and stained with antibodies to GpIbα. DAPI was used to visualize DNA.

In contrast to the above results, when HFF-hTERT-shp53 cells were treated with IR, they displayed significant increases in both their frequencies of anaphase bridges and the percentages of mislocalization of GpIbα, F-actin and filamin A during cytokinesis (Figure 38A). Similar

results were observed when I treated HFF-hTERT-vector cells with IR (data not shown), suggesting that anaphase bridges formed from IR-induced DNA DSBs indeed triggered the mislocalization of cytokinesis-related proteins. As overexpression of GpIbα was also observed to induce DSBs, anaphase bridges and cytokinesis protein mislocalization, it is possible to hypothesize that GpIbα overexpression first induced DSB DNA damage, similar to IR treatment, which in turn formed anaphase bridges, leading to cytokinesis defects and failure.

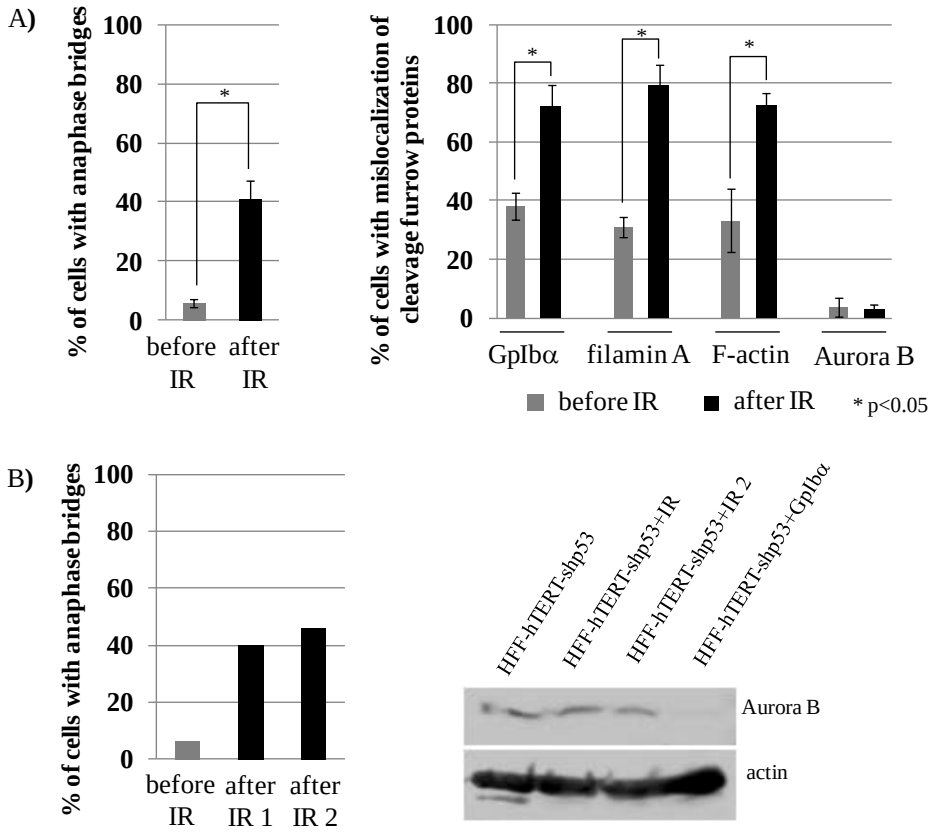

Figure 38 The IR treatment in the HFF-hTERT-shp53 cells triggers increases in anaphase bridges, as well as percentage of cytokinesis-related protein mislocalization.

(A) The percentages of anaphase bridges (left) and the mislocalization of GpIbα, filamin A, F-actin and Aurora B during cytokinesis (right) before and after the IR treatment in HFF-hTERT-shp53 cells. (B) Left: the percentage of anaphase bridges before and after the IR treatment in HFF-hTERT-shp53 cells. IR 1 and IR 2 indicate two independent experiments. Right: Western blot analysis of Aurora B's expression levels

in HFF-hTERT-shp53 cells before and after IR treatment, as well as in HFF-hTERT-shp53+GpIbα cells. Actin was used as a loading control.

The reasons behind why HFF-hTERT-shp53+GpIbα cells demonstrated a different phenotype from HFF-hTERT-shp53 or HFF-hTERT-vector cells after IR treatment are not known. However, one speculation could be that there is a threshold for the percentages of cytokinesis-related protein mislocalizations, which was already reached (or almost reached) in the untreated HFF-hHTERT-shp53+GpIbα cells. This speculation will be further explained in the section of "Speculations and discussions" in this chapter. Alternatively, these results might also be due to the fact that HFF-hTERT-shp53+GpIbα cells were a stable cell line, which had been under selection and cultured for a long time, therefore there might be an acquired adaptation, which prevented further cytokinesis defects in addition to the existing problems.

3.2.5.3 Aurora B down-regulation mediates the inhibition of cytokinesis caused by GpIbα overexpression

DSB DNA damage seems to be a transitional phenotype between GpIbα overexpression and cytokinesis defects, but how the DNA damage was caused by GpIbα overexpression is still under investigation. One promising candidate involved in this mechanism is Aurora B.

Aurora B down-regulation seems to be responsible for the anaphase bridges in the GpIbα overexpressing cells

Li *et al.* have demonstrated that GpIbα overexpression leads to a marked reduction in the protein level of Aurora B, which I have also verified in Figure 38B; more importantly, when Aurora B is re-expressed in these HFF-hTERT-shp53+GpIbα cells, the percentage of DSB DNA

damage is decreased (Li et al.), suggesting that Aurora B down-regulation is responsible for the elevated levels of DNA damage in the GpIbα-overexpressing cells. Therefore, it could be possible that GpIbα overexpression caused cytokinesis defects and binucleation, through down-regulating Aurora B to generate DNA damage and anaphase bridges.

In order to test this hypothesis, I first examined whether the re-expression of Aurora B could reduce the high percentage of anaphase bridges caused by GpIbα overexpression. As expected, the frequency of anaphase bridges in the HFF-hTERT-shp53+GpIbα+Aurora B cells was significantly reduced when compared with HFF-hTERT-shp53+GpIbα cells, and was almost unchanged when compared with the control HFF-hTERT-shp53 cells (Figure 39A), consistent with the DSB DNA damage levels observed in these three cell lines (Li et al.). Therefore, these results suggest that the reduced expression level of Aurora B was the (or one of the) cause(s) for the anaphase bridges observed in the GpIbα-overexpressing cells.

To rule out the possibility that Aurora B down-regulation was a result from DSB DNA damages, HFF-hTERT-shp53 cells were treated with IR and the protein levels of Aurora B were examined by Western blot analysis. As demonstrated in Figure 38B, although IR treatment induced a marked increase in the percentage of anaphase bridges, presumably by causing DNA DSBs, the protein level of Aurora B remained almost unchanged. This result confirmed that Aurora B down-regulation observed in GpIbα-overexpressing cells was not a result from anaphase bridge formation, rather, it was probably the (or one of the) cause(s) of the anaphase bridges.

Aurora B down-regulation is the reason for cytokinesis failure in GpIbα overexpressing cells

The next question I examined was whether the reduced expression of Aurora B was responsible for the cytokinesis failure and binucleation in the GpIbα-overexpressing cells. Indeed, when Aurora B was re-expressed in the HFF-hTERT-shp53+GpIbα cells, the percentages of cytokinesis failure and binucleation were both reduced to almost the same levels of the control HFF-hTERT-shp53 cells, as examined by live-cell imaging and immunofluorescence, respectively (Figure 39B), indicating that the reduced Aurora B caused by GpIbα overexpression led to cytokinesis failure in these cells.

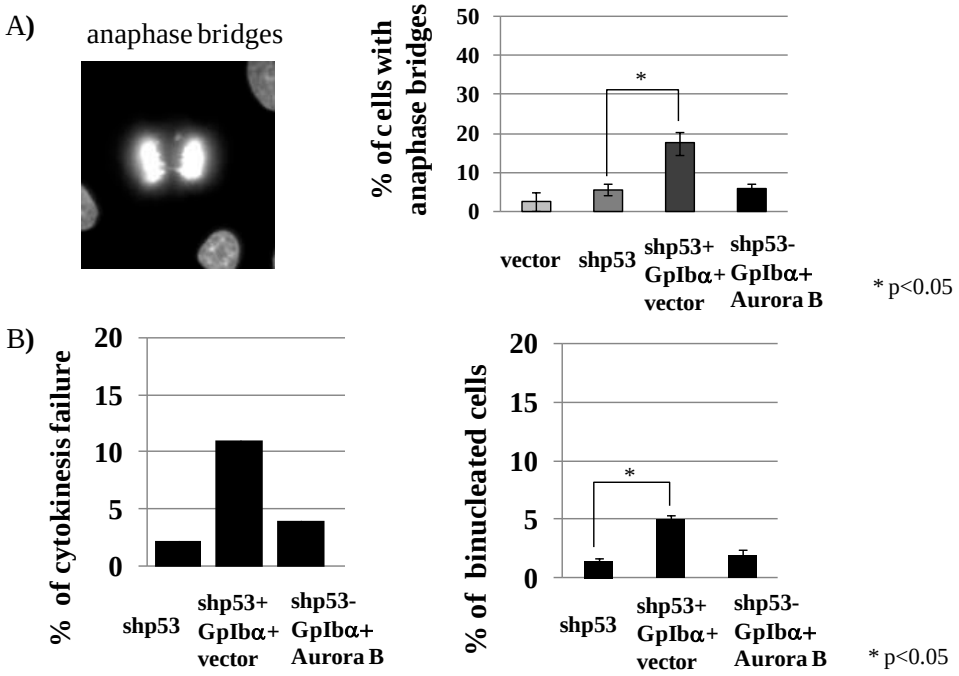

Figure 39 Aurora B down-regulation seems to mediate the mechanism through which the overexpressed GpIbα causes cytokinesis defects and final failure.

(A) Left: a representative picture of anaphase bridges in the HFF-hTERT-shp53+GpIbα cells. Right: quantifications of anaphase bridges in HFF-hTERT-vector, HFF-hTERT-shp53, HFF-hTERT-

shp53+GpIbα+vector, HFF-hTERT-shp53+GpIbα+Aurora B (HFF-hTERT-shp53+GpIbα cells stably overexpressing Aurora B) cells. Note that there is a significant increase in the percentage of cells with anaphase bridges after overexpression of GpIbα when compared with control (shp53 cells), however, there is no change in the percentage of anaphase bridges after the overexpression of GpIbα and Aurora B when compared with control (shp53 cells). (B) The percentages of cytokinesis failure and binucleation examined by live cell imaging and immunofluorescence, respectively, in HFF-hTERT-shp53, HFF-hTERT-shp53+GpIbα+vector, HFF-hTERT-shp53+GpIbα+Aurora B cells. Note that there is a significant increase in the percentage of binucleated cells after overexpression of GpIbα when compared with control (shp53 cells), however, there is no change in the percentage of binucleated cells after the overexpression of GpIbα and Aurora B when compared with control (shp53 cells).

Aurora B down-regulation is responsible for the mislocalization of cytokinesis-related proteins in GpIbα overexpressing cells

Lastly, I examined whether GpIbα overexpression caused mislocalization of cytokinesis-related proteins through down-regulation of Aurora B. The localizations of GpIbα, F-actin and filamin A during cytokinesis were analyzed by immunofluorescence. Interestingly, the quantification data suggest that after re-expression of Aurora B in these HFF-hTERT-shp53+GpIbα cells, the percentages of cells with mislocalization of GpIbα, F-actin and filamin A during cytokinesis were all reduced, when compared with their respective control cells, consistent with previous observation that re-expression of Aurora B rescued cytokinesis failure. Similarly, the asymmetrical distribution of RhoA during cytokinesis in the GpIbα-overexpressing cells was also rescued by the re-expression of Aurora B, while the localization of Aurora B itself was not affected, even at the presence of anaphase bridges (Figure 40A, B, C, D). As demonstrated earlier, GpIbα, F-actin and filamin A were found to be correctly localized or mislocalized in the same cell (data now shown), however the fixation protocol for RhoA was

different from the protocol used for the other proteins, therefore co-immunofluorescence could not be conducted to test whether RhoA was mislocalized in the same cell demonstrating GpIbα, F-actin or filamin A mislocalization during cytokinesis.

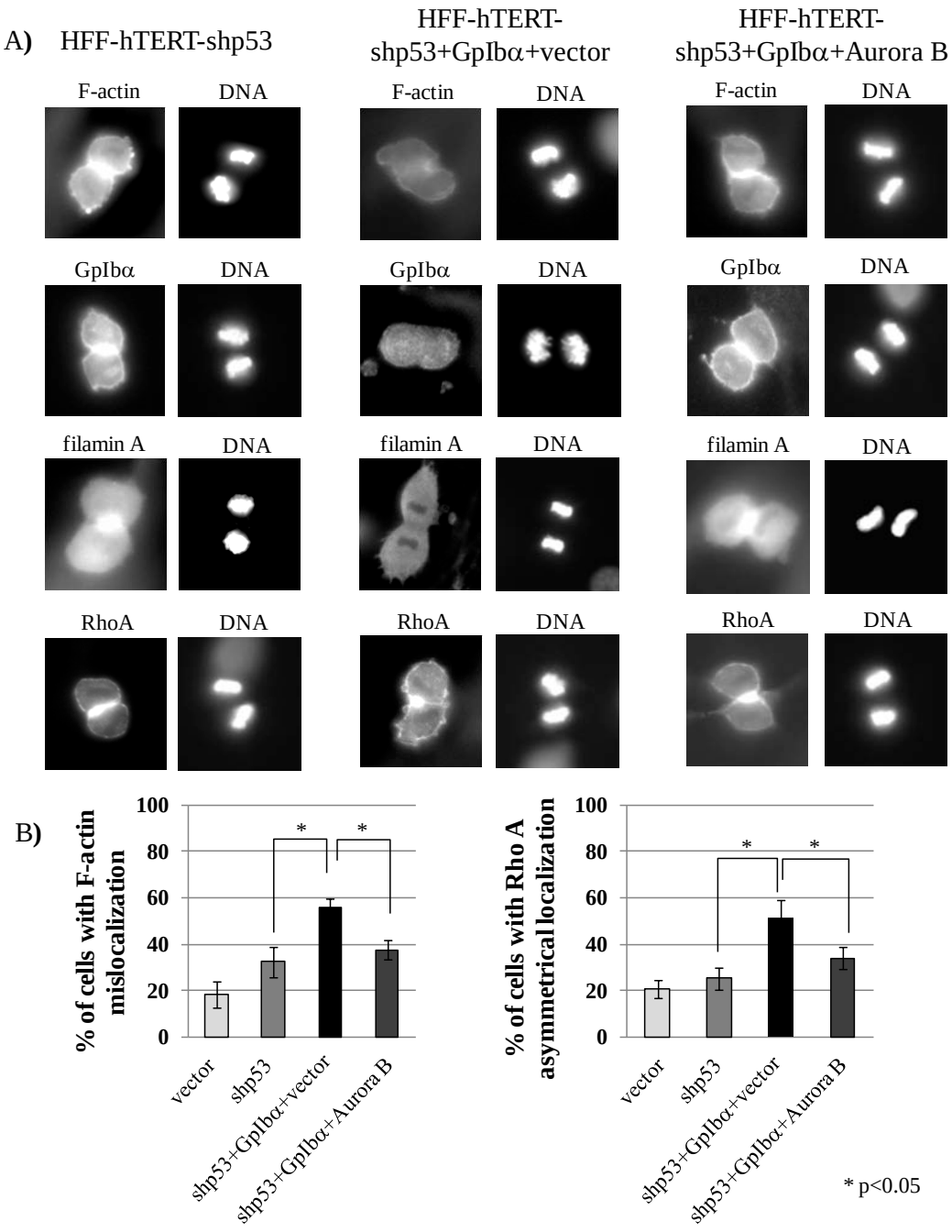

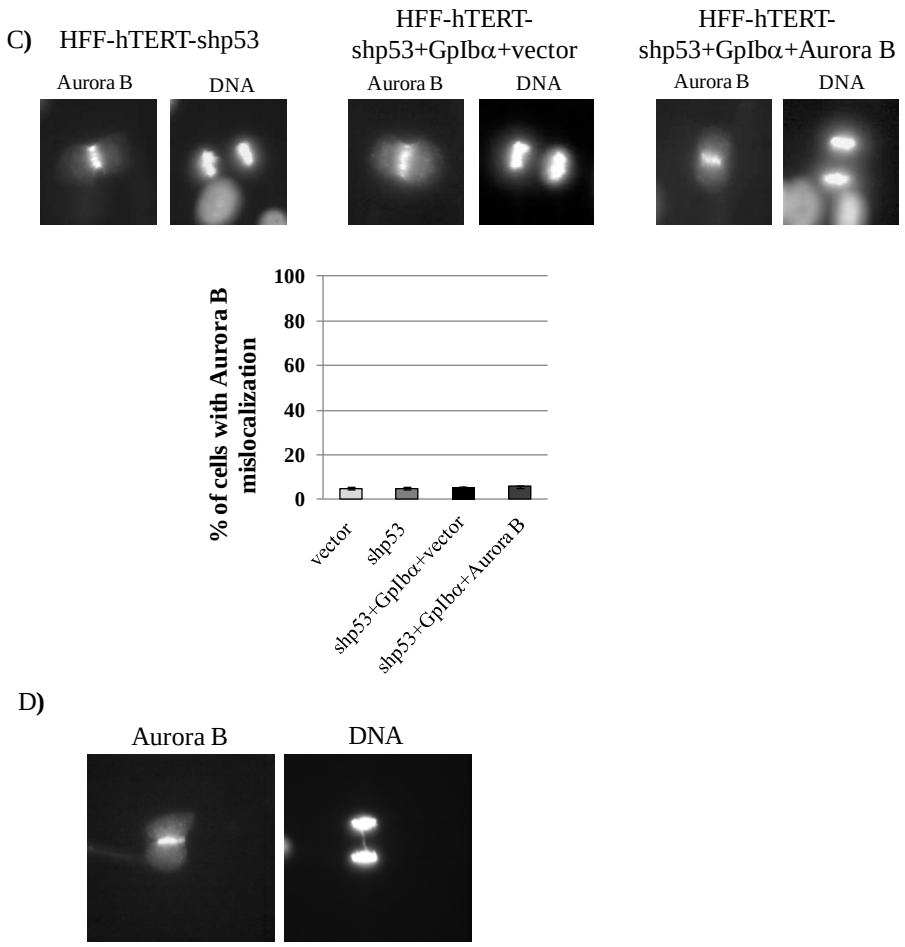

Figure 40 Aurora B down-regulation seems to be responsible for the cytokinesis-related protein mislocalization in the GpIbα-overexpressing cells, however its own localization is not affected.

(A) The mislocalization of F-actin, GpIbα and filamin A, as well as the asymmetrical localization of RhoA during cytokinesis were examined by immunofluorescence analyses. HFF-hTERT-shp53, HFF-hTERT-shp53+GpIbα+vector, HFF-hTERT-shp53+GpIbα+Aurora B cells were fixed and stained with respective antibodies. The nuclei were labeled by DAPI. (B) Quantifications of F-actin mislocalization and RhoA asymmetrical localization during cytokinesis in HFF-hTERT-vector, HFF-hTERT-shp53, HFF-hTERT-shp53+GpIbα+vector, HFF-hTERT-shp53+GpIbα+Aurora B cells. (C) Aurora B's cytokinesis localization was examined by immunofluorescence in the same cell lines as in (B). Top panel: representative images of Aurora B's localization during cytokinesis. Bottom: quantification of Aurora B mislocalization during cytokinesis. (D) Aurora B was enriched at the CF in the presence of anaphase bridges. HFF-hTERT-

shp53+GpIbα-vector cells were fixed and stained with antibodies against Aurora B. The nuclei were labeled with DAPI.

3.2.5.4 Other possible mechanisms to mediate cytokinesis failure in the GpIbα overexpressing cells

Besides the above-mentioned Aurora B pathway that was involved in the mechanism through which GpIbα overexpression led to cytokinesis failure, other factors might also contribute to this mechanism. One such example is cdc25B, which has been found to be overexpressed in GpIbα-overexpressing cells (Li & Prochownik, unpublished data). Hence, HFF-hTERT-shp53+GpIbα cells with cdc25B knockdown via shRNA were analyzed.

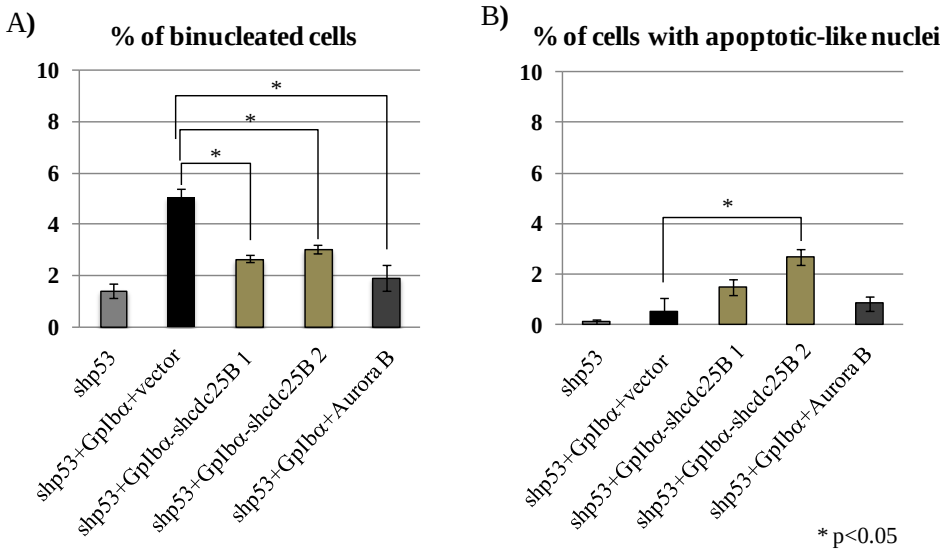

Figure 41 cdc25B may be involved in the mechanism by which GpIbα overexpression leads to binucleation.

(A) The percentages of binucleation in the HFF-hTERT-shp53, HFF-hTERT-shp53+GpIbα+vector, HFF-hTERT-shp53+GpIbα-shcdc25B (two stable clones of HFF-hTERT-shp53+GpIbα cells with cdc25B knockdown via shRNA), HFF-hTERT-shp53+GpIbα+Aurora B cells. (B) The percentages of apoptotic-like nuclei in the same cell lines as in (A).

After cdc25B knockdown, the frequency of binucleation decreased in the GpIbα-overexpressing cells (Figure 41A). However it was also interesting to note that these HFF-hTERT-shp53+GpIbα-shcdc25B cells demonstrated fragmented and apoptotic-like nuclei in the fixed cell population (Figure 41B). This observation suggested that although cdc25B knockdown was observed to reduce the binucleation caused by GpIbα overexpression, it might do so by activating cell death pathways, effectively eliminating the binucleated cells. This is opposite to the re-expression of Aurora B, as Aurora B directly corrected cytokinesis defects. This possibility will require further investigation.

My results so far suggested that the cortically localized GpIbα could interfere with cytokinesis when it was overexpressed, and generating binucleated cells. Aurora B down-regulation caused by GpIbα overexpression was shown to be a transitional step, which triggered anaphase bridges, thus affecting normal assembly of the cytokinesis machineries at the CF, and resulting in failure of cytokinesis. Meanwhile, up-regulation of cdc25B caused by GpIbα overexpression might also contribute to binucleation, through an undefined mechanism, which will be discussed in the section of "Speculations and discussions".

The above summary provides a plausible explanation for the mechanism of why GpIbα overexpression interferes with cytokinesis. However, there are two major parts missing in this model, the first is to answer how GpIbα overexpression leads to down-regulation of Aurora B, and the second is how Aurora B down-regulation induces DNA damages to form anaphase bridges. Besides, the exact importance for GpIbα interaction with filamin A is not clear. Therefore, the real mechanism for GpIbα overexpression to impair cytokinesis may be more complicated than it appears.

3.3 SUMMARY

GpIbα is the key subunit of the vWF receptors that are located on the cell surface of platelets, and the traditional function of GpIbα is thought to be in mediating platelet activation and aggregation. However, in this chapter, the novel roles for GpIbα, outside of the blood cell system, have begun to be uncovered. Without expression of the other vWF receptor subunits, GpIbα was partially localized to the cell cortex of non-platelet cells during interphase, and partially colocalized with F-actin filaments, suggesting a non-blood-cell-related function of GpIbα. More interestingly, GpIbα was observed to be enriched at the CF during cytokinesis in immortalized epithelial and fibroblast cells, colocalized with F-actin, myosin II and filamin A, therefore demonstrating a possible role for GpIbα in cytokinesis.

The overexpression of GpIbα in these epithelial and fibroblast cells has been demonstrated to cause cytokinesis defects, including anaphase bridges and mislocalization of cytokinesis-related proteins. Consistently, the percentages of cytokinesis failure and binucleation were elevated in these GpIbα-overexpressing cells. Furthermore, the endogenous overexpression of GpIbα was shown to be the cause of many mitotic and cytokinesis defects observed in HeLa cells, including binucleation, indicating a possible role for GpIbα overexpression in the tetraploidization of cancer cells. The mechanism of how GpIbα overexpression caused cytokinesis failure is still under investigation, and my current data supports work from the Prochownik lab showing that down-regulation of Aurora B seemed to be a major transitional step leading to cytokinesis failure after GpIbα overexpression, which might involve the interaction of GpIbα with filamin A.

3.4 SPECULATIONS AND DISCUSSIONS

During the exploration of the novel role(s) for GpIbα outside of the blood cell system, and the functions of overexpressed GpIbα in tumorigenesis, many interesting open-ended questions have arisen, some of which will be discussed below, and may be worth future investigations.

3.4.1 A fundamental question: why is a protein that has a *specific* function in platelet activation involved in *general* cellular events such as cytokinesis?

GpIbα is conventionally believed to be predominantly expressed in megakaryocytes and platelets, exerting critical functions in the blood clotting process; however in this chapter, its novel functions during cytokinesis and tetraploidization in non-megakaryocyte/platelet cells was suggested, which lead us to wonder why this GpIbα protein seems to play two completely distinct roles in different systems. Although it is possible that these two roles are not associated with each other, it is also likely that both of GpIbα's roles in megakaryocytes/platelets and non-megakaryocyte/platelet cells are inter-connected.

Prior to producing platelets, megakaryocytes need to undergo a unique cell division process, called endomitosis, which describes cells going through several rounds of DNA replication without cytokinesis (Jackson, 1990). A recent publication has demonstrated that, the endomitosis of megakaryocytes is a result of cytokinesis failure, which is associated with defective contractile rings and RhoA pathways (Lordier et al., 2008). Furthermore, it actually has been reported that the expression level of Aurora B is deceased in the polyploid megakaryocytes (Katayama et al., 1998; Kawasaki et al., 2001; Zhang et al., 2001). Hence, it is plausible to hypothesize that the endogenously overexpressed GpIbα in megakaryocytes

functions through down-regulating Aurora B to impair cytokinesis, and resulting in endomitosis, similar to it does in the HFF-hTERT-shp53+GpIbα cells. This hypothesis would suggest that the original and/or primary function of GpIbα might be in cytokinesis, and then it evolutionally acquired new functions in platelet activation, hence the two roles for GpIbα are in fact associated with one another, although this speculation requires more in-depth analysis.

3.4.2 The c-Myc-GpIbα-Aurora B/cdc25B model to mediate tumorigenesis

My research in this chapter was initiated when GpIba was identified as a major target of c-Myc. As suggested by Li *et al.*, the transforming and tumorigenic properties of c-Myc can be largely recapitulated by overexpression of GpIbα, and the overexpression of GpIba is observed in all of the cancer cells lines they examined (Li et al., 2008).

Besides cancer cell lines, GpIbα has also been found to be overexpressed in human cancer tissues. For example, significant elevated expression of GpIbα was observed in ovarian mucinous adenocarcinoma when compared with normal ovarian tissues, as identified from the microarray database that was analyzed by Oncomine™ (Compendia Bioscience, Ann Arbor, MI, 2010) (Figure 42). Similarly, higher levels of GpIbα transcripts were found in testicular tumors when compared with their control testicular tissues, in imatinib-resistant chronic myelogenous leukemia when compared with untreated chronic myelogenous leukemia, as well as in c-src-transformed primary human mammary epithelial cells when compared with non-transformed controls (Li et al., 2008). These data indicated that GpIbα is overexpressed in various types of human tumors, which is consistent with our observation of the various cancer cell lines that demonstrated GpIbα overexpression originating from different tumor tissues (Li et al., 2008).

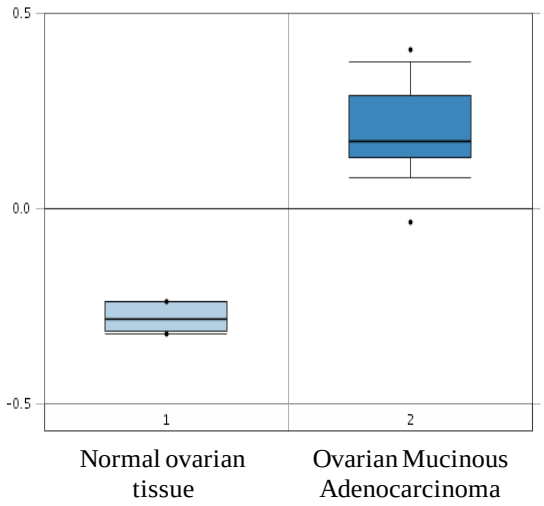

Figure 42 GpIbα overexpression in tumor tissues.

GpIbα expression levels in Hedrix Ovarian Mucinous Adenocarcinoma when compared with normal ovarian tissues. Data were analyzed and visualized by Oncomine and the original microarray data were reported by Hendrix ND, Wu R, Kuick R, Schwartz DR, Fearon ER, Cho KR. (2006) Cancer Res. 66(3): 1354-1362.

The GpIbα gene is localized at the short arm of chromosome 17 (17pter-p12). Although the amplification of whole chromosome 17 has been reported in some tumors, including neuroblastoma, renal metanephric adenoma, hepatocellular carcinoma, and adrenocortical adenomas (Brown et al., 1997; Plantaz et al., 1997; Yano et al., 2004; Zhao et al., 1999), GpIbα "is not significantly focally amplified across the entire dataset of 3131 tumors [examined] and is not located within a focal peak region of amplification", as demonstrated by a comprehensive database analysis that was completed by Tumorscape (the Broad Institute of MIT and Harvard). This suggests that the overexpression of GpIbα may not be due to a chromosomal amplification, rather, it may occur at a transcriptional or a post-transcriptional level. As GpIbα has been identified to be a down-stream target of c-Myc transcription factor (Li et al., 2007), it is plausible

to hypothesize that GpIbα overexpression in tumors is a result of elevated transcriptional activities by c-Myc.

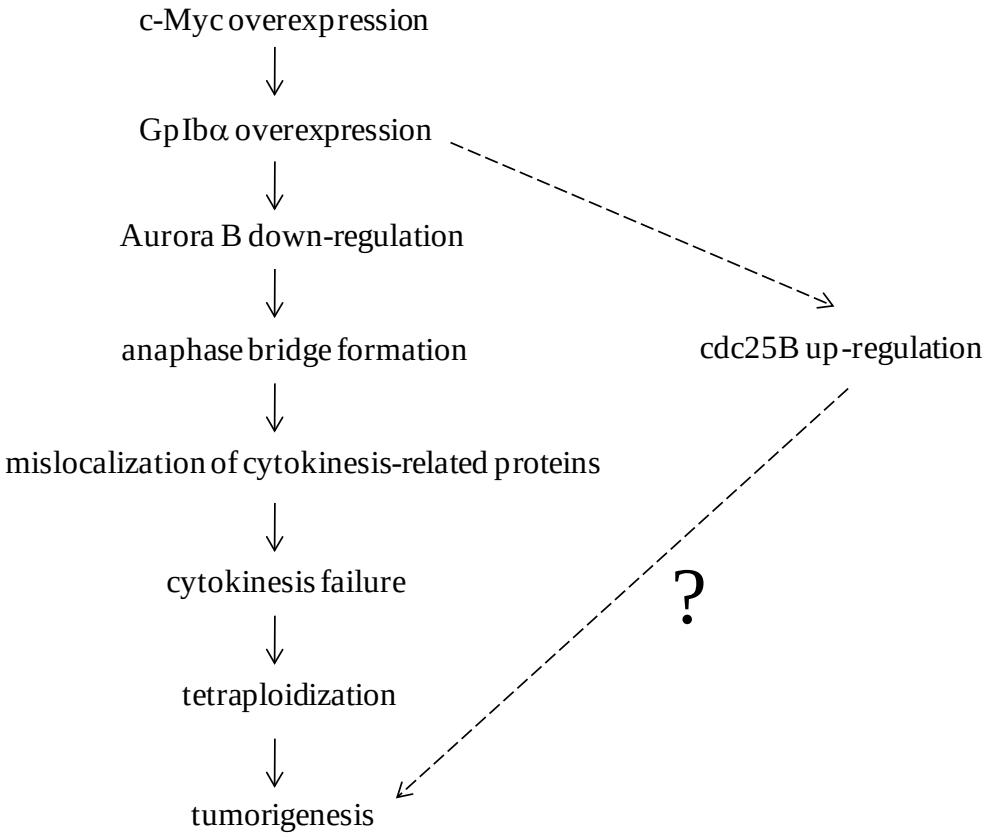

Figure 43 Model: how does overexpressed c-myc induce tumorigenesis?

c-Myc triggers GpIbα overexpression, which in turn down-regulates Aurora B (and up-regulates cdc25B). Aurora B down-regulation induces anaphase bridge formation, causing cytokinesis defects (such as mislocalization of cytokinesis-related proteins), and results in cytokinesis failure, therefore generating tetraploid cells, an intermediate towards carcinogenic transformation.

In my studies, GpIbα overexpression caused the cytokinesis defects and failure, which were mediated by the down-regulation of Aurora B, as well as other possible mechanisms such as the cdc25B up-regulation. As discussed in the "CYTOKINESIS FAILURE, TETRAPLOIDY AND TUMORIGENESIS" section of Chapter I, the outcome of cytokinesis failure is

tetraploidization, which is believed to be an intermediate step towards tumorigenesis. Therefore, taken together, all these information can be summarized into a c-Myc-GpIbα-Aurora B/cdc25B model, as demonstrated in Figure 43, which suggests a possibility that the classical oncoprotein c-Myc triggers tumorigenesis through impairing cytokinesis and generating tetraploid cells, mediated by GpIbα overexpression and consequential down-regulation of Aurora B (and/or up-regulation of cdc25B).

3.4.3 Cytokinesis defects and hyper-proliferation/tumorigenesis

It is intriguing to note that, the cells containing overexpressed GpIbα (or c-Myc) exhibit two major properties, one is the cytokinesis defects and/or cytokinesis failure, demonstrated by my studies in this chapter, and the other is the hyper-proliferation, observed by Li & Prochownik [unpublished data]. Interestingly, from a cell's point of view, cytokinesis defects are probably not favorable, while hyper-proliferation is probably favorable. The reason why a favorable phenotype and an unfavorable phenotype seem to appear hand by hand may be explained by the possibility that both of the two phenotypes, cytokinesis failure and hyper-proliferation, come from the same cause: the overexpression of GpIbα, or its origin c-Myc. In other words, cells containing overexpressed GpIbα/c-Myc gain the growth advantage of hyper-proliferation at the price of cytokinesis defects/failure, as these two phenotypes are 'bound together' by the same cause.

My data have already explored how GpIbα overexpression caused cytokinesis failure, but the mechanism through which GpIbα overexpression leads to hyper-proliferation is not known. One possible explanation is that upon GpIbα overexpression, Aurora B, a cytokinesis checkpoint

protein, is repressed, while cdc25B phophatase, a mitosis promoter, is boosted, which may suggest that GpIbα overexpression tends to accelerate the cell cycle, by affecting these cell cycle regulators.

Consequently, the cells containing overexpressed GpIbα can proliferate faster, and at the same time they are more prone to cell divisional defects and/or failure, for example these cells could continue their cell cycle and execute mitosis in the presence of unfixed DNA damage, and ultimately triggering cytokinesis failure. On the other hand, the tetraploid cells generated from the cytokinesis defects/failure caused by GpIbα overexpression may become aneuploid cells after further rounds of cell division, which possibly elicit tumorigenic properties, such as hyper-proliferation, therefore forming a positive loop between cytokinesis failure and hyper-proliferation, the key characteristic of tumorigenesis.

Therefore, the c-Myc-GpIbα-Aurora B/cdc25B model (Figure 43) seem to provide a novel mechanism to explain the divisional defects and the hyper-proliferation associated with c-Myc, both of which are observed in numerous tumors. These results hence open a new window for designing potential anti-cancer treatments, which may aim for eliminating the overexpressed GpIbα and/or its downstream effectors.

It is also important to point out that other than genomic instability and hyperproliferation, roles for GpIbα in other c-Myc-related tumorigenic pathways have not been studied (Figure 44), which may warrant future investigation.

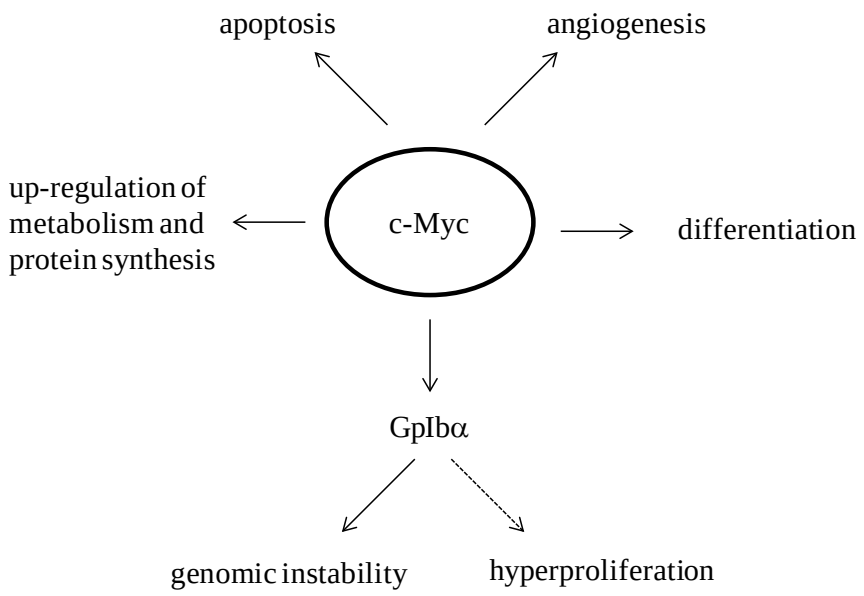

modified from Meyer and Penn, 2008

Figure 44 Effects of deregulated c-Myc that are associated with tumorigenesis.

Upregualted c-Myc can play roles in promoting cellular proliferation, differentiation, angiogenesis, apoptosis, genomic instability, as well as upregulation of metabolism and protein synthesis. Our data suggested that genomic instability induced by c-Myc was mediated by GpIbα.

3.4.4 p53 and cytokinesis

Interestingly, my data suggests that the knockdown of shp53 seemed to cause slight increases in some cytokinesis defects when compared with the control cells, for example, formation of anaphase bridges, and mislocalization of cytokinesis-related proteins, just to name a few. Similar to my observation, other reports have also demonstrated that the knockdown of p53 can lead to binucleation or multinucleation. For example, the polyploidization of differentiated megakaryocytes is found to increase upon p53 knockdown (Fuhrken et al., 2008). In addition, p53 is reported to reduce the binucleation frequency in the liver cells that are deficient in the

nucleotide excision repair pathways (Nunez et al., 2000). These reports and my data all suggest that p53 may function to prevent binucleation, hence down-regulation of p53 allows or even promotes binucleation.

The above observation might be explained by the fact that p53 is involved in the DNA damage response pathway, which is responsible for hindering cell cycle progression in the presence of DNA damage, as discussed in the "CELL CYCLE" section of Chapter I. Intuitively, the loss of p53 would attenuate the DNA damage response pathway, therefore allowing cell cycle progression in the presence of unrepaired DNA damage, leading to an accumulation of DNA damage, which may overwhelm the repair system. During mitosis, this unrepaired DNA damage could result in anaphase bridges, and cause mislocalization of the cytokinesis-related proteins, hindering the ingression of the CF, and leading to cytokinesis failure and binucleation.

Alternatively, the observation that the knockdown of p53 promotes cytokinesis defects, may be explained by the possibility that p53 is directly involved in cytokinesis. Recently, some cytokinesis regulators have been identified as targets of p53, including PRC1 and ECT2 (Li et al., 2004; Scoumanne and Chen, 2006). As p53 is a transcription factor that regulates the expression of numerous protein targets, it would not be surprising if more targets of p53 are found to be cytokinesis-related proteins. Deregulation of p53 may affect these protein expression levels, therefore resulting in an aberrant cytokinesis.

3.4.5 The organizations and functions of GpIbα, filamin A, F-actin, and RhoA in normal interphase or mitotic cells

Throughout my studies in this chapter, the localizations of GpIbα, filamin A, F-actin and RhoA were extensively examined, and my data suggests that a hypothetical complex may form, composed of these proteins, as discussed below.

3.4.5.1 The hypothetical complex of GpIbα/filamin A/F-actin

GpIbα has demonstrated colocalization with filamin A and F-actin on the cell cortex during interphase, as well as at the CF during cytokinesis, suggesting an association between these three proteins. It is highly possible that GpIbα, filamin A and F-actin form a complex (GpIbα/filamin A/F-actin complex) in the non-platelet cells, similar to what is reported in platelets (Nakamura et al., 2006), except without the rest of the vWF receptor subunits. This model needs to be tested further.

My results revealed that when the F-actin organization was disrupted by cytochalasin D, the organization of GpIbα was also disrupted, suggesting that GpIbα may be controlled by F-actin in interphase cells. This relationship may be mediated through filamin A, which is associated with both F-actin and GpIbα, and form the hypothetical GpIbα/filamin A/F-actin complex. It would be interesting to examine if when filamin A is disrupted, the localization of GpIbα would still be affected, which could test the dependency of GpIbα on filamin A.

Similarly, the mitotic arrangements and organizations of these three proteins may be similar to what they are in interphase. My data have suggested that the expression level of GpIbα influenced their localizations in cytokinesis, and additionally, filamin A and F-actin

would mislocalize at the same time as GpIbα did, supporting the hypothetical "GpIbα/filamin A/F-actin" complex during cytokinesis. It might be possible that GpIbα is recruited to the CF due to its interaction with F-actin through filamin A, however the exact role for GpIbα at the CF during cytokinesis remains to be examined.

3.4.5.2 The hypothetical complex of GpIbα/filamin A/(F-actin)/RhoA/ROCK during normal cytokinesis

One simple hypothesis for GpIbα's function at the CF is that it is required to form the "GpIbα/filamin A/F-actin" complexes during cytokinesis, which facilitates and/or maintains the correct conformations of GpIbα, filamin A and F-actin, providing accessible 'platforms' for their own binding partners.

RhoA may be one such binding partner of the "GpIbα/filamin A/F-actin" complexes, which is pivotal in regulating normal cytokinesis. RhoA has been demonstrated to control the phosphorylation of MRLC and activation of myosin II by regulating ROCK, as well as to influence F-actin assembly by regulating formin (Piekny et al., 2005). It is interesting that both RhoA and ROCK have been identified to bind to the C-terminal tail of filamin A (Pi et al., 2002; Ueda et al., 2003), suggesting that the hypothetical complex can interact with RhoA and ROCK, and may be indirectly involved in the regulation machinery of cytokinesis.

3.4.5.3 The other possible roles for filamin A in normal cytokinesis

Until now, the exact role for filamin A in cytokinesis has not been clearly identified, although its localization at the CF has been observed in my studies using cultured human cells, as well as in a previous report using chicken embryo cells (Nunnally et al., 1980). During

cytokinesis, filamin A might simply function as a structural mediator for the localizations of other cytokinesis regulators, for example, in the hypothetical complex of GpIbα/filamin A/F-actin as described above. In addition, filamin A might also exert its own function directly on the regulation of the actomyosin rings at the CF.

It is interesting to note that the well-established role for filamin A is to cross-link F-actin into gel-like networks, not anti-parallel bundle structures. As discussed previously in the "CYTOKINESIS" section of Chapter I, randomly oriented actin filaments, with myosin II motor proteins, are able to generate forces that could be used for contraction during cytokinesis (Figure 5B, C). Furthermore, in dividing yeast the F-actin filament were proposed to nucleate in irregular directions and this dynamic organization of F-actin was thought to allow the "advantageous plasticity" during the establishment of myosin node connections, for the contractile ring assembly (Vavylonis et al., 2008). Therefore, filamin A might play important roles in the assembly or the stabilization of these irregularly oriented F-actins during cytokinesis, and GpIbα-filamin A interaction might be involved in facilitating this process.

3.4.6 How does GpIbα overexpression cause cytokinesis failure?

The major theme of this chapter is to elucidate the mechanism of how GpIbα overexpression causes cytokinesis failure. There may be three possible models, as discussed below.

The first model is the anaphase bridge model, which is proposed earlier in Figure 43. In this model, GpIbα overexpression causes anaphase bridges as a primary cytokinesis defect, by down-regulating Aurora B. This in turn triggers mislocalization of cytokinesis proteins as a response to these bridge defects, therefore leading to failure of cytokinesis, and generating

binucleated daughter cells. In addition, up-regulation of cdc25B by GpIbα overexpression may also contribute the generation of binucleated cells. The details of this proposal will be expanded below.

3.4.6.1 How does GpIbα overexpression lead to Aurora B down-regulation?

It is not clear how GpIbα overexpression could result in down-regulation of Aurora B in HFF cells, however there are several possibilities. The first hypothesis involves c-Myc. As the overexpression of GpIbα has been shown to up-regulate c-Myc (Li & Prochownik, unpublished data), and as c-Myc is a well-known transcription factor that can either up-regulate or down-regulate its target proteins, it is plausible to propose that the transcription of Aurora B may be regulated by c-Myc, therefore indirectly influenced by GpIbα.

The second hypothesis involves interactants of GpIbα, such as filamin A and 14-3-3 proteins that have been demonstrated to bind to the C-terminal tail of GpIbα. 14-3-3 proteins are known to interact with various transcriptional regulators and chromatin modifiers, including histone deacetylases, histone acetyltransferases, TATA-binding proteins, p53, as well as histones (Bertos et al., 2001; Chen and Wagner, 1994; Imhof and Wolffe, 1999; Meek et al., 2004; Pan et al., 1999; Waterman et al., 1998). Therefore, affecting 14-3-3 proteins may result in deregulation of some protein transcription, for example Aurora B. It is possible that the overexpressed GpIbα might have titrated 14-3-3 proteins by binding to them, hence interfering with normal activity of 14-3-3 proteins needed for the transcription of Aurora B, and this results in the down-regulation of Aurora B. The other possible mediator of GpIbα overexpression is filamin A, which is known to have more than 20 binding partners, including integrins, RhoA and ROCK. These proteins have been demonstrated to be involved in the signaling pathways that

regulate transcription factors (Carson and Wei, 2000). Therefore, overexpression of GpIbα may affect these signal pathways via filamin A, and interfere with the transcriptional regulation of Aurora B, leading to its down-regulation.

3.4.6.2 The role for Aurora B in mediating cytokinesis failure caused by GpIbα overexpression

In this anaphase bridge model, a key question is why Aurora B down-regulation could induce an increase in anaphase bridge formation. One possible explanation is that Aurora B might be directly involved in the DNA damage monitoring and/or repair pathways, so that down-regulation of Aurora B would result in an attenuated or defective DNA damage response and/or repair pathways. This would therefore cause more DNA damage accumulating in the cell, and finally generating more anaphase bridges. A recent report has demonstrated that Aurora B is a substrate of chk1 (Peddibhotla et al., 2009; Zachos et al., 2007), one of the key transducer proteins in the DNA damage response system, hence Aurora B might be involved in the DNA damage response system, consistent with the above explanation.

Besides causing anaphase bridges to impair cytokinesis, there are other aspects of cytokinesis which the down-regulated Aurora B can affect, and leading to failure of the cell division. For example, Aurora B is the central protein for the NoCut-like cytokinesis checkpoint, as discussed in the "CYTOKINESIS" section of Chapter I, therefore, the down-regulation of Aurora B caused by GpIbα overexpression may directly attenuate the cytokinesis checkpoint. This may result in a higher chance of CF regression when anaphase bridges or chromosomes at the divisional site are present, thus contributing to an increase in the binucleated cells.

In addition to my studies in this chapter, down-regulation of Aurora B has already been reported to cause cytokinesis defects, as demonstrated in an experiment, where siRNA mediated knockdown of Aurora B prevents a midbody protein TACC1 from localizing to the midbody, and impairing cytokinesis, thus generating binucleated/multinucleated cells (Delaval et al., 2004). Hence, it would not be surprising if knockdown of Aurora B also interferes with other cytokinesis-related proteins' localization, therefore inhibiting the completion of cytokinesis.

Although the above-proposed scenarios may seem to be different from each other, they might actually overlap with each other. It is possible that Aurora B down-regulation caused by GpIbα overexpression can negatively affect various aspects of cell division, all leading to failure of cytokinesis.

3.4.6.3 The role for cdc25B in mediating cytokinesis failure caused by GpIbα overexpression

Besides Aurora B, another promising mediator in the mechanism through which GpIbα overexpression leads to cytokinesis failure could be cdc25B, which was found to be overexpressed in the GpIbα-overexpressing cells (Li & Prochownik, unpublished data). It is interesting to note that cdc25B overexpression has also been observed in numerous cancers (Gasparotto et al., 1997; Hu et al., 2001; Kudo et al., 1997; Ngan et al., 2003; Takemasa et al., 2000; Wu et al., 1998), similar to GpIbα, therefore suggesting a correlation between GpIbα, cdc25B and tumorigenesis, possibly through cytokinesis failure and tetraploidization.

It has been reported that cdc25B is up-regulated in cells with DNA damage, and facilitates the cell cycle progression of these cells (Bansal and Lazo, 2007). Similarly, another report demonstrated that overexpression of cdc25B results in premature mitosis (Karlsson et al.,

1999), which suggest that high expression levels of cdc25B tend to accelerate the cell cycle progression, regardless of damaged DNA. Therefore, in the GpIbα-overexpressing cells that already contain DNA damage, up-regulation of cdc25B may prevent normal cell cycle checkpoints, so that these cells continue to resume cell cycle, despite the presence of DNA damage. This would cause more damaged DNA accumulation within the cells, and triggering failure of cell division. Therefore, it is likely that the overexpressed cdc25B contribute to the elevated percentage of cytokinesis failure by allowing more cells with DNA damage to enter mitosis, which would potentially fail in cytokinesis.

Interestingly, when cdc25B was knockdown in the HFF-hTERT-shp53+GpIbα cells, I observed a higher frequency of apoptotic-like nuclei, although the binucleation frequency was indeed decreased (Figure 41). Additionally, abnormal cell morphology, such as flattened and enlarged cells, was sometimes perceived during cell culture (data not shown). These observations suggest that HFF-hTERT-shp53+GpIbα-shcdc25B cells seem to have a higher tendency to activate cell death. This may be due to the fact that in these cells, Aurora B was repressed by GpIbα overexpression, and cdc25B was knockdown by shRNA, in addition to p53 knockdown. Missing Aurora B, cdc25B, and p53 at the same time might be overwhelming to the cells when they proliferate, as their cell cycle regulation system and DNA damage monitoring/repair system are all attenuated. Hence, there may be too many unrepaired errors throughout the cell cycle, which may finally trigger cell death, and eliminate binucleated cells.

3.4.6.4 Alternative mechanisms through which GpIbα overexpression impairs cytokinesis, independent of the deregulation of Aurora B (or cdc25B)

Although this above model (Figure 43) is convincing, there might still be other possible models that may also contribute to the mechanism to some extent.

The first one is a RhoA-containing complex model. In this model, the abnormally high expression level of GpIbα interferes with the formation of the hypothetical "GpIbα/filamin A/(F-actin)/RhoA/ROCK complex", therefore affecting the localization of RhoA.

An additional model is a mechanical model which involves actin re-organization. In normal conditions, actin proteins need to be re-assembled and/or re-located to the CF, from other areas of the cell during cytokinesis (Cao and Wang, 1990). However when GpIbα was overexpressed, the excess GpIbα may abnormally "anchor" F-actin though filamin A to the original interphase locations, which prevents the re-organization of F-actin required for cytokinesis, hence causing cytokinesis failure.

A third model is that GpIbα overexpression may interfere with the membrane deposit/fusion pathways, which are essential for the completion of cell division. As GpIbα is a membrane protein that could interact with F-actin through filamin A, it would not be surprising if it was involved in the regulation of the actin-containing vesicles deposited at the CF during cytokinesis to separate two daughter cells, as introduced in the section of "CYTOKINESIS" of Chapter I. Therefore, overexpression of GpIbα may impair the normal formation and/or trafficking of these actin-containing vesicles, leading to failure of cytokinesis.

These above hypothetical models are independent of Aurora B (or cdc25B), and therefore might be used to explain the observation that re-expression of Aurora B did not correct

cytokinesis failure to exactly the level of control cells (Figure 39B), possibly due to the involvement of other mechanisms independent of Aurora B.

3.4.6.5 The role for filamin A in mediating cytokinesis failure caused by GpIbα overexpression

My data suggests that GpIbα's capability of binding to filamin A was essential for the mechanism through which GpIbα overexpression impaired cytokinesis. This could be due to direct involvement of filamin A in this mechanism, which may be similar to its hypothetical role as a structural mediator in normal cytokinesis, as proposed above. Or alternatively, filamin A may play an indirect role, by facilitating the post-ER trafficking of the overexpressed GpIbα.

It has been demonstrated that in platelets, the binding to filamin A is essential for stabilizing GpIbα for its intracellular trafficking towards the cell surface (Feng et al., 2005). Therefore, the overexpressed GpIbα in non-platelet cells may utilize a similar pathway, involving their interaction with filamin A, to localize to the cell cortex. Interestingly, the filamin A binding domain deleted GpIbα have been shown to accumulate in the ER fraction, when they are overexpressed in HFF-hTERT-shp53 cells (data by Li Y., not shown), supporting the hypothesis that the interaction with filamin A is needed for the post-ER trafficking of the overexpressed GpIbα towards the plasma membrane in HFF cells.

If this cortical localization is vital for the overexpressed GpIbα to interfere with cytokinesis, it would be intuitive to imagine that the binding of GpIbα to filamin A is indispensible in the mechanism, hence suggesting an indirect role for filamin A in mediating those cytokinesis defects caused by GpIbα overexpression.

3.4.7 Why does GpIbα knockdown in HeLa cells fail to correct the mislocalization of the cytokinesis-related proteins?

My results have demonstrated that GpIbα overexpression in noncancer (HFF) cells led to three types of cytokinesis defects: mislocalization of cytokinesis-related proteins, formation of anaphase bridges and generation of binucleated cells. On the other hand, GpIbα knockdown in HeLa cells significantly reduced the percentages of two cytokinesis defects: anaphase bridges and binucleation, however the mislocalizations of GpIbα, filamin A and F-actin during cytokinesis in HeLa cells were only marginally corrected by the knockdown of GpIbα.

These data suggest that some other factor(s), independent of the endogenous overexpression of GpIbα, may interfere with the localization of cytokinesis-related proteins in HeLa cells. Therefore, even when GpIbα was corrected to a near-normal level in HeLa cells by the shRNA-mediated knockdown (data by Li Y., not shown), the mislocalization of cytokinesis-related proteins was minimally improved. These factors might be deregulation of proteins involved in the membrane deposit pathways that functions during cytokinesis in HeLa cells, which can be independent of GpIbα.

One interesting fact about HeLa cells is that, unlike the HFF-hTERT-shp53+GpIbα cells which exhibited a reduced expression of Aurora B caused by GpIbα overexpression, HeLa cells demonstrate an elevated level of Aurora B (Giet et al., 2005; Meraldi et al., 2004). In the HFF-hTERT-shp53+GpIbα cells, the down-regulation of Aurora B triggered by GpIbα overexpression has been demonstrated to be the major cause for the anaphase bridge formation and binucleation. However, HeLa cells contain high protein levels of Aurora B, therefore, HeLa cells may possess other GpIbα overexpression-dependent but Aurora B downreuglation-

independent defects to induce anaphase bridges and binucleation, which could be rescued by GpIbα knockdown. One such defect might involve deregulation of cdc25B, which was discussed earlier. Similarly, there might be multiple causes for the mislocalization of cytokinesis-related proteins in HeLa cells, and GpIbα knockdown may only be one of them (probably only a minor one), therefore changing one of several causes may not be sufficient to correct the mislocalization phenotype.

3.4.8 Why does the IR treatment fail to induce higher percentages of cytokinesis protein mislocalization in the HFF-hTERT-shp53+GpIbα cells?

My data suggest that IR treatment markedly increased the frequency of anaphase bridges in the HFF-hTERT-shp53+GpIbα cells, but failed to increase the percentages of the mislocalization of cytokinesis-related proteins. On the contrary, when the HFF-hTERT-shp53 cells were treated with IR, percentages of anaphase bridges and cytokinesis protein mislocalization were both significantly increased (Figure 37, 38).

A possible explanation for the different responses of these two cell lines after IR treatment would be that the HFF-hTERT-shp53+GpIbα cells might have already reached a maximum percentage of protein mislocalization, which will be explained below. HFF-hTERT-shp53 cells did not demonstrate high percentages of cytokinesis protein mislocalization before the IR treatment, therefore these percentages may have more of a potential to increase after the IR treatment.

As mentioned previously in the “Results” section, combinations of the presence/absence of anaphase bridges and the presence/absence of the cytokinesis proteins at the CF were

observed in the IR treated HFF-hTERT-shp53+GpIbα cells. Four combinations observed include: A) with bridge, correct localization of cytokinesis proteins; B) with bridge, mislocalization of cytokinesis proteins; C) no bridge, mislocalization of cytokinesis proteins; D) no bridge, correct localization of cytokinesis proteins. These observations suggest that there might be a dynamic process for the localization changes of the cytokinesis-related proteins in response to the anaphase bridges, as proposed in Figure 45.

The combination A describes that a cell containing an anaphase bridge at the divisional site, starts with normal localization of the cytokinesis-related proteins at the CF, which might be due to the possibility that the organizations of cytokinesis-related proteins on the CF have already been established at an earlier stage of cell division.

As the CF ingresses to a certain degree, the anaphase bridge is detected, therefore triggering a cytokinesis checkpoint to hinder the CF ingression. This checkpoint can induce the disassembly of cytokinesis machineries on the CF, therefore leaving the cell with the anaphase bridge at the divisional site and mislocalized cytokinesis proteins, which is the combination B.

As the CF ingression is hindered, the cell has more time to cope with its anaphase bridge. If this DNA bridge is successfully resolved, the combination C would be observed, as a cells containing no bridge but still demonstrating cytokinesis protein mislocalization.

Lastly, if this cell is committed to resume cytokinesis, these cytokinesis-related proteins could reassemble, and cytokinesis continues, which is the combination D.

Alternatively, the combination D could also represent a normal condition, when cells do not have anaphase bridges or other types of cytokinesis defects, therefore demonstrating the correct localization of cytokinesis-related proteins at the CF. Meanwhile, the combination C

could describe that cells demonstrate mislocalized cytokinesis machineries, due to other cytokinesis defects, for example, chromosome nondisjunctions, besides anaphase bridges.

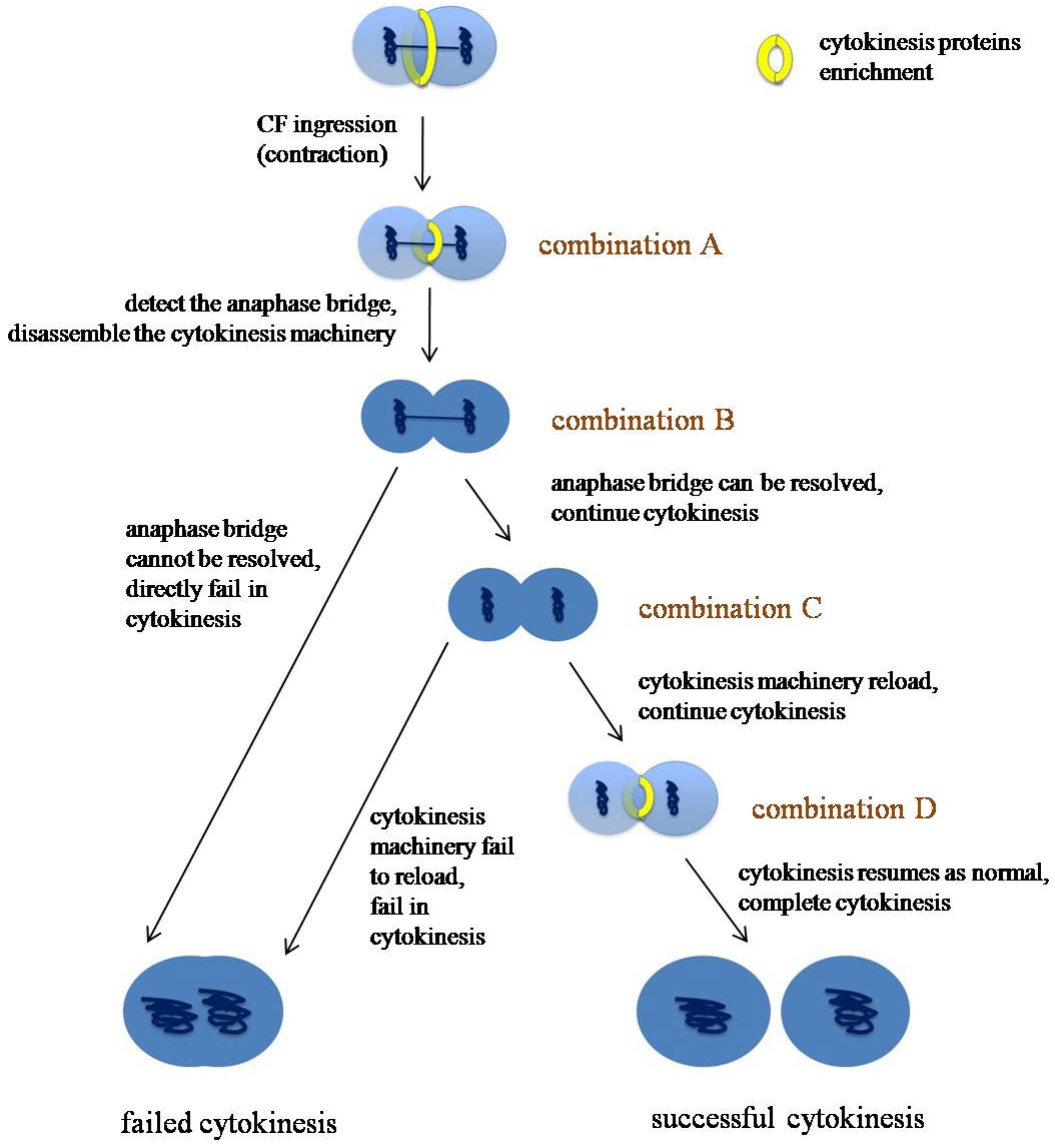

Figure 45 Model: how does a cell response to the anaphase bridge during cytokinesis?

There are four hypothetical phases, also described in the text. Phase 1: the cell has already assembled cytokinesis-related proteins at the CF before the detection of the anaphase bridge. Phase 2: as the CF ingresses, the anaphase bridge is detected (possibly due to cytokinesis checkpoints), therefore the cytokinesis-related proteins are disassembled from the CF. This cell may directly fail cytokinesis if the anaphase bridge is not resolved, generating a tetraploid cell. If the anaphase is resolved, the cell proceeds to

phase 3. Phase 3: the cell resolves the anaphase bridge, and may continue cytokinesis procedure to the phase 4; alternatively, this cell may contain other cytokinesis defects besides the anaphase bridge, such as nondisjunctions, which lead to cytokinesis failure, generating a tetraploid cell. Phase 4: the cytokinesis-related proteins are re-assembled at the CF in the cell when the anaphase bridge is resolved, and the normal progression of cytokinesis is executed. The end products are two diploid daughter cells, indicating a successful completion of cytokinesis.

If this dynamic model is what occurs in cells containing anaphase bridges and/or other divisional defects (nondisjunctions), the percentage of cytokinesis protein mislocalization, as examined by immunofluorescence using fixed cell populations, would have a maximum number. This maximum percentage of protein mislocalization will not be 100%, even if 100% of the cells possessed bridges/nondisjunctions, due to the following reason below.

Assuming 100% of cells had bridges/nondisjunctions, at any given time during cytokinesis, there would be mixed populations of cells showing combination A through D of the proposed model (Figure 45), within the same coverslip. Therefore, when this coverslip was fixed and analyzed, the percentage of cells demonstrating protein mislocalization would be calculated by: the time duration for combination B and C divided by the total time duration for the four combinations. This number will be the maximum percentage of protein mislocalization during cytokinesis, which cannot be further increased.

In the HFF-hTERT-shp53+GpIbα cells used in my study, the maximum percentage of protein mislocalization might have already been reached prior to the IR treatment, due to DNA damage, anaphase bridges, and/or other defects, exerted by GpIbα overexpression. Therefore, the observation that IR treatment in HFF-hTERT-shp53+GpIbα cells triggered an increase in the anaphase bridges, but not in the protein mislocalization during cytokinesis is due to the

possibility that the percentage of cytokinesis-related protein mislocalization has already reached to the maximum in these cells, and will not be able to further increase, even with the induction of additional bridges by the IR treatment.

4.0 CHAPTER IV. MATERIALS AND METHODS

4.1.1 Cell lines

HFF-hTERT vector only (human foreskin fibroblast immortalized with human telomerase reverse transcriptase), HFF-hTERT shp53 (stable-knockdown of p53), HFF-hTERT-GpIbα (stable-overexpression of GpIbα), HFF-hTERT-shp53+GpIbα, HFF-hTERT-shp53+Δsig-GpIbα, HFF-shp53+Δfil-GpIbα, HFF-hTERT-shp53+GpIbα+Aurora B, HFF-hTERT-shp53+GpIbα-shcdc25B cells (gifts from Dr. Edward Prochownik, University of Pittsburgh) were maintained in Dulbecco's Modified Eagle Medium (DMEM, Sigma) supplemented with 10% fetal bovine serum (FBS, Atlanta Biologicals) and 1% L-glutamine (Invitrogen). RPE-hTERT cells (retinal pigmented epithelial cell line stably transfected with human telomerase reverse transcriptase, also referred to as RPE1 cells) were maintained in DMEM/F12 supplemented with 10% FBS. UP3 (uvulopalatopharyngoplasty) cells (gift from Dr. Susanne Gollin) were maintained in KGM2 medium. Liver adenocarcinoma cell line SK-HEP (ATCC), lung adenocarcinoma epithelial cell line A549 (ATCC), and all UPCI:SCC cells (University of Pittsburgh Cancer Institute, oral squamous carcinomas cells, gifts from Dr. Susanne Gollin, University of Pittsburgh) cells were maintained in minimal essential medium (MEM, sigma) supplemented with 10% FBS and 1% non-essential amino acid (Invitrogen). Osteosarcoma cell line U-2 OS (ATCC) was maintained in McCoy's 5A medium (sigma) supplemented with 10% FBS. Human

cervical adenocarcinoma epithelial cell line HeLa and African green monkey SV40-transfected kidney fibroblast cell line COS-7 (ATCC) were maintained in DMEM supplemented with 10% FBS. All cells were cultured at 37°C with 5% CO2.

4.1.2 Plasmid transfections

10^5 cells were seeded on 22 x 22mm glass coverslips (VWR) in 6-well plates six hours prior to transfection. Each well of cells were transfected with 2μg of plasmid, using 6μl of the FuGENE6 transfection reagent (Roche Diagnostics) following the manufacture's protocol. Fresh medium was added 12 hours after transfection. Cells were examined 24-48 hours after transfection, unless where indicated. Alternatively, Lipofectamine 2000 (Invitrogen) and Tfx transfection reagents (Promega) were used following the manufacture's protocol, in the attempts to transfect plasmids into RPE-hTERT and HFF-hTERT cells.

4.1.3 p53 knockdown

Cells were seeded onto 60mm petri dishes five hour prior to siRNA transfection. sip53 (Qiagen) was transfected into cells using HiPerFect Transfection Reagent (Qiagen) following the manufacture's instruction. Fluorescently labeled scrambled siRNA was used as a control. 24-48 hours after transfection, western blotting was used to check the efficiency of p53 knockdown.

4.1.4 Immunofluorescence

Cells were fixed with 3.7% paraformaldehyde (weight/volume) in phosphate buffered saline buffer (PBS) at room temperature for 15 minutes, followed by a seven minute incubation of 0.1% triton X-100 (volume/volume) in PBS at 4°C. For visualizing RhoA, cells were fixed with 10% trichloroacetic acid (volume/volume) in PBS at 4°C for 15 minutes, followed by the same triton permeabilization. All cells were incubated in blocking buffer (1% bovine serum albumin (BSA, sigma) in PBS), for one hour at room temperature prior to immunostaining.

Primary antibodies include antibodies against α-tubulin (Abcam, Cambridge, MA, 1:500), cytochrome C (Santa Cruz Biotechnology, Santa Cruz, CA, 1:500), p150 (BD Pharmingen, San Diego, CA, 1:500), MHC (Sigma, 1:500), actin (Cytoskeleton, 1:100), filamin A (a gift from Dr. Nakamura, Translational Medicine Division, Brigham and Women's Hospital, Boston, MA, 1:500), Gp1bα (Emfret Analytics, Würzburg, Germany, 1:100), RhoA (Santa Cruz Biotechnology, 1: 100), Aurora B (BD Pharmingen, 1:100). Secondary antibodies are fluorescent labeled goat anti-rabbit or anti-mouse, or anti-rat Alexa Fluor488 or 568 (Molecular Probes, Invitrogen). All primary and secondary antibodies were diluted in blocking buffer and the incubations for primary and secondary antibodies were 30 minutes at room temperature, with three times of PBS washes in between. Rodamine-phalloidin (Cytoskeleton) was used to label F-actin, following the manufacture's protocol. DNA-specific fluorescent dye 4,6-diamidino-2-phenylindole (DAPI, Sigma, St. Louis) was used to visualize DNA by five minutes application on fixed cells. Samples were mounted with nail polish (VWR) and examined using a 40X or 100X oil immersion objective (UPlanApo) on an Olympus BX60 epifluorescence microscope. Images were taken using a Hamamatsu Argus-20 CCD camera (Hamamatsu Co., Bridgewater,

NJ). Confocal microscopy was performed using Nikon Eclipse E800 (Nikon) with BioRad Radiance 2000 system.

4.1.5 Quantification of phenotypes after microscopy analysis

Generally, at least 500 cells were analyzed to determine mitotic indexes, percentages of nuclear fragmentation, micronuclei, and binucleation/multinucleation in each experiment. At least 100 mitotic cells were analyzed to determine localization of cytokinesis-related proteins and anaphase bridges in each experiment. p values were determined by Student's unpaired two-tailed t-test, and $p < 0.05$ was considered to be 'significant'.

In order to objectively quantify the cytokinesis-related protein mislocalization in HeLa-shvector and HeLa-shGpIbα cells, blinded experiments were performed, where the labels of the coverslips that contained immunostained cells were hidden, until the counting was completed.

4.1.6 Live cell imaging

Cells transiently or stably transfected with GFP-related plasmids were cultured on 35-mm glass-bottom culture dish (MatTek Corporation, Ashland, MA). Differential interference contrast (DIC) and epifluorescence microscopy was performed on a Nikon TE2000-U inverted microscope with a CoolSNAP HQ digital camera (Roper Scientific Photometrics), while cells were maintained at 37°C in a moisturized and air-heated microscope chamber (Life Imaging Services, Reinach, Switzerland). Images were taken and analyzed using MetaMorph software (Molecular Devices). Quantification results of cytokinesis failure by live cell imaging were based on 50-120 samples analyzed for each category.

4.1.7 Cell proliferation and apoptosis assays

MTS assays were conducted using the CellTiter 96® AQ_{ueous} One Solution Cell Proliferation Assay kit (Promega) following the manufacture's instruction.

Annexin-V assays were performed following the Alex Fluor-conjugated annexin V detection kit (Molecular Probes, Invitrogen, CA), following the manufacture's instruction, with minor modifications. Briefly, Tetramethyl Rhodamine Methyl Ester (TMRM) diluted in regular buffer was used to label live cells at 37°C for 10 minutes, before the addition of annexin-V regents, which labeled the apoptotic cells. These samples were subjected to microscopy analysis by placing the coverslip upside-down for cells to face the general buffer in a chamber.

MitoTracker staining was performed by applying the fluorescent dye MitoTracker Red (Invitrogen, CA) to cells at 37°C for 10 minutes prior to fixation and microscopy analysis, following the manufacture's protocol.

4.1.8 *In vitro* MT polymerization

MTs were polymerized using the fluorescence-based tubulin polymerization assay kit (Cytoskeleton), following the manufacture's protocol.

4.1.9 Flow cytometry

Cells were fixed with cold 70% EtOH and stained with propidium iodide (Fluka: BioChemika, Switzerland) at a final concentration of 50 μg/ml. Analysis of flow cytometry was performed in the Flow Cytometry Facility in University of Pittsburgh Cancer Institute (UPCI).

4.1.10 Cellular fractionation

Cells were trypsinized and harvested by spinning at 2000 rpm for 2 minutes. The cell pellet was resuspended gently in digitonin buffer (10 mM Pipes pH6.8, 300 mM Sucrose, 100 mM NaCl, 3 mM MgCl2, 5 mM EDTA, 0.01% digitonin and 1 mM PMSF), by slowly pipetting the pellet for 20 times through an end-cut pipette tip. Cell suspension was incubated on ice for 15 minutes with gentle inversion every 5 minutes. After spinning at 2,000 rpm for 2 minutes at 4°C, the supernatant and pellets were separated. The supernatant was subjected to spinning at 6,000 rpm for 2 minutes at 4°C and the newly yielded supernatant was then transferred into a new tube and labeled as the cytoplasmic fraction. The pellet was resuspended in PBS and spun at 6,000rpm for 2 minutes at 4°C. The new pellet was resuspended in NP40 buffer (10 mM Pipes pH6.8, 300 mM Sucrose, 100 mM NaCl, 3 mM MgCl2, 3 mM EDTA, 1% NP40 and 1 mM PMSF). The suspension was incubated on ice for 15 minutes with mixing every 5 minutes and subjected to spinning at 10,000rpm for 15 minutes at 4°C. The supernatant was transferred into a new tube as the membrane-associated fraction. The pellet was resuspended in 2% sodium dodecyl sulfate (SDS) buffer as the detergent-insoluble fraction.

4.1.11 Western Blotting

Cell lysis was performed following one of the two protocols. In the RIPA protocol, cells were trypsinized and pelleted after PBS washes, followed by incubation with RIPA buffer (Tris 50mM, NaCl 150 mM, NP40 1%, with freshly added PMSF 1mM) on ice for 15 minutes, which were then subjected to centrifugation at 13,000rpm, 4°C for 15 minutes. The supernatant contained most of the proteins in cells. Alternatively, the cell pellet after trypsinizaiton and PBS

washes were lysed with 2X SDS buffer by boiling at 100 °C for 5 minutes, followed by repeated passage through syringe needle for 15 times to break the cells.

Samples were loaded onto 10% SDS-PAGE gels, and proteins were separated by electrophoresis and transferred onto PVDF membranes (Biorad, Hercules, CA). The membranes were incubated with blocking buffer 5% milk in tris-buffered Saline Tween-20 (TBST) (weight/volume) for one hour at room temperature. Primary antibodies include antibodies against cyclin B (BD, San Jose, CA), actin (Cytoskeleton, Denver, CO), p53 (Santa Cruz Biotechnology, Santa Cruz, CA), PARP1 (Cell Signaling Technology, Danvers, MA), CD44 (BD, San Jose, CA), calnexin (Stressgen, Ann Arbor, MI), GAPDH (Cell signaling, Danvers, MA), GFP (Abcam, Cambridge, MA), GP1Bα (Emfret Analytics, Würzburg, Germany). Membranes were incubated with the primary antibody diluted in blocking buffer overnight at 4°C. After 15 minute of TBST wash, membranes were then incubated with anti-mouse or anti-rabbit IgG-HRP-linked secondary antibodies (Amersham, GE Healthcare, UK) diluted in blocking buffer for one hour at room temperature. Results were visualized using an enhanced chemiluminescent kit (Pierce, Rockford, IL), following the manufacture's protocol.

4.1.12 Treatments

Cells were treated with 10 nM DZ or 100 nM vinblastine or 1 μM taxol (final concentration in the culture medium) for 38 hours at 37°C before analysis for most of the studies in Chapter II, unless where indicated. Vinblastine concentration was chosen to demonstrate a similar level of microtubule disruption as compared to 10 nM of DZ.

Cells were treated with 8 μM of cytochalasin D to disrupt the F-actin network, or with 33 μM of nocodazole to disrupt the MT network, in chapter III. Both treatments were done at 37°C for 30 minutes.

Cell permeable caspase inhibitors (caspase-3/7, -8, -9 inhibitors) (Calbiochem) were used as in reference Jennings JJ *et al.*, 2006 (Jennings et al., 2006).

H_2O_2 treatment was used to induce apoptosis. H_2O_2 was purchased from CVS or Giant Eagle and diluted into the regular cell culture medium. Cells were incubated with 10 mM of H_2O_2 for one hour before further analyses.

IR treatment was used to induce DSB DNA damage and anaphase bridge formation or induction of p53. Cells by subjected to 2 Gy of γ-radiation, followed by a release of 24 hours before further analyses.

BIBLIOGRAPHY

Acilan, C., Potter, D. M., and Saunders, W. S. (2007). DNA repair pathways involved in anaphase bridge formation. Genes Chromosomes Cancer 46, 522-531.

Adams, R. R., Tavares, A. A., Salzberg, A., Bellen, H. J., and Glover, D. M. (1998). pavarotti encodes a kinesin-like protein required to organize the central spindle and contractile ring for cytokinesis. Genes Dev 12, 1483-1494.

Adams, R. R., Wheatley, S. P., Gouldsworthy, A. M., Kandels-Lewis, S. E., Carmena, M., Smythe, C., Gerloff, D. L., and Earnshaw, W. C. (2000). INCENP binds the Aurora-related kinase AIRK2 and is required to target it to chromosomes, the central spindle and cleavage furrow. Curr Biol 10, 1075-1078.

Agarwal, M. L., Agarwal, A., Taylor, W. R., and Stark, G. R. (1995). p53 controls both the G2/M and the G1 cell cycle checkpoints and mediates reversible growth arrest in human fibroblasts. Proc Natl Acad Sci U S A 92, 8493-8497.

Albertson, R., Cao, J., Hsieh, T. S., and Sullivan, W. (2008). Vesicles and actin are targeted to the cleavage furrow via furrow microtubules and the central spindle. J Cell Biol 181, 777-790.

Allen, C., and Borisy, G. G. (1974). Structural polarity and directional growth of microtubules of Chlamydomonas flagella. J Mol Biol 90, 381-402.

Altaha, R., Fojo, T., Reed, E., and Abraham, J. (2002). Epothilones: a novel class of non-taxane microtubule-stabilizing agents. Curr Pharm Des 8, 1707-1712.

Amano, M., Ito, M., Kimura, K., Fukata, Y., Chihara, K., Nakano, T., Matsuura, Y., and Kaibuchi, K. (1996). Phosphorylation and activation of myosin by Rho-associated kinase (Rho-kinase). J Biol Chem 271, 20246-20249.

Andreassen, P. R., Martineau, S. N., and Margolis, R. L. (1996). Chemical induction of mitotic checkpoint override in mammalian cells results in aneuploidy following a transient tetraploid state. Mutat Res 372, 181-194.

Andrews, R. K., Gardiner, E. E., Shen, Y., Whisstock, J. C., and Berndt, M. C. (2003). Glycoprotein Ib-IX-V. Int J Biochem Cell Biol 35, 1170-1174.

Apodaca, G. (2001). Endocytic traffic in polarized epithelial cells: role of the actin and microtubule cytoskeleton. Traffic 2, 149-159.

Appella, E. (2001). Modulation of p53 function in cellular regulation. Eur J Biochem 268, 2763.

Appella, E., and Anderson, C. W. (2001). Post-translational modifications and activation of p53 by genotoxic stresses. Eur J Biochem 268, 2764-2772.

Arnal, I., and Wade, R. H. (1995). How does taxol stabilize microtubules? Curr Biol 5, 900-908.

Arnold, J. M. (1969). Cleavage furrow formation in a telolecithal egg (Loligo pealii). I. Filaments in early furrow formation. J Cell Biol 41, 894-904.

Askham, J. M., Vaughan, K. T., Goodson, H. V., and Morrison, E. E. (2002). Evidence that an interaction between EB1 and p150(Glued) is required for the formation and maintenance of a radial microtubule array anchored at the centrosome. Mol Biol Cell 13, 3627-3645.

Atherton-Fessler, S., Parker, L. L., Geahlen, R. L., and Piwnica-Worms, H. (1993). Mechanisms of p34cdc2 regulation. Mol Cell Biol 13, 1675-1685.

Augenlicht, L. H., Wadler, S., Corner, G., Richards, C., Ryan, L., Multani, A. S., Pathak, S., Benson, A., Haller, D., and Heerdt, B. G. (1997). Low-level c-myc amplification in human colonic carcinoma cell lines and tumors: a frequent, p53-independent mutation associated with improved outcome in a randomized multi-institutional trial. Cancer Res 57, 1769-1775.

Baglia, F. A., Badellino, K. O., Li, C. Q., Lopez, J. A., and Walsh, P. N. (2002). Factor XI binding to the platelet glycoprotein Ib-IX-V complex promotes factor XI activation by thrombin. J Biol Chem 277, 1662-1668.

Banerjee, T., Nath, S., and Roychoudhury, S. (2009). DNA damage induced p53 downregulates Cdc20 by direct binding to its promoter causing chromatin remodeling. Nucleic Acids Res 37, 2688-2698.

Banin, S., Moyal, L., Shieh, S., Taya, Y., Anderson, C. W., Chessa, L., Smorodinsky, N. I., Prives, C., Reiss, Y., Shiloh, Y., and Ziv, Y. (1998). Enhanced phosphorylation of p53 by ATM in response to DNA damage. Science 281, 1674-1677.

Bansal, P., and Lazo, J. S. (2007). Induction of Cdc25B regulates cell cycle resumption after genotoxic stress. Cancer Res 67, 3356-3363.

Becker, K. F., Allmeier, H., and Hollt, V. (1992). New mechanisms of hormone secretion: MDR-like gene products as extrusion pumps for hormones? Horm Metab Res 24, 210-213.

Bellanger, J. M., Astier, C., Sardet, C., Ohta, Y., Stossel, T. P., and Debant, A. (2000). The Rac1- and RhoG-specific GEF domain of Trio targets filamin to remodel cytoskeletal actin. Nat Cell Biol 2, 888-892.

Bement, W. M., Mandato, C. A., and Kirsch, M. N. (1999). Wound-induced assembly and closure of an actomyosin purse string in Xenopus oocytes. Curr Biol 9, 579-587.

Benink, H. A., and Bement, W. M. (2005). Concentric zones of active RhoA and Cdc42 around single cell wounds. J Cell Biol 168, 429-439.

Berndt, M. C., Du, X. P., and Booth, W. J. (1988). Ristocetin-dependent reconstitution of binding of von Willebrand factor to purified human platelet membrane glycoprotein Ib-IX complex. Biochemistry 27, 633-640.

Berridge, M. V., and Tan, A. S. (1993). Characterization of the cellular reduction of 3-(4,5-dimethylthiazol-2-yl)-2,5-diphenyltetrazolium bromide (MTT): subcellular localization, substrate dependence, and involvement of mitochondrial electron transport in MTT reduction. Arch Biochem Biophys 303, 474-482.

Berry, L. D., and Gould, K. L. (1996). Regulation of Cdc2 activity by phosphorylation at T14/Y15. Prog Cell Cycle Res 2, 99-105.

Bertos, N. R., Wang, A. H., and Yang, X. J. (2001). Class II histone deacetylases: structure, function, and regulation. Biochem Cell Biol 79, 243-252.

Beumer, S., Heijnen, H. F., MJ, I. J., Orlando, E., de Groot, P. G., and Sixma, J. J. (1995). Platelet adhesion to fibronectin in flow: the importance of von Willebrand factor and glycoprotein Ib. Blood 86, 3452-3460.

Bharti, A. C., Takada, Y., and Aggarwal, B. B. (2005). PARP cleavage and caspase activity to assess chemosensitivity. Methods Mol Med 111, 69-78.

Blagosklonny, M. V. (2007). Mitotic arrest and cell fate: why and how mitotic inhibition of transcription drives mutually exclusive events. Cell Cycle 6, 70-74.

Blagosklonny, M. V., Darzynkiewicz, Z., Halicka, H. D., Pozarowski, P., Demidenko, Z. N., Barry, J. J., Kamath, K. R., and Herrmann, R. A. (2004). Paclitaxel induces primary and postmitotic G1 arrest in human arterial smooth muscle cells. Cell Cycle 3, 1050-1056.

Blagosklonny, M. V., Demidenko, Z. N., Giovino, M., Szynal, C., Donskoy, E., Herrmann, R. A., Barry, J. J., and Whalen, A. M. (2006). Cytostatic activity of paclitaxel in coronary artery smooth muscle cells is mediated through transient mitotic arrest followed by permanent post-mitotic arrest: comparison with cancer cells. Cell Cycle 5, 1574-1579.

Bollag, D. M., McQueney, P. A., Zhu, J., Hensens, O., Koupal, L., Liesch, J., Goetz, M., Lazarides, E., and Woods, C. M. (1995). Epothilones, a new class of microtubule-stabilizing agents with a taxol-like mechanism of action. Cancer Res 55, 2325-2333.

Bolton, M. A., Lan, W., Powers, S. E., McCleland, M. L., Kuang, J., and Stukenberg, P. T. (2002). Aurora B kinase exists in a complex with survivin and INCENP and its kinase activity is stimulated by survivin binding and phosphorylation. Mol Biol Cell 13, 3064-3077.

Bonnefoy, A., Daenens, K., Feys, H. B., De Vos, R., Vandervoort, P., Vermylen, J., Lawler, J., and Hoylaerts, M. F. (2006). Thrombospondin-1 controls vascular platelet recruitment and thrombus adherence in mice by protecting (sub)endothelial VWF from cleavage by ADAMTS13. Blood 107, 955-964.

Bradford, H. N., Dela Cadena, R. A., Kunapuli, S. P., Dong, J. F., Lopez, J. A., and Colman, R. W. (1997). Human kininogens regulate thrombin binding to platelets through the glycoprotein Ib-IX-V complex. Blood 90, 1508-1515.

Bradford, H. N., Pixley, R. A., and Colman, R. W. (2000). Human factor XII binding to the glycoprotein Ib-IX-V complex inhibits thrombin-induced platelet aggregation. J Biol Chem 275, 22756-22763.

Brinkley, B. R., and Stubblefield, E. (1966). The fine structure of the kinetochore of a mammalian cell in vitro. Chromosoma 19, 28-43.

Brito, D. A., and Rieder, C. L. (2006). Mitotic checkpoint slippage in humans occurs via cyclin B destruction in the presence of an active checkpoint. Curr Biol 16, 1194-1200.

Brotschi, E. A., Hartwig, J. H., and Stossel, T. P. (1978). The gelation of actin by actin-binding protein. J Biol Chem 253, 8988-8993.

Brown, E., and Hogg, N. (1996). Where the outside meets the inside: integrins as activators and targets of signal transduction cascades. Immunol Lett 54, 189-193.

Brown, J. A., Anderl, K. L., Borell, T. J., Qian, J., Bostwick, D. G., and Jenkins, R. B. (1997). Simultaneous chromosome 7 and 17 gain and sex chromosome loss provide evidence that renal metanephric adenoma is related to papillary renal cell carcinoma. J Urol 158, 370-374.

Cai, J., Yang, J., and Jones, D. P. (1998). Mitochondrial control of apoptosis: the role of cytochrome c. Biochim Biophys Acta 1366, 139-149.

Calderwood, D. A., Shattil, S. J., and Ginsberg, M. H. (2000). Integrins and actin filaments: reciprocal regulation of cell adhesion and signaling. J Biol Chem 275, 22607-22610.

Canman, C. E., Lim, D. S., Cimprich, K. A., Taya, Y., Tamai, K., Sakaguchi, K., Appella, E., Kastan, M. B., and Siliciano, J. D. (1998). Activation of the ATM kinase by ionizing radiation and phosphorylation of p53. Science 281, 1677-1679.

Cao, L. G., and Wang, Y. L. (1990). Mechanism of the formation of contractile ring in dividing cultured animal cells. I. Recruitment of preexisting actin filaments into the cleavage furrow. J Cell Biol 110, 1089-1095.

Carlier, M. F. (1982). Guanosine-5'-triphosphate hydrolysis and tubulin polymerization. Review article. Mol Cell Biochem 47, 97-113.

Carlier, M. F., and Pantaloni, D. (1978). Kinetic analysis of cooperativity in tubulin polymerization in the presence of guanosine di- or triphosphate nucleotides. Biochemistry 17, 1908-1915.

Carlier, M. F., and Pantaloni, D. (1981). Kinetic analysis of guanosine 5'-triphosphate hydrolysis associated with tubulin polymerization. Biochemistry 20, 1918-1924.

Carson, J. A., and Wei, L. (2000). Integrin signaling's potential for mediating gene expression in hypertrophying skeletal muscle. J Appl Physiol 88, 337-343.

Carvalho, A., Desai, A., and Oegema, K. (2009). Structural memory in the contractile ring makes the duration of cytokinesis independent of cell size. Cell 137, 926-937.

Casares, S., Rodriguez, J. M., Martin, A., and Parrado, A. (1993). Rearrangements of c-myc and c-abl genes in tumour cells in Burkitt's lymphoma. J Clin Pathol 46, 778-779.

Chalamalasetty, R. B., Hummer, S., Nigg, E. A., and Sillje, H. H. (2006). Influence of human Ect2 depletion and overexpression on cleavage furrow formation and abscission. J Cell Sci 119, 3008-3019.

Chan, K. L., North, P. S., and Hickson, I. D. (2007). BLM is required for faithful chromosome segregation and its localization defines a class of ultrafine anaphase bridges. EMBO J 26, 3397-3409.

Chaturvedi, P., Eng, W. K., Zhu, Y., Mattern, M. R., Mishra, R., Hurle, M. R., Zhang, X., Annan, R. S., Lu, Q., Faucette, L. F., et al. (1999). Mammalian Chk2 is a downstream effector of the ATM-dependent DNA damage checkpoint pathway. Oncogene 18, 4047-4054.

Chaudhuri, A. R., Tomita, I., Mizuhashi, F., Murata, K., and Luduena, R. F. (1998). Distinct and overlapping binding sites for IKP104 and vinblastine on tubulin. J Protein Chem 17, 685-690.

Cheeseman, I. M., Anderson, S., Jwa, M., Green, E. M., Kang, J., Yates, J. R., 3rd, Chan, C. S., Drubin, D. G., and Barnes, G. (2002). Phospho-regulation of kinetochore-microtubule attachments by the Aurora kinase Ipl1p. Cell 111, 163-172.

Chen, F., and Wagner, P. D. (1994). 14-3-3 proteins bind to histone and affect both histone phosphorylation and dephosphorylation. FEBS Lett 347, 128-132.

Chew, T. L., Wolf, W. A., Gallagher, P. J., Matsumura, F., and Chisholm, R. L. (2002). A fluorescent resonant energy transfer-based biosensor reveals transient and regional myosin light chain kinase activation in lamella and cleavage furrows. J Cell Biol 156, 543-553.

Chiu, L. Y., Ko, J. L., Lee, Y. J., Yang, T. Y., Tee, Y. T., and Sheu, G. T. L-type calcium channel blockers reverse docetaxel and vincristine-induced multidrug resistance independent of ABCB1 expression in human lung cancer cell lines. Toxicol Lett 192, 408-418.

Cimini, D., Moree, B., Canman, J. C., and Salmon, E. D. (2003). Merotelic kinetochore orientation occurs frequently during early mitosis in mammalian tissue cells and error correction is achieved by two different mechanisms. J Cell Sci 116, 4213-4225.

Cimini, D., Wan, X., Hirel, C. B., and Salmon, E. D. (2006). Aurora kinase promotes turnover of kinetochore microtubules to reduce chromosome segregation errors. Curr Biol 16, 1711-1718.

Clemetson, K. J., and Clemetson, J. M. (1995). Platelet GPIb-V-IX complex. Structure, function, physiology, and pathology. Semin Thromb Hemost 21, 130-136.

Cooper, J. A. (1987). Effects of cytochalasin and phalloidin on actin. J Cell Biol 105, 1473-1478.

Cooper, S. (2003). Reappraisal of serum starvation, the restriction point, G0, and G1 phase arrest points. FASEB J 17, 333-340.

Cory, A. H., Owen, T. C., Barltrop, J. A., and Cory, J. G. (1991). Use of an aqueous soluble tetrazolium/formazan assay for cell growth assays in culture. Cancer Commun 3, 207-212.

Crews, S., Barth, R., Hood, L., Prehn, J., and Calame, K. (1982). Mouse c-myc oncogene is located on chromosome 15 and translocated to chromosome 12 in plasmacytomas. Science 218, 1319-1321.

Dalla-Favera, R., Bregni, M., Erikson, J., Patterson, D., Gallo, R. C., and Croce, C. M. (1982). Human c-myc onc gene is located on the region of chromosome 8 that is translocated in Burkitt lymphoma cells. Proc Natl Acad Sci U S A 79, 7824-7827.

Dammermann, A., Desai, A., and Oegema, K. (2003). The minus end in sight. Curr Biol 13, R614-624.

Daniels, M. J., Wang, Y., Lee, M., and Venkitaraman, A. R. (2004). Abnormal cytokinesis in cells deficient in the breast cancer susceptibility protein BRCA2. Science 306, 876-879.

Darenfed, H., and Mandato, C. A. (2005). Wound-induced contractile ring: a model for cytokinesis. Biochem Cell Biol 83, 711-720.

Darwiche, N., Freeman, L. A., and Strunnikov, A. (1999). Characterization of the components of the putative mammalian sister chromatid cohesion complex. Gene 233, 39-47.

David-Pfeuty, T., Erickson, H. P., and Pantaloni, D. (1977). Guanosinetriphosphatase activity of tubulin associated with microtubule assembly. Proc Natl Acad Sci U S A 74, 5372-5376.

Debili, N., Issaad, C., Masse, J. M., Guichard, J., Katz, A., Breton-Gorius, J., and Vainchenker, W. (1992). Expression of CD34 and platelet glycoproteins during human megakaryocytic differentiation. Blood 80, 3022-3035.

Delaval, B., Ferrand, A., Conte, N., Larroque, C., Hernandez-Verdun, D., Prigent, C., and Birnbaum, D. (2004). Aurora B -TACC1 protein complex in cytokinesis. Oncogene 23, 4516-4522.

Delos, S. E., Burdick, M. J., and White, J. M. (2002). A single glycosylation site within the receptor-binding domain of the avian sarcoma/leukosis virus glycoprotein is critical for receptor binding. Virology 294, 354-363.

DeLuca, J. G., Gall, W. E., Ciferri, C., Cimini, D., Musacchio, A., and Salmon, E. D. (2006). Kinetochore microtubule dynamics and attachment stability are regulated by Hec1. Cell 127, 969-982.

Demidenko, Z. N., and Blagosklonny, M. V. (2004). Flavopiridol induces p53 via initial inhibition of Mdm2 and p21 and, independently of p53, sensitizes apoptosis-reluctant cells to tumor necrosis factor. Cancer Res 64, 3653-3660.

Denis, C., Methia, N., Frenette, P. S., Rayburn, H., Ullman-Cullere, M., Hynes, R. O., and Wagner, D. D. (1998). A mouse model of severe von Willebrand disease: defects in hemostasis and thrombosis. Proc Natl Acad Sci U S A 95, 9524-9529.

DeRosier, D. J., and Tilney, L. G. (2000). F-actin bundles are derivatives of microvilli: What does this tell us about how bundles might form? J Cell Biol 148, 1-6.
Donjerkovic, D., and Scott, D. W. (2000). Regulation of the G1 phase of the mammalian cell cycle. Cell Res 10, 1-16.
Dotto, G. P. (2000). p21(WAF1/Cip1): more than a break to the cell cycle? Biochim Biophys Acta 1471, M43-56.
Du, X. (2007). Signaling and regulation of the platelet glycoprotein Ib-IX-V complex. Curr Opin Hematol 14, 262-269.
Duelli, D., and Lazebnik, Y. (2007). Cell-to-cell fusion as a link between viruses and cancer. Nat Rev Cancer 7, 968-976.
Duelli, D. M., Hearn, S., Myers, M. P., and Lazebnik, Y. (2005). A primate virus generates transformed human cells by fusion. J Cell Biol 171, 493-503.
Duelli, D. M., Padilla-Nash, H. M., Berman, D., Murphy, K. M., Ried, T., and Lazebnik, Y. (2007). A virus causes cancer by inducing massive chromosomal instability through cell fusion. Curr Biol 17, 431-437.
Dulic, V., Kaufmann, W. K., Wilson, S. J., Tlsty, T. D., Lees, E., Harper, J. W., Elledge, S. J., and Reed, S. I. (1994). p53-dependent inhibition of cyclin-dependent kinase activities in human fibroblasts during radiation-induced G1 arrest. Cell 76, 1013-1023.
Dulyaninova, N. G., and Bresnick, A. R. (2004). The long myosin light chain kinase is differentially phosphorylated during interphase and mitosis. Exp Cell Res 299, 303-314.
Duriez, P. J., and Shah, G. M. (1997). Cleavage of poly(ADP-ribose) polymerase: a sensitive parameter to study cell death. Biochem Cell Biol 75, 337-349.
Dussmann, H., Rehm, M., Kogel, D., and Prehn, J. H. (2003). Outer mitochondrial membrane permeabilization during apoptosis triggers caspase-independent mitochondrial and caspase-dependent plasma membrane potential depolarization: a single-cell analysis. J Cell Sci 116, 525-536.
Dutrillaux, B., Gerbault-Seureau, M., Remvikos, Y., Zafrani, B., and Prieur, M. (1991). Breast cancer genetic evolution: I. Data from cytogenetics and DNA content. Breast Cancer Res Treat 19, 245-255.
Eda, M., Yonemura, S., Kato, T., Watanabe, N., Ishizaki, T., Madaule, P., and Narumiya, S. (2001). Rho-dependent transfer of Citron-kinase to the cleavage furrow of dividing cells. J Cell Sci 114, 3273-3284.
Eggert, U. S., Mitchison, T. J., and Field, C. M. (2006). Animal cytokinesis: from parts list to mechanisms. Annu Rev Biochem 75, 543-566.
el-Deiry, W. S., Harper, J. W., O'Connor, P. M., Velculescu, V. E., Canman, C. E., Jackman, J., Pietenpol, J. A., Burrell, M., Hill, D. E., Wang, Y., and et al. (1994). WAF1/CIP1 is induced in p53-mediated G1 arrest and apoptosis. Cancer Res 54, 1169-1174.
Elhajouji, A., Cunha, M., and Kirsch-Volders, M. (1998). Spindle poisons can induce polyploidy by mitotic slippage and micronucleate mononucleates in the cytokinesis-block assay. Mutagenesis 13, 193-198.
Elnakady, Y. A., Sasse, F., Lunsdorf, H., and Reichenbach, H. (2004). Disorazol A1, a highly effective antimitotic agent acting on tubulin polymerization and inducing apoptosis in mammalian cells. Biochem Pharmacol 67, 927-935.
Erisman, M. D., Rothberg, P. G., Diehl, R. E., Morse, C. C., Spandorfer, J. M., and Astrin, S. M. (1985). Deregulation of c-myc gene expression in human colon carcinoma is not accompanied by amplification or rearrangement of the gene. Mol Cell Biol 5, 1969-1976.

Escot, C., Theillet, C., Lidereau, R., Spyratos, F., Champeme, M. H., Gest, J., and Callahan, R. (1986). Genetic alteration of the c-myc protooncogene (MYC) in human primary breast carcinomas. Proc Natl Acad Sci U S A 83, 4834-4838.

Evans, L., Mitchison, T., and Kirschner, M. (1985). Influence of the centrosome on the structure of nucleated microtubules. J Cell Biol 100, 1185-1191.

Ewers, S. B., Langstrom, E., Baldetorp, B., and Killander, D. (1984). Flow-cytometric DNA analysis in primary breast carcinomas and clinicopathological correlations. Cytometry 5, 408-419.

Fang, G., Yu, H., and Kirschner, M. W. (1998). The checkpoint protein MAD2 and the mitotic regulator CDC20 form a ternary complex with the anaphase-promoting complex to control anaphase initiation. Genes Dev 12, 1871-1883.

Faull, R. J., and Ginsberg, M. H. (1996). Inside-out signaling through integrins. J Am Soc Nephrol 7, 1091-1097.

Feng, S., Lu, X., and Kroll, M. H. (2005). Filamin A binding stabilizes nascent glycoprotein Ibalpha trafficking and thereby enhances its surface expression. J Biol Chem 280, 6709-6715.

Feng, S., Resendiz, J. C., Lu, X., and Kroll, M. H. (2003). Filamin A binding to the cytoplasmic tail of glycoprotein Ibalpha regulates von Willebrand factor-induced platelet activation. Blood 102, 2122-2129.

Fielding, A. B., Schonteich, E., Matheson, J., Wilson, G., Yu, X., Hickson, G. R., Srivastava, S., Baldwin, S. A., Prekeris, R., and Gould, G. W. (2005). Rab11-FIP3 and FIP4 interact with Arf6 and the exocyst to control membrane traffic in cytokinesis. EMBO J 24, 3389-3399.

Foley, E. A., and Kapoor, T. M. (2009). Chromosome congression: on the bi-orient express. Nat Cell Biol 11, 787-789.

Fuhrken, P. G., Apostolidis, P. A., Lindsey, S., Miller, W. M., and Papoutsakis, E. T. (2008). Tumor suppressor protein p53 regulates megakaryocytic polyploidization and apoptosis. J Biol Chem 283, 15589-15600.

Fujiwara, T., Bandi, M., Nitta, M., Ivanova, E. V., Bronson, R. T., and Pellman, D. (2005). Cytokinesis failure generating tetraploids promotes tumorigenesis in p53-null cells. Nature 437, 1043-1047.

Fuller, B. G., Lampson, M. A., Foley, E. A., Rosasco-Nitcher, S., Le, K. V., Tobelmann, P., Brautigan, D. L., Stukenberg, P. T., and Kapoor, T. M. (2008). Midzone activation of aurora B in anaphase produces an intracellular phosphorylation gradient. Nature 453, 1132-1136.

Furnari, B., Rhind, N., and Russell, P. (1997). Cdc25 mitotic inducer targeted by chk1 DNA damage checkpoint kinase. Science 277, 1495-1497.

Galipeau, P. C., Cowan, D. S., Sanchez, C. A., Barrett, M. T., Emond, M. J., Levine, D. S., Rabinovitch, P. S., and Reid, B. J. (1996). 17p (p53) allelic losses, 4N (G2/tetraploid) populations, and progression to aneuploidy in Barrett's esophagus. Proc Natl Acad Sci U S A 93, 7081-7084.

Garcia-Campayo, V., Sugahara, T., and Boime, I. (2002). Unmasking a new recognition signal for O-linked glycosylation in the chorionic gonadotropin beta subunit. Mol Cell Endocrinol 194, 63-70.

Gasparotto, D., Maestro, R., Piccinin, S., Vukosavljevic, T., Barzan, L., Sulfaro, S., and Boiocchi, M. (1997). Overexpression of CDC25A and CDC25B in head and neck cancers. Cancer Res 57, 2366-2368.

Georgatos, S. D., Pyrpasopoulou, A., and Theodoropoulos, P. A. (1997). Nuclear envelope breakdown in mammalian cells involves stepwise lamina disassembly and microtubule-drive deformation of the nuclear membrane. J Cell Sci 110 (Pt 17), 2129-2140.

George, S. P., Wang, Y., Mathew, S., Srinivasan, K., and Khurana, S. (2007). Dimerization and actin-bundling properties of villin and its role in the assembly of epithelial cell brush borders. J Biol Chem 282, 26528-26541.

Giaccia, A. J., and Kastan, M. B. (1998). The complexity of p53 modulation: emerging patterns from divergent signals. Genes Dev 12, 2973-2983.

Giansanti, M. G., Bonaccorsi, S., Bucciarelli, E., and Gatti, M. (2001). Drosophila male meiosis as a model system for the study of cytokinesis in animal cells. Cell Struct Funct 26, 609-617.

Giansanti, M. G., Bonaccorsi, S., Williams, B., Williams, E. V., Santolamazza, C., Goldberg, M. L., and Gatti, M. (1998). Cooperative interactions between the central spindle and the contractile ring during Drosophila cytokinesis. Genes Dev 12, 396-410.

Giet, R., Petretti, C., and Prigent, C. (2005). Aurora kinases, aneuploidy and cancer, a coincidence or a real link? Trends Cell Biol 15, 241-250.

Glotzer, M. (2004). Cleavage furrow positioning. J Cell Biol 164, 347-351.

Glotzer, M., Murray, A. W., and Kirschner, M. W. (1991). Cyclin is degraded by the ubiquitin pathway. Nature 349, 132-138.

Goeckeler, Z. M., Masaracchia, R. A., Zeng, Q., Chew, T. L., Gallagher, P., and Wysolmerski, R. B. (2000). Phosphorylation of myosin light chain kinase by p21-activated kinase PAK2. J Biol Chem 275, 18366-18374.

Gomez-Roman, N., Felton-Edkins, Z. A., Kenneth, N. S., Goodfellow, S. J., Athineos, D., Zhang, J., Ramsbottom, B. A., Innes, F., Kantidakis, T., Kerr, E. R., et al. (2006). Activation by c-Myc of transcription by RNA polymerases I, II and III. Biochem Soc Symp, 141-154.

Goode, B. L., and Eck, M. J. (2007). Mechanism and function of formins in the control of actin assembly. Annu Rev Biochem 76, 593-627.

Gromley, A., Yeaman, C., Rosa, J., Redick, S., Chen, C. T., Mirabelle, S., Guha, M., Sillibourne, J., and Doxsey, S. J. (2005). Centriolin anchoring of exocyst and SNARE complexes at the midbody is required for secretory-vesicle-mediated abscission. Cell 123, 75-87.

Gu, Y., Rosenblatt, J., and Morgan, D. O. (1992). Cell cycle regulation of CDK2 activity by phosphorylation of Thr160 and Tyr15. EMBO J 11, 3995-4005.

Hanson, P. I., Roth, R., Lin, Y., and Heuser, J. E. (2008). Plasma membrane deformation by circular arrays of ESCRT-III protein filaments. J Cell Biol 180, 389-402.

Hardwick, K. G., Johnston, R. C., Smith, D. L., and Murray, A. W. (2000). MAD3 encodes a novel component of the spindle checkpoint which interacts with Bub3p, Cdc20p, and Mad2p. J Cell Biol 148, 871-882.

Hardwick, K. G., Li, R., Mistrot, C., Chen, R. H., Dann, P., Rudner, A., and Murray, A. W. (1999). Lesions in many different spindle components activate the spindle checkpoint in the budding yeast Saccharomyces cerevisiae. Genetics 152, 509-518.

Harrington, W. F., and Rodgers, M. E. (1984). Myosin. Annu Rev Biochem 53, 35-73.

Hau, P. M., Siu, W. Y., Wong, N., Lai, P. B., and Poon, R. Y. (2006). Polyploidization increases the sensitivity to DNA-damaging agents in mammalian cells. FEBS Lett 580, 4727-4736.
Heiskanen, K. M., Bhat, M. B., Wang, H. W., Ma, J., and Nieminen, A. L. (1999). Mitochondrial depolarization accompanies cytochrome c release during apoptosis in PC6 cells. J Biol Chem 274, 5654-5658.
Hernandez-Verdun, D., and Gautier, T. (1994). The chromosome periphery during mitosis. Bioessays 16, 179-185.
Higuchi, T., and Uhlmann, F. (2005). Stabilization of microtubule dynamics at anaphase onset promotes chromosome segregation. Nature 433, 171-176.
Himes, R. H., Kersey, R. N., Heller-Bettinger, I., and Samson, F. E. (1976). Action of the vinca alkaloids vincristine, vinblastine, and desacetyl vinblastine amide on microtubules in vitro. Cancer Res 36, 3798-3802.
Hirokawa, N. (2006). mRNA transport in dendrites: RNA granules, motors, and tracks. J Neurosci 26, 7139-7142.
Hodge, T. P., Cross, R., and Kendrick-Jones, J. (1992). Role of the COOH-terminal nonhelical tailpiece in the assembly of a vertebrate nonmuscle myosin rod. J Cell Biol 118, 1085-1095.
Hoffman, D. B., Pearson, C. G., Yen, T. J., Howell, B. J., and Salmon, E. D. (2001). Microtubule-dependent changes in assembly of microtubule motor proteins and mitotic spindle checkpoint proteins at PtK1 kinetochores. Mol Biol Cell 12, 1995-2009.
Hoffman, W. H., Biade, S., Zilfou, J. T., Chen, J., and Murphy, M. (2002). Transcriptional repression of the anti-apoptotic survivin gene by wild type p53. J Biol Chem 277, 3247-3257.
Holland, A. J., and Taylor, S. S. (2006). Cyclin-B1-mediated inhibition of excess separase is required for timely chromosome disjunction. J Cell Sci 119, 3325-3336.
Holloway, S. L., Glotzer, M., King, R. W., and Murray, A. W. (1993). Anaphase is initiated by proteolysis rather than by the inactivation of maturation-promoting factor. Cell 73, 1393-1402.
Honda, R., Korner, R., and Nigg, E. A. (2003). Exploring the functional interactions between Aurora B, INCENP, and survivin in mitosis. Mol Biol Cell 14, 3325-3341.
Hopkins, C. D., and Wipf, P. (2009). Isolation, biology and chemistry of the disorazoles: new anti-cancer macrodiolides. Nat Prod Rep 26, 585-601.
Hotani, H., and Miyamoto, H. (1990). Dynamic features of microtubules as visualized by dark-field microscopy. Adv Biophys 26, 135-156.
Hotulainen, P., and Lappalainen, P. (2006). Stress fibers are generated by two distinct actin assembly mechanisms in motile cells. J Cell Biol 173, 383-394.
Howell, B. J., McEwen, B. F., Canman, J. C., Hoffman, D. B., Farrar, E. M., Rieder, C. L., and Salmon, E. D. (2001). Cytoplasmic dynein/dynactin drives kinetochore protein transport to the spindle poles and has a role in mitotic spindle checkpoint inactivation. J Cell Biol 155, 1159-1172.
Hoyt, M. A., Totis, L., and Roberts, B. T. (1991). S. cerevisiae genes required for cell cycle arrest in response to loss of microtubule function. Cell 66, 507-517.
Hu, Y. C., Lam, K. Y., Law, S., Wong, J., and Srivastava, G. (2001). Identification of differentially expressed genes in esophageal squamous cell carcinoma (ESCC) by cDNA expression array: overexpression of Fra-1, Neogenin, Id-1, and CDC25B genes in ESCC. Clin Cancer Res 7, 2213-2221.

Hwang, L. H., Lau, L. F., Smith, D. L., Mistrot, C. A., Hardwick, K. G., Hwang, E. S., Amon, A., and Murray, A. W. (1998). Budding yeast Cdc20: a target of the spindle checkpoint. Science 279, 1041-1044.

Ikebe, M., and Hartshorne, D. J. (1985a). Phosphorylation of smooth muscle myosin at two distinct sites by myosin light chain kinase. J Biol Chem 260, 10027-10031.

Ikebe, M., and Hartshorne, D. J. (1985b). The role of myosin phosphorylation in the contraction-relaxation cycle of smooth muscle. Experientia 41, 1006-1010.

Ikebe, M., Hartshorne, D. J., and Elzinga, M. (1986). Identification, phosphorylation, and dephosphorylation of a second site for myosin light chain kinase on the 20,000-dalton light chain of smooth muscle myosin. J Biol Chem 261, 36-39.

Iliakis, G., Wang, Y., Guan, J., and Wang, H. (2003). DNA damage checkpoint control in cells exposed to ionizing radiation. Oncogene 22, 5834-5847.

Imhof, A., and Wolffe, A. P. (1999). Purification and properties of the Xenopus Hat1 acetyltransferase: association with the 14-3-3 proteins in the oocyte nucleus. Biochemistry 38, 13085-13093.

Inoue, S., and Ritter, H., Jr. (1975). Dynamics of mitotic spindle organization and function. Soc Gen Physiol Ser 30, 3-30.

Jackson, C. W. (1990). Megakaryocyte endomitosis: a review. Int J Cell Cloning 8, 224-226.

Jansen, R., Irschik, H., Reichenbach, H., Wray, V., and Hofle, G. (1994). Antibiotics from gliding bacteria, LIX: Disorazoles, highly cytotoxic metabolites from the sorangicin-producing bacterium sorangium cellulosum strain. Liebigs Annalen der Chemie 8**.**

Jantsch-Plunger, V., Gonczy, P., Romano, A., Schnabel, H., Hamill, D., Schnabel, R., Hyman, A. A., and Glotzer, M. (2000). CYK-4: A Rho family gtpase activating protein (GAP) required for central spindle formation and cytokinesis. J Cell Biol 149, 1391-1404.

Janz, M., Stuhmer, T., Vassilev, L. T., and Bargou, R. C. (2007). Pharmacologic activation of p53-dependent and p53-independent apoptotic pathways in Hodgkin/Reed-Sternberg cells. Leukemia 21, 772-779.

Jennings, J. J., Jr., Zhu, J. H., Rbaibi, Y., Luo, X., Chu, C. T., and Kiselyov, K. (2006). Mitochondrial aberrations in mucolipidosis Type IV. J Biol Chem 281, 39041-39050.

Johnson, D. G. (1995). Regulation of E2F-1 gene expression by p130 (Rb2) and D-type cyclin kinase activity. Oncogene 11, 1685-1692.

Jones, J. M., Attardi, L., Godley, L. A., Laucirica, R., Medina, D., Jacks, T., Varmus, H. E., and Donehower, L. A. (1997). Absence of p53 in a mouse mammary tumor model promotes tumor cell proliferation without affecting apoptosis. Cell Growth Differ 8, 829-838.

Jurk, K., Clemetson, K. J., de Groot, P. G., Brodde, M. F., Steiner, M., Savion, N., Varon, D., Sixma, J. J., Van Aken, H., and Kehrel, B. E. (2003). Thrombospondin-1 mediates platelet adhesion at high shear via glycoprotein Ib (GPIb): an alternative/backup mechanism to von Willebrand factor. FASEB J 17, 1490-1492.

Kaitna, S., Mendoza, M., Jantsch-Plunger, V., and Glotzer, M. (2000). Incenp and an aurora-like kinase form a complex essential for chromosome segregation and efficient completion of cytokinesis. Curr Biol 10, 1172-1181.

Kallioniemi, O. P., Punnonen, R., Mattila, J., Lehtinen, M., and Koivula, T. (1988). Prognostic significance of DNA index, multiploidy, and S-phase fraction in ovarian cancer. Cancer 61, 334-339.

Kamasaki, T., Osumi, M., and Mabuchi, I. (2007). Three-dimensional arrangement of F-actin in the contractile ring of fission yeast. J Cell Biol 178, 765-771.

Karlsson, C., Katich, S., Hagting, A., Hoffmann, I., and Pines, J. (1999). Cdc25B and Cdc25C differ markedly in their properties as initiators of mitosis. J Cell Biol 146, 573-584.

Kastan, M. B., Zhan, Q., el-Deiry, W. S., Carrier, F., Jacks, T., Walsh, W. V., Plunkett, B. S., Vogelstein, B., and Fornace, A. J., Jr. (1992). A mammalian cell cycle checkpoint pathway utilizing p53 and GADD45 is defective in ataxia-telangiectasia. Cell 71, 587-597.

Katayama, H., Ota, T., Morita, K., Terada, Y., Suzuki, F., Katoh, O., and Tatsuka, M. (1998). Human AIM-1: cDNA cloning and reduced expression during endomitosis in megakaryocyte-lineage cells. Gene 224, 1-7.

Kawasaki, A., Matsumura, I., Miyagawa, J., Ezoe, S., Tanaka, H., Terada, Y., Tatsuka, M., Machii, T., Miyazaki, H., Furukawa, Y., and Kanakura, Y. (2001). Downregulation of an AIM-1 kinase couples with megakaryocytic polyploidization of human hematopoietic cells. J Cell Biol 152, 275-287.

Kelley, C. A., Sellers, J. R., Goldsmith, P. K., and Adelstein, R. S. (1992). Smooth muscle myosin is composed of homodimeric heavy chains. J Biol Chem 267, 2127-2130.

Kelly, A. E., Sampath, S. C., Maniar, T. A., Woo, E. M., Chait, B. T., and Funabiki, H. (2007). Chromosomal enrichment and activation of the aurora B pathway are coupled to spatially regulate spindle assembly. Dev Cell 12, 31-43.

Khleif, S. N., DeGregori, J., Yee, C. L., Otterson, G. A., Kaye, F. J., Nevins, J. R., and Howley, P. M. (1996). Inhibition of cyclin D-CDK4/CDK6 activity is associated with an E2F-mediated induction of cyclin kinase inhibitor activity. Proc Natl Acad Sci U S A 93, 4350-4354.

Khmelinskii, A., Lawrence, C., Roostalu, J., and Schiebel, E. (2007). Cdc14-regulated midzone assembly controls anaphase B. J Cell Biol 177, 981-993.

King, J. M., Hays, T. S., and Nicklas, R. B. (2000). Dynein is a transient kinetochore component whose binding is regulated by microtubule attachment, not tension. J Cell Biol 151, 739-748.

Kirschner, M. W., and Mitchison, T. (1986). Microtubule dynamics. Nature 324, 621.

Knowlton, A. L., Lan, W., and Stukenberg, P. T. (2006). Aurora B is enriched at merotelic attachment sites, where it regulates MCAK. Curr Biol 16, 1705-1710.

Koc, A., Wheeler, L. J., Mathews, C. K., and Merrill, G. F. (2004). Hydroxyurea arrests DNA replication by a mechanism that preserves basal dNTP pools. J Biol Chem 279, 223-230.

Konopka, C. A., Schleede, J. B., Skop, A. R., and Bednarek, S. Y. (2006). Dynamin and cytokinesis. Traffic 7, 239-247.

Konrad, R. J., and Kudlow, J. E. (2002). The role of O-linked protein glycosylation in beta-cell dysfunction. Int J Mol Med 10, 535-539.

Kosako, H., Goto, H., Yanagida, M., Matsuzawa, K., Fujita, M., Tomono, Y., Okigaki, T., Odai, H., Kaibuchi, K., and Inagaki, M. (1999). Specific accumulation of Rho-associated kinase at the cleavage furrow during cytokinesis: cleavage furrow-specific phosphorylation of intermediate filaments. Oncogene 18, 2783-2788.

Kosako, H., Yoshida, T., Matsumura, F., Ishizaki, T., Narumiya, S., and Inagaki, M. (2000). Rho-kinase/ROCK is involved in cytokinesis through the phosphorylation of myosin light chain and not ezrin/radixin/moesin proteins at the cleavage furrow. Oncogene 19, 6059-6064.

Kruczynski, A., Barret, J. M., Etievant, C., Colpaert, F., Fahy, J., and Hill, B. T. (1998). Antimitotic and tubulin-interacting properties of vinflunine, a novel fluorinated Vinca alkaloid. Biochem Pharmacol 55, 635-648.

Kruse, K., Camalet, S., and Julicher, F. (2001). Self-propagating patterns in active filament bundles. Phys Rev Lett 87, 138101.

Kruse, K., and Julicher, F. (2000). Actively contracting bundles of polar filaments. Phys Rev Lett 85, 1778-1781.

Kruse, K., and Julicher, F. (2003). Self-organization and mechanical properties of active filament bundles. Phys Rev E Stat Nonlin Soft Matter Phys 67, 051913.

Kudo, Y., Yasui, W., Ue, T., Yamamoto, S., Yokozaki, H., Nikai, H., and Tahara, E. (1997). Overexpression of cyclin-dependent kinase-activating CDC25B phosphatase in human gastric carcinomas. Jpn J Cancer Res 88, 947-952.

Kulkarni, S., Dopheide, S. M., Yap, C. L., Ravanat, C., Freund, M., Mangin, P., Heel, K. A., Street, A., Harper, I. S., Lanza, F., and Jackson, S. P. (2000). A revised model of platelet aggregation. J Clin Invest 105, 783-791.

Kuppens, I. E. (2006). Current state of the art of new tubulin inhibitors in the clinic. Curr Clin Pharmacol 1, 57-70.

Lange, B. M., and Gull, K. (1996). Structure and function of the centriole in animal cells: progress and questions. Trends Cell Biol 6, 348-352.

Lanni, J. S., and Jacks, T. (1998). Characterization of the p53-dependent postmitotic checkpoint following spindle disruption. Mol Cell Biol 18, 1055-1064.

Lengauer, C., Kinzler, K. W., and Vogelstein, B. (1997). DNA methylation and genetic instability in colorectal cancer cells. Proc Natl Acad Sci U S A 94, 2545-2550.

Li, C., Lin, M., and Liu, J. (2004). Identification of PRC1 as the p53 target gene uncovers a novel function of p53 in the regulation of cytokinesis. Oncogene 23, 9336-9347.

Li, F., and Higgs, H. N. (2005). Dissecting requirements for auto-inhibition of actin nucleation by the formin, mDia1. J Biol Chem 280, 6986-6992.

Li, Y., Lu, J., Cohen, D., and Prochownik, E. V. (2008). Transformation, genomic instability and senescence mediated by platelet/megakaryocyte glycoprotein Ibalpha. Oncogene 27, 1599-1609.

Li, Y., Lu, J., and Prochownik, E. V. (2007). c-Myc-mediated genomic instability proceeds via a megakaryocytic endomitosis pathway involving Gp1balpha. Proc Natl Acad Sci U S A 104, 3490-3495.

Li, Y., Lu, J., and Prochownik, E. V. (2009). Modularity of the oncoprotein-like properties of platelet glycoprotein Ibalpha. J Biol Chem 284, 1410-1418.

Li, Y., Xu, F. L., Lu, J., Saunders, W. S., and Prochownik, E. V. Widespread genomic instability mediated by a pathway involving glycoprotein Ib alpha and aurora B kinase. J Biol Chem.

Liang, S. H., and Clarke, M. F. (2001). Regulation of p53 localization. Eur J Biochem 268, 2779-2783.

Liang, X. H., Mungal, S., Ayscue, A., Meissner, J. D., Wodnicki, P., Hockenbery, D., Lockett, S., and Herman, B. (1995). Bcl-2 protooncogene expression in cervical carcinoma cell lines containing inactive p53. J Cell Biochem 57, 509-521.

Lin, C. M., and Hamel, E. (1981). Effects of inhibitors of tubulin polymerization on GTP hydrolysis. J Biol Chem 256, 9242-9245.

Little, C. D., Nau, M. M., Carney, D. N., Gazdar, A. F., and Minna, J. D. (1983). Amplification and expression of the c-myc oncogene in human lung cancer cell lines. Nature 306, 194-196.

Lopez, J. A., Andrews, R. K., Afshar-Kharghan, V., and Berndt, M. C. (1998). Bernard-Soulier syndrome. Blood 91, 4397-4418.

Lordier, L., Jalil, A., Aurade, F., Larbret, F., Larghero, J., Debili, N., Vainchenker, W., and Chang, Y. (2008). Megakaryocyte endomitosis is a failure of late cytokinesis related to defects in the contractile ring and Rho/Rock signaling. Blood 112, 3164-3174.

Losada, A. (2007). Cohesin regulation: fashionable ways to wear a ring. Chromosoma 116, 321-329.

Lowe, J., Li, H., Downing, K. H., and Nogales, E. (2001). Refined structure of alpha beta-tubulin at 3.5 A resolution. J Mol Biol 313, 1045-1057.

Luo, S. Z., Mo, X., Afshar-Kharghan, V., Srinivasan, S., Lopez, J. A., and Li, R. (2007). Glycoprotein Ibalpha forms disulfide bonds with 2 glycoprotein Ibbeta subunits in the resting platelet. Blood 109, 603-609.

Maccioni, R. B., and Cambiazo, V. (1995). Role of microtubule-associated proteins in the control of microtubule assembly. Physiol Rev 75, 835-864.

MacNeal, R. K., and Purich, D. L. (1978). Stoichiometry and role of GTP hydrolysis in bovine neurotubule assembly. J Biol Chem 253, 4683-4687.

MacPherson, M., and Fagerholm, S. C. Filamin and filamin-binding proteins in integrin-regulation and adhesion. Focus on: "FilaminA is required for vimentin-mediated cell adhesion and spreading". Am J Physiol Cell Physiol 298, C206-208.

Madaule, P., Eda, M., Watanabe, N., Fujisawa, K., Matsuoka, T., Bito, H., Ishizaki, T., and Narumiya, S. (1998). Role of citron kinase as a target of the small GTPase Rho in cytokinesis. Nature 394, 491-494.

Maeda, K., Rosch, A., Maeda, Y., Kalbitzer, H. R., and Wittinghofer, A. (1991). Rabbit skeletal muscle myosin. Unfolded carboxyl-terminus and its role in molecular assembly. FEBS Lett 281, 23-26.

Maerki, S., Olma, M. H., Staubli, T., Steigemann, P., Gerlich, D. W., Quadroni, M., Sumara, I., and Peter, M. (2009). The Cul3-KLHL21 E3 ubiquitin ligase targets aurora B to midzone microtubules in anaphase and is required for cytokinesis. J Cell Biol 187, 791-800.

Maiato, H., DeLuca, J., Salmon, E. D., and Earnshaw, W. C. (2004). The dynamic kinetochore-microtubule interface. J Cell Sci 117, 5461-5477.

Mallavarapu, A., Sawin, K., and Mitchison, T. (1999). A switch in microtubule dynamics at the onset of anaphase B in the mitotic spindle of Schizosaccharomyces pombe. Curr Biol 9, 1423-1426.

Mariani-Costantini, R., Escot, C., Theillet, C., Gentile, A., Merlo, G., Lidereau, R., and Callahan, R. (1988). In situ c-myc expression and genomic status of the c-myc locus in infiltrating ductal carcinomas of the breast. Cancer Res 48, 199-205.

Marine, J. C., and Lozano, G. Mdm2-mediated ubiquitylation: p53 and beyond. Cell Death Differ 17, 93-102.

Marshall, W. F. (2001). Centrioles take center stage. Curr Biol 11, R487-496.

Maser, R. S., and DePinho, R. A. (2002). Connecting chromosomes, crisis, and cancer. Science 297, 565-569.

Mastronarde, D. N., McDonald, K. L., Ding, R., and McIntosh, J. R. (1993). Interpolar spindle microtubules in PTK cells. J Cell Biol 123, 1475-1489.

Matsumura, F., Totsukawa, G., Yamakita, Y., and Yamashiro, S. (2001). Role of myosin light chain phosphorylation in the regulation of cytokinesis. Cell Struct Funct 26, 639-644.
Matsuoka, S., Huang, M., and Elledge, S. J. (1998). Linkage of ATM to cell cycle regulation by the Chk2 protein kinase. Science 282, 1893-1897.
Maupin, P., and Pollard, T. D. (1986). Arrangement of actin filaments and myosin-like filaments in the contractile ring and of actin-like filaments in the mitotic spindle of dividing HeLa cells. J Ultrastruct Mol Struct Res 94, 92-103.
Medalia, O., Beck, M., Ecke, M., Weber, I., Neujahr, R., Baumeister, W., and Gerisch, G. (2007). Organization of actin networks in intact filopodia. Curr Biol 17, 79-84.
Meek, S. E., Lane, W. S., and Piwnica-Worms, H. (2004). Comprehensive proteomic analysis of interphase and mitotic 14-3-3-binding proteins. J Biol Chem 279, 32046-32054.
Melhem, M. F., Meisler, A. I., Finley, G. G., Bryce, W. H., Jones, M. O., Tribby, II, Pipas, J. M., and Koski, R. A. (1992). Distribution of cells expressing myc proteins in human colorectal epithelium, polyps, and malignant tumors. Cancer Res 52, 5853-5864.
Mendoza, M., Norden, C., Durrer, K., Rauter, H., Uhlmann, F., and Barral, Y. (2009). A mechanism for chromosome segregation sensing by the NoCut checkpoint. Nat Cell Biol 11, 477-483.
Meraldi, P., Honda, R., and Nigg, E. A. (2004). Aurora kinases link chromosome segregation and cell division to cancer susceptibility. Curr Opin Genet Dev 14, 29-36.
Mercier, C., Masseguin, C., Roux, F., Gabrion, J., and Scherrmann, J. M. (2004). Expression of P-glycoprotein (ABCB1) and Mrp1 (ABCC1) in adult rat brain: focus on astrocytes. Brain Res 1021, 32-40.
Meyer, N., and Penn, L. Z. (2008). Reflecting on 25 years with MYC. Nat Rev Cancer 8, 976-990.
Mitchison, T., and Kirschner, M. (1984). Dynamic instability of microtubule growth. Nature 312, 237-242.
Moran, N., Morateck, P. A., Deering, A., Ryan, M., Montgomery, R. R., Fitzgerald, D. J., and Kenny, D. (2000). Surface expression of glycoprotein ib alpha is dependent on glycoprotein ib beta: evidence from a novel mutation causing Bernard-Soulier syndrome. Blood 96, 532-539.
Morgan, D. O. (1999). Regulation of the APC and the exit from mitosis. Nat Cell Biol 1, E47-53.
Morisaki, H., Ando, A., Nagata, Y., Pereira-Smith, O., Smith, J. R., Ikeda, K., and Nakanishi, M. (1999). Complex mechanisms underlying impaired activation of Cdk4 and Cdk2 in replicative senescence: roles of p16, p21, and cyclin D1. Exp Cell Res 253, 503-510.
Moritz, M., Braunfeld, M. B., Guenebaut, V., Heuser, J., and Agard, D. A. (2000). Structure of the gamma-tubulin ring complex: a template for microtubule nucleation. Nat Cell Biol 2, 365-370.
Mueller, P. R., Coleman, T. R., Kumagai, A., and Dunphy, W. G. (1995). Myt1: a membrane-associated inhibitory kinase that phosphorylates Cdc2 on both threonine-14 and tyrosine-15. Science 270, 86-90.
Munzel, P., Marx, D., Kochel, H., Schauer, A., and Bock, K. W. (1991). Genomic alterations of the c-myc protooncogene in relation to the overexpression of c-erbB2 and Ki-67 in human breast and cervix carcinomas. J Cancer Res Clin Oncol 117, 603-607.
Muranyi, A., MacDonald, J. A., Deng, J. T., Wilson, D. P., Haystead, T. A., Walsh, M. P., Erdodi, F., Kiss, E., Wu, Y., and Hartshorne, D. J. (2002). Phosphorylation of the myosin phosphatase target subunit by integrin-linked kinase. Biochem J 366, 211-216.

Murata-Hori, M., Fumoto, K., Fukuta, Y., Iwasaki, T., Kikuchi, A., Tatsuka, M., and Hosoya, H. (2002). Myosin II regulatory light chain as a novel substrate for AIM-1, an aurora/Ipl1p-related kinase from rat. J Biochem (Tokyo) 128, 903-907.

Musacchio, A., and Hardwick, K. G. (2002). The spindle checkpoint: structural insights into dynamic signalling. Nat Rev Mol Cell Biol 3, 731-741.

Nakamura, F., Pudas, R., Heikkinen, O., Permi, P., Kilpelainen, I., Munday, A. D., Hartwig, J. H., Stossel, T. P., and Ylanne, J. (2006). The structure of the GPIb-filamin A complex. Blood 107, 1925-1932.

Nasmyth, K. (2005). How might cohesin hold sister chromatids together? Philos Trans R Soc Lond B Biol Sci 360, 483-496.

Ngan, E. S., Hashimoto, Y., Ma, Z. Q., Tsai, M. J., and Tsai, S. Y. (2003). Overexpression of Cdc25B, an androgen receptor coactivator, in prostate cancer. Oncogene 22, 734-739.

Nguyen, H. G., Makitalo, M., Yang, D., Chinnappan, D., St Hilaire, C., and Ravid, K. (2009). Deregulated Aurora-B induced tetraploidy promotes tumorigenesis. FASEB J 23, 2741-2748.

Nilsson, I., and Hoffmann, I. (2000). Cell cycle regulation by the Cdc25 phosphatase family. Prog Cell Cycle Res 4, 107-114.

Norbury, C., Blow, J., and Nurse, P. (1991). Regulatory phosphorylation of the p34cdc2 protein kinase in vertebrates. EMBO J 10, 3321-3329.

Norden, C., Mendoza, M., Dobbelaere, J., Kotwaliwale, C. V., Biggins, S., and Barral, Y. (2006). The NoCut pathway links completion of cytokinesis to spindle midzone function to prevent chromosome breakage. Cell 125, 85-98.

Nunez, F., Chipchase, M. D., Clarke, A. R., and Melton, D. W. (2000). Nucleotide excision repair gene (ERCC1) deficiency causes G(2) arrest in hepatocytes and a reduction in liver binucleation: the role of p53 and p21. FASEB J 14, 1073-1082.

Nunnally, M. H., D'Angelo, J. M., and Craig, S. W. (1980). Filamin concentration in cleavage furrow and midbody region: frequency of occurrence compared with that of alpha-actinin and myosin. J Cell Biol 87, 219-226.

Nurse, P. (1990). Universal control mechanism regulating onset of M-phase. Nature 344, 503-508.

Ogle, B. M., Cascalho, M., and Platt, J. L. (2005). Biological implications of cell fusion. Nat Rev Mol Cell Biol 6, 567-575.

Oguri, T., Ozasa, H., Uemura, T., Bessho, Y., Miyazaki, M., Maeno, K., Maeda, H., Sato, S., and Ueda, R. (2008). MRP7/ABCC10 expression is a predictive biomarker for the resistance to paclitaxel in non-small cell lung cancer. Mol Cancer Ther 7, 1150-1155.

Ohi, R., Coughlin, M. L., Lane, W. S., and Mitchison, T. J. (2003). An inner centromere protein that stimulates the microtubule depolymerizing activity of a KinI kinesin. Dev Cell 5, 309-321.

Ohta, Y., Suzuki, N., Nakamura, S., Hartwig, J. H., and Stossel, T. P. (1999). The small GTPase RalA targets filamin to induce filopodia. Proc Natl Acad Sci U S A 96, 2122-2128.

Olaharski, A. J., Sotelo, R., Solorza-Luna, G., Gonsebatt, M. E., Guzman, P., Mohar, A., and Eastmond, D. A. (2006). Tetraploidy and chromosomal instability are early events during cervical carcinogenesis. Carcinogenesis 27, 337-343.

Olovnikov, I. A., Kravchenko, J. E., and Chumakov, P. M. (2009). Homeostatic functions of the p53 tumor suppressor: regulation of energy metabolism and antioxidant defense. Semin Cancer Biol 19, 32-41.

Orren, D. K., Petersen, L. N., and Bohr, V. A. (1995). A UV-responsive G2 checkpoint in rodent cells. Mol Cell Biol 15, 3722-3730.

Otomo, T., Otomo, C., Tomchick, D. R., Machius, M., and Rosen, M. K. (2005). Structural basis of Rho GTPase-mediated activation of the formin mDia1. Mol Cell 18, 273-281.

Ozaki, Y., Asazuma, N., Suzuki-Inoue, K., and Berndt, M. C. (2005). Platelet GPIb-IX-V-dependent signaling. J Thromb Haemost 3, 1745-1751.

Pan, S., Sehnke, P. C., Ferl, R. J., and Gurley, W. B. (1999). Specific interactions with TBP and TFIIB in vitro suggest that 14-3-3 proteins may participate in the regulation of transcription when part of a DNA binding complex. Plant Cell 11, 1591-1602.

Parness, J., and Horwitz, S. B. (1981). Taxol binds to polymerized tubulin in vitro. J Cell Biol 91, 479-487.

Peddibhotla, S., Lam, M. H., Gonzalez-Rimbau, M., and Rosen, J. M. (2009). The DNA-damage effector checkpoint kinase 1 is essential for chromosome segregation and cytokinesis. Proc Natl Acad Sci U S A 106, 5159-5164.

Peled, A., Zipori, D., and Rotter, V. (1996). Cooperation between p53-dependent and p53-independent apoptotic pathways in myeloid cells. Cancer Res 56, 2148-2156.

Pelletier, O., Pokidysheva, E., Hirst, L. S., Bouxsein, N., Li, Y., and Safinya, C. R. (2003). Structure of actin cross-linked with alpha-actinin: a network of bundles. Phys Rev Lett 91, 148102.

Peng, C. Y., Graves, P. R., Thoma, R. S., Wu, Z., Shaw, A. S., and Piwnica-Worms, H. (1997). Mitotic and G2 checkpoint control: regulation of 14-3-3 protein binding by phosphorylation of Cdc25C on serine-216. Science 277, 1501-1505.

Pfaff, M., Liu, S., Erle, D. J., and Ginsberg, M. H. (1998). Integrin beta cytoplasmic domains differentially bind to cytoskeletal proteins. J Biol Chem 273, 6104-6109.

Pfleger, C. M., and Kirschner, M. W. (2000). The KEN box: an APC recognition signal distinct from the D box targeted by Cdh1. Genes Dev 14, 655-665.

Pi, M., Spurney, R. F., Tu, Q., Hinson, T., and Quarles, L. D. (2002). Calcium-sensing receptor activation of rho involves filamin and rho-guanine nucleotide exchange factor. Endocrinology 143, 3830-3838.

Piekny, A., Werner, M., and Glotzer, M. (2005). Cytokinesis: welcome to the Rho zone. Trends Cell Biol 15, 651-658.

Plantaz, D., Mohapatra, G., Matthay, K. K., Pellarin, M., Seeger, R. C., and Feuerstein, B. G. (1997). Gain of chromosome 17 is the most frequent abnormality detected in neuroblastoma by comparative genomic hybridization. Am J Pathol 150, 81-89.

Polager, S., and Ginsberg, D. (2009). p53 and E2f: partners in life and death. Nat Rev Cancer 9, 738-748.

Pollard, T. D., and Berro, J. (2009). Mathematical models and simulations of cellular processes based on actin filaments. J Biol Chem 284, 5433-5437.

Pollard, T. D., and Cooper, J. A. (2009). Actin, a central player in cell shape and movement. Science 326, 1208-1212.

Poperechnaya, A., Varlamova, O., Lin, P. J., Stull, J. T., and Bresnick, A. R. (2000). Localization and activity of myosin light chain kinase isoforms during the cell cycle. J Cell Biol 151, 697-708.

Powers, J., Bossinger, O., Rose, D., Strome, S., and Saxton, W. (1998). A nematode kinesin required for cleavage furrow advancement. Curr Biol 8, 1133-1136.

Prasanth, S. G., Prasanth, K. V., and Stillman, B. (2002). Orc6 involved in DNA replication, chromosome segregation, and cytokinesis. Science 297, 1026-1031.

Prives, C., and Hall, P. A. (1999). The p53 pathway. J Pathol 187, 112-126.

Rachid, S., Krug, D., Kunze, B., Kochems, I., Scharfe, M., Zabriskie, T. M., Blocker, H., and Muller, R. (2006). Molecular and biochemical studies of chondramide formation-highly cytotoxic natural products from Chondromyces crocatus Cm c5. Chem Biol 13, 667-681.

Raich, W. B., Moran, A. N., Rothman, J. H., and Hardin, J. (1998). Cytokinesis and midzone microtubule organization in Caenorhabditis elegans require the kinesin-like protein ZEN-4. Mol Biol Cell 9, 2037-2049.

Rappaport, R. (1961). Experiments concerning the cleavage stimulus in sand dollar eggs. J Exp Zool 148, 81-89.

Rappaport, R. (1985). Repeated furrow formation from a single mitotic apparatus in cylindrical sand dollar eggs. J Exp Zool 234, 167-171.

Ravelli, R. B., Gigant, B., Curmi, P. A., Jourdain, I., Lachkar, S., Sobel, A., and Knossow, M. (2004). Insight into tubulin regulation from a complex with colchicine and a stathmin-like domain. Nature 428, 198-202.

Reichenbach, H. (2001). Myxobacteria, producers of novel bioactive substances. J Ind Microbiol Biotechnol 27, 149-156.

Rieder, C. L. (1982). The formation, structure, and composition of the mammalian kinetochore and kinetochore fiber. Int Rev Cytol 79, 1-58.

Ris, H., and Witt, P. L. (1981). Structure of the mammalian kinetochore. Chromosoma 82, 153-170.

Rivera, J., Lozano, M. L., Corral, J., Gonzalez-Conejero, R., Martinez, C., and Vicente, V. (2000). Platelet GP Ib/IX/V complex: physiological role. J Physiol Biochem 56, 355-365.

Roger, L., Gadea, G., and Roux, P. (2006). Control of cell migration: a tumour suppressor function for p53? Biol Cell 98, 141-152.

Rogulski, K., Li, Y., Rothermund, K., Pu, L., Watkins, S., Yi, F., and Prochownik, E. V. (2005a). Onzin, a c-Myc-repressed target, promotes survival and transformation by modulating the Akt-Mdm2-p53 pathway. Oncogene 24, 7524-7541.

Rogulski, K. R., Cohen, D. E., Corcoran, D. L., Benos, P. V., and Prochownik, E. V. (2005b). Deregulation of common genes by c-Myc and its direct target, MT-MC1. Proc Natl Acad Sci U S A 102, 18968-18973.

Romano, A., Guse, A., Krascenicova, I., Schnabel, H., Schnabel, R., and Glotzer, M. (2003). CSC-1: a subunit of the Aurora B kinase complex that binds to the survivin-like protein BIR-1 and the incenp-like protein ICP-1. J Cell Biol 161, 229-236.

Roof, D. M., Meluh, P. B., and Rose, M. D. (1992). Kinesin-related proteins required for assembly of the mitotic spindle. J Cell Biol 118, 95-108.

Rowinsky, E. K., Cazenave, L. A., and Donehower, R. C. (1990). Taxol: a novel investigational antimicrotubule agent. J Natl Cancer Inst 82, 1247-1259.

Rowinsky, E. K., and Donehower, R. C. (1991). The clinical pharmacology and use of antimicrotubule agents in cancer chemotherapeutics. Pharmacol Ther 52, 35-84.

Sabry, J. H., O'Connor, T. P., Evans, L., Toroian-Raymond, A., Kirschner, M., and Bentley, D. (1991). Microtubule behavior during guidance of pioneer neuron growth cones in situ. J Cell Biol 115, 381-395.

Sachdeva, M., Zhu, S., Wu, F., Wu, H., Walia, V., Kumar, S., Elble, R., Watabe, K., and Mo, Y. Y. (2009). p53 represses c-Myc through induction of the tumor suppressor miR-145. Proc Natl Acad Sci U S A 106, 3207-3212.

Saito, S., Liu, X. F., Kamijo, K., Raziuddin, R., Tatsumoto, T., Okamoto, I., Chen, X., Lee, C. C., Lorenzi, M. V., Ohara, N., and Miki, T. (2004). Deregulation and mislocalization of the cytokinesis regulator ECT2 activate the Rho signaling pathways leading to malignant transformation. J Biol Chem 279, 7169-7179.

Salina, D., Bodoor, K., Eckley, D. M., Schroer, T. A., Rattner, J. B., and Burke, B. (2002). Cytoplasmic dynein as a facilitator of nuclear envelope breakdown. Cell 108, 97-107.

Sanchez, Y., Wong, C., Thoma, R. S., Richman, R., Wu, Z., Piwnica-Worms, H., and Elledge, S. J. (1997). Conservation of the Chk1 checkpoint pathway in mammals: linkage of DNA damage to Cdk regulation through Cdc25. Science 277, 1497-1501.

Sanger, J. M., and Sanger, J. W. (1980). Banding and polarity of actin filaments in interphase and cleaving cells. J Cell Biol 86, 568-575.

Sasse, F., Steinmetz, H., Heil, J., Hofle, G., and Reichenbach, H. (2000). Tubulysins, new cytostatic peptides from myxobacteria acting on microtubuli. Production, isolation, physico-chemical and biological properties. J Antibiot (Tokyo) 53, 879-885.

Sawin, K. E., LeGuellec, K., Philippe, M., and Mitchison, T. J. (1992). Mitotic spindle organization by a plus-end-directed microtubule motor. Nature 359, 540-543.

Scarlett, J. L., Sheard, P. W., Hughes, G., Ledgerwood, E. C., Ku, H. H., and Murphy, M. P. (2000). Changes in mitochondrial membrane potential during staurosporine-induced apoptosis in Jurkat cells. FEBS Lett 475, 267-272.

Schlosser, I., Holzel, M., Murnseer, M., Burtscher, H., Weidle, U. H., and Eick, D. (2003). A role for c-Myc in the regulation of ribosomal RNA processing. Nucleic Acids Res 31, 6148-6156.

Schroeder, T. E. (1968). Cytokinesis: filaments in the cleavage furrow. Exp Cell Res 53, 272-276.

Schroeder, T. E. (1970). The contractile ring. I. Fine structure of dividing mammalian (HeLa) cells and the effects of cytochalasin B. Z Zellforsch Mikrosk Anat 109, 431-449.

Schroeder, T. E. (1972). The contractile ring. II. Determining its brief existence, volumetric changes, and vital role in cleaving Arbacia eggs. J Cell Biol 53, 419-434.

Schroeder, T. E. (1975). Dynamics of the contractile ring. Soc Gen Physiol Ser 30, 305-334.

Scoumanne, A., and Chen, X. (2006). The epithelial cell transforming sequence 2, a guanine nucleotide exchange factor for Rho GTPases, is repressed by p53 via protein methyltransferases and is required for G1-S transition. Cancer Res 66, 6271-6279.

Sellers, J. R. (2000). Myosins: a diverse superfamily. Biochim Biophys Acta 1496, 3-22.

Shackney, S. E., Smith, C. A., Miller, B. W., Burholt, D. R., Murtha, K., Giles, H. R., Ketterer, D. M., and Pollice, A. A. (1989). Model for the genetic evolution of human solid tumors. Cancer Res 49, 3344-3354.

Shannon, K. B., Canman, J. C., and Salmon, E. D. (2002). Mad2 and BubR1 function in a single checkpoint pathway that responds to a loss of tension. Mol Biol Cell 13, 3706-3719.

Sharma, C. P., Ezzell, R. M., and Arnaout, M. A. (1995). Direct interaction of filamin (ABP-280) with the beta 2-integrin subunit CD18. J Immunol 154, 3461-3470.

Shelden, E., and Wadsworth, P. (1993). Observation and quantification of individual microtubule behavior in vivo: microtubule dynamics are cell-type specific. J Cell Biol 120, 935-945.

Shen-Ong, G. L., Keath, E. J., Piccoli, S. P., and Cole, M. D. (1982). Novel myc oncogene RNA from abortive immunoglobulin-gene recombination in mouse plasmacytomas. Cell 31, 443-452.

Shi, Q., and King, R. W. (2005). Chromosome nondisjunction yields tetraploid rather than aneuploid cells in human cell lines. Nature 437, 1038-1042.

Shieh, S. Y., Ikeda, M., Taya, Y., and Prives, C. (1997). DNA damage-induced phosphorylation of p53 alleviates inhibition by MDM2. Cell 91, 325-334.

Simon, G. C., Schonteich, E., Wu, C. C., Piekny, A., Ekiert, D., Yu, X., Gould, G. W., Glotzer, M., and Prekeris, R. (2008). Sequential Cyk-4 binding to ECT2 and FIP3 regulates cleavage furrow ingression and abscission during cytokinesis. EMBO J 27, 1791-1803.

Skop, A. R., Liu, H., Yates, J., 3rd, Meyer, B. J., and Heald, R. (2004). Dissection of the mammalian midbody proteome reveals conserved cytokinesis mechanisms. Science 305, 61-66.

Small, J. V. (1994). Lamellipodia architecture: actin filament turnover and the lateral flow of actin filaments during motility. Semin Cell Biol 5, 157-163.

Snyder, J. P., Nettles, J. H., Cornett, B., Downing, K. H., and Nogales, E. (2001). The binding conformation of Taxol in beta-tubulin: a model based on electron crystallographic density. Proc Natl Acad Sci U S A 98, 5312-5316.

Soldani, C., and Scovassi, A. I. (2002). Poly(ADP-ribose) polymerase-1 cleavage during apoptosis: an update. Apoptosis 7, 321-328.

Somma, M. P., Fasulo, B., Cenci, G., Cundari, E., and Gatti, M. (2002). Molecular dissection of cytokinesis by RNA interference in Drosophila cultured cells. Mol Biol Cell 13, 2448-2460.

Sorenson, C. M., and Eastman, A. (1988a). Influence of cis-diamminedichloroplatinum(II) on DNA synthesis and cell cycle progression in excision repair proficient and deficient Chinese hamster ovary cells. Cancer Res 48, 6703-6707.

Sorenson, C. M., and Eastman, A. (1988b). Mechanism of cis-diamminedichloroplatinum(II)-induced cytotoxicity: role of G2 arrest and DNA double-strand breaks. Cancer Res 48, 4484-4488.

Spiegelman, B. M., Penningroth, S. M., and Kirschner, M. W. (1977). Turnover of tubulin and the N site GTP in Chinese hamster ovary cells. Cell 12, 587-600.

Stegmeier, F., Visintin, R., and Amon, A. (2002). Separase, polo kinase, the kinetochore protein Slk19, and Spo12 function in a network that controls Cdc14 localization during early anaphase. Cell 108, 207-220.

Steigemann, P., Wurzenberger, C., Schmitz, M. H., Held, M., Guizetti, J., Maar, S., and Gerlich, D. W. (2009). Aurora B-mediated abscission checkpoint protects against tetraploidization. Cell 136, 473-484.

Stewenius, Y., Gorunova, L., Jonson, T., Larsson, N., Hoglund, M., Mandahl, N., Mertens, F., Mitelman, F., and Gisselsson, D. (2005). Structural and numerical chromosome changes in colon cancer develop through telomere-mediated anaphase bridges, not through mitotic multipolarity. Proc Natl Acad Sci U S A 102, 5541-5546.

Storchova, Z., Breneman, A., Cande, J., Dunn, J., Burbank, K., O'Toole, E., and Pellman, D. (2006). Genome-wide genetic analysis of polyploidy in yeast. Nature 443, 541-547.

Stossel, T. P., Condeelis, J., Cooley, L., Hartwig, J. H., Noegel, A., Schleicher, M., and Shapiro, S. S. (2001). Filamins as integrators of cell mechanics and signalling. Nat Rev Mol Cell Biol 2, 138-145.

Sudakin, V., Chan, G. K., and Yen, T. J. (2001). Checkpoint inhibition of the APC/C in HeLa cells is mediated by a complex of BUBR1, BUB3, CDC20, and MAD2. J Cell Biol 154, 925-936.

Sudakin, V., Ganoth, D., Dahan, A., Heller, H., Hershko, J., Luca, F. C., Ruderman, J. V., and Hershko, A. (1995). The cyclosome, a large complex containing cyclin-selective ubiquitin ligase activity, targets cyclins for destruction at the end of mitosis. Mol Biol Cell 6, 185-197.

Takamatsu, J., Horne, M. K., 3rd, and Gralnick, H. R. (1986). Identification of the thrombin receptor on human platelets by chemical crosslinking. J Clin Invest 77, 362-368.

Takemasa, I., Yamamoto, H., Sekimoto, M., Ohue, M., Noura, S., Miyake, Y., Matsumoto, T., Aihara, T., Tomita, N., Tamaki, Y., et al. (2000). Overexpression of CDC25B phosphatase as a novel marker of poor prognosis of human colorectal carcinoma. Cancer Res 60, 3043-3050.

Takiguchi, K. (1991). Heavy meromyosin induces sliding movements between antiparallel actin filaments. J Biochem 109, 520-527.

Tanaka-Takiguchi, Y., Kakei, T., Tanimura, A., Takagi, A., Honda, M., Hotani, H., and Takiguchi, K. (2004). The elongation and contraction of actin bundles are induced by double-headed myosins in a motor concentration-dependent manner. J Mol Biol 341, 467-476.

Tanenbaum, M. E., Macurek, L., Galjart, N., and Medema, R. H. (2008). Dynein, Lis1 and CLIP-170 counteract Eg5-dependent centrosome separation during bipolar spindle assembly. EMBO J 27, 3235-3245.

Taub, R., Kirsch, I., Morton, C., Lenoir, G., Swan, D., Tronick, S., Aaronson, S., and Leder, P. (1982). Translocation of the c-myc gene into the immunoglobulin heavy chain locus in human Burkitt lymphoma and murine plasmacytoma cells. Proc Natl Acad Sci U S A 79, 7837-7841.

Taylor, S. S., Scott, M. I., and Holland, A. J. (2004). The spindle checkpoint: a quality control mechanism which ensures accurate chromosome segregation. Chromosome Res 12, 599-616.

Thompson, H. M., Skop, A. R., Euteneuer, U., Meyer, B. J., and McNiven, M. A. (2002). The large GTPase dynamin associates with the spindle midzone and is required for cytokinesis. Curr Biol 12, 2111-2117.

Thompson, S. L., and Compton, D. A. (2008). Examining the link between chromosomal instability and aneuploidy in human cells. J Cell Biol 180, 665-672.

Tierno, M. B., Kitchens, C. A., Petrik, B., Graham, T. H., Wipf, P., Xu, F. L., Saunders, W. S., Raccor, B. S., Balachandran, R., Day, B. W., et al. (2009). Microtubule binding and disruption and induction of premature senescence by disorazole C(1). J Pharmacol Exp Ther 328, 715-722.

Trivedi, M., Budihardjo, I., Loureiro, K., Reid, T. R., and Ma, J. D. (2008). Epothilones: a novel class of microtubule-stabilizing drugs for the treatment of cancer. Future Oncol 4, 483-500.

Tsou, M. F., and Stearns, T. (2006). Mechanism limiting centrosome duplication to once per cell cycle. Nature 442, 947-951.

Tucker, J. B. (1971). Microtubules and a contractile ring of microfilaments associated with a cleavage furrow. J Cell Sci 8, 557-571.

Ueda, K., Ohta, Y., and Hosoya, H. (2003). The carboxy-terminal pleckstrin homology domain of ROCK interacts with filamin-A. Biochem Biophys Res Commun 301, 886-890.

Uhlmann, F. (2004). The mechanism of sister chromatid cohesion. Exp Cell Res 296, 80-85.

Uhlmann, F., Lottspeich, F., and Nasmyth, K. (1999). Sister-chromatid separation at anaphase onset is promoted by cleavage of the cohesin subunit Scc1. Nature 400, 37-42.

Ulsemer, P., Strassel, C., Baas, M. J., Salamero, J., Chasserot-Golaz, S., Cazenave, J. P., De La Salle, C., and Lanza, F. (2001). Biosynthesis and intracellular post-translational processing of normal and mutant platelet glycoprotein GPIb-IX. Biochem J 358, 295-303.

van Engeland, M., Nieland, L. J., Ramaekers, F. C., Schutte, B., and Reutelingsperger, C. P. (1998). Annexin V-affinity assay: a review on an apoptosis detection system based on phosphatidylserine exposure. Cytometry 31, 1-9.

Varga, V., Leduc, C., Bormuth, V., Diez, S., and Howard, J. (2009). Kinesin-8 motors act cooperatively to mediate length-dependent microtubule depolymerization. Cell 138, 1174-1183.

Vavylonis, D., Wu, J. Q., Hao, S., O'Shaughnessy, B., and Pollard, T. D. (2008). Assembly mechanism of the contractile ring for cytokinesis by fission yeast. Science 319, 97-100.

Vermes, I., Haanen, C., Steffens-Nakken, H., and Reutelingsperger, C. (1995). A novel assay for apoptosis. Flow cytometric detection of phosphatidylserine expression on early apoptotic cells using fluorescein labelled Annexin V. J Immunol Methods 184, 39-51.

Vorobjev, I. A., and Nadezhdina, E. S. (1987). The centrosome and its role in the organization of microtubules. Int Rev Cytol 106, 227-293.

Vousden, K. H. (2000). p53: death star. Cell 103, 691-694.

Wada, I., Rindress, D., Cameron, P. H., Ou, W. J., Doherty, J. J., 2nd, Louvard, D., Bell, A. W., Dignard, D., Thomas, D. Y., and Bergeron, J. J. (1991). SSR alpha and associated calnexin are major calcium binding proteins of the endoplasmic reticulum membrane. J Biol Chem 266, 19599-19610.

Walker, R. A., O'Brien, E. T., Pryer, N. K., Soboeiro, M. F., Voter, W. A., Erickson, H. P., and Salmon, E. D. (1988). Dynamic instability of individual microtubules analyzed by video light microscopy: rate constants and transition frequencies. J Cell Biol 107, 1437-1448.

Wallar, B. J., Stropich, B. N., Schoenherr, J. A., Holman, H. A., Kitchen, S. M., and Alberts, A. S. (2006). The basic region of the diaphanous-autoregulatory domain (DAD) is required for autoregulatory interactions with the diaphanous-related formin inhibitory domain. J Biol Chem 281, 4300-4307.

Wanger, M., Keiser, T., Neuhaus, J. M., and Wegner, A. (1985). The actin treadmill. Can J Biochem Cell Biol 63, 414-421.

Wanger, M., and Wegner, A. (1985). Equilibrium constant for binding of an actin filament capping protein to the barbed end of actin filaments. Biochemistry 24, 1035-1040.

Ware, J., Russell, S., and Ruggeri, Z. M. (2000). Generation and rescue of a murine model of platelet dysfunction: the Bernard-Soulier syndrome. Proc Natl Acad Sci U S A 97, 2803-2808.

Waterman, M. J., Stavridi, E. S., Waterman, J. L., and Halazonetis, T. D. (1998). ATM-dependent activation of p53 involves dephosphorylation and association with 14-3-3 proteins. Nat Genet 19, 175-178.

Weaver, B. A., and Cleveland, D. W. (2006). Does aneuploidy cause cancer? Curr Opin Cell Biol 18, 658-667.

Weihing, R. R. (1985). The filamins: properties and functions. Can J Biochem Cell Biol 63, 397-413.
Weisenberg, R. C., Deery, W. J., and Dickinson, P. J. (1976). Tubulin-nucleotide interactions during the polymerization and depolymerization of microtubules. Biochemistry 15, 4248-4254.
White, J. G. (2005). The astral relaxation theory of cytokinesis revisited. Bioessays 2, 267-72.
Wijkstrom, H., Granberg-Ohman, I., and Tribukait, B. (1984). Chromosomal and DNA patterns in transitional cell bladder carcinoma. A comparative cytogenetic and flow-cytofluorometric DNA study. Cancer 53, 1718-1723.
Williams, B. C., Riedy, M. F., Williams, E. V., Gatti, M., and Goldberg, M. L. (1995). The Drosophila kinesin-like protein KLP3A is a midbody component required for central spindle assembly and initiation of cytokinesis. J Cell Biol 129, 709-723.
Wipf, P., and Graham, T. H. (2004). Total synthesis of (-)-disorazole C1. J Am Chem Soc 126, 15346-15347.
Wipf, P., Graham, T. H., Vogt, A., Sikorski, R. P., Ducruet, A. P., and Lazo, J. S. (2006). Cellular analysis of disorazole C and structure-activity relationship of analogs of the natural product. Chem Biol Drug Des 67, 66-73.
Wirth, K. G., Wutz, G., Kudo, N. R., Desdouets, C., Zetterberg, A., Taghybeeglu, S., Seznec, J., Ducos, G. M., Ricci, R., Firnberg, N., et al. (2006). Separase: a universal trigger for sister chromatid disjunction but not chromosome cycle progression. J Cell Biol 172, 847-860.
Wiseman, H., and Halliwell, B. (1996). Damage to DNA by reactive oxygen and nitrogen species: role in inflammatory disease and progression to cancer. Biochem J 313 (Pt 1), 17-29.
Wollert, T., Wunder, C., Lippincott-Schwartz, J., and Hurley, J. H. (2009). Membrane scission by the ESCRT-III complex. Nature 458, 172-177.
Wolpert, L. (1960). The mechanics and mechanism of cleavage. Int Rev Cytol 10, 163–216.
Wu, G., Lin, Y. T., Wei, R., Chen, Y., Shan, Z., and Lee, W. H. (2008). Hice1, a novel microtubule-associated protein required for maintenance of spindle integrity and chromosomal stability in human cells. Mol Cell Biol 28, 3652-3662.
Wu, H., Lan, Z., Li, W., Wu, S., Weinstein, J., Sakamoto, K. M., and Dai, W. (2000). p55CDC/hCDC20 is associated with BUBR1 and may be a downstream target of the spindle checkpoint kinase. Oncogene 19, 4557-4562.
Wu, W., Fan, Y. H., Kemp, B. L., Walsh, G., and Mao, L. (1998). Overexpression of cdc25A and cdc25B is frequent in primary non-small cell lung cancer but is not associated with overexpression of c-myc. Cancer Res 58, 4082-4085.
Wulf, E., Deboben, A., Bautz, F. A., Faulstich, H., and Wieland, T. (1979). Fluorescent phallotoxin, a tool for the visualization of cellular actin. Proc Natl Acad Sci U S A 76, 4498-4502.
Xu, F. L., Rbaibi, Y., Kiselyov, K., Lazo, J. S., Wipf, P., and Saunders, W. S. Mitotic slippage in non-cancer cells induced by a microtubule disruptor, disorazole C1. BMC Chem Biol 10, 1.
Xu, W., Xie, Z., Chung, D. W., and Davie, E. W. (1998). A novel human actin-binding protein homologue that binds to platelet glycoprotein Ibalpha. Blood 92, 1268-1276.
Yamamoto, N., Greco, N. J., Barnard, M. R., Tanoue, K., Yamazaki, H., Jamieson, G. A., and Michelson, A. D. (1991). Glycoprotein Ib (GPIb)-dependent and GPIb-independent pathways of thrombin-induced platelet activation. Blood 77, 1740-1748.

Yamashiro, S., Totsukawa, G., Yamakita, Y., Sasaki, Y., Madaule, P., Ishizaki, T., Narumiya, S., and Matsumura, F. (2003). Citron kinase, a Rho-dependent kinase, induces di-phosphorylation of regulatory light chain of myosin II. Mol Biol Cell 14, 1745-1756.

Yano, H., Nanashima, A., Hidaka, S., Haseba, M., Tanaka, K., Yamaguchi, H., Nakagoe, T., Tagawa, Y., and Nagayasu, T. (2004). Numerical aberrations of chromosome 17 and the p53 locus in small hepatocellular carcinomas. Anticancer Res 24, 111-115.

Yokoyama, T., Goto, H., Izawa, I., Mizutani, H., and Inagaki, M. (2005). Aurora-B and Rho-kinase/ROCK, the two cleavage furrow kinases, independently regulate the progression of cytokinesis: possible existence of a novel cleavage furrow kinase phosphorylates ezrin/radixin/moesin (ERM). Genes Cells 10, 127-137.

Zachos, G., Black, E. J., Walker, M., Scott, M. T., Vagnarelli, P., Earnshaw, W. C., and Gillespie, D. A. (2007). Chk1 is required for spindle checkpoint function. Dev Cell 12, 247-260.

Zhang, W., Tong, Q., Li, S., Wang, X., and Wang, Q. (2008). MG-132 inhibits telomerase activity, induces apoptosis and G(1) arrest associated with upregulated p27kip1 expression and downregulated survivin expression in gastric carcinoma cells. Cancer Invest 26, 1032-1036.

Zhang, Y., Sun, S., Chen, W. C., Kaluzhny, Y., Chinnappan, D., Yu, G., and Ravid, K. (2001). Repression of AIM-1 kinase mRNA as part of a program of genes regulated by Mpl ligand. Biochem Biophys Res Commun 282, 844-849.

Zhao, J., Speel, E. J., Muletta-Feurer, S., Rutimann, K., Saremaslani, P., Roth, J., Heitz, P. U., and Komminoth, P. (1999). Analysis of genomic alterations in sporadic adrenocortical lesions. Gain of chromosome 17 is an early event in adrenocortical tumorigenesis. Am J Pathol 155, 1039-1045.

Zimmet, J., and Ravid, K. (2000). Polyploidy: occurrence in nature, mechanisms, and significance for the megakaryocyte-platelet system. Exp Hematol 28, 3-16.

Zou, H., McGarry, T. J., Bernal, T., and Kirschner, M. W. (1999). Identification of a vertebrate sister-chromatid separation inhibitor involved in transformation and tumorigenesis. Science 285, 418-422.

Zumdieck, A., Kruse, K., Bringmann, H., Hyman, A. A., and Julicher, F. (2007). Stress generation and filament turnover during actin ring constriction. PLoS One 2, e696.